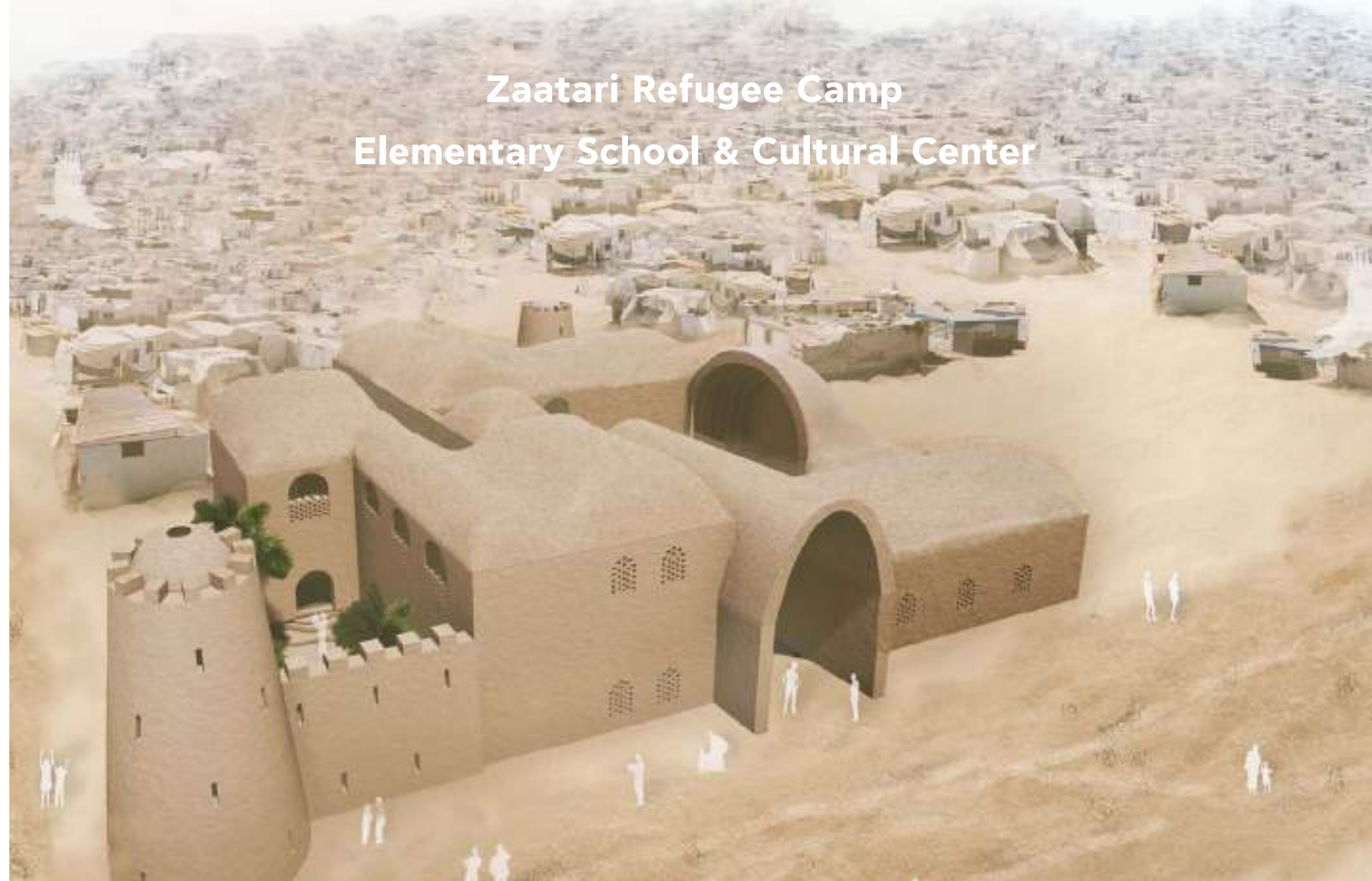


SANDCASTLE

Zaatari Refugee Camp
Elementary School & Cultural Center



AR3B011 Earthy TU Delft Group_04

Delft University of Technology

Faculty of Architecture and the Built Environment

Department of Architectural Engineering and Technology

Master of Science in Architecture, Urbanism and Building Sciences

Track Building Technology

AR3B011 EARTHY 2019/2020

DESIGN TEAM

Konstantina Chouliara	4744292
Maria Dimas	4893344
Steven Engels	4813022
Daniella Naous	4290038
Bart van Nimwegen	4484770
Ronald Rijsterborgh	4483014

INSTRUCTORS

Prof. Dr. Ir. Sevil Sariyildiz
Dr. Ir. Fred Veer
Dr. Ir. Pirouz Nourian
Ir. Hans Hoogenboom
Ir. Dirk Rinze Visser
Ir. Shervin Azadi
Ir. Frank Schnater

ABSTRACT

As part of the Building Technology Studio AR3B011 Earthy students were assigned to propose an urban plan and design earthy architectural solutions for the Syrian refugees in Zaatari Camp in Jordan. The aim was to provide Zaatari refugees with facility buildings and housing solutions that gives them dignity, security, comfort, a sense of belonging, and simultaneously restores cultural vibes and supply their socioeconomic needs. Because, refugee camps are not allowed to erect any permanent buildings, earthy architecture has the potential of providing a high quality solution, while being a 100% circular destructible structure.

Research and analysis of the camp showed that there is an insufficient school network. After planning the enhanced school network on the urban scale, the report elaborates on the design of one school. The layout of the floor plans resulted through graph theoretical methods and the combination of vernacular desert architecture and castle architecture, to create a comfortable and appealing environment.

The volumes of the complex had to be in line with the material's nature. Adobe bricks cannot withstand tension forces and therefore can be used only be used in compression-only structures. The principles of catenary arched geometries were implemented through parametric computational tools. After creating such geometries, their structural endurance was tested. Finally, the construction techniques suggested for the project were analysed.

CONTENTS

1	ANALYSIS	6
2	URBAN CONFIGURATION	21
3	LAYOUT CONFIGURATION	31
4	FORM FINDING	55
5	STRUCTURAL ANALYSIS	70
6	CONSTRUCTION	82
7	CONCLUSION	125
8	REFERENCES	127
9	APPENDIX	131

INTRODUCTION

As part of the Building Technology Studio AR3B011 Earthy, students have been assigned to plan urban and design earthy architectural solutions for the Syrian refugees in Zaatari Camp in Jordan. At the same time refugees have been there since 2013 and are expected to stay there for a considerable amount of years in the future. Therefore, it is only reasonable to provide Zaatari refugees with facility buildings and housing solutions that gives them dignity, security, comfort, a sense of belonging, restores cultural vibes, and supplies their socioeconomic needs.

Refugee camps are not allowed to erect any permanent buildings. Earthy architecture has the potential of providing such a high quality solution, and yet be a temporary structure. Earthy architecture is cheap since dirt (earth) is available on site and requires low-tech processing. Earth bricks (or adobe bricks) are environmentally friendly because they are 100% 'demountable', and circular. Demolished earth is just earth!

Despite all of the advantages of using earth as a building material, earth has a very challenging structural mechanics limitations. The material is brittle. Adobe bricks cannot withstand tension forces and therefore can be used only be used in compression-only structures. Antoni Gaudi's inspiring example of mirrored hanging catenary arched geometries is a good example to follow when designing compression only structures. In this Project the same principles used by Gaudi

are mimicked using parametric computational tools including grasshopper and kangaroo, mesh+, python, weaverbird, karamba as plug-ins.

Other computational algorithms were used in this course like the configurative approach for layout planning through the graph theoretical methods for design and analysis of spatial configurations of floor plans. The bridge between architecture, mathematics, material science, structural analysis, parametric design, and computational layout configuration was articulated in this course.

First though, an analysis was conducted and the camp was researched inorder to find what is the situation there? What are their greatest needs? And what can be done to make things better?

1 ANALYSIS

The world is currently suffering from an unprecedented refugee crisis (Steadman, 2018). The amount of registered Syrian refugees counts 5,644,769 heads. Most syrian refugee camps are in Turkey, followed by Lebanon and Jordan. Although Jordan has several refugee camps, not only for Syrians, the Zaatri camp is by far the largest Syrian refugee camp in Jordan, housing 78,597 refugees. Zaatri Camp demographics were analyzed in order to get an insight into the main target groups of the refugees. The design of the camp, and choice of additional facilities should adhere to the needs of the prevailing demographic group with highest demand and shortest supply to its necessities.

Regardless of the age groups, 43.9% of the refugees are female and 56.1% are male (UNHCR, 2019). From the 78,597 refugees, 12,005 (15.3%) have work permits and 1,680 (14%) are working women (figure 1). It is worth mentioning, that 20% of the families on the camp are female headed households (Omondi et al., 2019).

Most refugees originate from Daráa, which is 60km away from the camp, while the rest come from Damascus or other rural areas. The rate of the camp growth experienced an external shock in 2013 of new influx; fortunately, by 2019 it had stabilized to a normal urban internal growth rate (figure 2). However, the dwelling supply growth rate still did not match the demand. Therefore, an urban plan was required to improve the quality and increase the quantity of the accommodating structure and facilities of the camp.

Figure 1 | Working permits statistics (UNHCR, 2019)

Figure 2 | Growth of inhabitants (UNHCR, 2019)



Figure 1

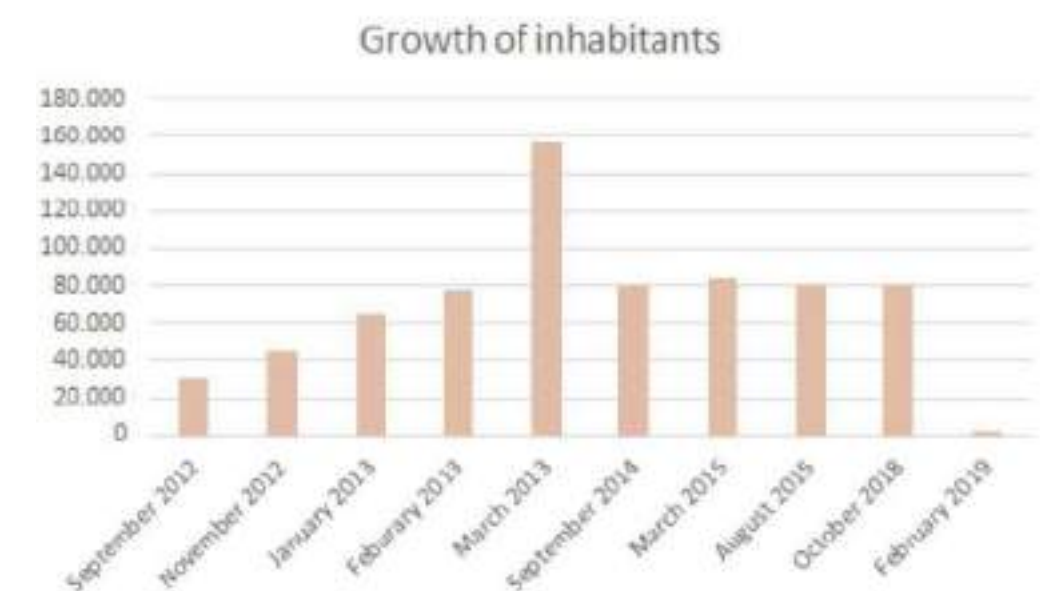
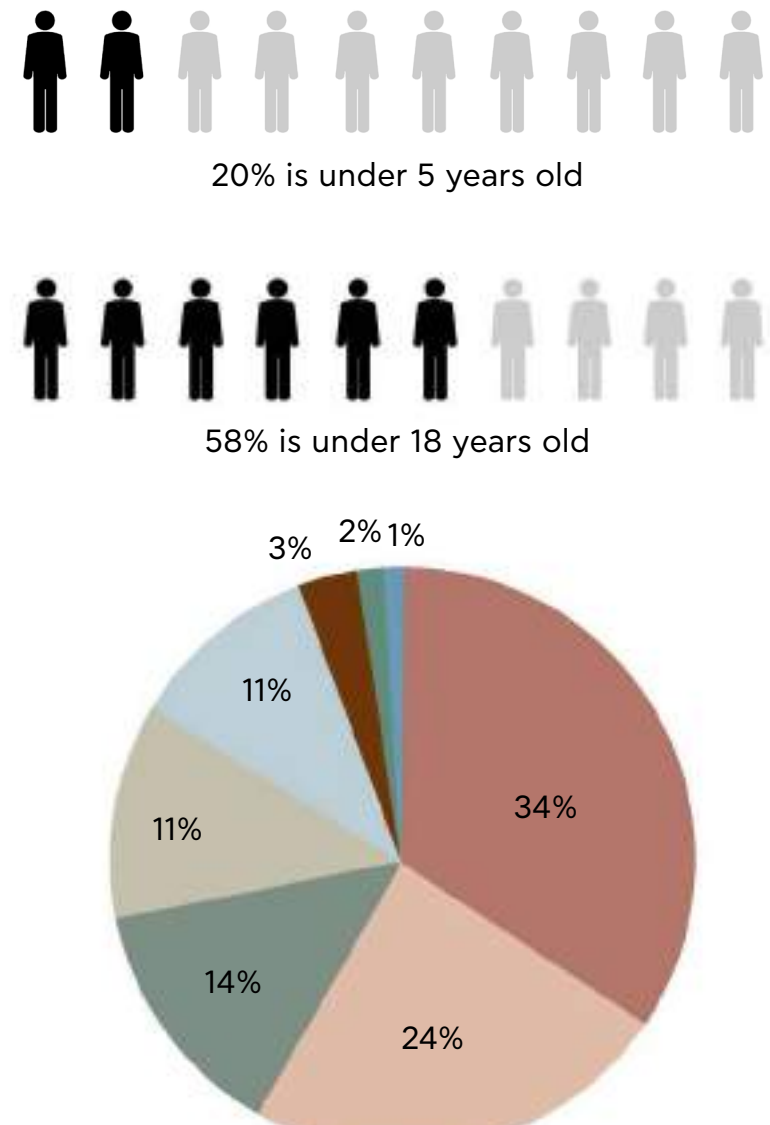


Figure 2

According to the research, 20% of the camp are under 5 years old, and 58% are under 18 years old (figure 3). This means that the youth make up more than half of the camp's population. Inhabitants within this age-band, should still be enrolled in school under normal circumstances (Omondi et al., 2019).

Considering elementary school education of higher priority than secondary school, and that within a couple of years the 20% of children below 5 years old will become of age of primary education, this analysis focused on the current age group lying between 6 and 12 years old. Statistics indicate that there are 18.493 children between 6 and 12 years old (Omondi et al., 2019). There are only 32 schools available in 13 locations. That would mean that 578 children are enrolled per school (figure 4). However, these schools are not specified. Not all of them are elementary schools and some of them could be vocational training centers for 18+'s. Hence, the demand is larger than it could initially be deduced.

Figure 3 | Demographic statistics (Omondi et al., 2019)

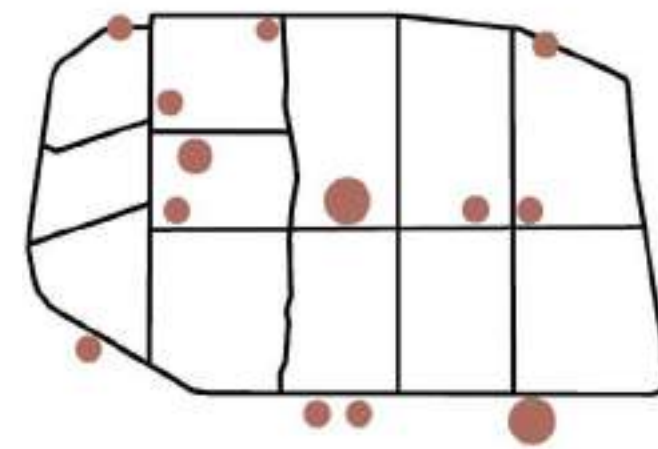




18.493 children



32 schools



13 school locations

578 children per school?

Figure 4 | Amount of children
from 6-12, schools and school
locations on camp

"Zaatari is divided into 12 districts. Representatives from each district serve on a camp committee to help maintain dialogue with SRAD on key issues related to life in the camp, such as services." (Soulié & Ababsa, 2018).

After zooming into each district, the shortage between demand and supply of elementary education became evident. The percentage of children between the ages of 6 and 12 who are enrolled in school never exceeded 45%. This is an alarming percentage of unenrolled children (figure 5) (UNHCR., 2019; UNICEF-REACH, 2016c). Henceforth, it was decided to focus on planning and designing elementary schools for the refugee camp. Before that, the reasons causing this low enrolment rate should be understood for the plan to counteract these causes.



Figure 5 | Map of households with age appropriate children enrolled in school (UNHCR., 2019; UNICEF-REACH, 2016c)

0 100 200 500 1000 (m)

<38% 38-40% 40-42% >42%



One reason some families might have decided not to send their female children to school, is the threat of harassment on the road. To counteract this threat, a design rule was established to have a school within every 400m radius (figure 6). The shorter the distance pupils need to walk from home, the safer they would feel. Another solution was creating two shifts of school hours. The morning shift will exclude the boys for the safety of the girls. Evening shifts will host the boys, and therefore girls could go home early during daytime.

Another aspect could be the route. If schools are placed in the middle of the district, children would have to walk on deserted small and crampy roads. On the other hand, if schools are placed on the main paved streets dividing the districts, this could be dangerous due to cars and large crowds. Therefore, new schools would preferably be placed just one street inwards, parallel to the main street. That way students would have a balanced route option between both contextual advantages.

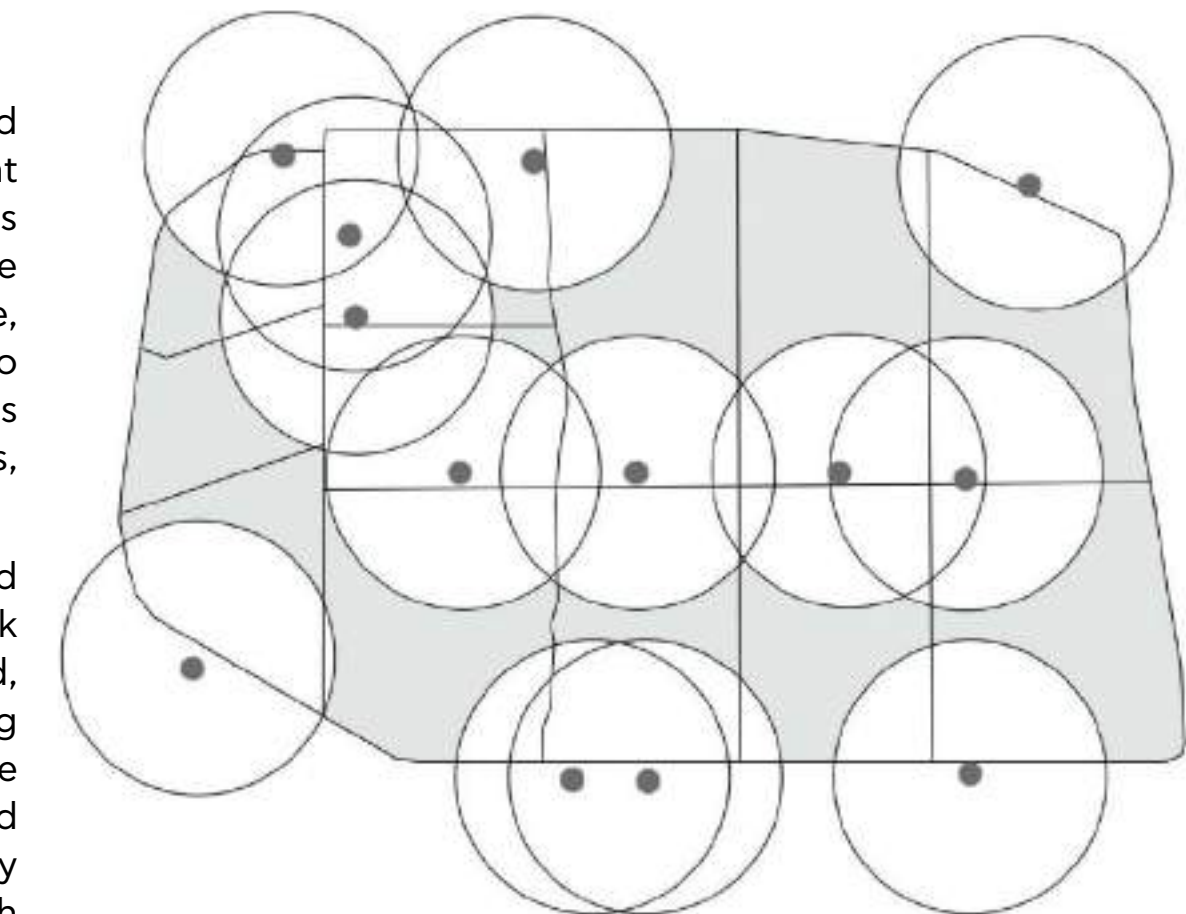
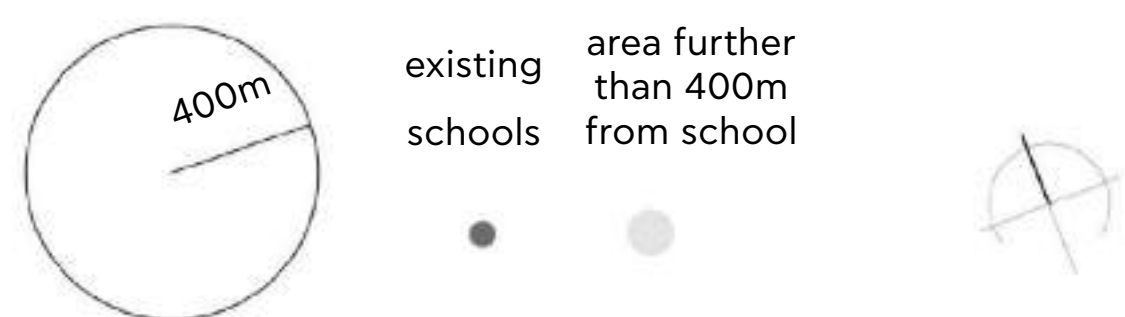


Figure 6 | Map of camp areas further than 400m from existing school locations

0 100 200 500 1000 (m)

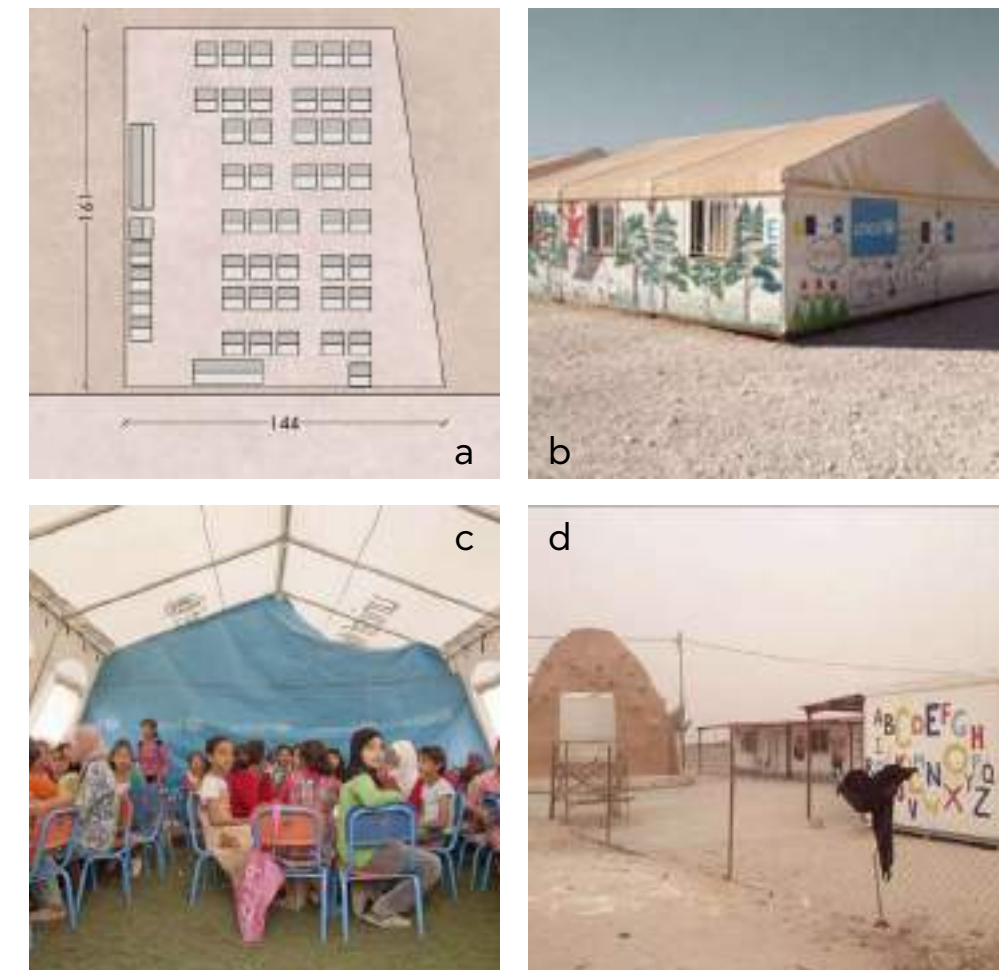


Another reason behind the low rate of attendance could be the kids lack of motivation. The existing schools are made out of drab looking containers, that are no different than the existing housing containers. New school designs that would appeal to the kids taste and attract their attention would be a creative solution.

In addition to their lack of appeal, current school do not have a designated play space (figure 7a). Looking at the map and satellite photos, only some schools are in the proximity of an independent separate sports field, and they only have some empty space in between the containers creating the schools. Therefore newly designed schools must house in a designated playground.

Last but not least, the low rate of enrolment could be due to the shortage of adequate quantity, quality and size of the available schools. Therefore, a study was conducted to identify the areas where there is no school within 400 meter distance, in link with the percentage of unenrolled students per district. Two types of interventions were introduced; upgrade, and addition. Schools that only need a quality improvement, would receive an upgrade intervention, whereas a new school construction project will be provided to locations without any schools within close proximity.

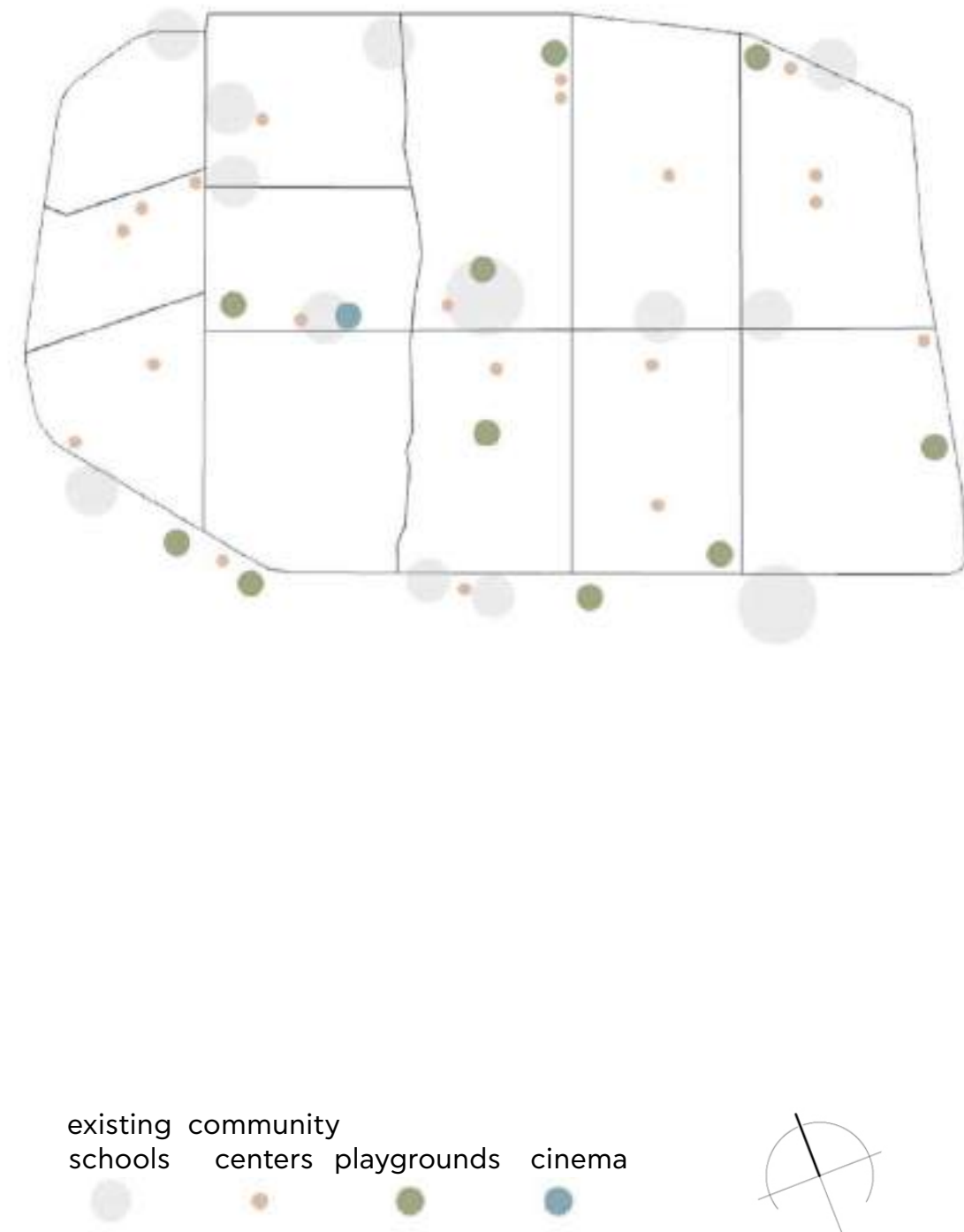
Figure 7 | a. plan of school on camp
 b. exterior view of school (Graham Brown, 2013)
 c. interior view of school ("Future Learning Space," 2015)
 d. exterior view of school ("Field Ready | Post," 2017)



As can be seen in Figure 8 there is a need for communal spaces for activities. The map shows few communal facilities and playgrounds, that are not in a 400m proximity of all planned and existing schools. Schools however, often make use of extra curricular activity rooms. If some schools could accommodate a multifunctional room this could satisfy both the students and the community's needs, through efficient space utilization and organizational flexibility.

0 100 200 500 1000 (m)

Figure 8 | Map of existing schools, community centers, and playgrounds



By now, the need for schools is clear; however, where would the teachers be brought from? How would the addition of these schools fit in and have an impact on the social and employment structure? As mentioned above 15.3% of the refugees have work permits, while the total unemployment mounts upto 35%. According to statistics there is a significant amount of the unemployed refugees that are educated or somehow qualified. Creating schools would create jobs to the educated unemployed population. A social structure cycle would be created by creating more schools (figure 9). Today's pupils would form the new generation of educated and skilled individuals of the camp and would become the future teachers or builders of schools. (Ledwith, 2014)

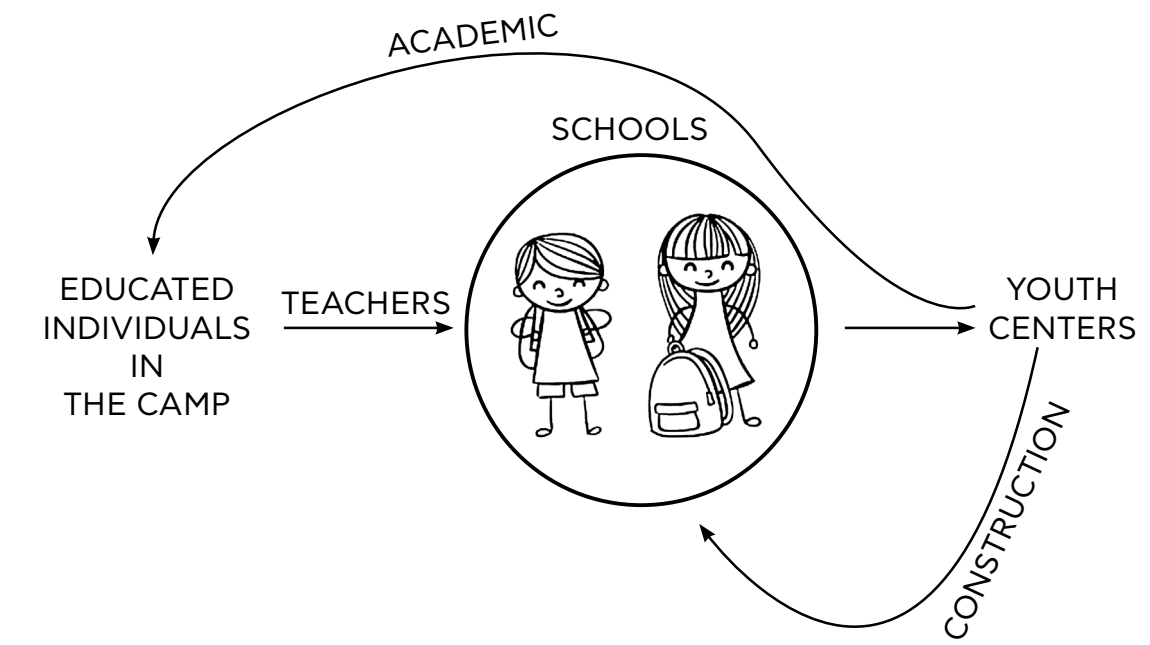


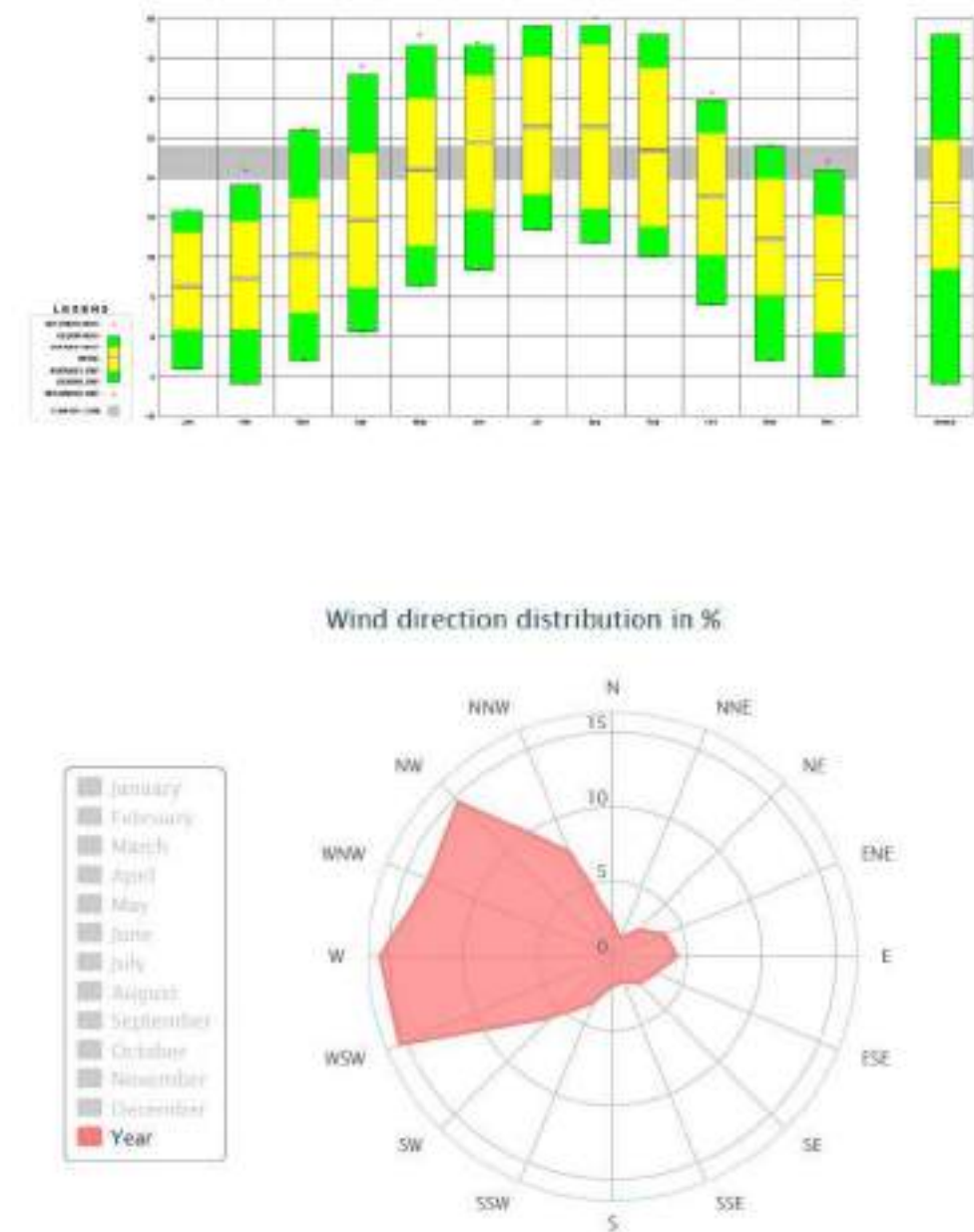
Figure 9 | Social structure diagram after adding schools

Jordan has a dry and hot climate. The place where the Zaatri camp is located, can be categorized as desert. Annually, the average temperature ranges between 6-26°C (Ligget et al., 2018) (figure 10). Wind speed averages between 2 and 4 Bft annually, with the prevailing winds coming from the west (Windfinder, 2019) (figure 11). Zaatri Camp gets 189 mm of rainfall annually. (SamSamWater Foundation, 2018) Additional information about the climate can be found in Appendix A. This climate is ideal for earthy buildings, because of its low humidity. (Ligget et al., 2018) Due to the use of their thermal mass, earthy buildings can create cool interiors, which are much needed in this climate.

In this project, it was crucial that the designs for the schools would be adapted to the climate. By using central courtyards, controlling the orientation of rooms, and mindfully placing the openings, eventually the architectural expression of the building could result in a very comfortable environment.

Figure 10 | Chart of annual average temperatures (Ligget et al., 2018)

Figure 11 | Annual windrose of Amman airport (Windfinder, 2019)



The soil around the Al Zaatri camp is quite untypical for a place in the desert, since it contains on average only 20% of fine sand. The soil composition shown in Figure 12, is an average of four separate measurements all done in the direct area of the camp. The reason why the soil is not really desert like, is probably because the camp is situated near an old river bedding. This river dried out over the past years, but if it has flowed for thousands of years, it is likely that it left a lot of settlement behind in the area, causing the high percentages of clay and silt in the soil.

Looking to the soil composition on a larger scale shows that the camp is situated in an area where the desert slowly turns into a landscape with more vegetation. Moving north and west, are the fertile landscapes of southern Syria and the Jordan Valley. This fertility could be declared by looking into the soil composition of the area. Figures 13-15 show respectively the percentage of sand, clay and silt in the large surroundings of the camp, at a depth of 30 centimeters.

One may notice that the further east you go, the more desert like the landscape becomes. The percentage of fine sand in the soil rises towards 80% and the presence of clay and silt become very minimal. It is worth mentioning, that the Al Zaatri camp is situated in an area with a relative high amount of silt, compared to its surroundings. This could almost only be declared by assuming that there must have been much more water in that area than there is present at this moment.

Figure 12 | Soil composition
(Tomislav Hengl, Jorge Samuel
Mendes de Jesus, 2019)

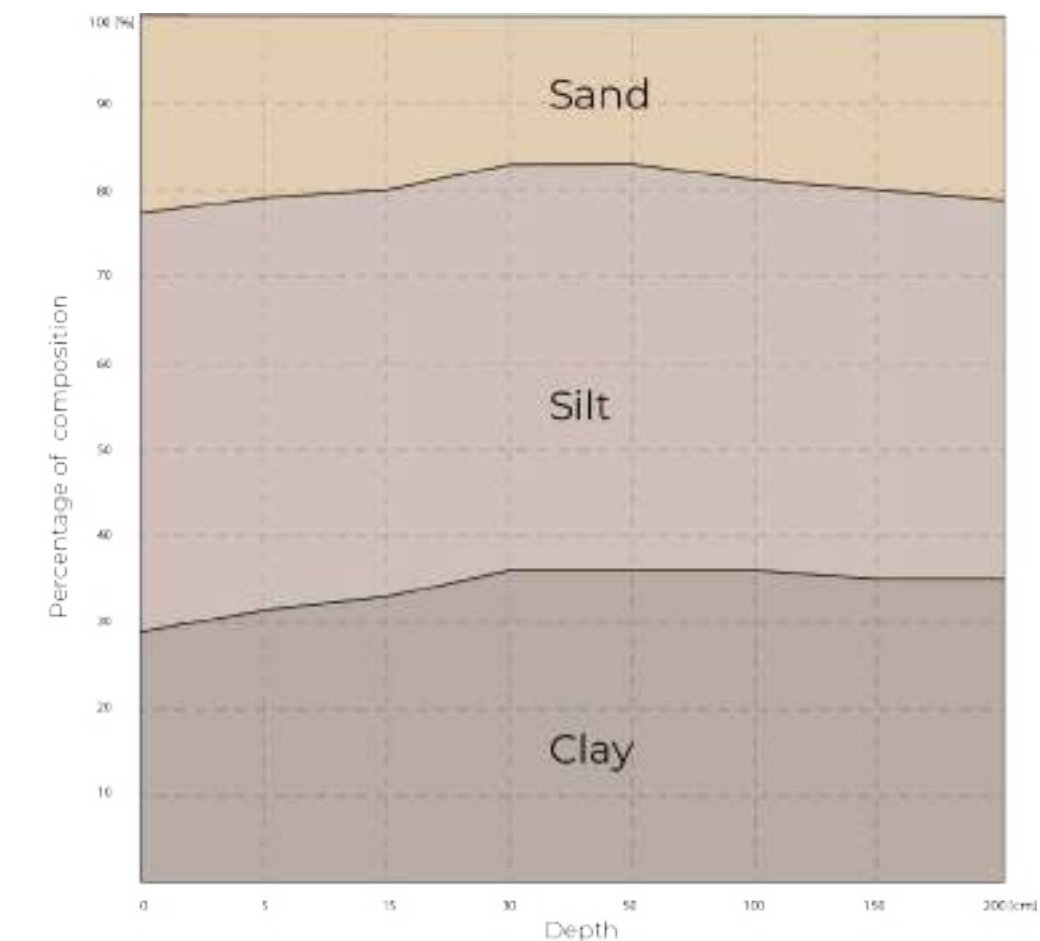




Figure 13
SAND

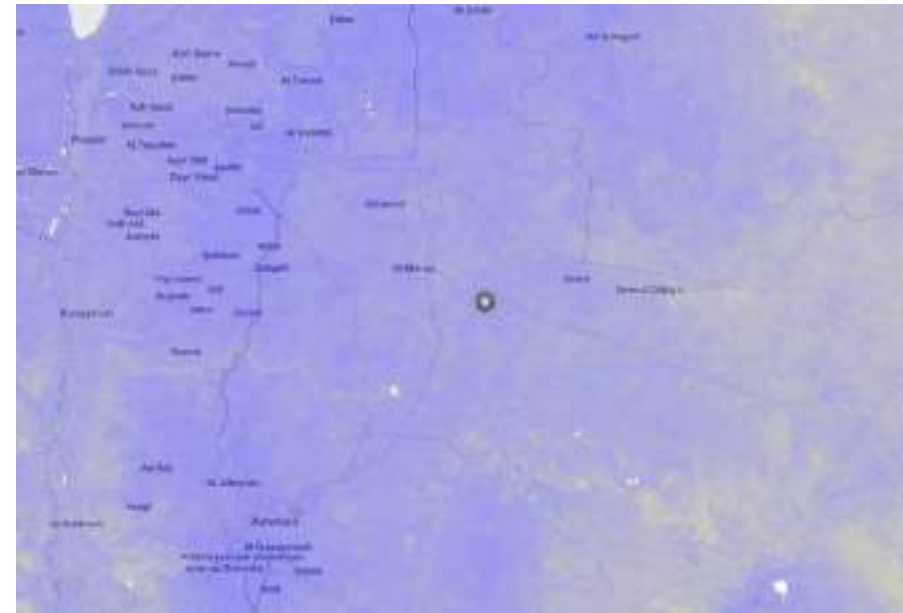
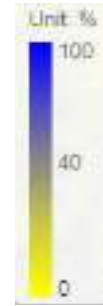


Figure 14
CLAY

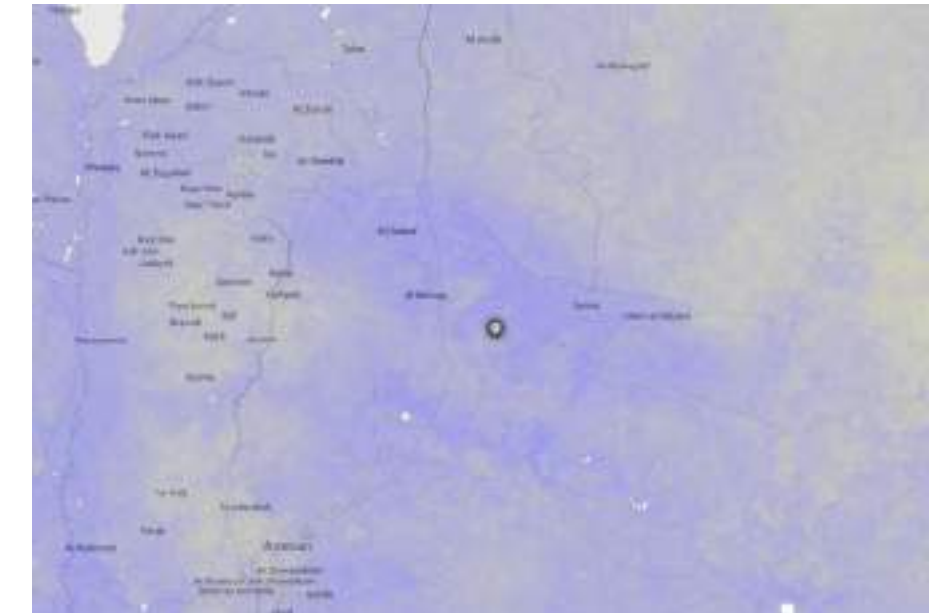
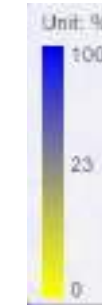


Figure 15
SILT



Figure 13-15 | Soil composition
(Tomislav Hengl, Jorge Samuel
Mendes de Jesus, 2019)

This project followed a customized version of the commonly known engineering design process or cycle. The simplest engineering design process starts with analysing the problem and researching the needs and constraints. Afterwards, a variety of alternative possible solutions are generated. The best solution is elaborated into a detailed design. The results are prototyped, evaluated and tested. At the end the design is refined and based on the evaluation. Then it is reevaluated and the cycle is repeated. Research and design are intertwined throughout the process (Strimel, 2014; van Dooren, 2013)

For this project the process was planned beforehand, yet adapted to the circumstantial changes while in progress. This global flowchart describes the process of this project. The process can be identified by 6 main stages (figures 16, 17). Research and urban analysis, Urban configuration, architectural layout configuration, form finding, structural verification, and construction methodology.

Research and urban analysis started with gathering information and data from reports, maps, news articles, interviews, and previous research. This lead to identifying the missing connections, facilities, buildings, supply and current demand in the camp. It also recognized the proximity of communal facilities, and amount of unenrolled children per district. This phase resulted in a master plan document

with a list of requirements in every district.

Urban configuration used a grasshopper algorithm that grouped every 100 unenrolled students into clusters within each district. These lead to an urban plan with all school related interventions; schools in need for an upgrade, and the locations of the new required schools.

Architectural layout configuration phase focused on designing the new school projects. The process took as an input the master plan of the camp including the new locations for schools, the proximity between the project location and other communal facilities, and the number of unenrolled children.

Research was conducted for input about general requirements of a school facility. A list of the functional rooms, the min LUX requirement, minimum height, minimum floor area, and recommended orientation and accessibility were defined. A relationship (REL) chart between the different rooms was made to determine which room had to be close and easily accessible via which room. This was finally translated into a justified bubble diagram that combined the floor area with the connections to other rooms.

The program of requirements of each school was customized based on the proximity between the project location and other communal facilities, and the number of unenrolled

children within 400m. The most elaborate program of requirements (Priority 3) was chosen to be detailed. The 2D bubble diagram was translated into a 3D volumetric and mass configuration study using LEGO. Schematic floor plans were generated and later refined using grasshopper and python scripts. The final meshed floor plan is sent to form finding.

Form finding processed the floor plan meshed into a relaxed compression shape. This phase tessellates the meshes, which affects the final shape and route of forces transfer. The tessellated and refined meshes were welded into other meshes that had to be connected for a smoother shape. Those were dynamically relaxed using kangaroo mimicking Antoni Gaudi's method of the catenary chained curves computationally. These resulted theoretically in a compression only structure form, however it had to be verified.

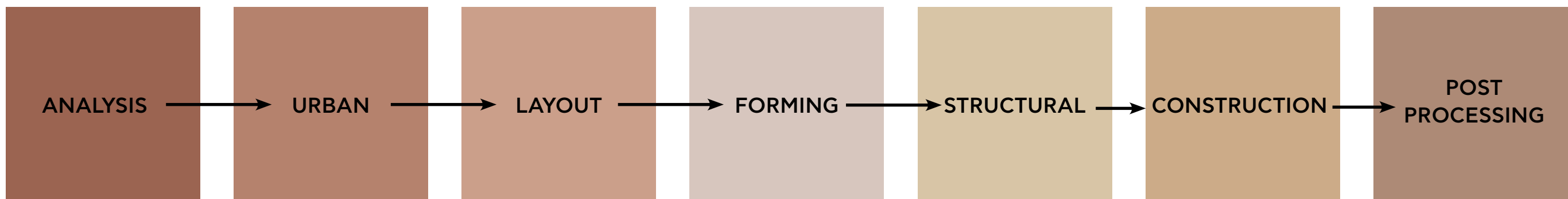
Structural verification was the processing step that ensured that the structure would pass all structural safety requirements given the assigned material, dimensions, and

after applying possible external horizontal and vertical forces. In this step the structure was tested whether it would be free from tension forces even after maximum deformation and force line eccentricities. If the structure did not pass the evaluation the design process went back to the form finding phase for redesign. Then again retested. This back and forth cycle between form finding and structural verification kept looping until a success alternative was found.

Construction methodology. In this stage bricklaying pattern and bonds were chosen. A construction manual was made. A bricklaying script was generated to enclose the surfaces. In some cases the design was retaken back to the form finding to match the bricklaying pattern chosen.

Post processing: For presentation purposes, floor plans and section views were annotated, renders and walk through impressions were generated. The final product and process were evaluated, reflected upon and further developments were suggested.

Figure 16 | Block flow chart



6 FLOWCHART

ANALYSIS

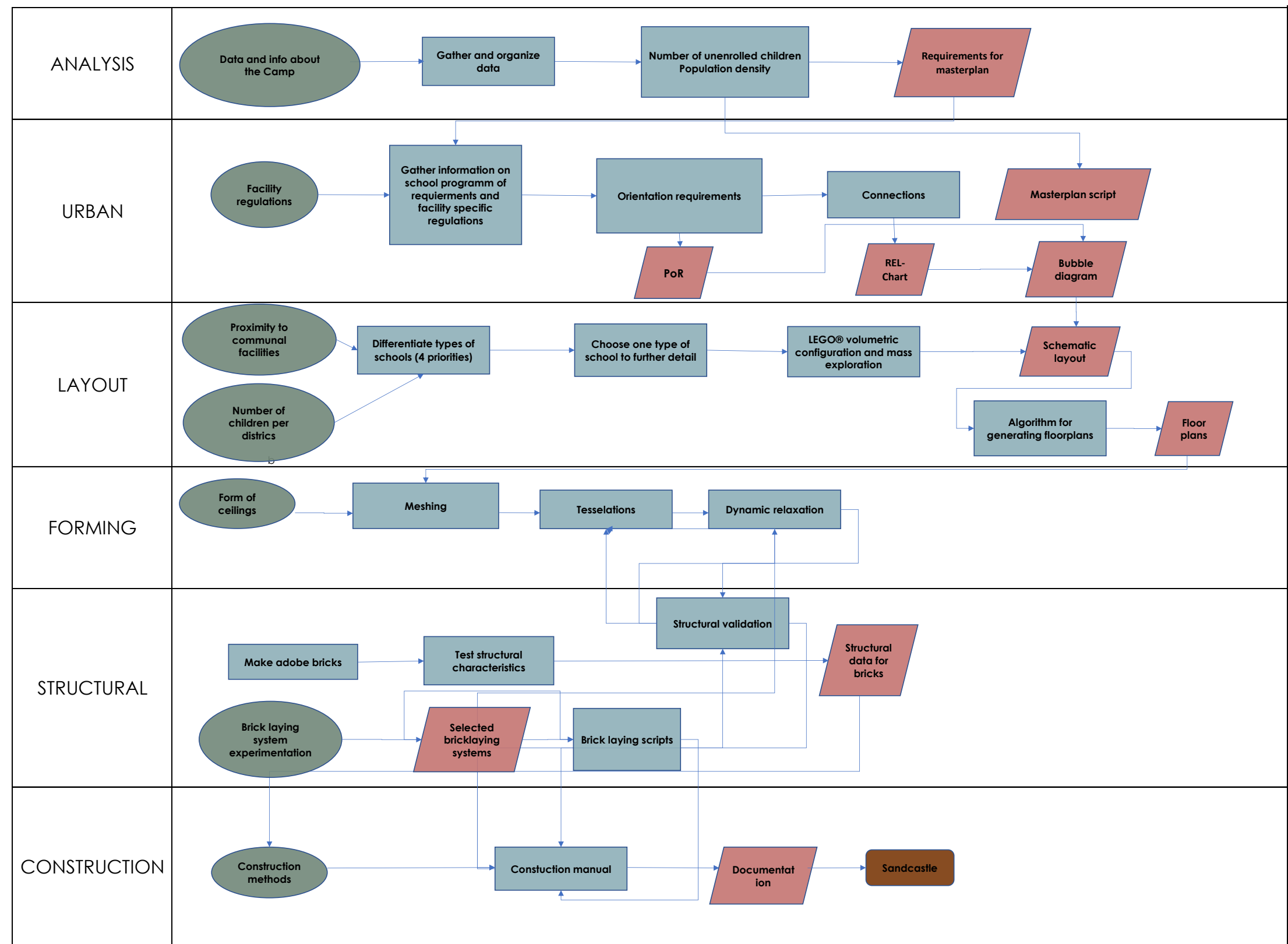


Figure 17 | General Flowchart

2 URBAN CONFIGURATION

To cope with the accessibility issues, the goal was to enhance the existing school network in a way that would eliminate kids from crossing paved streets and would comply with the 5 minute walk restriction. In addition the new schools were to be placed in existing empty location of the camp, to avoid disturbing housing. The two aspects under examination, to determine the new school locations, were child population density and the empty spaces in the camp. Initially, the population of children aged 6-12 was calculated for each district (figures 18-19). In comparison to the density of this age group per district, it was clear that the needs of the camp varied depending on the neighborhood.

CHILD POPULATION

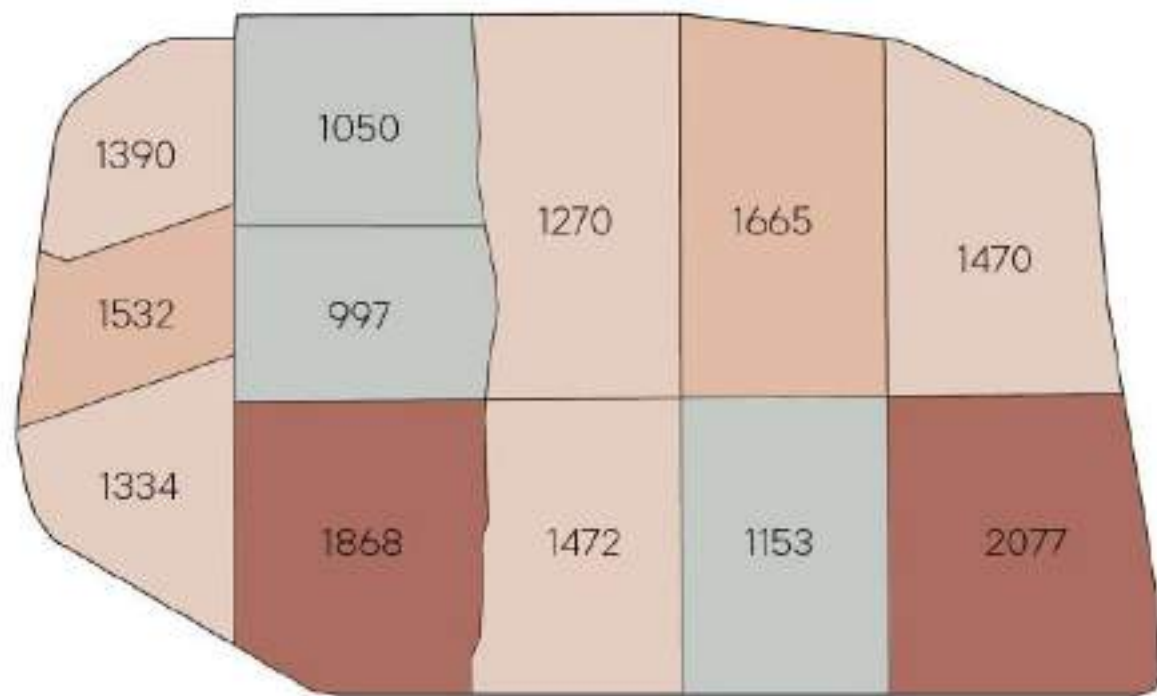


Figure 18 | Map of child population

CHILD DENSITY

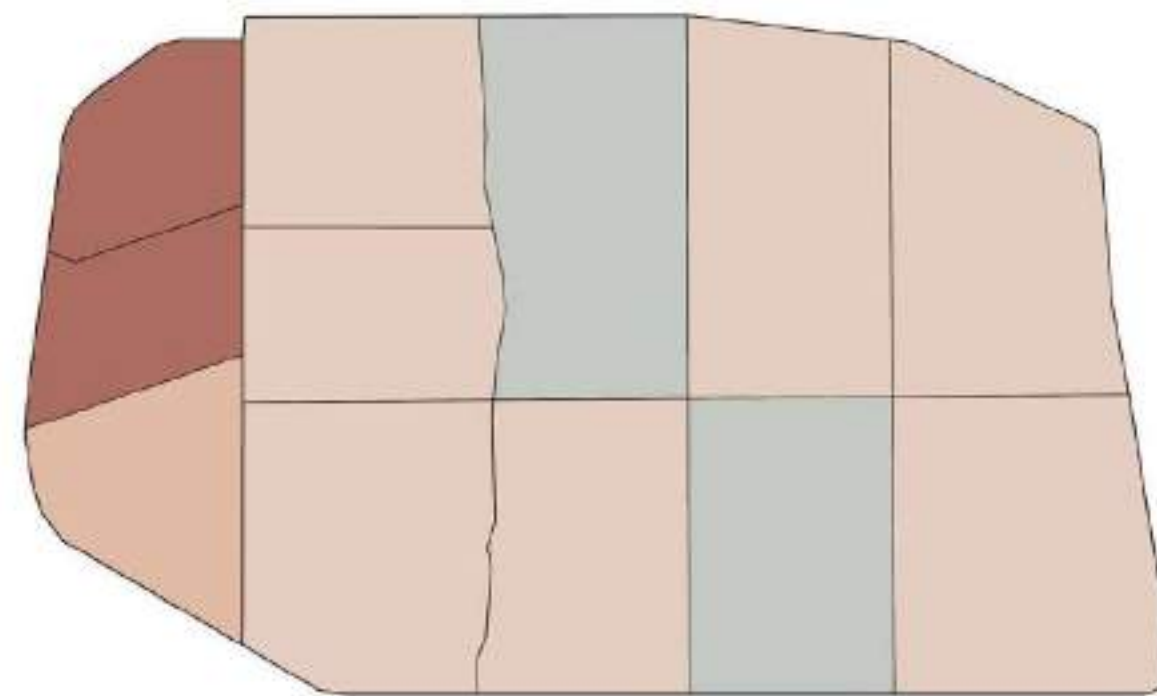
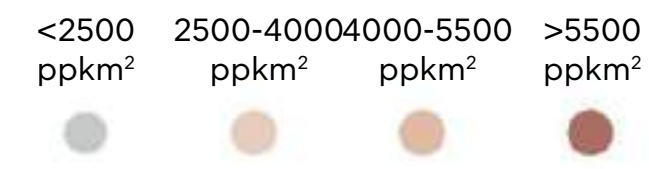


Figure 19 | Map of child desnity



The goal was to divide the districts parts equal to the children living there, gaining perspective on the population density. As the numbers were in the thousands, instead the districts were partitioned in areas representing the hundreds of children. As a result, the numbers were divided by 100, and then rounded up to the nearest integer. Having obtained the number of partitions per district, the voronoi diagram was used for the tessellation, combined with a galapagos optimization that ensured all areas within a district were approximately equal. Each centroid of these subdivisions, represented 100 children (figure 20).

These points were to be clustered into groups that would be accommodated by the same school. To reduce the amount of new facilities, the schools were to have two shifts: a morning and an evening one. Such an approach would also facilitate the separation of girls and boys, which is common in the local culture. A school serving over 200 children in one shift seemed excessive and under 100 seemed too little, so taking into consideration the double shifts, the points were to be clustered in groups of 2,3, or 4 points. The second limitation of clustering, which was adjusted manually, was that the clusters should not cross over paved streets, because the traffic is too dangerous for children walking to school. By applying K-means clustering and some minor manual adjustments, the groups of Figure 21 occurred.

DENSITY POINTS

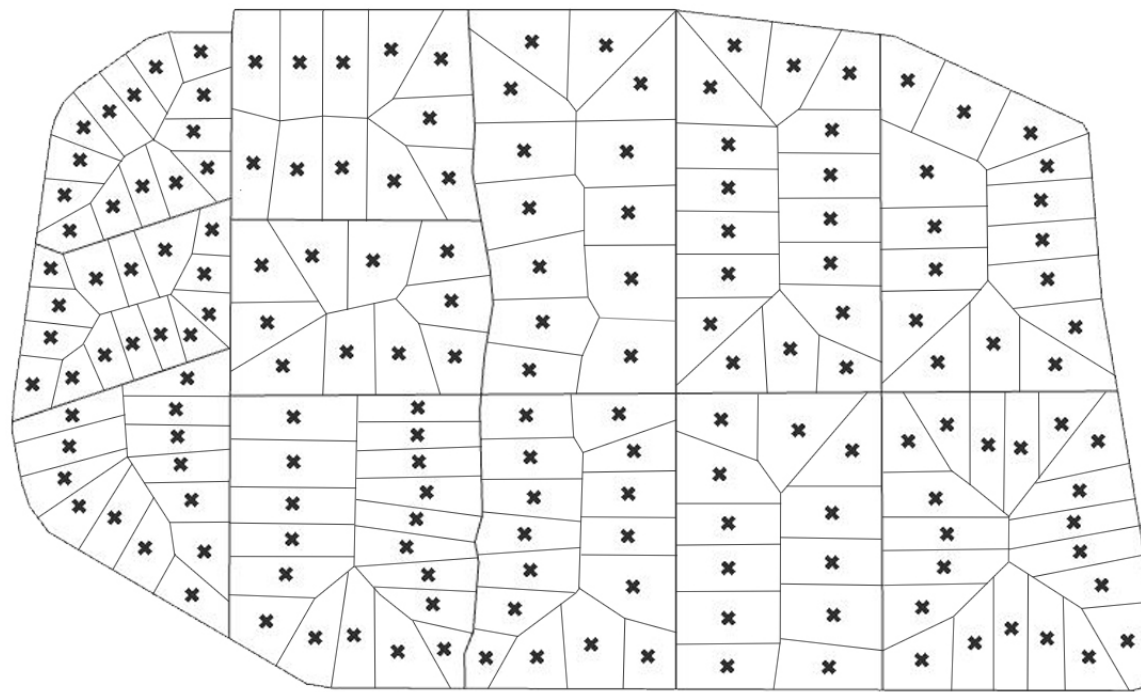


Figure 20 | Map of child population

CLUSTERS

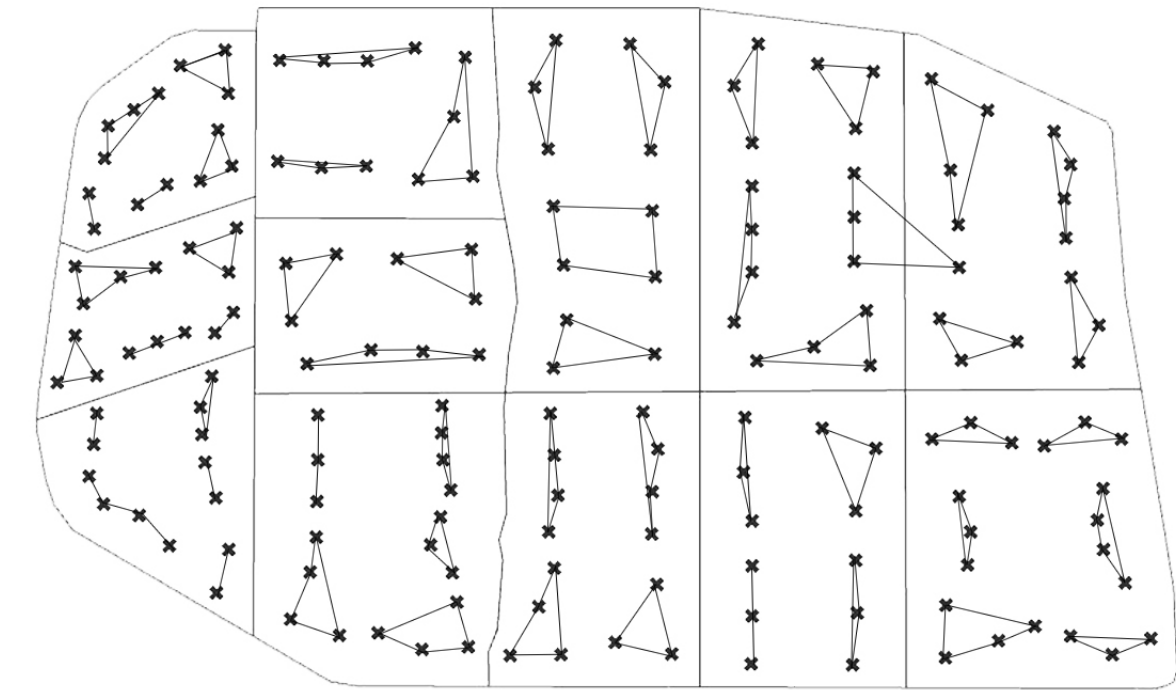


Figure 21 | Map of clusters

0 100 200 500 1000 (m)

100 children clusterings



In order to minimize interference with the existing facilities, it was decided that the new schools would only be placed in areas of the camp that are currently empty. Ideally, those would not fall within the center of a district, to leave housing undisturbed. By using the image sampler on an image of the map, those areas were easily unveiled. The image used was a black and white depiction of the occupied and free spaces on camp (black for occupied and white for empty). When a white area was detected, the point would be lifted higher than the rest, as can be seen in Figure 22. From the entire camp, the greatest challenge was located in districts 1 and 2, as no available empty spaces were identified (figures 23, 24).

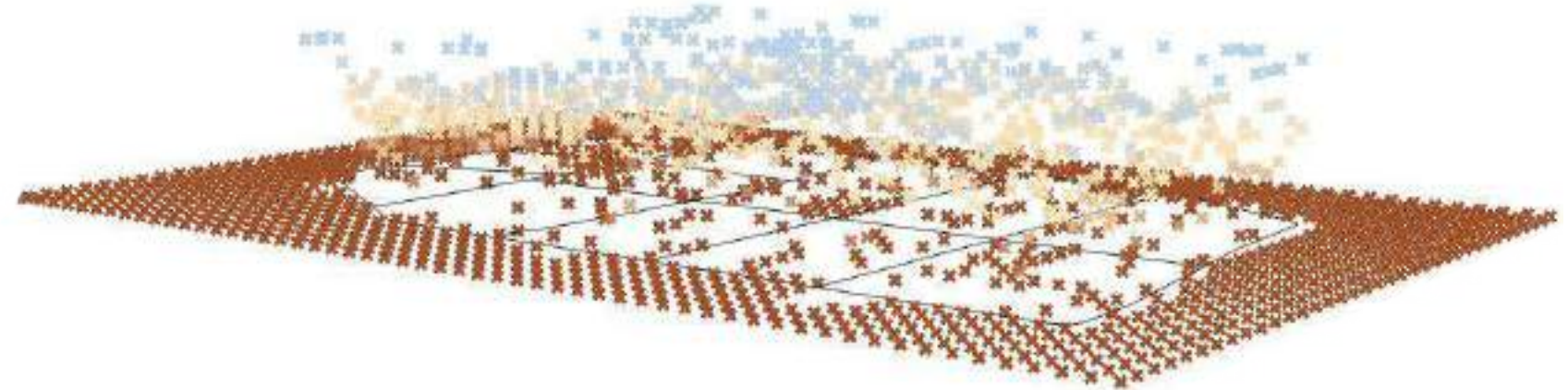


Figure 22 | General Flowchart



SPACE AVAILABILITY

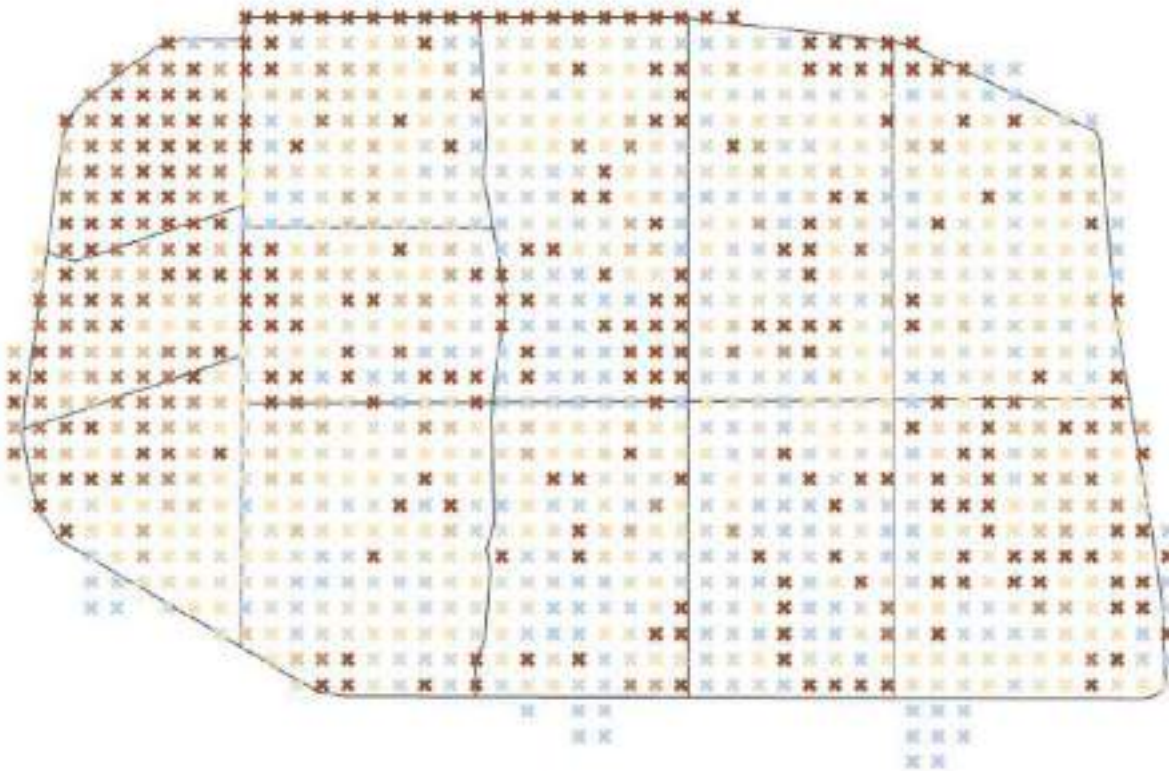


Figure 23 | Map space availability

EMPTY SPACES

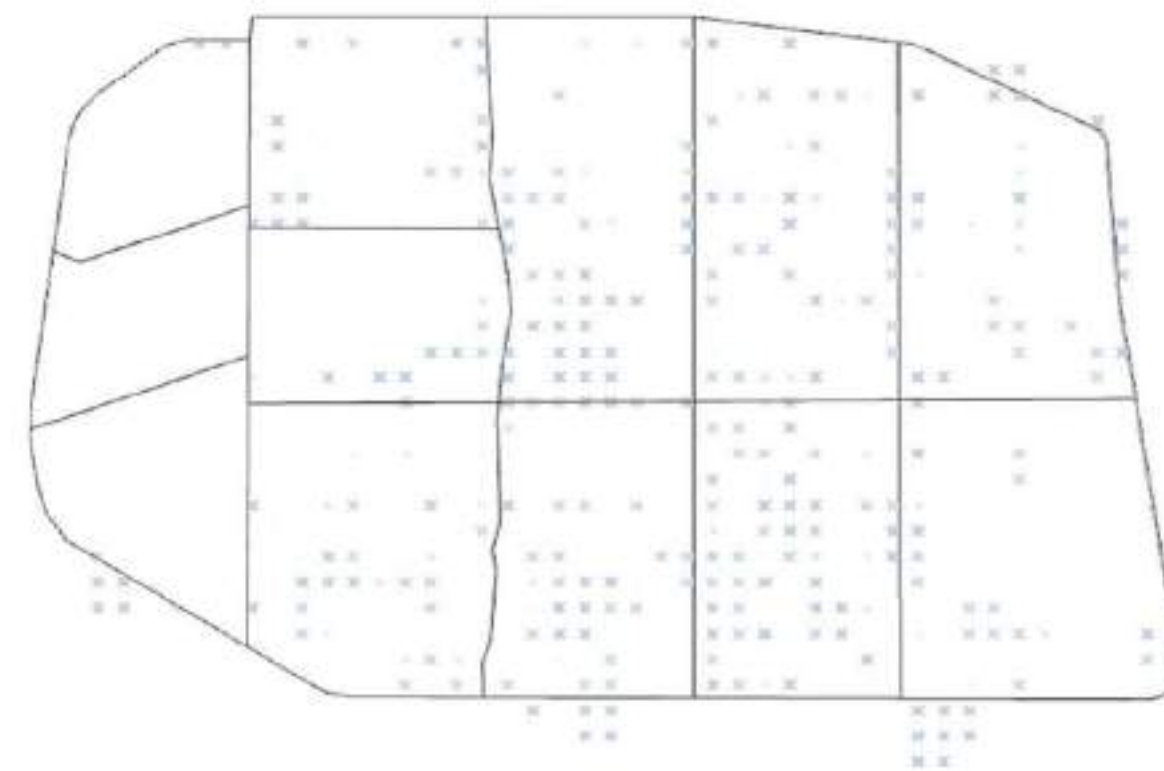


Figure 24 | Map of empty spaces



By combining the above information, the school locations could be defined. First, the clusters that could be accommodated from the existing schools were chosen (figure 25). Then, the new schools were placed in the nearest empty spaces to each cluster. Although the procedure ran smoothly for most districts, as mentioned above, district 1 and 2 were more challenging. To minimize interference, school placement was approached slightly differently. Some of the new schools were placed on the border of the camp, like certain existing schools in the South are. Then, as the existing school grounds bordering districts 1 and 2 are quite large (approximately 7000m² each), it was decided that they could co-host two schools. Finally, left within the district were only new schools accommodating the least amount of children (100 per shift), in other words the smallest possible facility (figure 26). Despite the density of the districts, after looking closer, certain empty plots were found, so the new schools are not considered a major disturbance.

EXISTING SCHOOLS

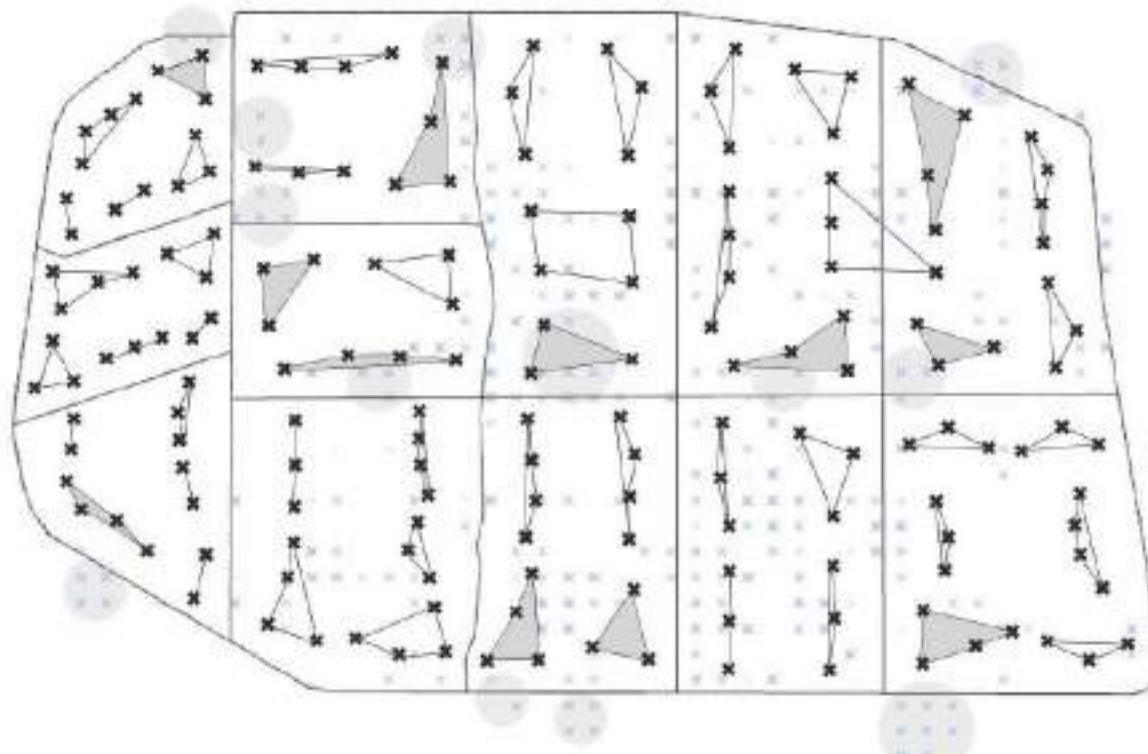


Figure 25 | Map of clusters accommodated by existing schools

NEW SCHOOLS

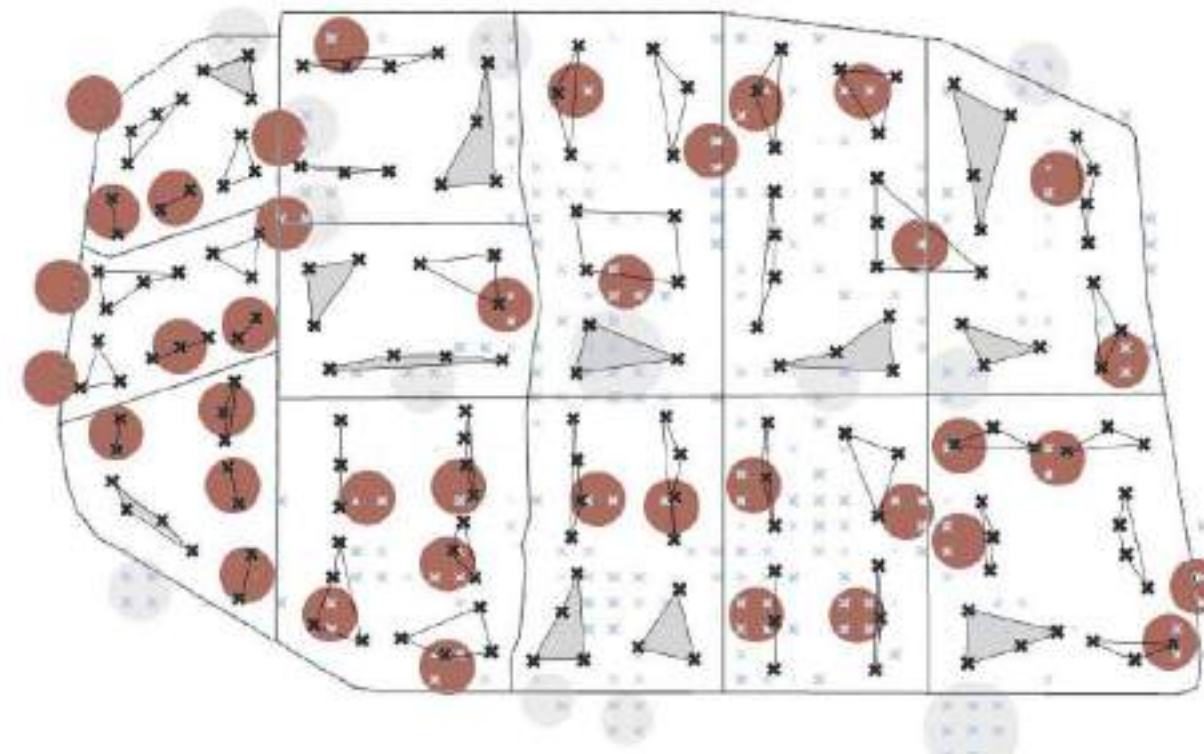
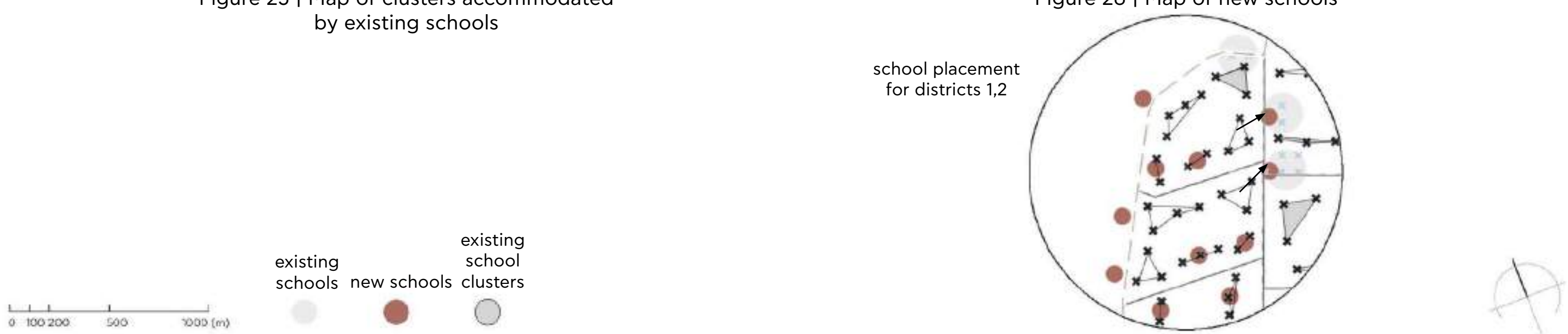


Figure 26 | Map of new schools



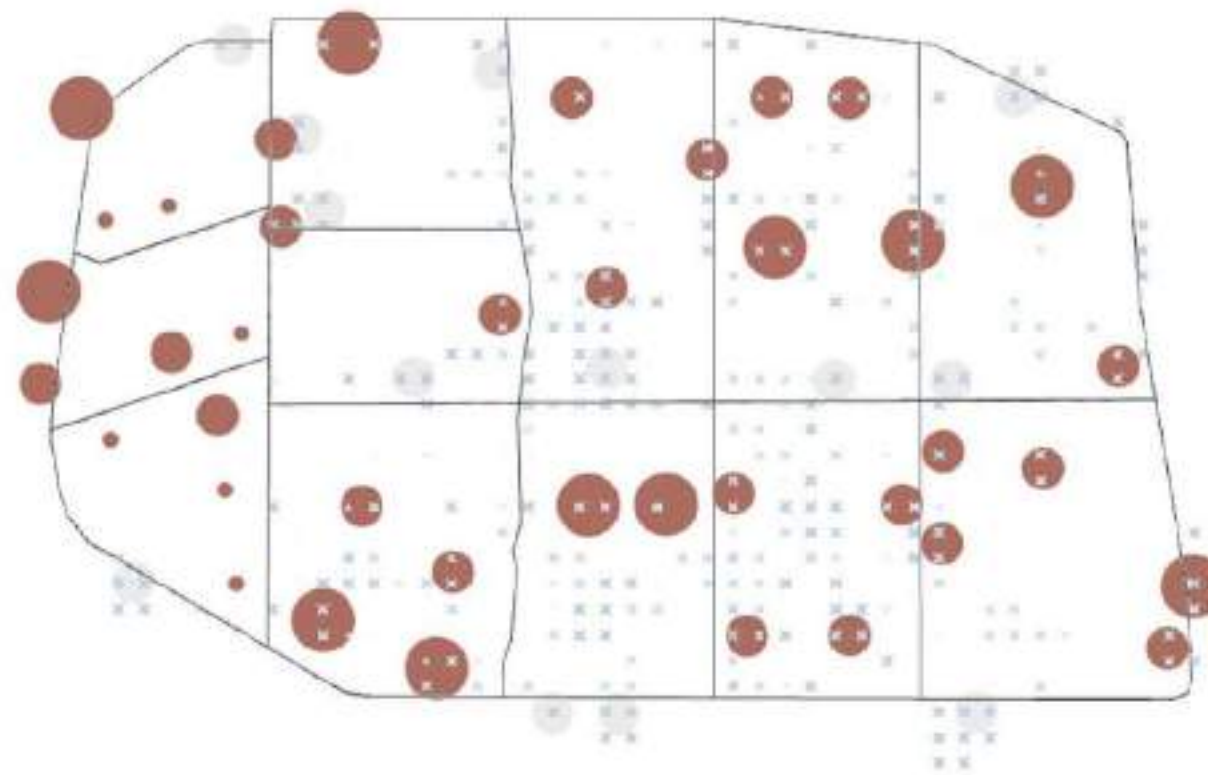


Figure 27 | Map of masterplan

The described process, resulted in a strong school network, capable of accommodating all the children in the camp. The new schools vary in size (small, medium, big), depending on the amount of children they account for. From the initial amount of 13 schools, the final master plan includes a total of 52 schools (39 new), easily accessible by everyone in the camp (figure 27).



3 LAYOUT CONFIGURATION

Since each district has different needs, and conditions, a flowchart algorithm was constructed to customize the program of requirements (PoR) of each school (see Appendix C). The main determining factors of the school's PoR are the number of unenrolled children, and proximity to other facilities. This set up lead to 3 main priority school types. (figure 28, Appendix D)

First is the amount of children is calculated, and divided into two shifts (morning and evening). Based on that each class room will accommodate 30 pupils, the number of required classrooms is calculated.

Priority 0 If the number of classrooms needed is less than 2, then an upgrade to an existing school will take place and no new school will be needed.

Priority 1 If the amount of required classrooms is between 2 and 4, the following basic functional areas will be included in the PoR: classrooms, Restrooms, teacher rooms, Court yard, Gallery, and entrance.

Classrooms: Based on the number of unenrolled children per district, the amount of classrooms is calculated per school. Each class room will accommodate 30 pupils in a minimum floor plan area of 45 square meters ($1.5m^2$ per person).

All class rooms were initially placed in one cluster, later on they got split into two. This had an influence on the

Bubble diagram, REL chart, and eventually the floorplan configuration. The separation would give more privacy to the younger students and create a safer environment for them away from the older kids. This has a larger impact when the school is large.

Courtyards: Splitting the classrooms into two clusters was accompanied by creating two courtyards instead of one. Courtyards size is proportional to the peripheral rooms surrounding it. The courtyard is always in the center and is open air. If the school is too small, both courtyards get merged into one. This has a larger impact when the school is large.

Teachers lounge: This room is designated as a resting area for teachers, but it could include some desks in addition to sofas for teacher to use in preparation for classes.

Entrance: Since the Castle has one entrance, this entrance need to be glamorous, big and beautiful. The entrance should be inviting yet give the vibe of a defence line. Everyone inside this castle is important and protected behind these walls

Restrooms: Restrooms will be split based on gender and separate staff from students.

Galleries: These are covered passages open at the one side facing the courtyards, making for a pleasant semi-open space to spend time in.

Priority 2 If the amount of required classrooms is between 4 and 6, a multi functional room and storage area are added to the PoR of priority 1. This multifunctional room is made either private or public depending on the distance to the closest communal facility in the area. If the proximity is less than 100m, the room is made private, while if it is further than a 100m the room is made public.

Multifunctional room: This room is meant to host music, art, drama and gym courses along any other extra curricular activities. This room can host parents-teachers meeting days and teacher workshops. It will be available to rent by other community organizations or groups to host their events. Therefore it should be close to the main entrance for easy access by the public.

Storage: This will store chairs and tables for the multi-functional room. It might also store audio, video, music instruments and equipment. Art and theatre material can be placed there as well.

Priority 3 If the amount of required classrooms is between 6 and 8, an administration room, a Liwan, a canteen and a kitchen is added to the PoR of priority 1 and 2. The same rule described under priority 2 conditions, applies to the multifunctional room here. If the closest communal library in the

surrounding area is less than 100m away, no library is added. But if the closest library is further than 100m away, a communal library is added to the school's program of requirements.

Administration offices: The administration will have offices. Any division between the offices can be done via curtains or asian accordion partition walls.

Canteen and Kitchen: The canteen is more like a kiosk for events and teachers. The multi functional room can host eating tables if needed. Students are expected to bring food from home, and therefore this canteen is not expected to feed the students daily. The Kitchen needs a logistics point to get things in and out. Therefore it is located on the wall of the castle. These are also in close proximity to the multi-functional room

Liwan: Is a semi-open lounge; it is closed from one side, yet open to the courtyard from the other side. This lounge is cool because it is open air but yet shaded from the sun. Its south positioning (northern-orientation) is crucial for its thermal comfort. The Liwan has a minimum double story free height of 5400mm. This has been designed to face an amphitheater shaped courtyard. The courtyard with the amphitheatre steps can be used to sit on for eating lunch, space to play during school recess. But it can also be used as seats to watch the Liwan when functioning as an open air stage.

Winter living room: This is a lounge for the recess during winter. It is oriented north of courtyard. This means that the sun hits it from the south

Library: The library has two stories, on the ground floor the library and on the top floor a reading area. The Library is only made public outside of school hours.

This is the complete list of functional areas present in Priority 3: Classrooms, a multifunctional, a communal library, restrooms, courtyards, canteen, kitchen, teachers lounge, administration offices, entrance, storage, liwan, and a winter living room. Each of these functions proximity, and routing relation to the other was specified. Other specified properties were the orientation, minimum surface area, and light requirements. Please look at the table of PoR (Appendix B).

This project further developed a Priority 3 design that has 7 class rooms. Each class room will accommodate 30 pupils in a minimum floor plan area of 45 square meters ($1.5m^2$ per person). This means the school will host about 400 students in both evening and morning shifts (200 students per shift).

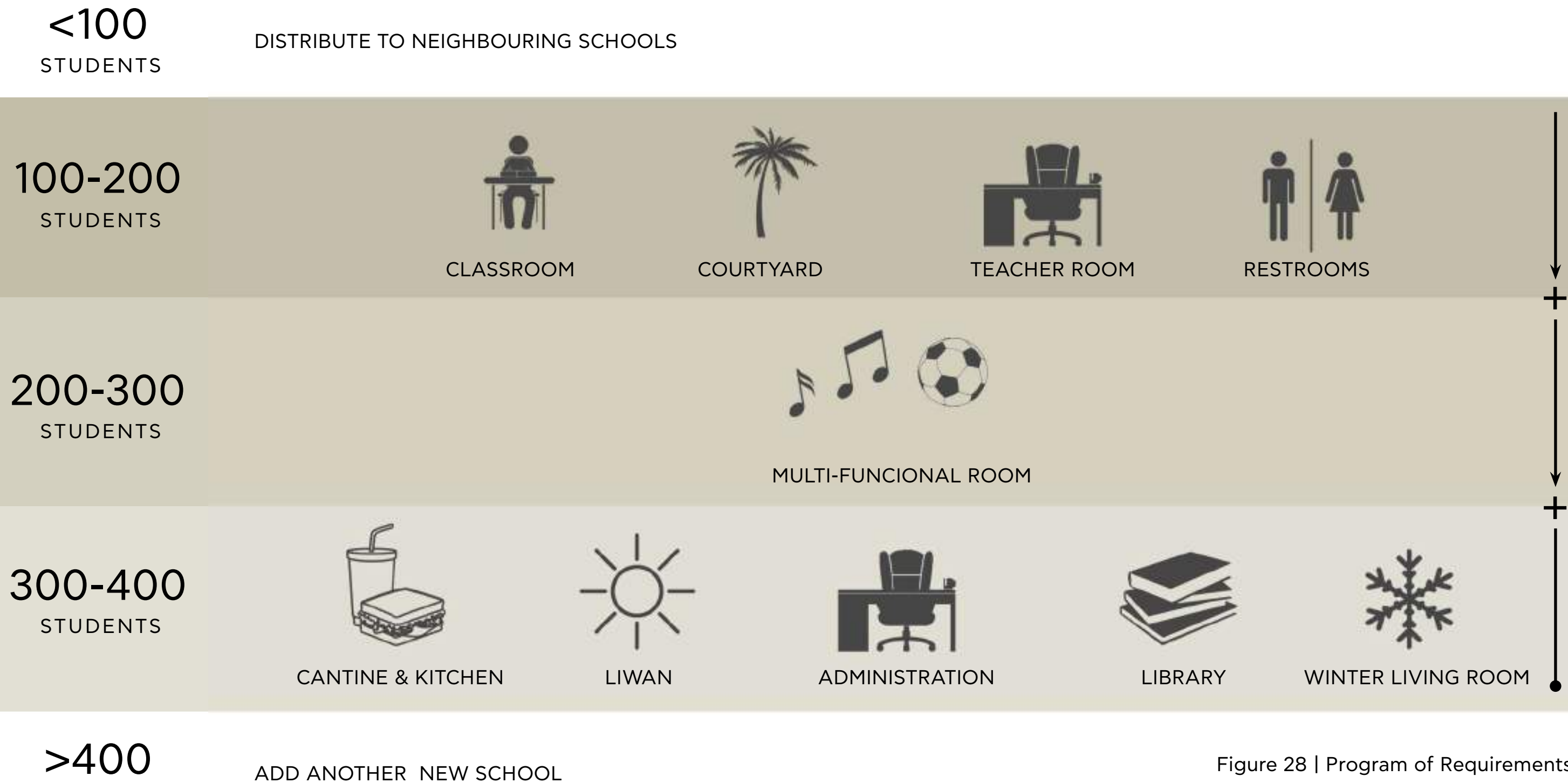


Figure 28 | Program of Requirements

The first idea, inspired by vernacular architecture, was to create a courtyard school. Such an approach, when combined with a single entrance, would ensure the feeling of safety, while also being a pleasant familiar space.

The reasoning for using such a configuration in vernacular desert architecture, lies in climate related issues. The courtyard often includes a fountain and vegetation, to create a more comfortable climate, through evaporative cooling. In addition, the courtyard enables wind circulation of the hot air, contributing to the comfort level of the space (figure 29). After a closer analysis of the typical courtyard house, certain additional spaces from the typical house rooms (kitchen, bedrooms etc) were revealed. The liwan and the winter living room are often used in vernacular examples to exaggerate the air circulation effect. These spaces are double heighed and semi-open, facing the north and the south respectively, making for ideal spaces to be in the winter and summer. The double height leads the hot air up and out of the main courtyard area (figure 30).

Figure 29 | Air circulation in courtyard

Figure 30 | Liwan (Retlaw Snellac Photography, n.d.)

Figure 31 | Sabat passage ("Sabat," n.d.)

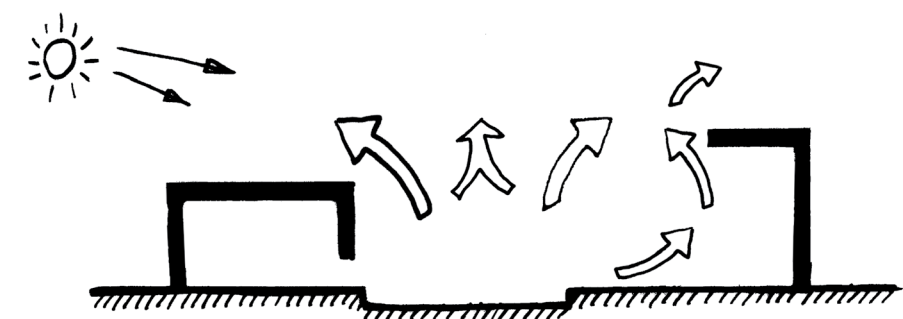


Figure 29



Figure 30



Figure 31

block dust from entering the building. Instead, windows with many small openings are preferred, such as the wooden mashrabiya latticework. This type of shading works very well for a constant ventilation and lighting, without however exposing the interior of the building to outsiders (figure 32).

The combination of all these effects result in a cooler environment which is the main concern in this climate and were talking into account in the configuration of the school.

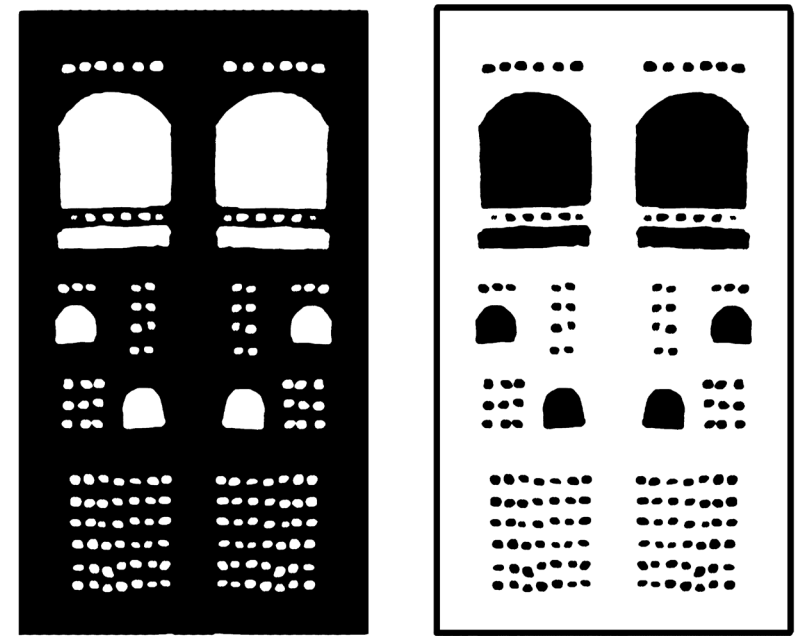


Figure 32 | Mashrabiya windows

Initially the inspiration from vernacular arabic architecture was translated into layout by having one big central courtyard in the middle of the site. The other functions were also placed around the courtyard. More specifically, the classrooms were located on the north-west side of the site, whereas on the east side the multifunctional room was placed to separate the public function from the private function of elementary school. On the south, the entrance and the library were placed in immediate connection to the multifunctional room since they were also part of the cultural center. The liwan was located on the south and the winter living room on the north according to vernacular architecture in order to provide a space with a pleasant temperature during summer (liwan) and winter (winter living room)(figure 33).

To furthermore examine the relations between the different spaces, REL charts and bubble diagrams were made. In the bubble diagram (figure 34) the relationship and the proximity among the rooms is depicted. The magnitude of the bubbles corresponds to the area and the lines refer to immediate connections (through doors). In the justified diagram (figure 35) the different levels of depth are presented. At depth 0 lies the courtyard that is the center of interest. From there, the rest functions are connected (depth 1) and the most private rooms (such as restrooms) belong to the last level of depth.

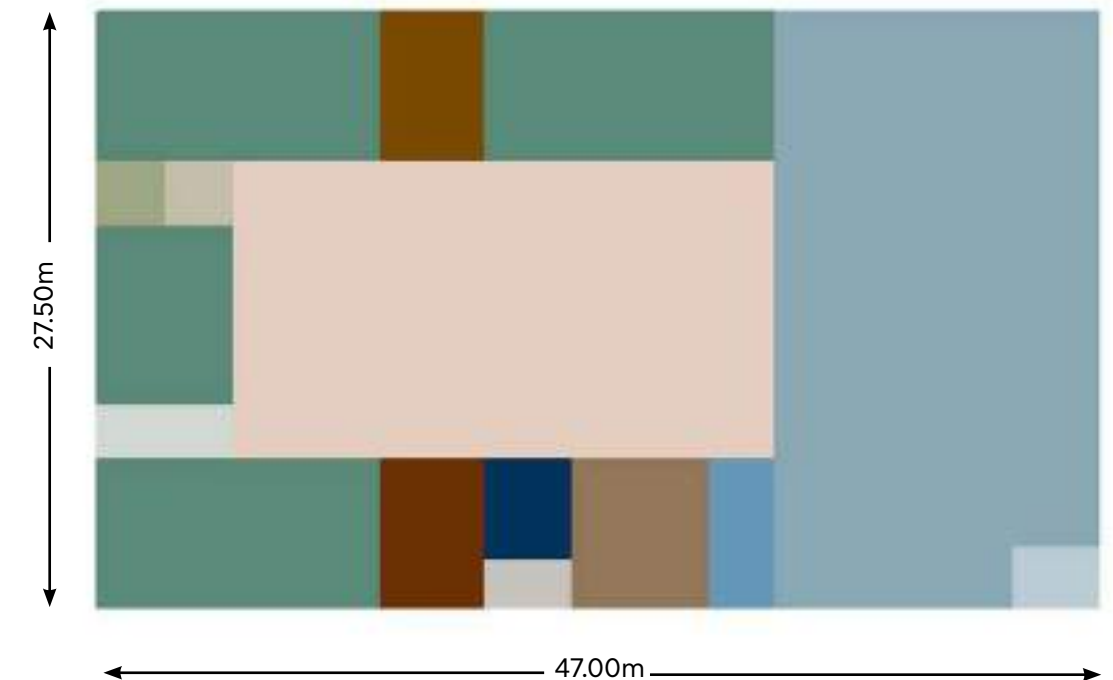
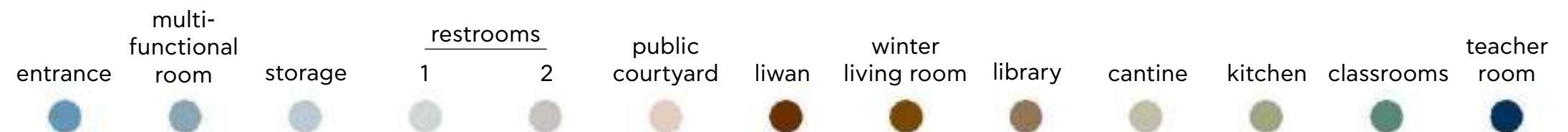


Figure 33 | Courtyard layout



Finally the REL chart (figure 36) expresses the existence of an immediate connection (1) or of no connection (0).

This configuration solved the problem of safety since the building was closed to the outside and there was only one main entrance, controlling the visitors. The playground in the courtyard was visible from everywhere, easing the children's supervision. However, it became clear from the justified graph and the REL chart, that the complexity level was low, leading to certain problems. Although the safety issues had been addressed, the result was too spread out and lacked originality, therefore could not be considered inspiring enough for the children. In addition, the separation of private and public spaces was less successful than intended. Finally, the size of the multifunctional room was way too big and overshadowed the primary purpose of the complex: elementary school. These remarks set off a series of alternative designs with the aim of 'knitting' all the desired results into the ultimate configuration.

B U B B L E D I A G R A M

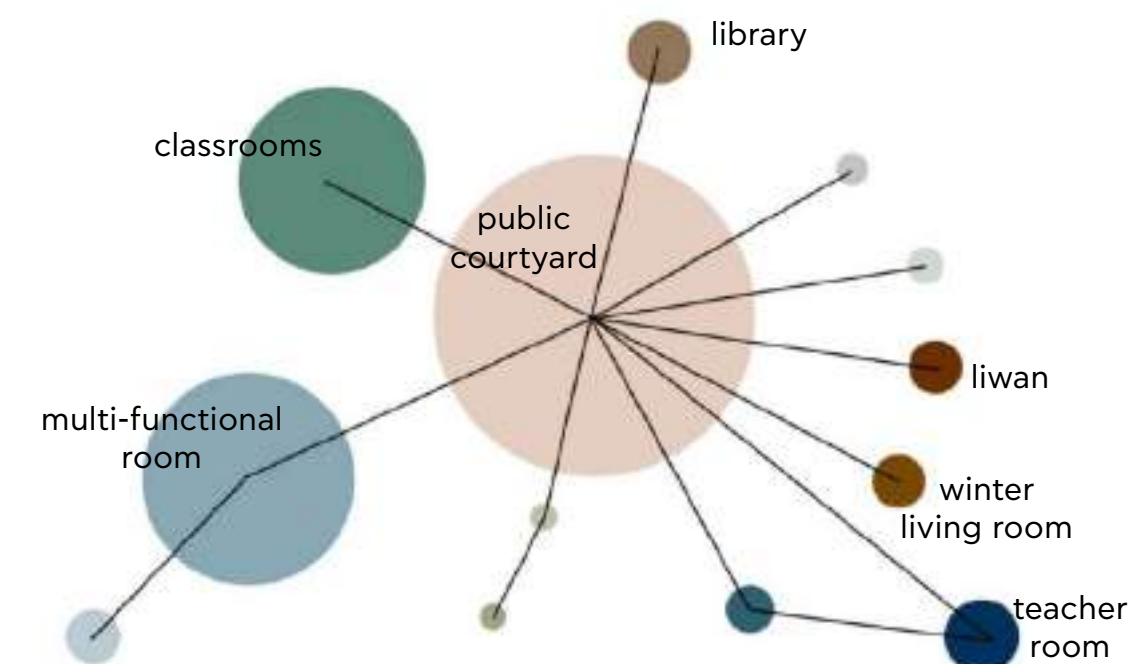
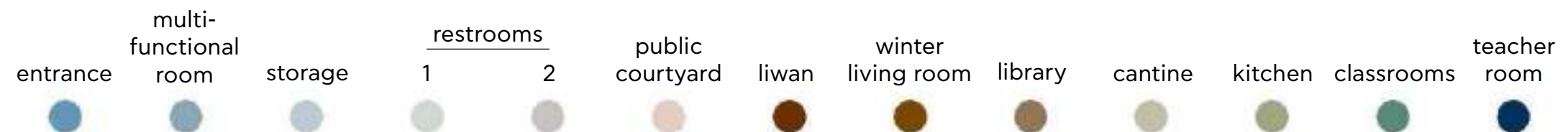


Figure 34 | Bubble Diagram
(Nourian, n.d.)



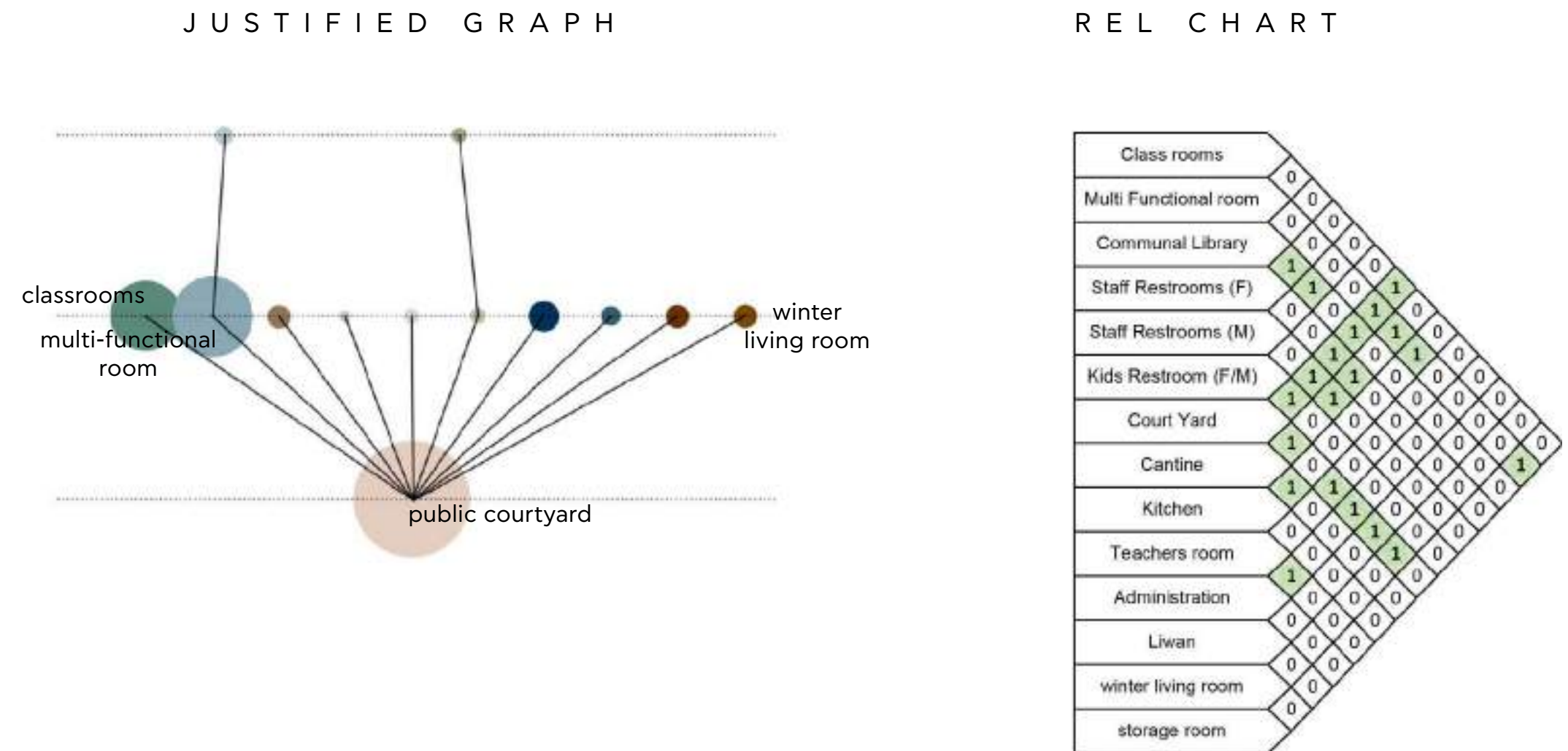


Figure 35 | Justified graph

Figure 36 | REL Chart



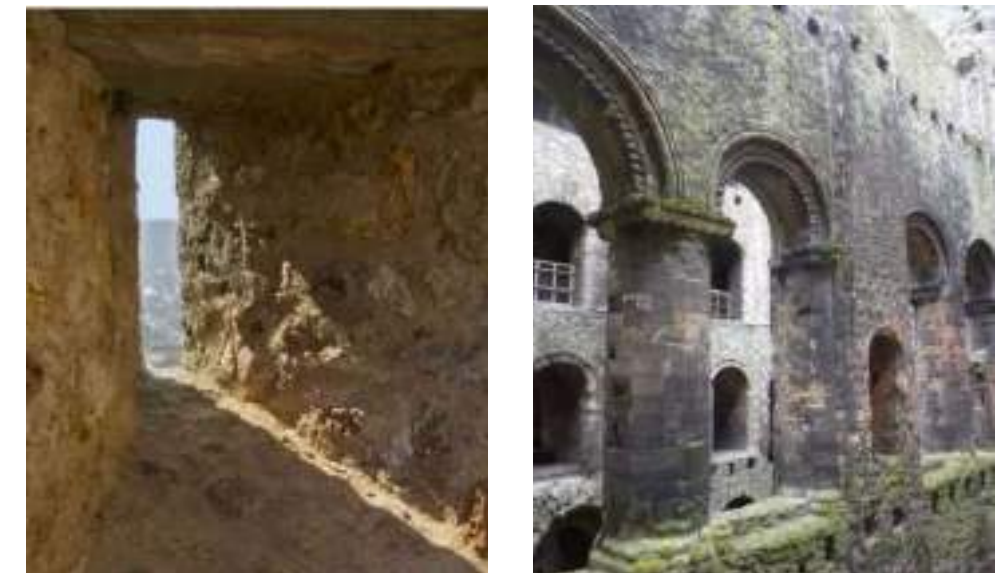
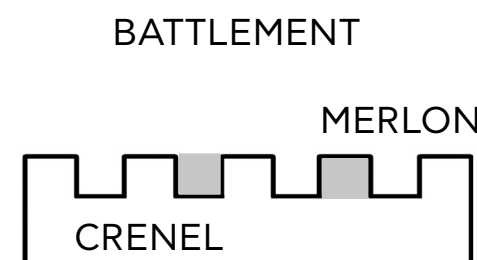
After brainstorming on the image of the school, the idea of a castle-school came up. A castle also expresses an enclosed space, meant to be protected from outsiders, has few openings towards the public and makes use of courtyards. Furthermore, the idea of a castle, introduced the stacking of rooms, to save space, and result in a more compact floor plan.

Looking deeper into the architectural expression of a castle, representative elements the team wanted to introduce in the project were found. The maze-like layout castles tend to have, with tunnels, narrow paths and small staircases were ideas that could arouse the children's imagination and encourage exploring the school. From the outside, the castles border, is defined by a defensive wall, recognizable from the battlement on top of these walls (figure 37). Such detailing would not be hard to construct, but would upgrade the ambience of the school. Typically, in the corners of the castle walls, towers are placed. Another element, the team felt would fit in well, was the arcade, or gallery, which could be placed around a courtyard (figure 39).

Figure 37 | Battlement

Figure 38 | Arrow loop(Jebulon, 2018)

Figure 39 | Arcade/gallery(Mball93,2018)



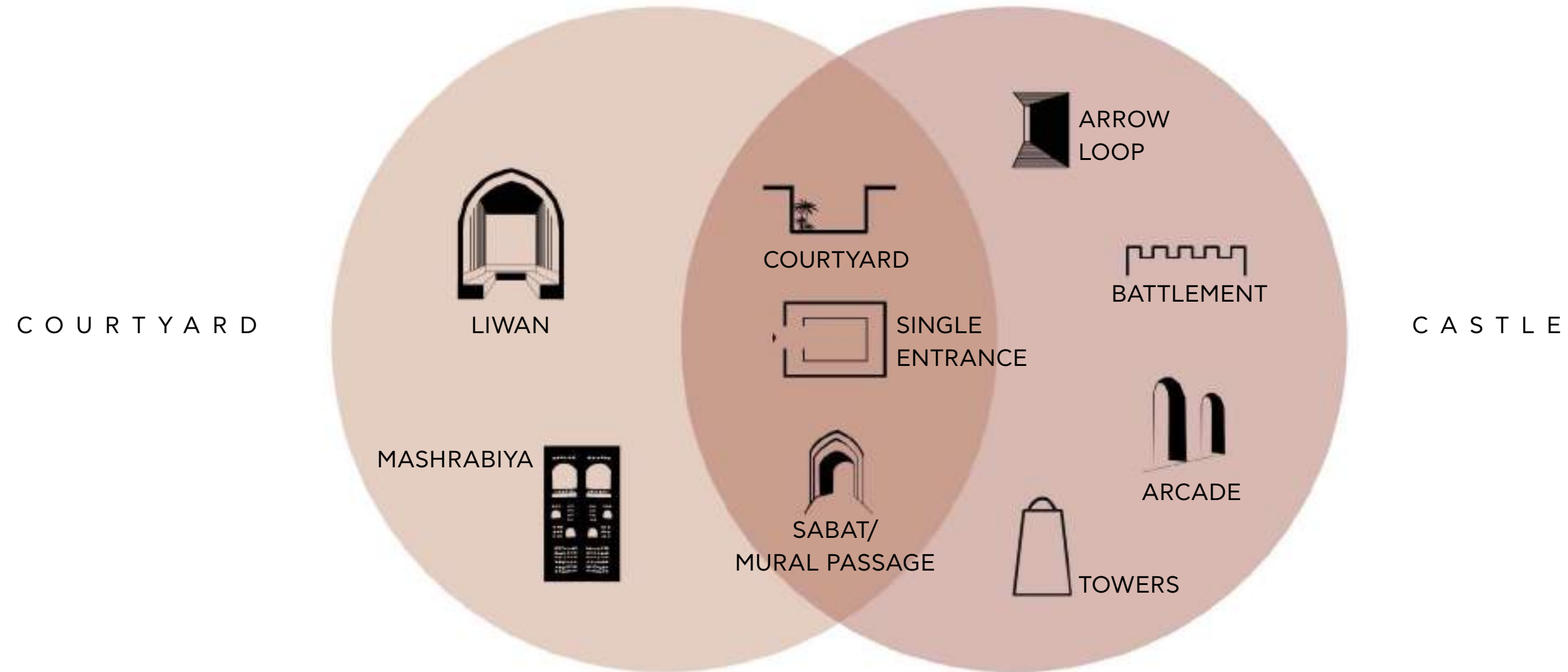
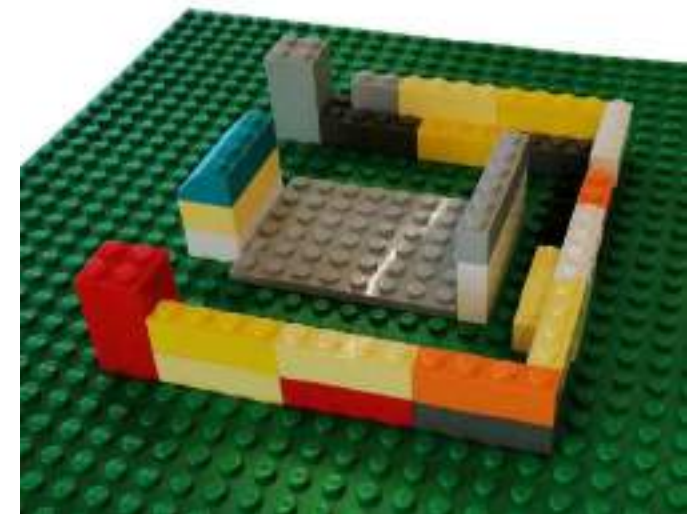
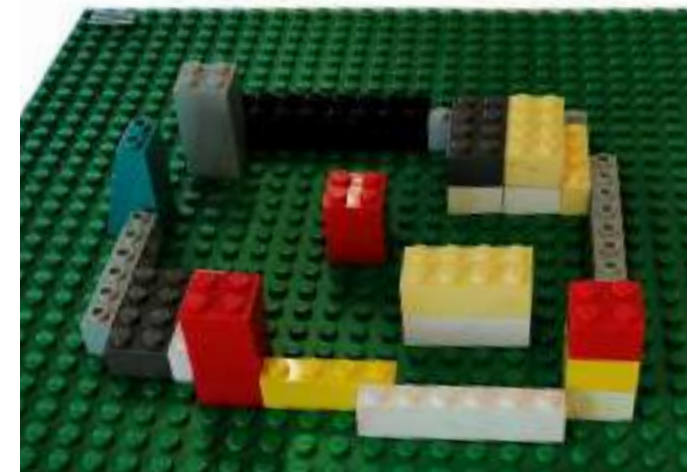


Figure 40 | Courtyard and Castle architectural elements

Interestingly enough, the two layouts, of a castle and a courtyard house had many things in common. The common elements would definitely be incorporated, while additional characteristics from both types were chosen to serve the comfort and appeal of the building (figure 40).

A means to find the best configuration for the purpose was to explore in 3D. To do so we experimented with stacking LEGO pieces starting from the initial courtyard configuration (figure 41). Soon it was observed that in order to achieve the desired privacy the multifunctional room had to be more clearly separated from the school and also to reduce in size. The area of the site was a restrictive parameter so the idea of moving some rooms to an upper level was created so as to fit all functions without crowding. The most satisfying outcome (figure 41) was selected to be developed further.

single courtyard

break up the space
more height variations

make dense

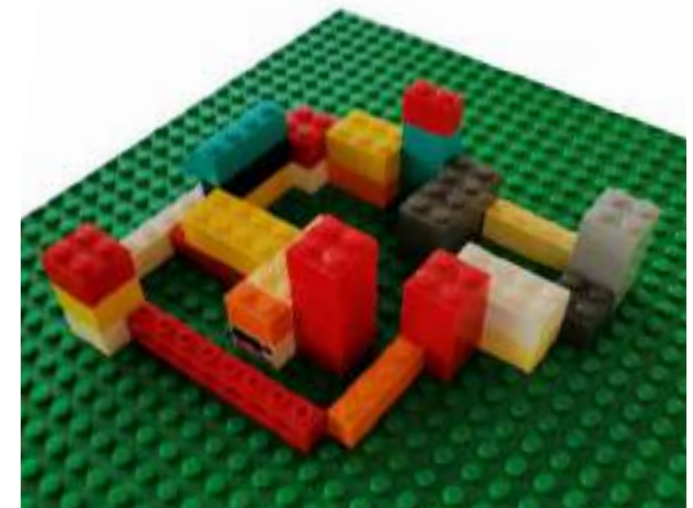
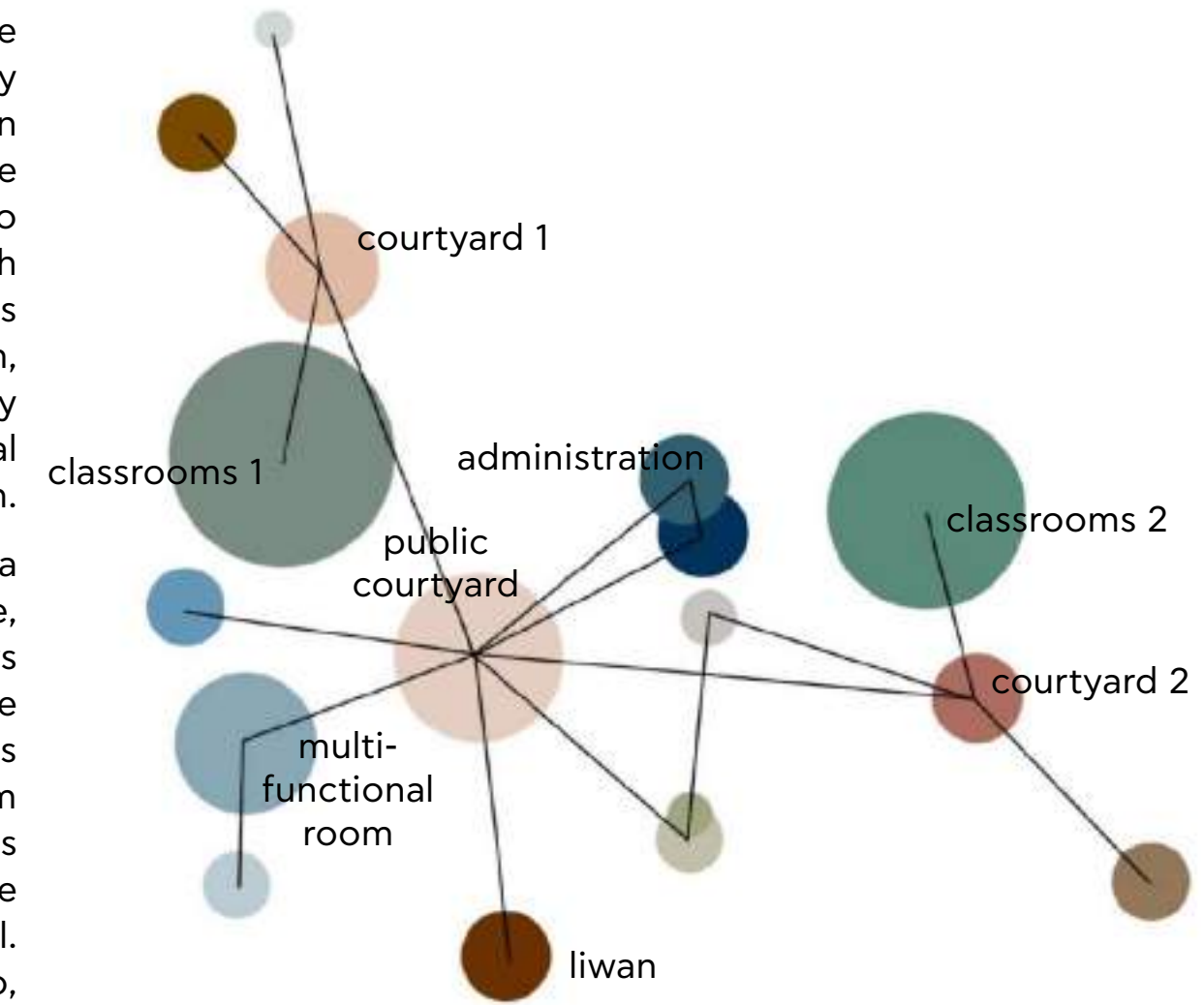


Figure 41 | Lego experimentation

B U B B L E D I A G R A M



The bubble diagram of the final configuration shows the connections and adjacency between the rooms. It is easily noted that the level of complexity is much higher than in the initial design (figures 42-44). The principal change is the fragmentation of functions in three districts, namely two private clusters for the school and one for the public. Each cluster is comprised of the relative functions, courtyard 1 is surrounded by four classrooms and the winter living room, courtyard 2 by three classrooms and the library and finally the public courtyard is surrounded by the multifunctional room, the administration room, the canteen and the kitchen.

The justified graph shows the hierarchy of functions from a user's perspective. At the first level (depth 0) is the entrance, where the user is introduced into the building, then follows the public courtyard (depth 1), which has a strong connective role as in the initial design. Depth 2 comprises of the rooms that are available for public use and a user has access from the public courtyard. The last level of the graph corresponds to the most private parts of the complex, that are mainly the classrooms and the supporting rooms of the multifunctional. The increased complexity can be seen in the REL chart too, as the 1's are more dispersed than in the previous layout (figures 34-36)

Figure 42 | Bubble Diagram



J U S T I F I E D G R A P H

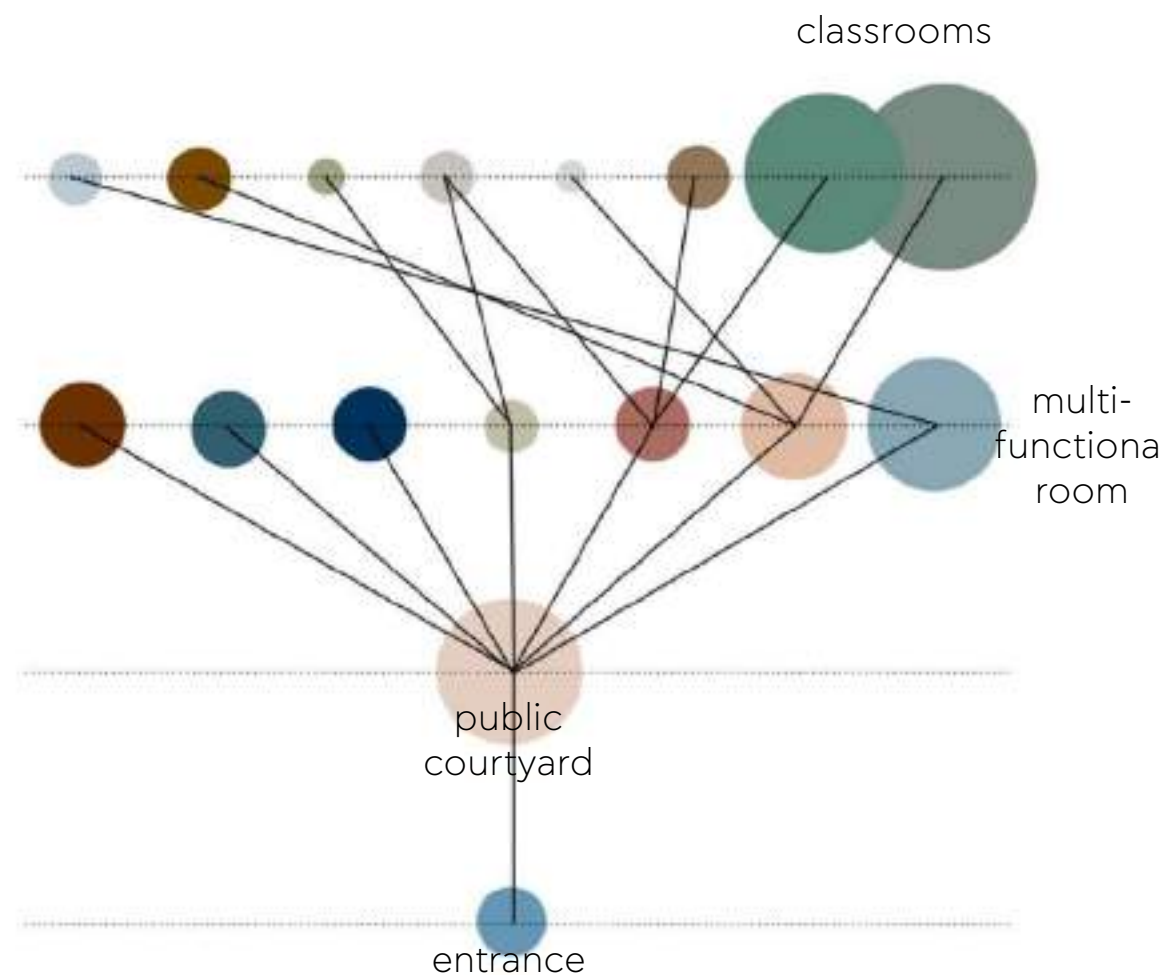


Figure 43 | Justified graph

Figure 44 | REL Chart

R E L C H A R T

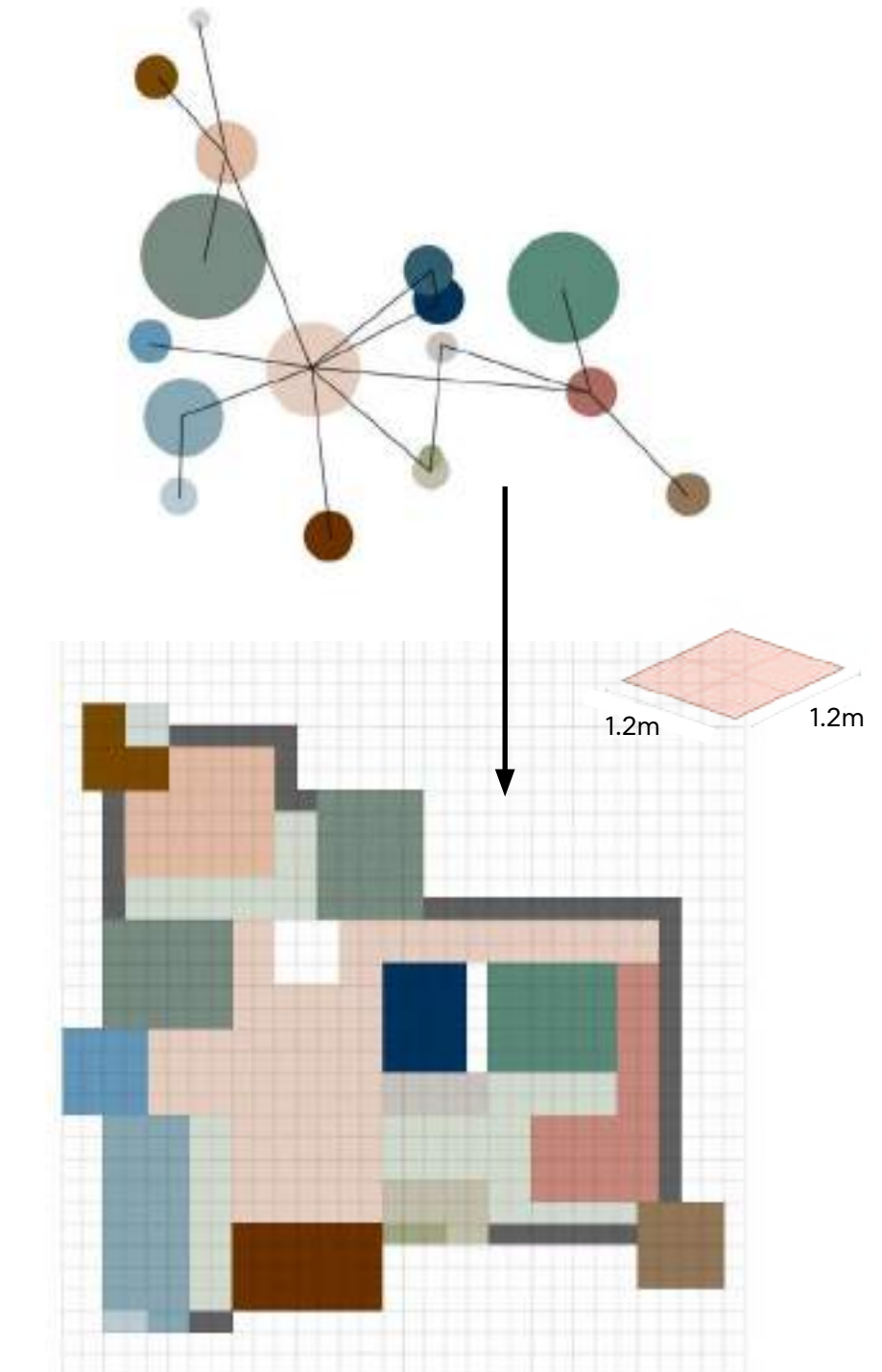
	Entrance	Class rooms young	Class rooms old	Public courtyard	Courtyard 1	Courtyard 2	Restrooms 1	Restrooms 2	Teachers room	Administration	Communal library	Multifunctional room	Cantine	Kitchen	Liwan	Winter living room	Storage room
Entrance	0	0	0	0	0	0	0	0	0	0	0	0	0	0	0	0	0
Class rooms young	0	0	1	0	0	0	0	0	0	0	0	0	0	0	0	0	0
Class rooms old	0	0	0	1	0	0	0	0	0	0	0	0	0	0	0	0	0
Public courtyard	0	0	0	0	0	0	0	0	0	0	0	0	0	0	0	0	0
Courtyard 1	1	1	0	0	0	0	0	0	0	0	0	0	0	0	0	0	0
Courtyard 2	0	1	0	0	0	0	0	0	0	0	0	0	0	0	0	0	0
Restrooms 1	1	0	1	0	0	0	0	0	0	0	0	0	0	0	0	0	0
Restrooms 2	0	0	0	1	0	0	0	0	0	0	0	0	0	0	0	0	0
Teachers room	0	0	0	0	0	0	0	0	0	0	0	0	0	0	0	0	0
Administration	1	0	0	0	1	0	0	0	0	1	0	0	0	0	0	0	0
Communal library	0	0	0	0	0	0	0	0	0	0	0	0	0	0	0	0	0
Multifunctional room	0	0	0	0	0	0	0	0	0	0	0	0	0	0	0	0	0
Cantine	0	0	0	0	0	0	0	0	0	0	0	0	0	0	0	0	0
Kitchen	1	0	0	0	0	0	0	0	0	0	0	0	0	0	0	0	0
Liwan	0	0	0	0	0	0	0	0	0	0	0	0	0	0	1	0	0
Winter living room	0	0	0	0	0	0	0	0	0	0	0	0	0	0	0	0	0
Storage room	0	0	0	0	0	0	0	0	0	0	0	0	0	0	0	0	0



The bubble diagram of the final configuration had an extra layer of information compared to the initial one: the spatial correspondence with the site. The translation from bubbles to spaces is not an automated process, but requires human interpretation. As can be seen in figure 45 the lines from bubble diagram are translated to corridors not only in 2D but also in 3D. A corridor is translated in 3D to stairs, so one main staircase is added in each school cluster to serve the vertical circulation.

The transition was based on an architectural module, which was multiplied to reach the required areas of each room. The decided the module dimensions was 1.20x1.20m because it complied with the aforementioned rule and also was in direct proportion to the human body. The grid was not only applied in floorplan but also in the z axis for the same reasons. The size was capable to accommodate the different spaces efficiently (1 module width for stairs, 2 for corridors etc). Later on, the same module would define the brick size to facilitate the construction process. More details on the design decisions are presented in the floorplan pseudocode (see pseudocode floor plan flowchart in Appendix E).

Figure 45 | Transition from bubble diagram to layout, with use of architectural module



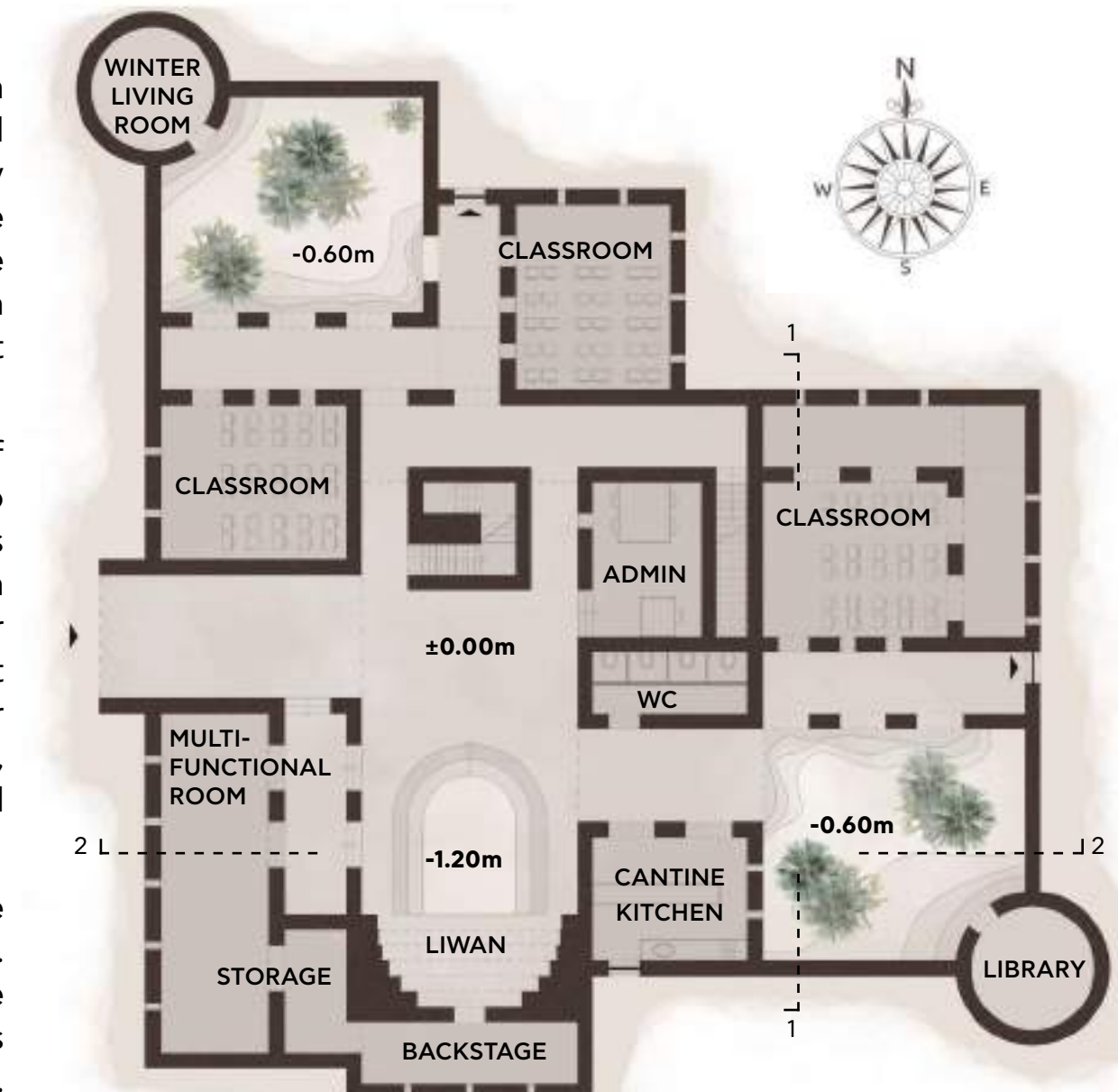
The next step was to translate this final layout into an architectural floor plan. In the figure 45 (bubble diagram and layout diagram) the various functions were depicted only by their clear area. At this stage the walls and openings are added to define the connections and disconnections of the spaces. Small adjustments were necessary in order to create a smooth traffic flow. But in general, the floorplan does not differ a lot from the layout diagram.

The entrance of the building is located on the west side of the castle. Walking through the entrance will bring you to the large public courtyard. The south side of the courtyard is closed off by the liwan. This liwan is a very common space in the vernacular architecture of the region. During hot summer days, it is the coolest place of the building, since it is not exposed to direct sunlight. Other buildings which border the main courtyard are the multi functional room, canteen, administration room and restrooms, all functions which could be used when public events are held in the amphitheater.

The other two courtyards are much more private than the first one and thereby placed much deeper into the building. They are accessible via the two sabats, which define the barrier between public and private spaces in the castle. This barrier is not very hard, but it creates a smaller darker space, which, compared to the light, open main courtyard, hints towards an entrance of a more private part of the building.

Figure 46 | Ground floor floorplan

0 12 5 10m



Passing through the sabats will lead to the courtyards of the classrooms. The classrooms on ground floor are connected to the courtyards via the galleries. This not only provides some privacy, it also is very beneficial for the indoor climate of the classrooms. The air temperature in the galleries will be lower than the outside air temperature. So the galleries also create a thermal barrier between the hot outside air, and the mild indoor climate, created by the heavy adobe walls. Opposed to the galleries, the castle's towers are placed. These towers are the highest structures in the building. In the eastern one, the library is located, while the western tower is designed as a winter living room. The courtyards are eventually closed off by the castle walls, creating a safe and closed space where kids can have fun and hang out together.

On the second floor, four more classrooms are located, alongside with the teacher room. The layout of this second floor is very comparable to the one of the ground floor, again with the galleries, which separate the classrooms from the courtyards. This second layer can be accessed from the ground floor by two different stairs. The first option is using the stair tower in the main courtyard. This will lead to the elevated gallery of the northern courtyard. The second stairs can be accessed by the corridor north of the stair tower and will end at the gallery of the eastern courtyard.

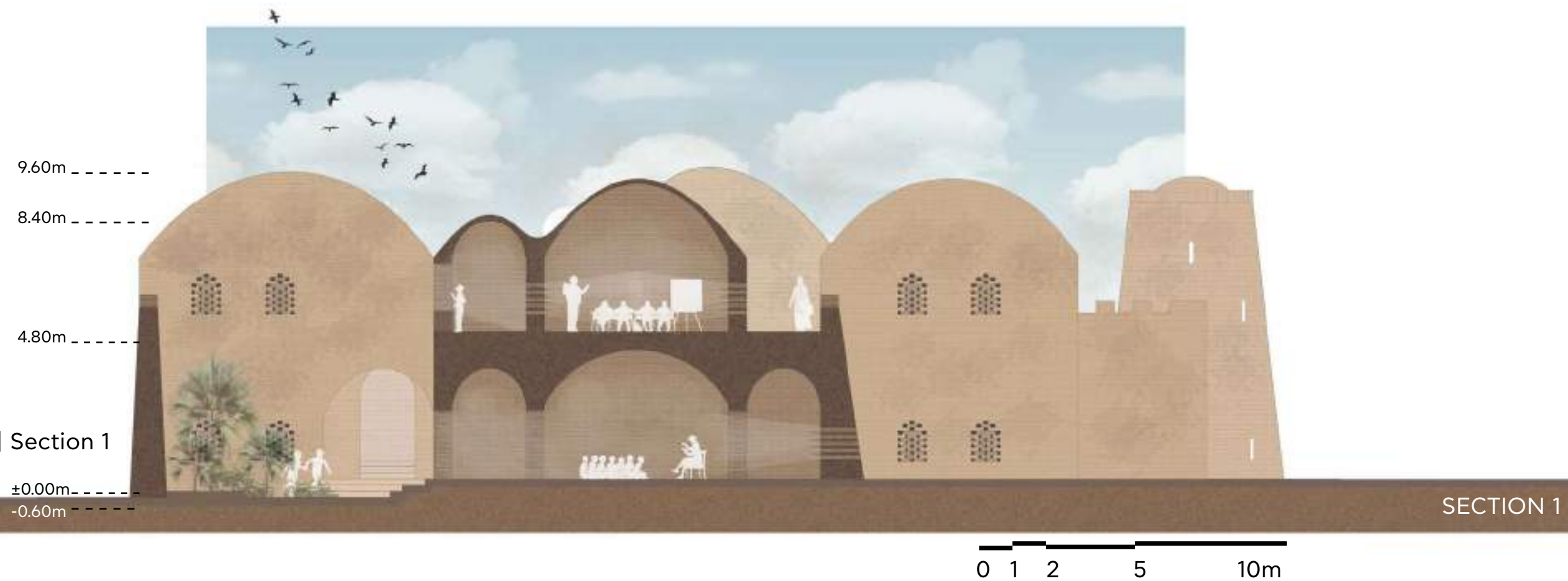
Figure 47 | First floor floorplan

0 12 5 10m



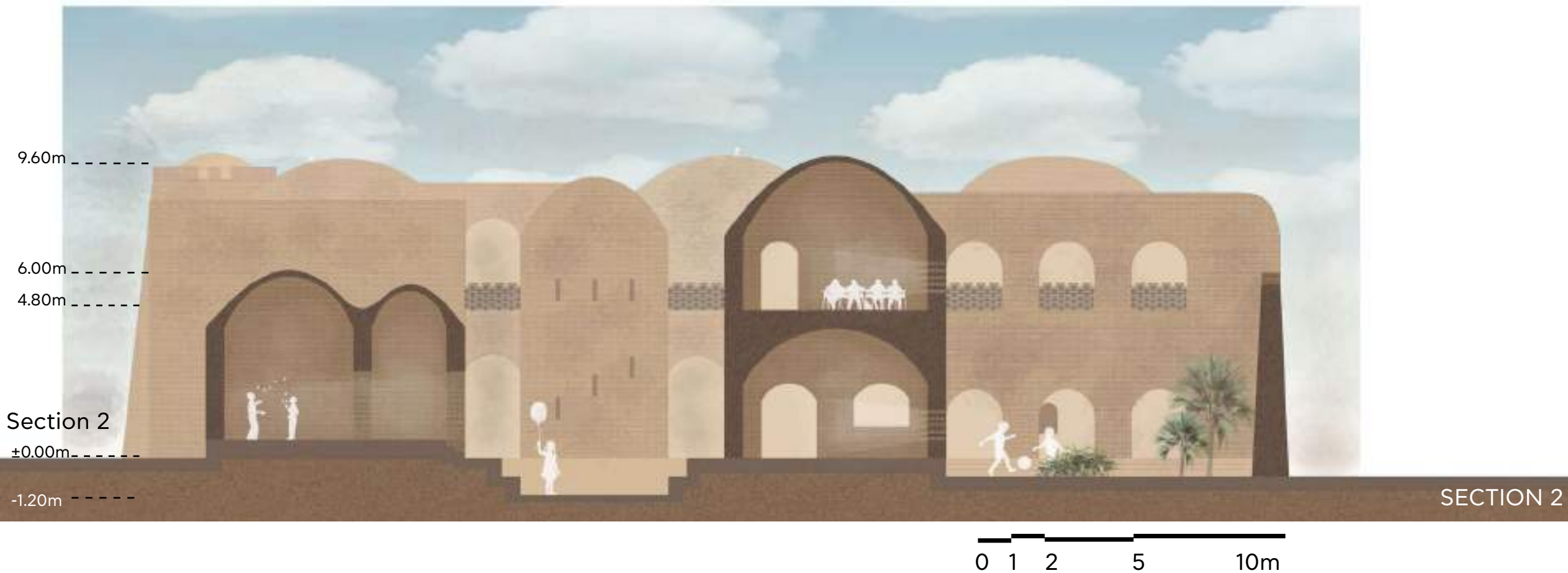
Also on the second floor, the two courtyards are connected to each other. With the elevated corridor, running alongside the castle wall, it is possible to get from one courtyard to the other. This connection is not only useful for traffic purposes, but also adds quality to the castle. Besides being an archetypal and recognisable element in the castle typology, it also adds to the maze like layout, by creating a backdoor connection between two parts of the building. This elevated connection can be clearly seen in the section below.

This section also shows how the two stories are related to each other. For structural reasons, it was very important that the load bearing walls would be positioned on top of each other. That is why the galleries and classrooms are placed exactly on top of each other. The only differences between the floors are the height of the ceilings. Because of the presence of the second floor, the ceiling height of the ground floor could not be too high. On the first floor there was no restriction, allowing for higher ceilings, by using a different relaxation. This process will be explained in chapter 4.6.



In section 2 both the public, on the left, and private courtyards, on the right, are visible. There is a 0,6 meter height difference between the two, which makes it harder to look through the sabats, and thereby adding strength to their public-private barrier function. An advantage of digging out the courtyards is that the earth could be used for construction purposes. Besides a height difference between the two courtyards, there is also a vertical distance between all the rooms and courtyards. This distance of 0.6 meters is to make sure that there is no water coming in during a heavy rain storms.

On the next page a route is created through the castle were all discussed building elements are shown in 3D (figure 50). Explanatory flowcharts about the different routes different users can take can be found in Appendix F.



6 SECTIONS

COURTYARD IN PLAN

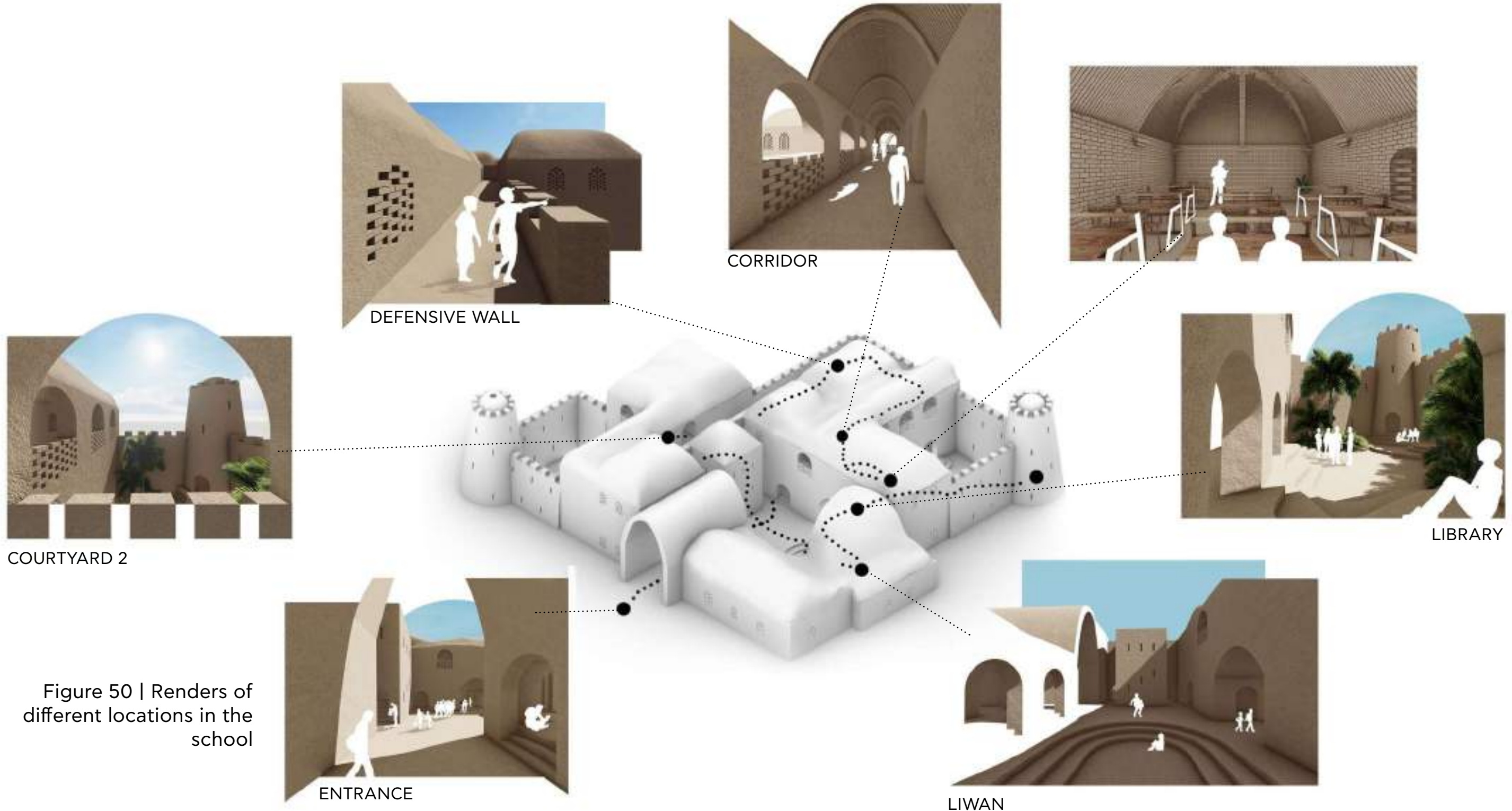
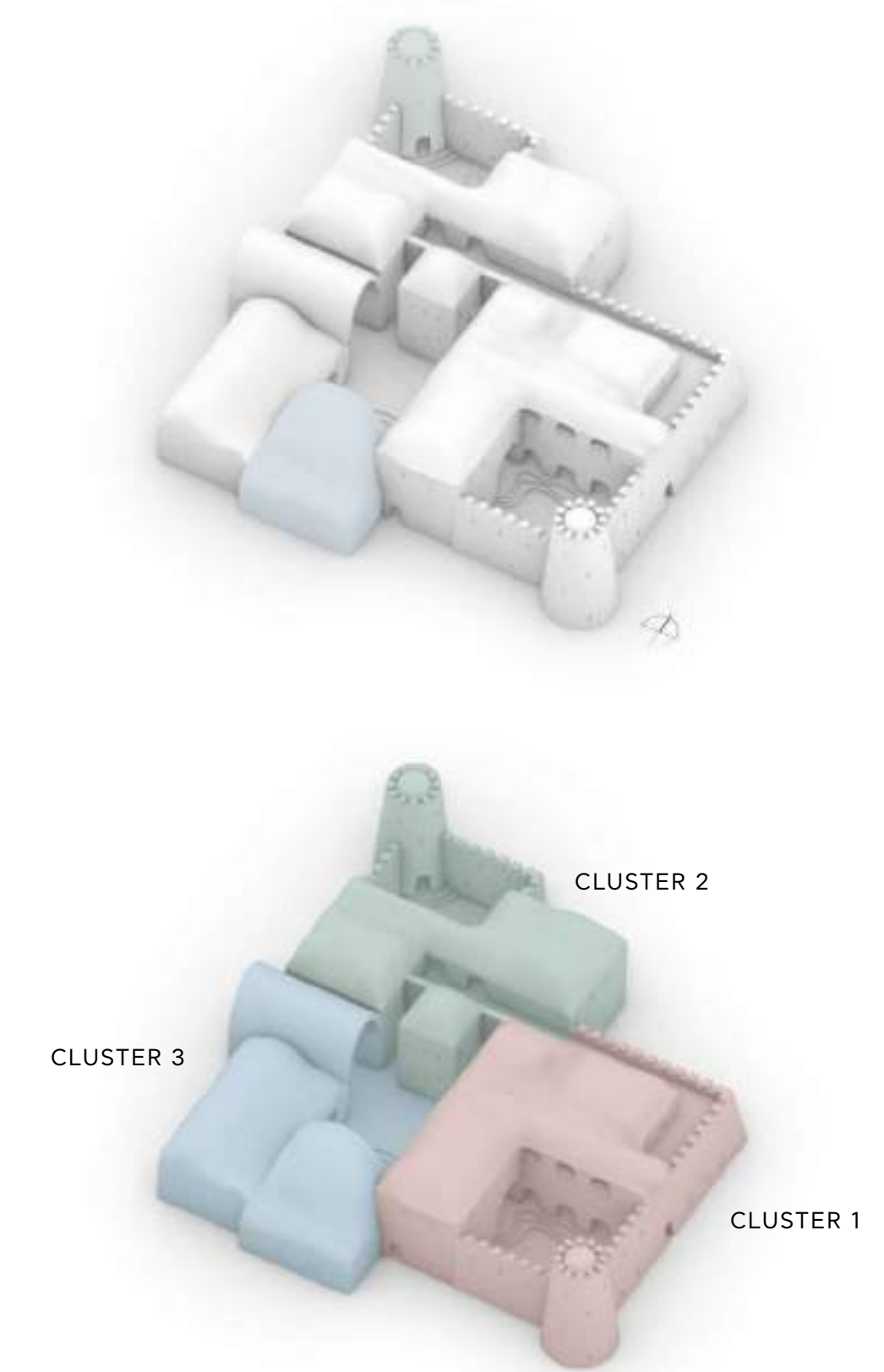


Figure 50 | Renders of different locations in the school

In climates such as in Jordan, one of the biggest causes of discomfort is heat. In this proposal the heating problem was addressed by suggesting thick adobe walls (60cm) with high thermal insulation (R-value), small openings to the streets and larger towards the courtyards. The double height of the liwan as well as the existence of a courtyard in front of it, improves the microclimate as it creates an airflow from the bottom to the top. Apart from that, by placing the liwan to the south and the winter living room to the north the users would have a favorable place to use throughout the year (figure 51).

Figure 51 | Winter living room and liwan

Figure 52 | Different clusters



In the final configuration the distinction of the three clusters was clear and complied with the privacy intention. Clusters 1 and 2 are private (school), while cluster 3 is public (communal uses). However, the distinction of the three courtyards did not only serve the architectural purpose but also the climate design. Considering that the two courtyards of the school (clusters 1 and 2) would be covered with vegetation as much as possible, the temperature there, would be lower than in the public, dry courtyard (figure 53). As a result, even in the days of stillness, the temperature difference between the courtyards, in combination with the two tunnel openings on the ground floor would create a natural airflow pushing the hot air away from the complex as seen in figure 54.

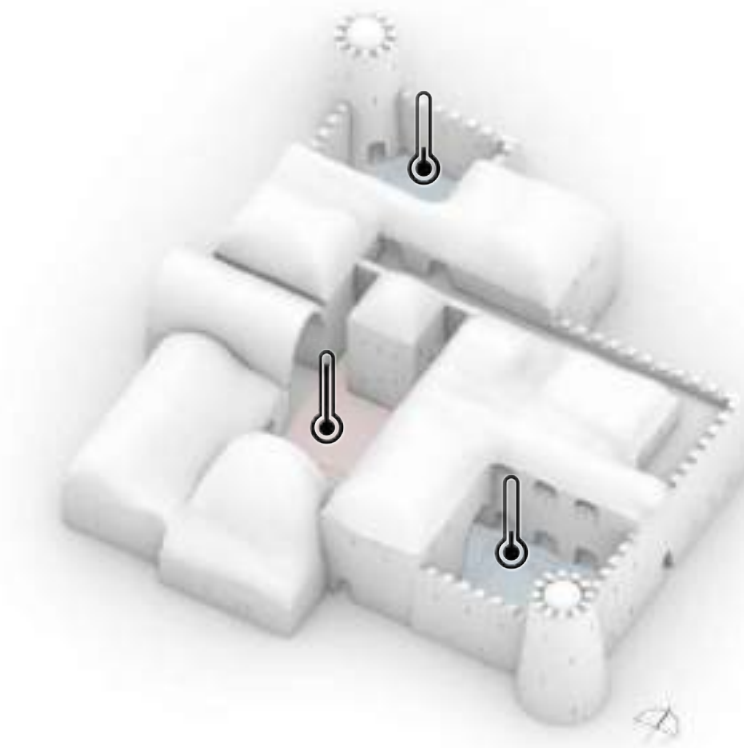


Figure 53 | Different courtyard temperatures

Figure 54 | Air flow from courtyards through tunnel



SECTION 2

0 1 2 5 10m



Figure 55 | Renders
overlooking courtyard 2

4 FORM FINDING

For form finding we decided to work parametrically in the Grasshopper environment. In certain tasks the use of meshes instead of b-reps was preferred to minimize the processing time the GPU needs to display objects, whereas in tasks that required more advanced editing b-reps were preferred. Different phases, required use of various softwares and plug-ins, as shown in the Computational Flowchart (figure 56). For sharing items within Grasshopper Speckle was used, while other files were shared in a common Google Drive folder.

1 FLOWCHART

FORM FINDING

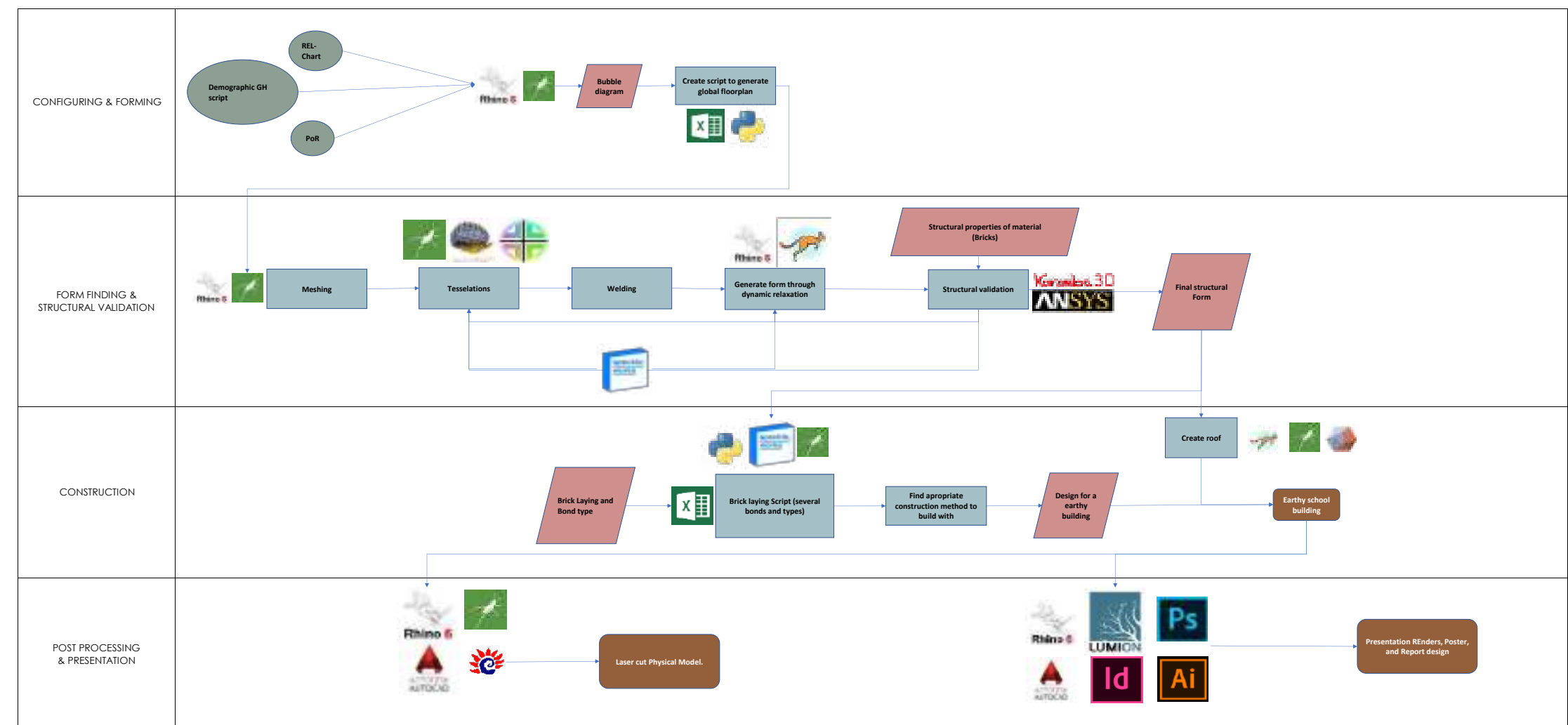


Figure 56 | Computational flowchart

The next step was to turn the floorplan into a 3D model. This was done by using the Grasshopper plug-in Kangaroo. With this software, it was possible to relaxate the volume, needed to create a compression only structure. This paragraph describes the process of how the 3D model was made and prepared for the relaxation.

The first idea was to make the meshes with only Grasshopper. The image below shows a part of this script. Here, one of the rooms of the Sand Castle is positioned and made. It starts at the left side, where the correct position of the grid is chosen. This point will be the origin of a rectangle which will become the floor of the room. Thereafter the walls around the room are added, before all the surfaces are transformed into meshes.

There were however a lot of problems by making the meshes in the way shown above. This script was only for making one single room, so when this has to be made for all rooms in the castle, it would become quite a mess. Besides this, this script still only produced a 2D mesh, as the ceiling height was not included yet. Of course, this could be added, but from this point, we started thinking about other possibilities to make these meshes. In this phase we were pointed to Python. This would be easier to make and much more accurate than the Grasshopper script initially used (figure 57).

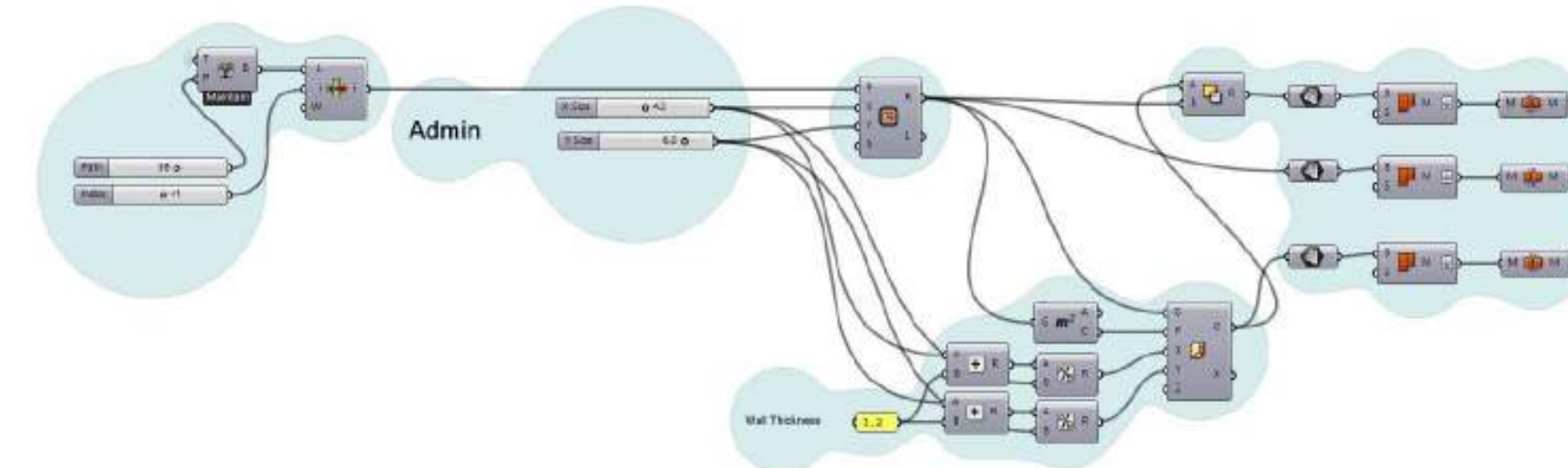


Figure 57 | Grasshopper mesh script

The process can be split into two parts. The first part is about collecting and structuring the data needed for the python script. The second part is a Python script which made the meshes that were eventually relaxed.

The first part starts with making a grid in Grasshopper. This grid exists out of points, which are all placed at a distance of 0.6 meters from each other. The thought behind this distance is that 0.6 meter is the smallest size an object can be in our floorplan. The architectural module is 1.2 meters, but since the walls had an estimated thickness of 0.6 meters, this distance was preferred over 1.2 meter.

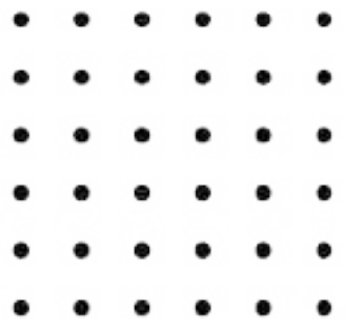
The next step was to select point out of this grid, which eventually will form the origin point of each room of the Sand Castle. This was done manually by using the 'Tree Branch' and 'List Item' components in Grasshopper.

Thereafter, the coordinates of these points were exported to an Excel file, using the 'Write to Excel' tool. By structuring the exported data, the Excel file contained three columns, for the X, Y and Z- coordinates of the origin points.

In a separate Excel file, the dimensions of each room were written. This has to be done very carefully, otherwise the wrong dimensions would be assigned to the wrong origin point in a later stage of the process. So the items in each of the data lists needed to be ordered in the same way, so that the rooms will have the correct position and dimensions.

Subsequently, these two Excel sheets were imported in the Grasshopper file, using the 'Read Excel' tool. Thereafter the two data trees were cleaned and structured, so that all empty or useless cells were removed from the lists and it only contained data which was necessary in the python script.

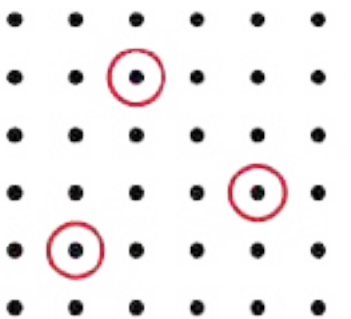
Finally the data was imported into the 'Python Script' component. However, before doing this, the data lists in Grasshopper needed to be rewritten into a list which python could read. After doing this, all datasets were ready to be imported into the python script (figure 58).



Step 1: Create a grid of points,
0.6 meter from each other



Step 2: Create an Excel sheet
which assigns every room to
a point on the grid



Step 3: Place the correct
points into an ordered
Grasshopper List



Step 4: Create an Excel sheet
with dimensions in X,Y and Z
of each room

(1)
0 7.2
1 6
2 2.4
(2)
0 13.2
1 2.4
2 2.4
(3)
0 6
1 7.2
2 2.4

Step 5: Make a Grasshopper
List with the properties of
each room



Step 6: Insert the two made
lists into the Python script

Figure 58 | Excel point import

The second phase entirely happens in the 'Python Script' component of Grasshopper. Besides the data sets, described above, the only other thing imported in the script was the mesh of one module, a two-dimensional object of 0.6 meters squared. This mesh was imported and was the starting point of the entire script. The first step was to copy this mesh and moving one tile to each of the imported origin points. This tile is the start of building each room.

The next step was to duplicate this tile over the XY-plane. To do this, the dimensions of each room were divided by 0.6, which gave the amount of tiles that were needed in both the X and Y direction. This created a surface which eventually would become the ceiling of the room.

Thereafter, the tiles of two of the four sides of the ceiling were duplicated and rotated 90 degrees over the edge of the ceiling surface. These tiles were the starting point of the walls of the room.

To create these walls, the edge tiles were multiplied in the Z-direction to create the correct height for each room in the Sand Castle. These walls were still only made on two edges of the ceiling. The final step would thereby be to duplicate these walls and move them to the other side of the ceiling. This resulted in each room having a ceiling and four walls (figure 59).

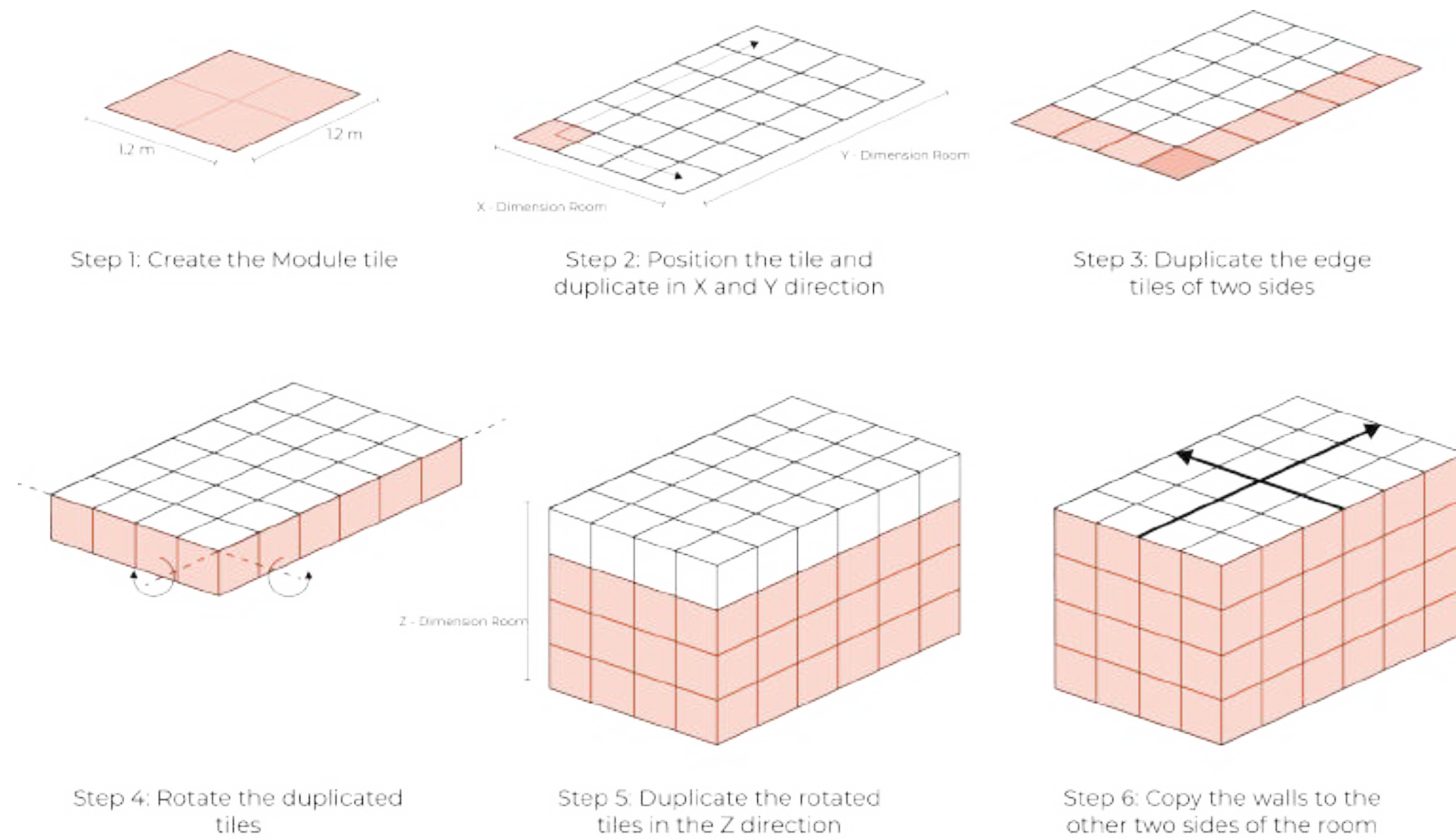


Figure 59 | Python meshing

Since the whole complex was to be built purely from adobe blocks (that have no tensile strength) the structures had to be compression-only. A way to achieve compression-only structures was by dynamically relaxing the shape. To achieve a well-structured and controllable dynamic relaxation the following steps had to be taken beforehand: mesh definition, tessellation and welding.

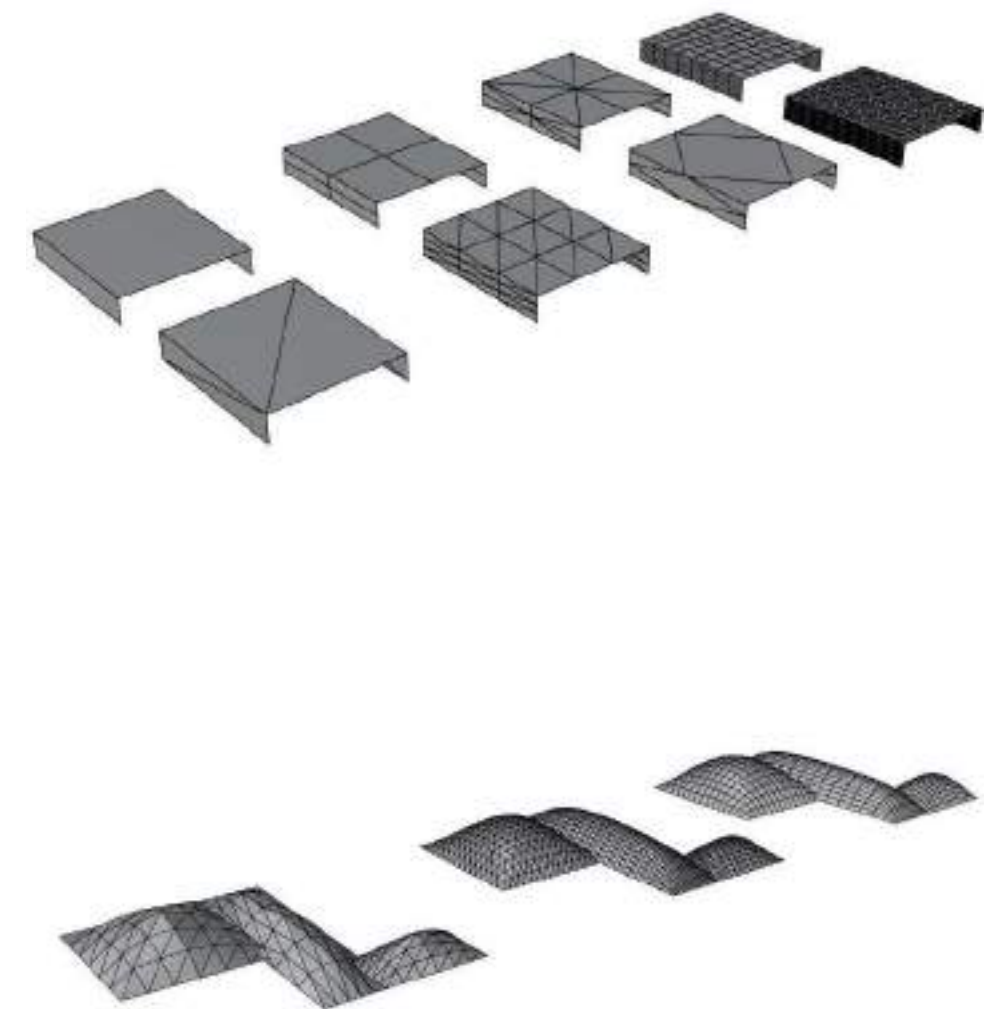
By completing the tessellation with as much precision as possible the mesh to be later tested in Karamba3D would provide us with more accurate results. This is why the tessellation should be refined but without exaggerating, because the computational time to proceed would increase respectively.

The first trials were made before completing the python script, so the mesh tested was a mesh surface of the whole room. It was suggested that the dynamic relaxation started from the walls and not from the floor, to avoid unusable spaces due to small height under a slanted wall. The ceiling would rest on the walls, so the trials were focused on finding the optimal tessellation pattern (figure 60).

It should be noted that each tessellation method had different effect on the relaxation. Some examples of different tessellations on connected meshes are shown in figure 61.

Figure 60 | Alternative tessellations

Figure 61 | Relaxation of alternative tessellations



After doing numerous trials with grasshopper components from plug-ins such as Weaverbird, Mesh+ and Lunchbox we ended up using the following:

For the vaults:

Weaverbird Constant Quads Split Subdivision was used. It calculates an all-quad and same-looking mesh, which is derived by adding a face for any edge to the original mesh. For the refinement the level in constant quads was set to 3 which is the maximum number of subdividing iterations for each face (figure 62).

For the domes:

Mesh+ Weighted Loop Subdivision is based on the implementation of Weaverbirds' subdivision the Loop subdivision. It introduces the option to modify the weight of smoothing or displacement from the original vertices. For subdividing the dome's surface two loops were used (figure 63).

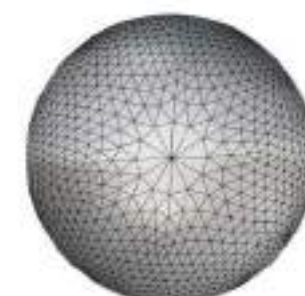


Figure 62 | Vault relaxation



Figure 63 | Dome relaxation



After having created the meshes with python script, the geometry was re-imported to Grasshopper environment. This time only the objects that would participate in the relaxation were added, that is the ceiling and the top row of the supporting walls. The tessellation was applied on each module (instead of the whole area of the room), providing higher levels of subdivision. On the right, the meshes generated from the python script can be seen.

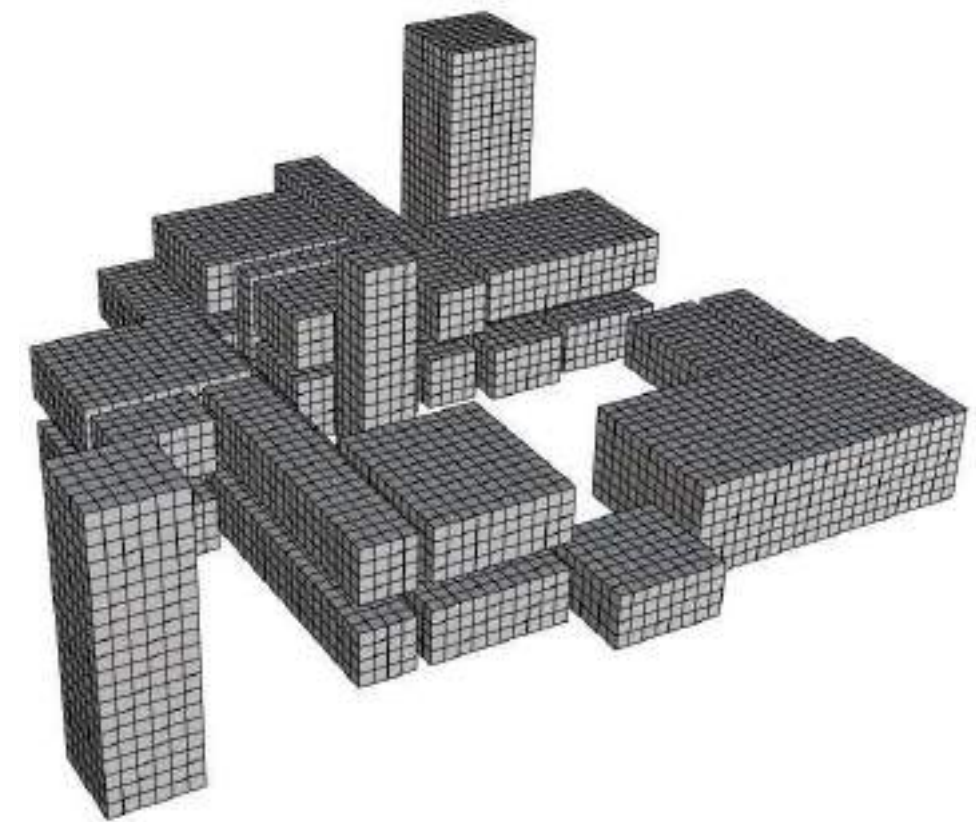
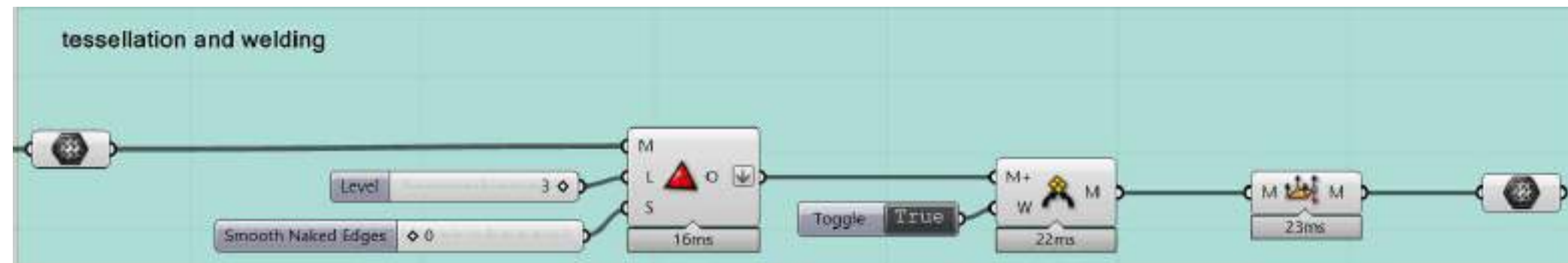


Figure 64 | Python script
mesh

One of the main challenges of the design was to combine the ceiling of the classrooms with the ceiling of the galleries. For this operation it was essential to make sure that all vertices of one mesh would match exactly with the other's. This is what welding is about. In order for it to work best the most accurate way to provide correct meshes was by creating them in python (as mentioned in chapter 4.3). By doing so, it was certain that the meshes of the grid would have exactly the same number of vertices on each edge.

For welding not as many options as for tessellation were available. From the three found in Grasshopper environment (Mesh Weld Vertices, Weld Mesh and Weaverbird Join Meshes and Weld) the latter was chosen. It returns a singular mesh object made out of a list of meshes. The new mesh is lighter meaning that the footprint of the new mesh is less than the sum of the originals. The final step before passing the data to kangaroo was to fix any inconsistencies in the directions of the mesh surfaces'. For this purpose the component Mesh Unify Normal was used (figure 65).

Figure 65 | Welding
Grasshopper script



The initial relaxation trials were done on the ceilings of the classroom and the gallery placed adjacent to each other. Immediately, certain problems appeared. By relaxing only the ceilings, the landing of the relaxed surface on the wall did not occur gradually. Also, as the surfaces were adjacent, there was no space for the wall to be placed afterwards. Finally, when the two surfaces we relaxed as one, due to the different span size, the height difference between the gallery and the classroom was too much (figure 66).

A first approach to solve the above mentioned issues was to we created a manifold. By including not only the surface of interest but also part of the surrounding walls the relaxation would be more realistic since the ceilings would actually rest on the walls. Also a row of modules would be added between the meshes, to show where the wall was.

As it can be seen in figures 67, 68 indeed the manifold technique was successful. However the significant height difference when relaxed remained. This was a problem, especially for the ground floor, where a more shallow geometry was preferred.

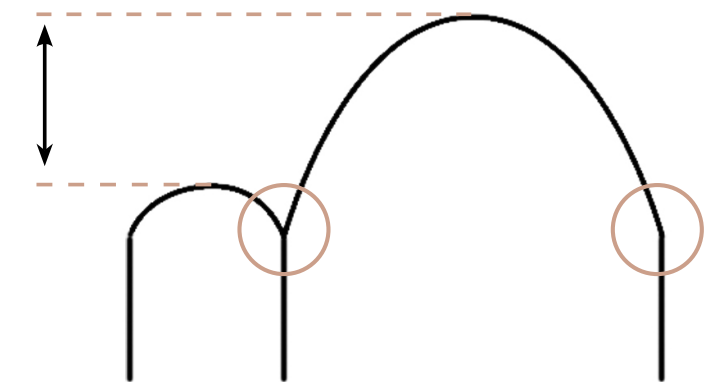


Figure 66 | Relaxation problems

Figure 67 | Manifold relaxation

Kangaroo2 was the Gh plug-in used to dynamically relax the meshes. In order to achieve a precise relaxation the following script was developed (see Appendix H). In this definition the mesh edges are assigned a certain strength, and the anchor points are imported manually from rhino. A vertical load is applied on the mesh surface to produce the relaxed mesh.

After trying different techniques such as changing anchor points, load strength, spring strength, etc the big height difference problem remained. The unified mesh was imported in Kangaroo2 as a whole even if it was a manifold the result was still dissatisfying. For this reason it was decided that the dynamic relaxation of the ceilings should be done separately (figure 70).

Apart from that, using the united mesh for the relaxation resulted in irregular shapes that were rejected, because the geometries were too complex to be built by inexperienced builders and adobe bricks (figure 69).

Eventually, the ground floor and the top floor were decided to be relaxated differently, as different specifications were required. The ceilings of the classrooms on the ground floor had to be less steep than the ones in the top floor (max height 1.8m). The ceilings of the galleries both in the ground and the top floor were of 1.20m height. Both the ceilings of the galleries and the classrooms of the ground floor would be constructed as plain vaults for ease of construction.

Figure 68 | Manifold relaxation

Figure 69 | Gallery opening relaxation

Figure 70 | Separate relaxation



The ceilings of the classrooms at the top floor could be higher, since no other floor would be added. Thus, the height of the ceiling was 2.4m. The galleries remained the same as in the ground floor (1.2m). On the top floor, the intention was to anchor all four sides to the walls, so as to avoid having sharp edges exposed to weather corrosion. This meant the construction technique used in ground floor, could not be used. A technique that could be incorporated in the castle idea was the ribbed vault.

To define the position and pattern of the rib vaults a series of manual tessellations was made (figure 71). The tessellations initially were done for the separate geometries of each room. Gradually, the tessellation included more spaces, in an effort to have a single tessellation for the entire cluster. A limitation of the tessellation patterns was to not create a vault with a larger span than 6m for structural reasons. However, when these unified tessellations were relaxed, the resulting geometries included complex geometries, such as vaults of varying height. Due to the difficult constructability, they were eventually rejected.

The selected tessellation when relaxated, produced relatively simple geometries whose construction was feasible. The lines (except for the perimeter) show the principal rib vaults (figure 72). The middle part would be constructed as normal vault, whereas only at the edges, the rib vault technique would be used (see chapter 6).

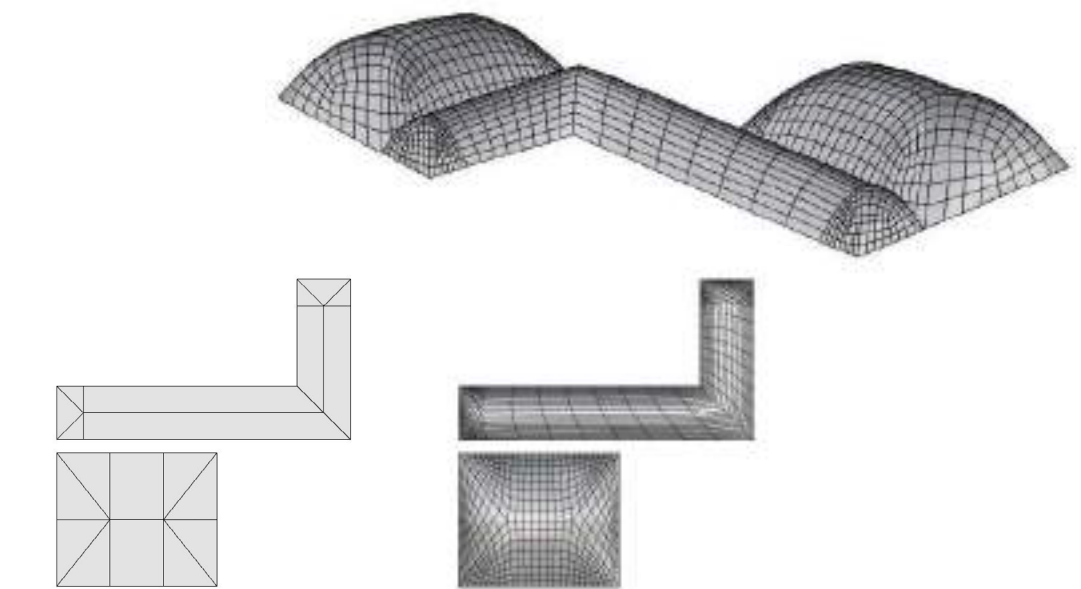
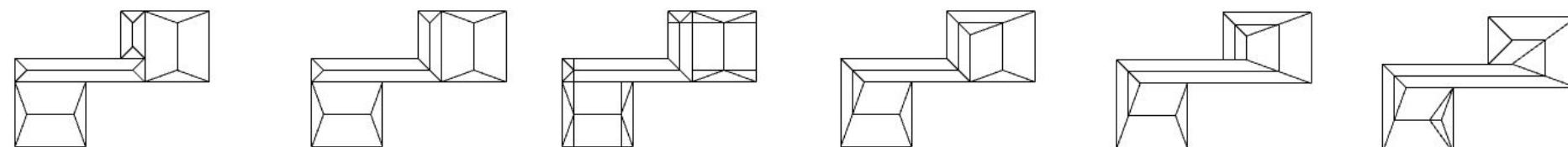


Figure 71 | Alternative tessellations

Figure 72 | Final relaxation



5 STRUCTURAL ANALYSIS

To determine the failure stress of adobe, laboratory experiments were done with self-handmade adobe bricks. To acquire these specifications specimens were made and tested by the students of this course. The thirty different specimens which were tested, were self-handmade with the same given basic recipe and with any selected additives.

The specimens with straw as an addition were the strongest from this research with a strength of 3.5 Mpa. If the statistical estimation of imprecision or 95% confidence was removed to be safe, a calculation value of 2.6 Mpa remained. A safety factor for adobe would be 2.5 to weaken the material in the calculation to make the final structure strong enough, a safe over-dimensioned structure.

All details of this research and the results and calculations can be found in the brick breaking report in Appendix I.

Tabel 1 shows the Calculation of the E-modules for two cases. The first value is the calculated value that was obtained from the brick breaking experiment. For this an average displacement was calculated. The second value is the one we used for all the hand, Karamba3D and Ansys calculations. (Gubasheva, 2017)

Table 1 | E-modulus calculation

E-modulus calculation						
	Height sample (mm)	Avg. Displ. (mm)	ϵ (mm/mm)	Mpa Sample	E modulus Cal.	
Calculated	60	12,6	0,21	2	9,523809524	
Used	60	1,2	0,02	2	100	

This second value was used because the data from the experiment was deemed unreliable. There were two factors that caused this. The first one was that the samples were not fully dried when they were tested. This caused the stones to be less strong. The second factor was the way the testing was done. The sample was placed onto a piece of plywood during the compression testing. This piece of plywood started to bend at a much earlier stage than that the sample would deform, causing an error in deformation readings. Various other sources also gave E-modulus values that were about 10-15 times higher than that we calculated. This gave us enough reason to multiply our results by a conservative 10 times.

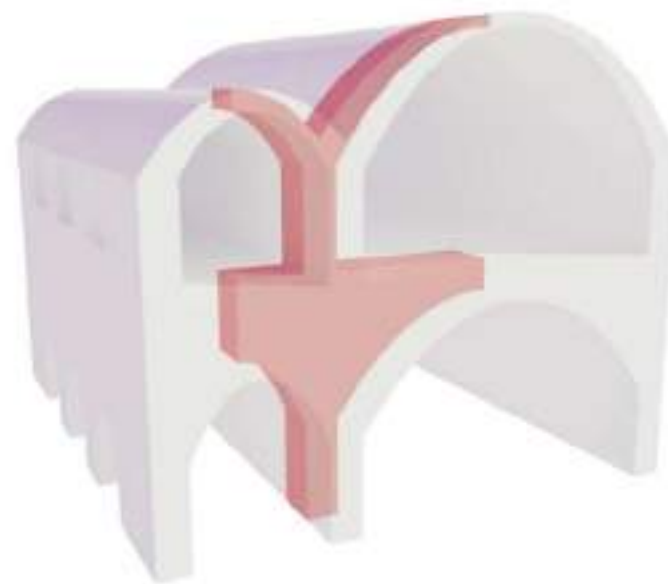
The structural verification was done for all the main elements of the plan. The calculations were done in two steps. The first step was doing the hand calculations to easily verify if certain design options were doable. The second step was to verify the meshes that were generated by the meshing scripts. This was done using karamba3D. The last step was to make solid models of the meshes and import them into Ansys. With Ansys the results were compared with karamba3D in order to verify them.

The hand calculations are a useful means of quickly checking whether the construction meets the set values. For the hand calculations, the maximum stress has been calculated in three different places of a characteristic part of the building, classrooms with a gallery. The failure stress was determined in the brick breaking report and can be found in Appendix I. The section area of the walls and the loads on construction are known. There are two ways to see if the structure meets the requirements. Method 1: Calculate the stress by dividing the total loads in the section area and then see if the calculated stress is lower than the maximum failure stress. Method 2: Calculate the maximum allowable loads by using the maximum failure stress and the section area and then see if this maximum forces are higher than actual loads on the structure.

For the loads on the construction, own weight, permanent floor loads and variable floor loads are used. 19.6 kN / m³ was used for adobe density. The wall thicknesses are 600 mm. 1.35 kN / m² was used for permanent floor load and 1.5 kN / m³ for variable floor load. These are the values that are applied to the floors of schools and utility buildings in addition to the own weight of the structure. These loads are multiplied by a safety factor of 1.5, so that calculations are made with even higher loads, so that the structure is ultimately safer, over-dimensioned.

The hand calculations are visible in the tables below. Each table has a figure that shows where the calculation is applied in the building. With every calculation, the stress is calculated in the section at the bottom of the wall. The three chosen places in the building are: 1. Wall between classroom and gallery. 2. Wall between opening in the gallery. 3. Wall of classroom (figure 73).

In all three cases the unity checks are lower than 1 (Tables 2-4). All cases therefore meet the imposed requirements.



WALL BETWEEN
CLASSROOM AND GALLERY

Table 2 | Hand calculations

Handcalculations location 1	
Volume [m³]:	11,76
Floor area [m²]:	4,2
Wall thickness [mm]:	600
Wall length [mm]:	1000
Section area [mm²]:	600000
Density [kN/m³]	19,6
Stress max [Mpa]:	2,6
Permanent floor load [kN/m²]:	1,35
Variable floor load [kN/m²]:	1,5
Safety factor material:	2,5
Safety factor loads:	1,5
Force calculated [kN] (included sf):	363,70
Force allowed [kN]:	624,00
U.C. force:	0,6
Stress calculated [Mpa] (included sf):	0,61
U.C. Stress:	0,6

Figure 73 | Hand calculation areas



WALL BETWEEN
GALLERY OPENINGS

Table 3 | Hand calculations

Handcalculations location 2	
Volume [m³]:	20,07
Floor area [m²]:	3,6
Wall thickness [mm]:	600
Wall length [mm]:	1200
Section area [mm²]:	720000
Density [kN/m³]	19,6
Stress max [Mpa]:	2,6
Permanent floor load [kN/m²]:	1,35
Variable floor load [kN/m²]:	1,5
Safety factor material:	2,5
Safety factor loads:	1,5
Force calculated [kN] (included sf):	605,45
Force allowed [kN]:	748,80
U.C. force:	0,8
Stress calculated [Mpa] (included sf):	0,84
U.C. Stress:	0,8



EDGE WALL

Table 4 | Hand calculations

Handcalculations location 3	
Volume [m³]:	8,95
Floor area [m²]:	3
Wall thickness [mm]:	600
Wall length [mm]:	1000
Section area [mm²]:	600000
Density [kN/m³]	19,6
Stress max [Mpa]:	2,6
Permanent floor load [kN/m²]:	1,35
Variable floor load [kN/m²]:	1,5
Safety factor material:	2,5
Safety factor loads:	1,5
Force calculated [kN] (included sf):	275,96
Force allowed [kN]:	624,00
U.C. force:	0,4
Stress calculated [Mpa] (included sf):	0,46
U.C. Stress:	0,4

One of the studies we did was to see if the catenary arcs of the ribs could be approximated by an ellipsoid arc (figure 74). This was done because this would simplify the marking and building of the formwork on site. The analysis was done using Ansys, see figure 75. When we analysed the results from Ansys we could conclude that the catenary arch is much more efficient in transferring the loads than the ellipsoid arch. Part of the reason why the difference was so big was because the arch was very shallow. If the arch would have been taller/steeper the ellipsoid arch would become more efficient and probably usable. In the end the arches used in the project remained catenary in shape because of their efficiency (figure 75).

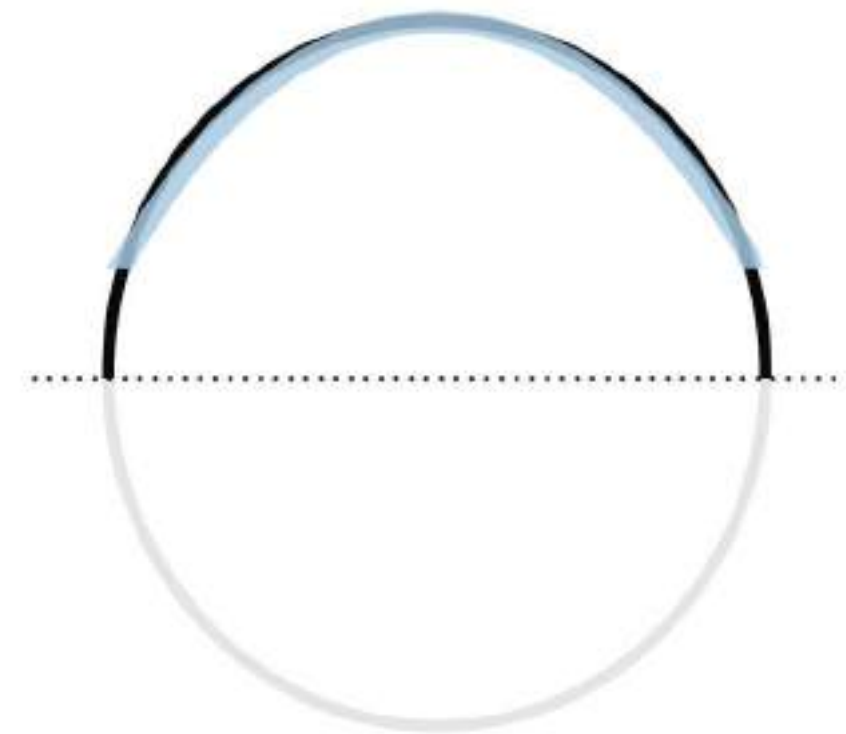


Figure 74 | Ellipsoid arc and catenary curve

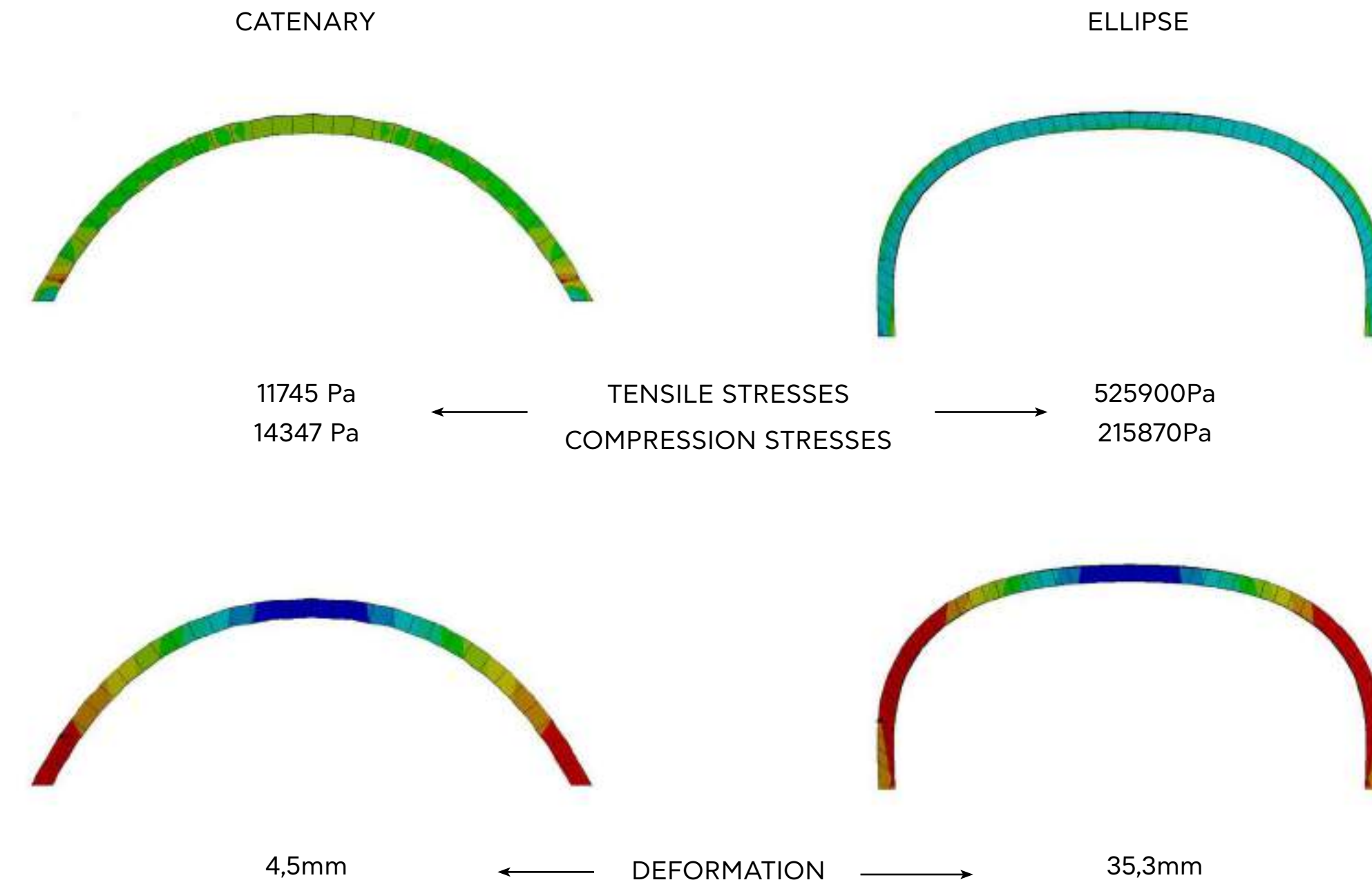


Figure 75 | Ellipsoid arc
and catenary curve ANSYS
analysis

Figure 76 shows the analysis of the classroom and gallery vault. For the gallery, classroom vault combo, Karamba3D was only used to estimate if the thrust line was correct. This was done because at the time it was difficult to achieve a reliable result that matched the hand calculations and the Ansys results. The reason for this was that above these two vaults, another floor was placed. This combination of a vault ceiling that supported another floor was difficult.

To make the results more reliable we did two things. The first was that the Karamba results for this part of the buildings construction was used to determine if the trust line was already mostly in compression. The second step we took was to import a solid model into Ansys to determine the stability of the two storey structure. The solid was less difficult to simulate and to get results that were more in line with the hand calculations.

As seen in Figure 76 the ceiling structure is in compression but also in tension. At first this appears to be a relatively undesirable thrust line. But there are several things to consider when looking at this figure. The top floor was not simulated,

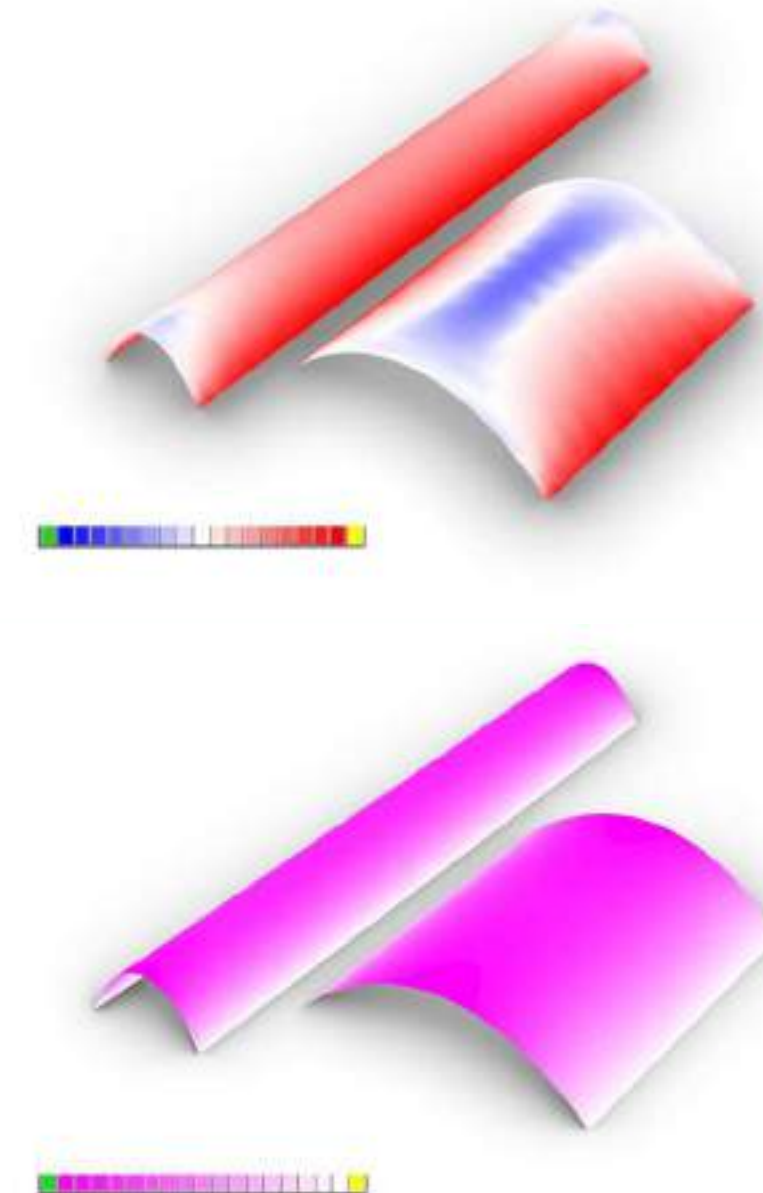


Table 5 | Karamba analysis results

Karamba Results						
Vaults	Cross section (mm)	Max Disp.	Princ. Stress 1 (Mpa)		Princ. Stress 2 (Mpa)	
			Max.	Min.	Max.	Min.
Gallery F0	210	7.3 mm	-0,009120	0,001770	-0,039700	-0,009730
Classroom F0	210	15 mm	-0,024200	0,003040	-0,125000	-0,043100
Classroom F1 cluster 1	210	11 mm	-0,051500	0,019400	-0,082200	0,009180

Figure 76 | Classroom and gallery vault Karamba analysis

which means that additional forces will be put on the sides of the arch. This would cause the thrust line to change and become more towards a compression construction. Another thing to consider is that the tension forces are relatively small and within limits, therefore they are acceptable.

When we analysed the outcome of the Karamba mesh in figure 76 and table 5 we saw the following; the total structure was indeed mostly in compression only and the tension forces were low enough not to cause any structural problems.

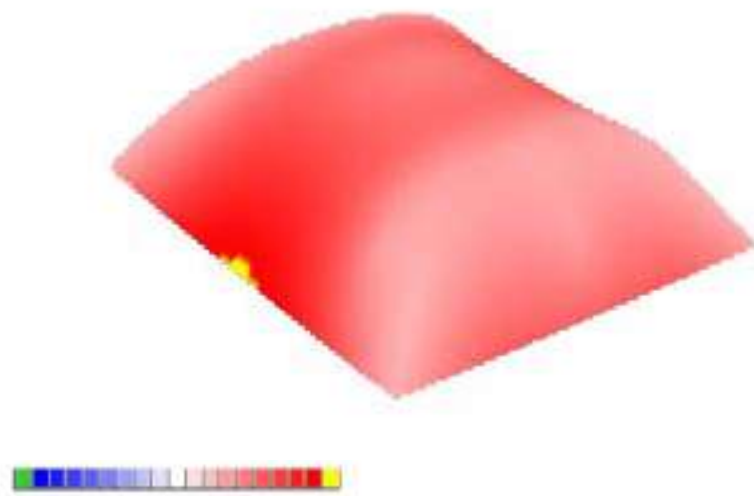


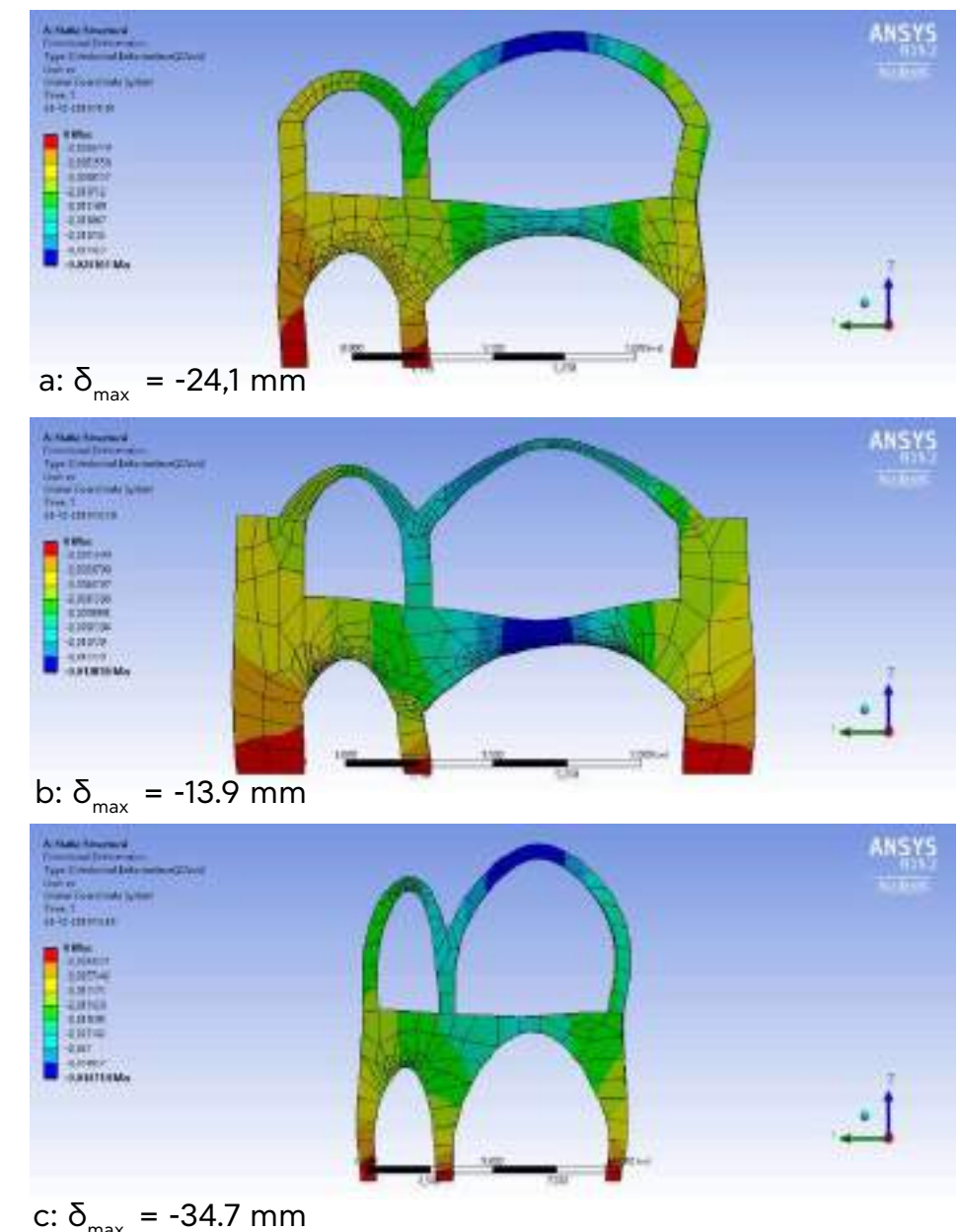
Figure 77 | Top floor classroom Karamba analysis

The advantage of ANSYS simulations in comparison with Karamba3D is that an entire building can be placed in it instead of a surface. For these ANSYS simulations, the same piece was taken from the entire design, classrooms with galleries. With these simulations, a search was made for the correct shape of the building. The ANSYS simulations looked at stresses and deformations. Compression stresses matched the structural requirements from the beginning, but the problem was in the deformation. Figure 78a shows the results of the deflection of the very first model.

Various options were tried to limit deformation. One of the best working options was to make the outer walls thicker. Figure 78b shows the model with walls of 1.6 meters. These walls ensured that the building kept its shape with less bending as a result, but a building with walls of 1.60m was not desirable.

An attempt was also made to make the form steeper. The consequence of this was that the building became much higher and that the stairs in the building would no longer fit, because they also became longer (figure 78c). The expectation was that this form would work best. The results do not show this. This was probably because the shape was not dynamic relaxed again, but scaled. The forces in this form did not therefore run as they should have.

Figure 78 | Ansys analysis
 a. Initial mesh
 b. Thicker walls
 c. Steeper vaults



In the figures 79 and 80 the results of the final chosen shape are shown. The finest mesh that was possible with this license was used for these simulations. The maximum compression stress in this shape was 0.235 MPa. There was also slight tension in this shape, 0.257 MPa. This tension is 1/10 of the maximum allowable stress (compression). This is expected to be small enough to remain standing. The deflection was 1/33 of the thickness of the floor. This was still within the rule of thumb of 1/6 (15%). To see if this deformation was too much, a model was been made with this deflection and then simulated again. If too much tension would occur, this deflection would be too much. This simulation showed that the tension had increased, but was still very small compared to the maximum allowable compression stress. (Table 6).

Figure 79 | Ansys stress analysis of final mesh

Figure 80 | Ansys deformation analysis of final mesh

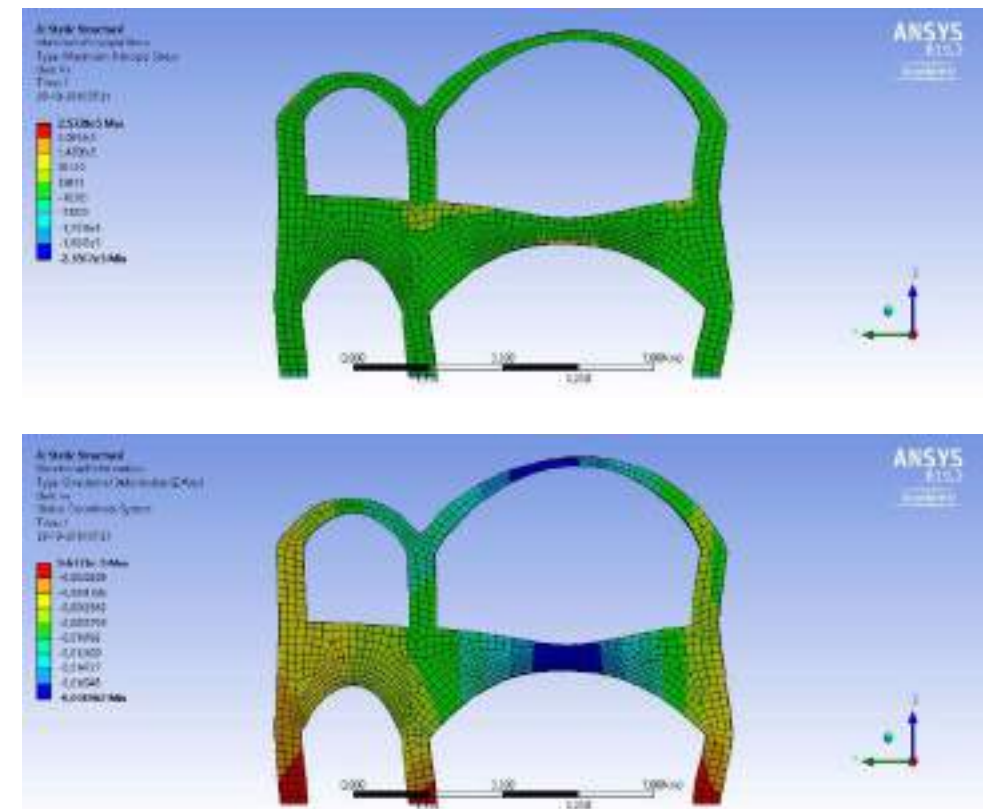


Table 6 | ANSYS analysis results

Ansys Results Vaults	Cross section	Max Disp.	Princ. Stress	
			Max.	Min.
Classroom and gallery	210	18,7 mm	-0,214 MPa	0,171 Mpa

As seen in the construction part of this report, the top floor classroom is a combination of a vault combined with a rib structure. Because the construction exists from these two different elements we had to look at them individually. The stresses from the vault can be seen in the total mesh from Table 5. The ribs however had to be calculated and simulated on their own.

First hand calculations were made if the Adobe material could handle the loads from the weight of the infill bricks. From we calculations we could conclude that it was possible with a cross section of 130*130 mm (16750 mm^2). However, in the end it was decided that the cross section had to be increased for two reasons. Firstly, because the calculated cross section the standardized brick size would not fit. The second reason was because the ribs fulfilled a very essential part in the construction. Therefore, an extra layer of security was added. This was done in the form of an increased size of the cross section so that more bricks were added. This reduced the risk of failing adobe bricks in the case of low quality bricks. In the end this resulted in a cross section of 210*150 mm (31500 mm^2) almost doubling the capacity of the rib.

The last step of the rib analysis was to model and simulate the ribs in Karamba, figure 83 and Table 7. This analysis showed that compressive and tension forces where within limits. The same counts for the deformation numbers. The only factor that Karamba did not account for was the fact

that the ribs were not loaded from the top e.g. a beam and floor combination. But the ribs were loaded from the sides. This would mean that the total capacity of the rib would not be used to support the weight of the infill bricks. This is illustrated in figures 81, 82. We could not simulate what the total used area of the rib would be due to time constraints, and because we deemed the overcapacity of the ribs to be large enough to support the loads. But if this were to be simulated this would have to be done in Ansys, in order to obtain this would give the most accurate results.

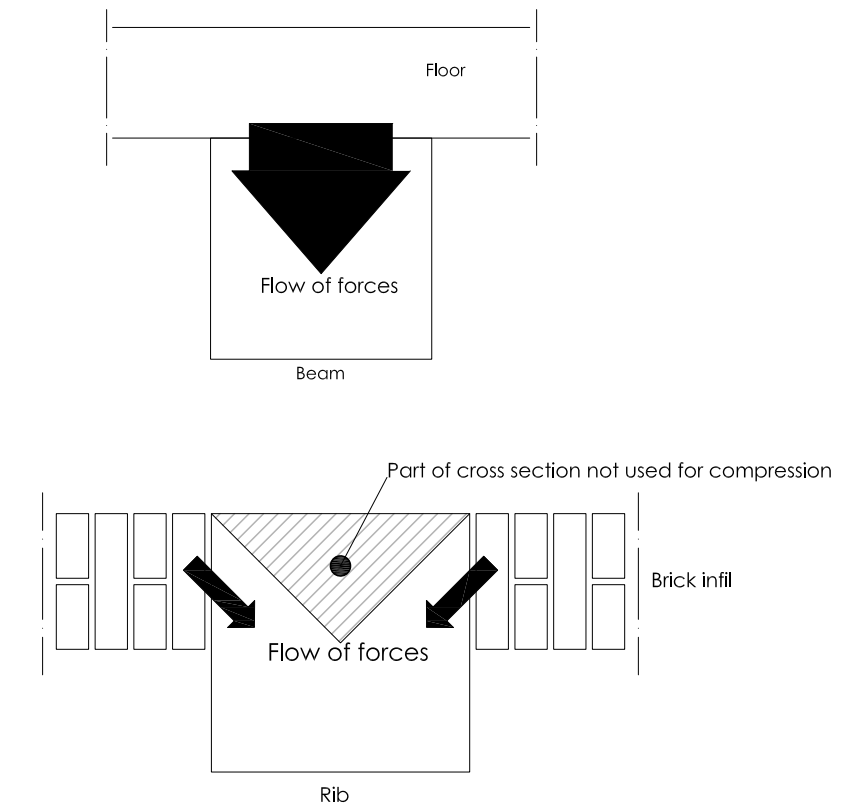


Figure 81 | Force flow of typical beam structure

Figure 82 | Force flow of rib structure

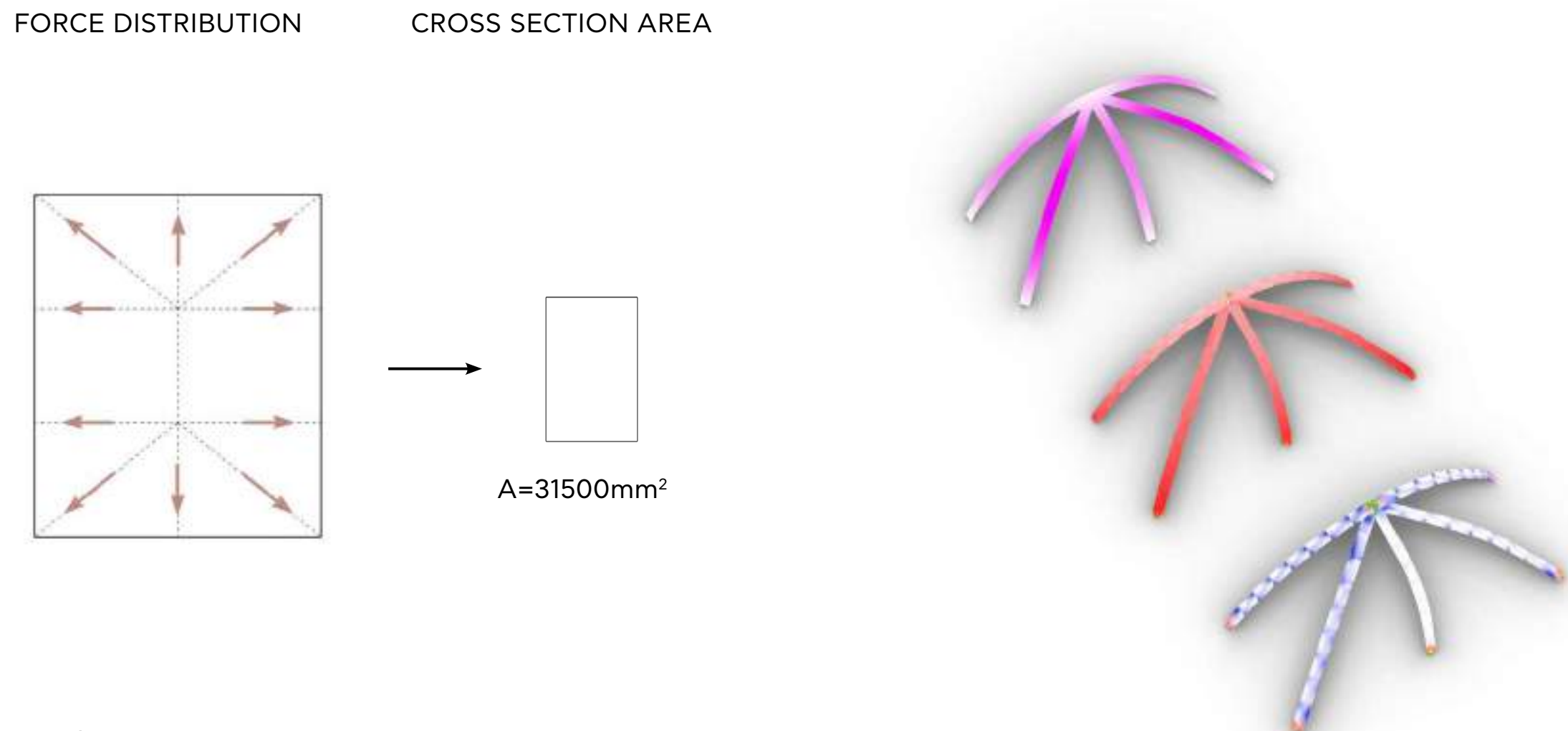


Table 7 | Karamba analysis results

Calculated cross section Ribs					
Avg. Stress on ribs (N)	Mpa Sample	mm ² needed	Cal. Cross.	Used Cross. (mm)	mm ²
33500	2	16750	129,4*129,6	210*150	31500
Rib's					
Cross section (mm)		Max Disp.	Princ. Stress 1 (Mpa)	Princ. Stress 2	
			Max. (Mpa)	Min.	Max.
Rib classroom	210	15.8 mm	-0,116000	0,234000	-0,349000

Figure 83 | Rib Karamba analysis

6 CONSTRUCTION MANUAL

Having completed the forming and structural verification of the complex, step by step instructions are provided to guide the builders through an easy construction process. The analysis starts with the work planning, the necessary materials and tools. Then the brick making and drying process is explained. The construction of each building element is explained (walls, ceilings, roof etc.) and finally the details of the building (stairs, openings).

To begin organizing the process, all the materials and tools should be gathered. One of the main goals was to minimize the import of materials and make use of those that are already available on the camp. The main construction material is adobe brick. So for the brick making the materials needed would be: clay (from the camp), coarse and fine sand (from the camp), straw (from the creek west of the camp) and water (from the water tanks of the camp). The additional materials listed below in Table 8 are needed for the foundations, measurements and formwork.



Table 8 | Material table

APPLICATION	flooring bricks mortar coating	flooring bricks mortar coating	foundation	flooring bricks	measurement tool	preparation tool	preparation tool	formwork brick molds	formwork
SOURCE	on site	on site	on site	creek west of the camp	on site	on site	waste on site	waste on site	waste on site
RE-USABILITY	yes	yes	yes		yes	yes	yes	yes	yes

Apart from standard tools such as shovels, pickaxes etc, the above mentioned materials also have to be altered to act as DIY tools. The use of cardboard is explained further on (chapter 6.8). The scrap wood is meant to be used for the brick molds and for formwork of the vaults in the top floor. After having obtained the curve meant to be followed by the formwork (chapter 6.8), wooden planks need to be placed following the curve and nailed together. Additional diagonal pieces should be added or the stability of the structure (figure 84).

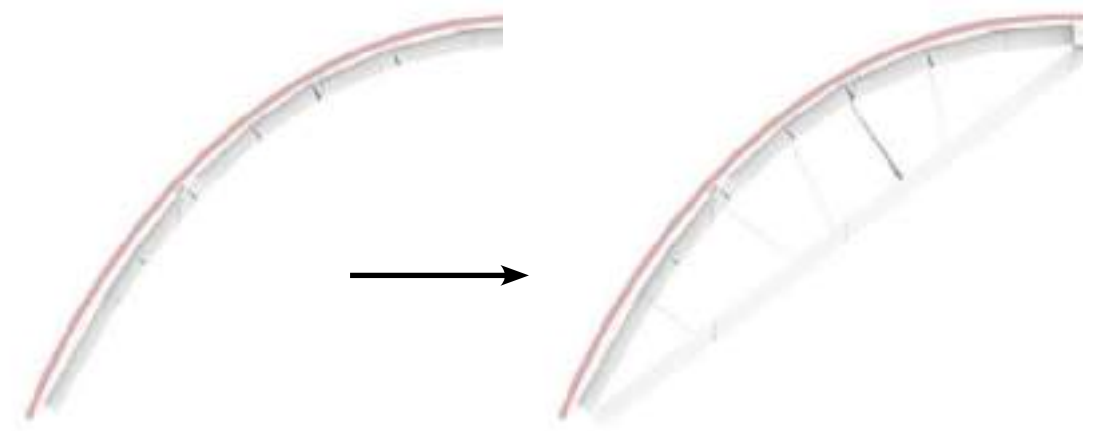


Figure 84 | Rib formwork

After completing the brick making and breaking workshop, calculations were done and the consistency of the strongest mixture was chosen (see Appendix I). Four different additives were tested, within the pure adobe mixture: rubber bands, cotton textile, straw and wood chips. Out of those four the mixture with the straw gave the best results (see Appendix I).

The exact composition within the mixture is 27.3% clay, 27.3% fine sand, 36.4% coarse sand and 9.1% water. The brick sizes are mainly two: type A, meant for walls and stairs has a size of 300x145x90mm (2 headers+mortar=1 stretcher, for bricklaying) and weighs 8kg (figure 85). It is a subdivision of the architectural module set during the layout configuration. For the laying of the corners a brick with half the width is required, so much less of this brick type will be needed. Finally, for the vaults and arches, a lighter brick was required for construction reasons (figure 87). That is brick type C, which has a size of 210x10x50mm and weighs only 2 kg per brick. This means that three different molds types should be made on site, giving priority to types A and B, which will be the first to be used for the walls.

For the drying to be uniform throughout the bricks, they should be dried in the shade. Usually the bricks are laid in rows on the ground, otherwise they may be placed in columns, allowing air to pass through them (figure 86).

Figure 85 | Adobe mixture materials

Figure 86 | Brick drying placement in rows and columns

BASIC MIXTURE



27.3% CLAY
27.3% FINE SAND
36.4% COARSE SAND
9.1% WATER

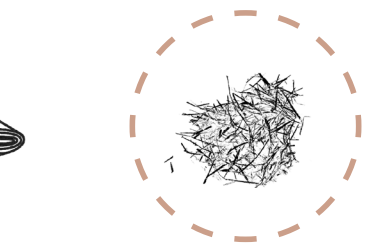
ALTERNATIVE ADDITIVES



RUBBER BANDS



COTTON FABRIC

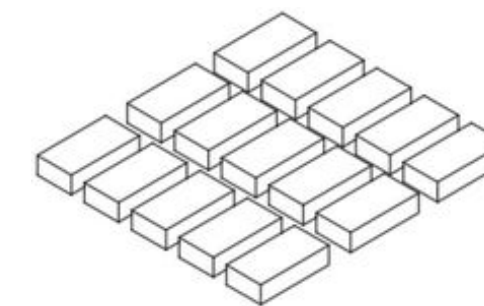


STRAW



WOODCHIPS

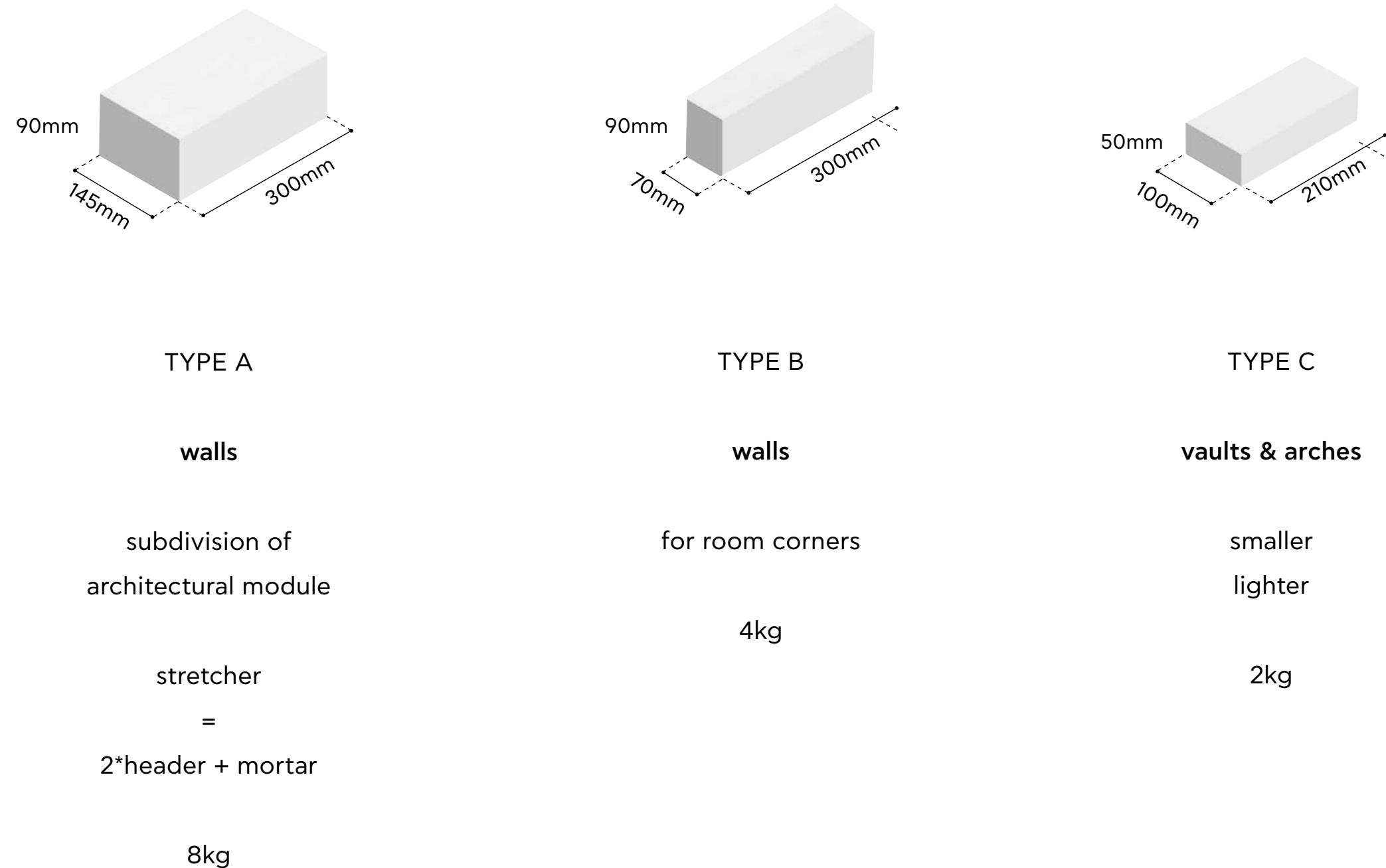
BRICK DRYING



ROWS



COLUMNS



One of the first tasks in order to build the foundation is to define the building outline. This can than be used to excavate earth for the foundations. Considering the building was designed based on an architectural module, ropes could be used as a measurement tool, by tying knots per 1.2m. To ensure that the rectangles marked are indeed rectangles (figure 88), the length of the diagonals can be used as a verification.

The foundations are meant to prevent moisture from getting into the adobe walls. Considering the wall thickness is 600mm, the trench dug out should have a width of 1200mm. The suggested depth of the trench is 400mm. The trenches need a stable base, for which rammed sand will be used. On top of that natural stones should be placed, protruding 600mm over floor level, to create a water resistant base for the structure. Alternatively, if natural stone cannot be found, burnt bricks can be used (figure 89).

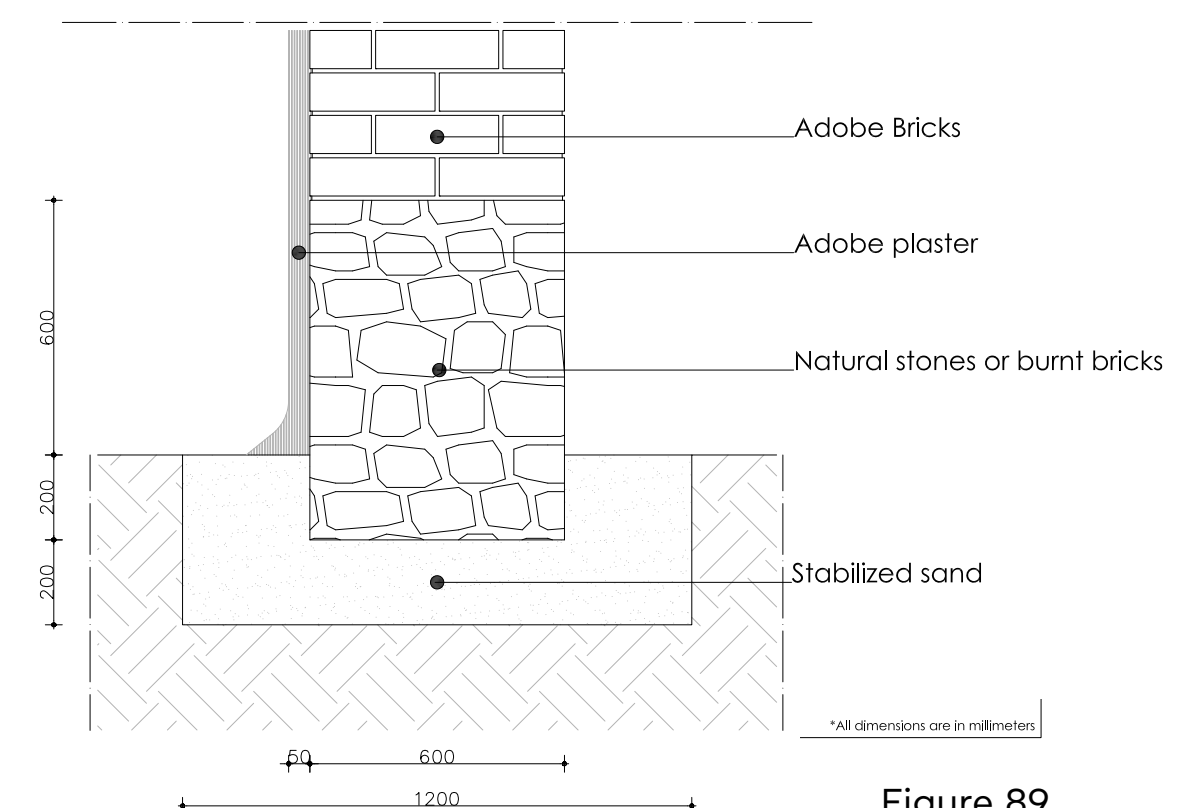


Figure 89

Figure 88 | Marking of room outline method

Figure 89 | Foundation section

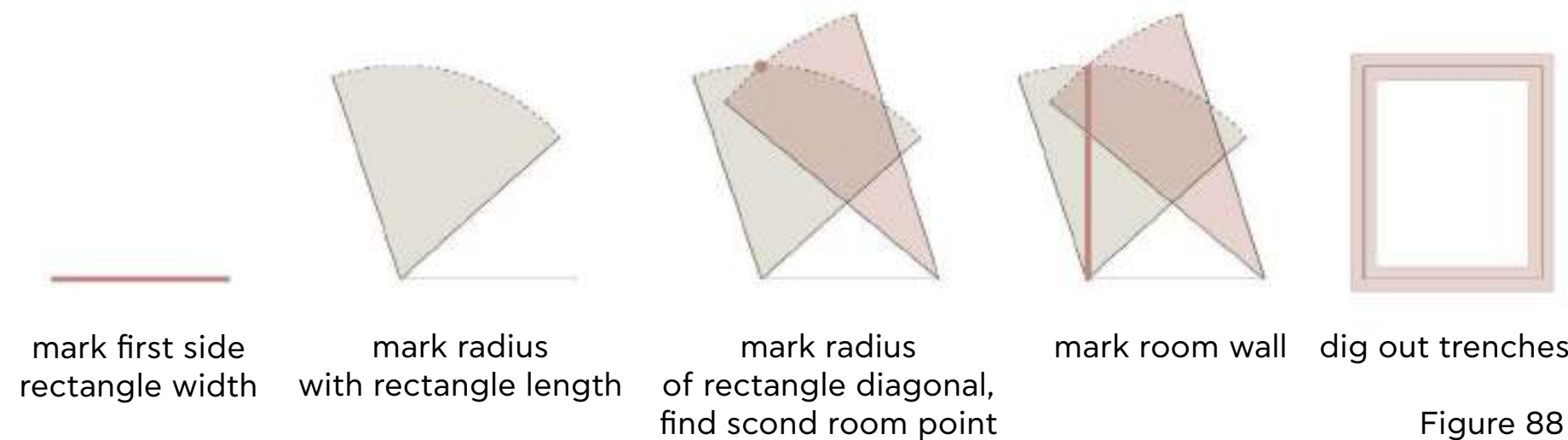


Figure 88

Our proposal consists of straight on which the ceiling structures land. For the bricklaying the english bond was chosen, as it is a simple pattern to explain to inexperienced builders and results in a strong bond. There are two patterns which are alternating one on top of the other (figure 90). The walls all have a thickness of 600mm (half an architectural module) and a height of 2.4m (two architectural modules in the z direction). Another benefit of this bricklaying is that it can easily be adapted to a wall of an increasing thickness, by building from the outside inwards (figure 91). The bricks used for the walls are type A and type B is added in corners or intersections (figure 90).

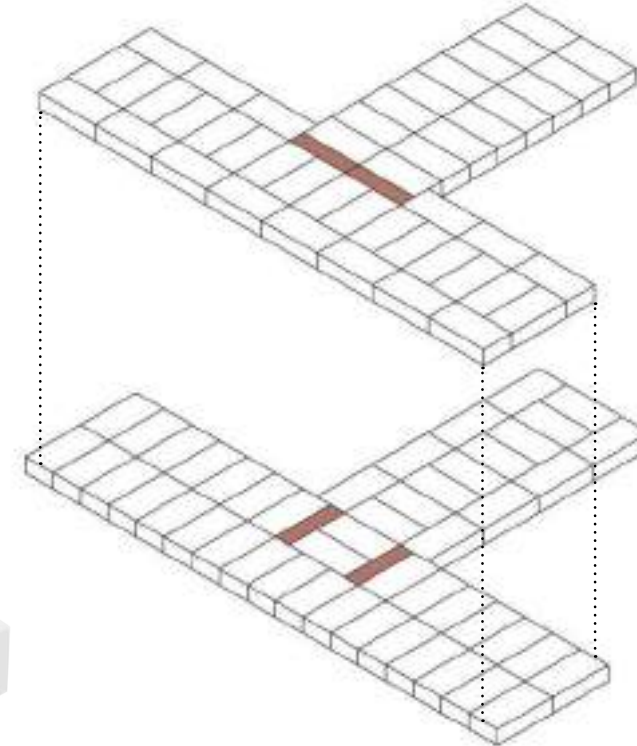
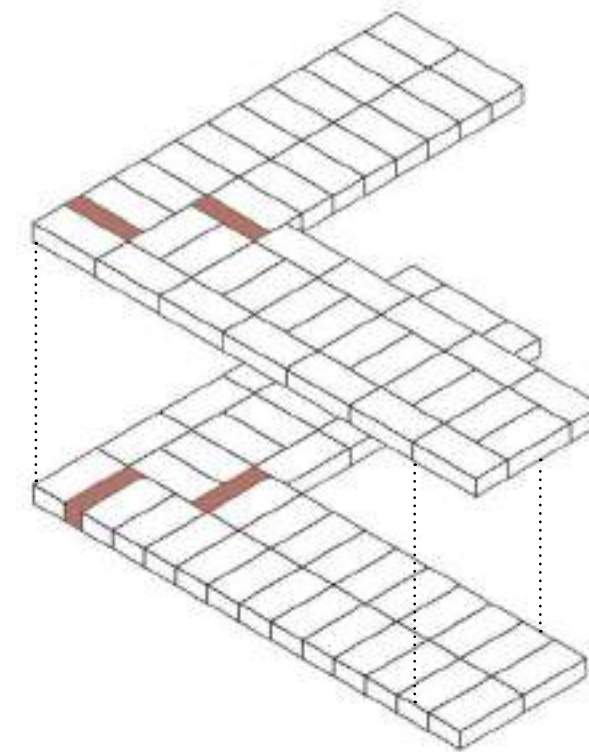


Figure 90 | Wall corner and intersection bricklaying

WALLS	TYPE BRICKLAYING	BRICK TYPE A & B	A 3D rendering of a single grey rectangular brick.	A 3D rendering of a single grey rectangular brick.
-------	---------------------	---------------------	--	--

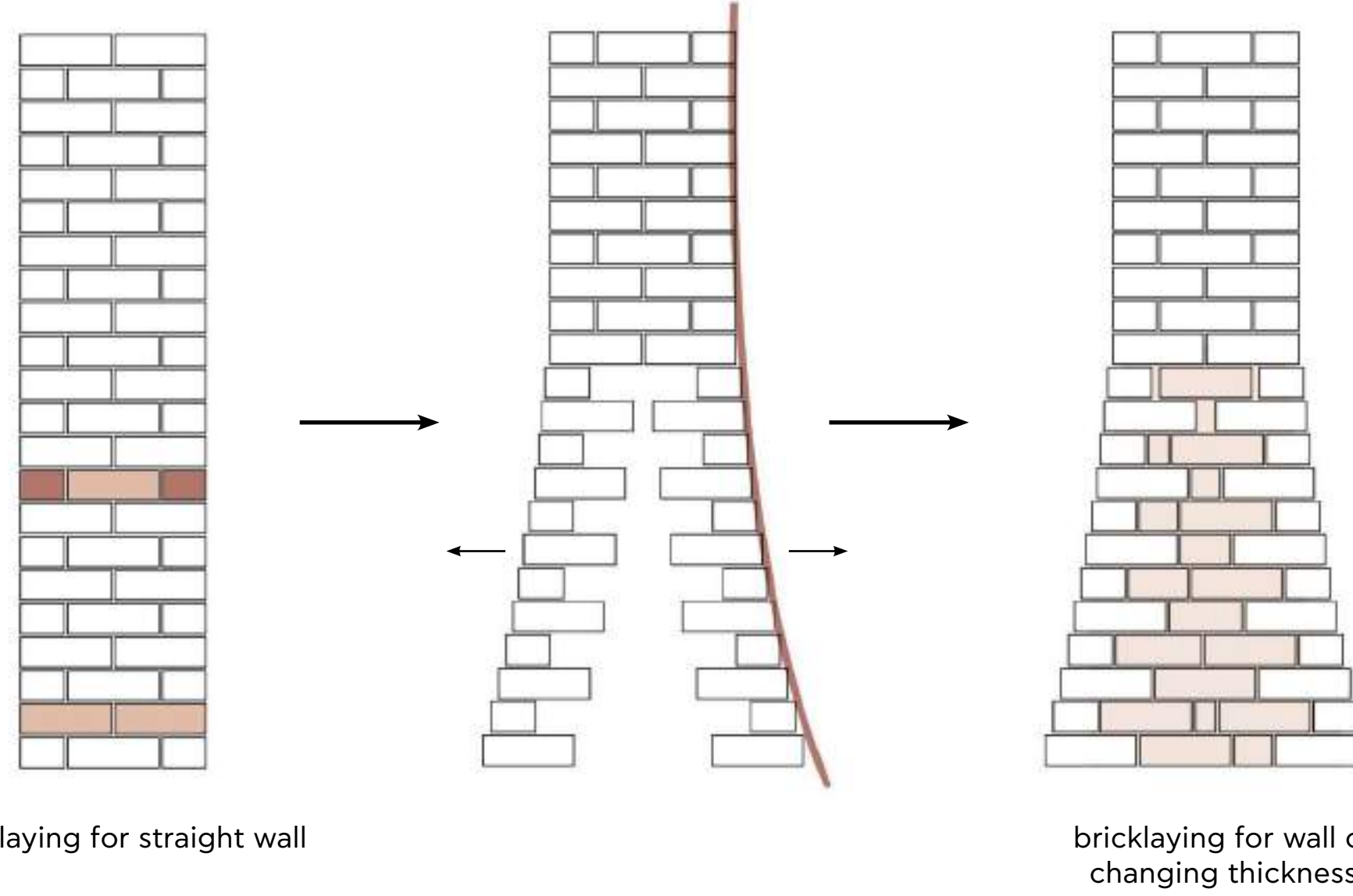
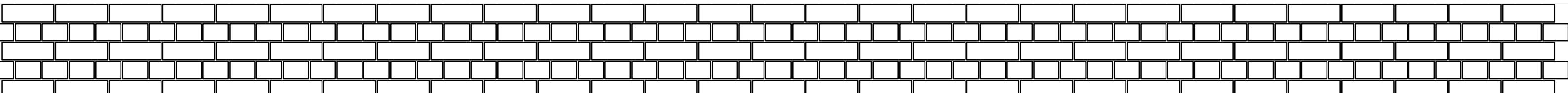


Figure 91 | Bricklaying for wall with increasing thickness

BRICKLAYING PATTERN



Since the castle is a large complex, it cannot be assumed that it will be built altogether from the start. Instead it should be built in phases, just as castles usually are. There are three different clusters, as mentioned in the layout chapter. Construction should begin from cluster one, since it is the most inclusive with classrooms, administration, restrooms and the canteen. The construction analysis will be focused on cluster one, which is representative of the rest of the complex.

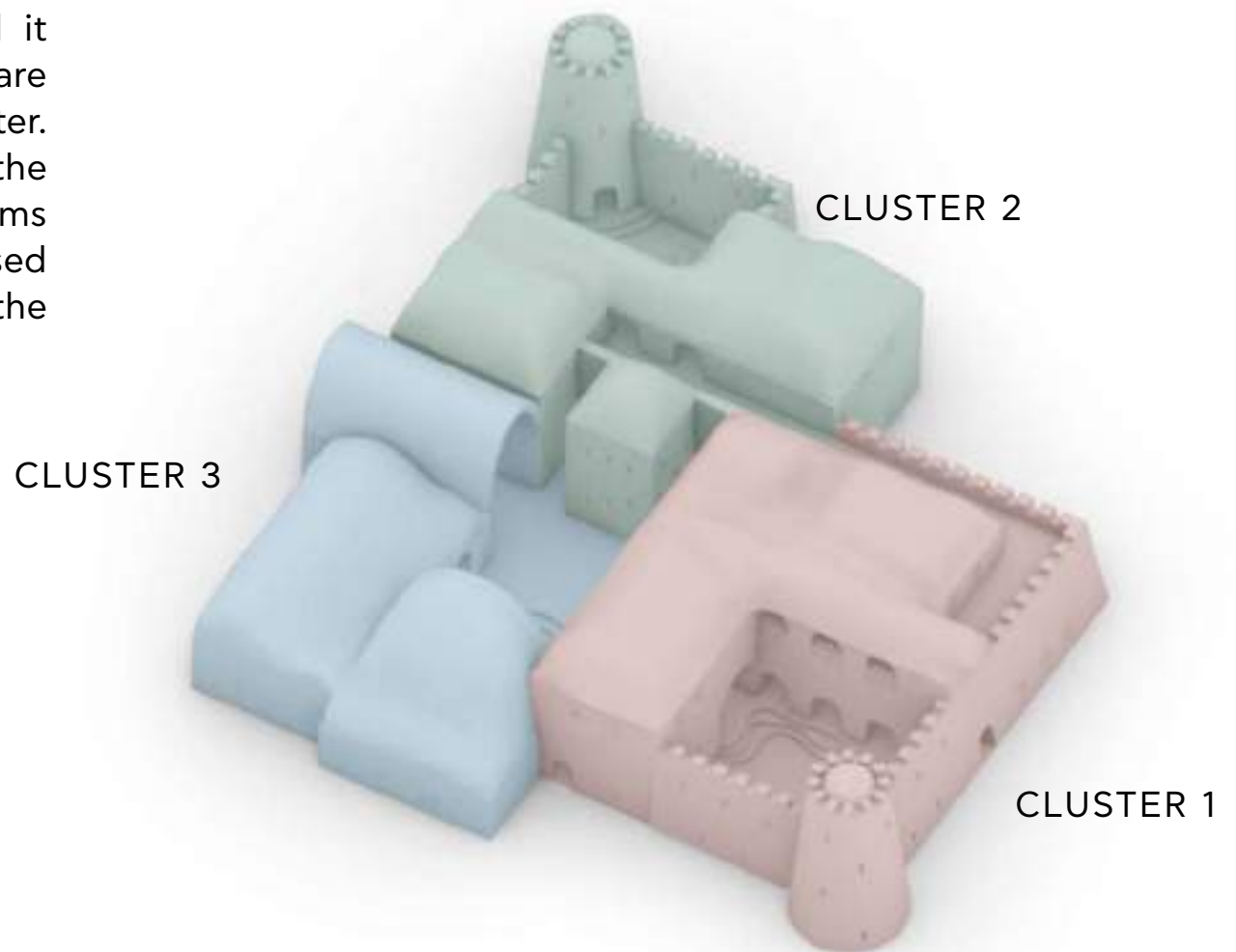


Figure 92 | Construction phases of clusters

For the ground floor, as mentioned in chapter x.6, the desired ceiling for the classroom was a quite shallow vault. This was to reduce the height difference between the classroom and the gallery, thus reducing the material needed for filling and for stairs. Initially stacking methods with a conventional brick were tried, however due to the curve this construction method had to be rejected (figure 94).

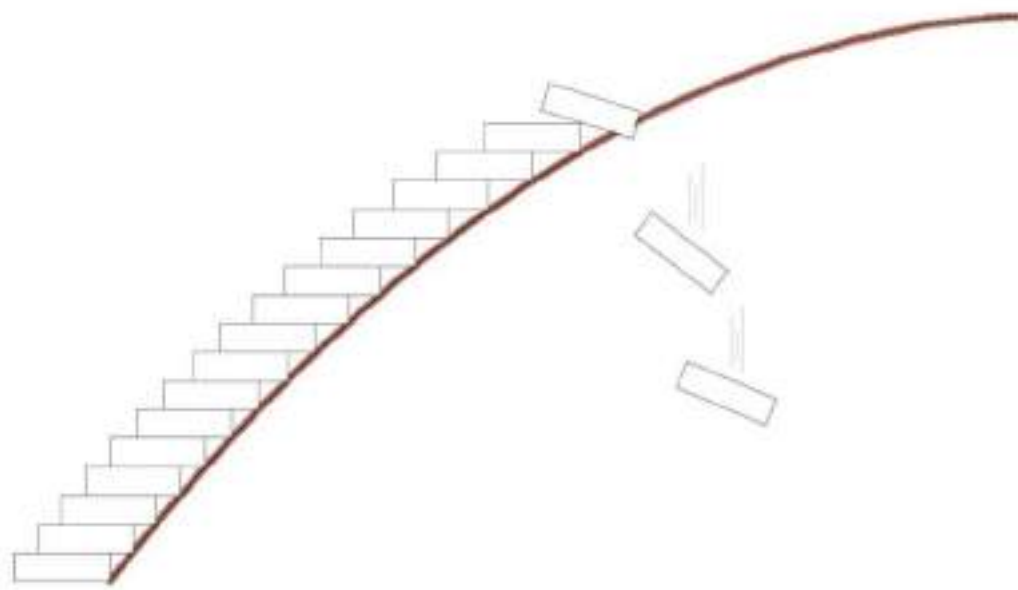
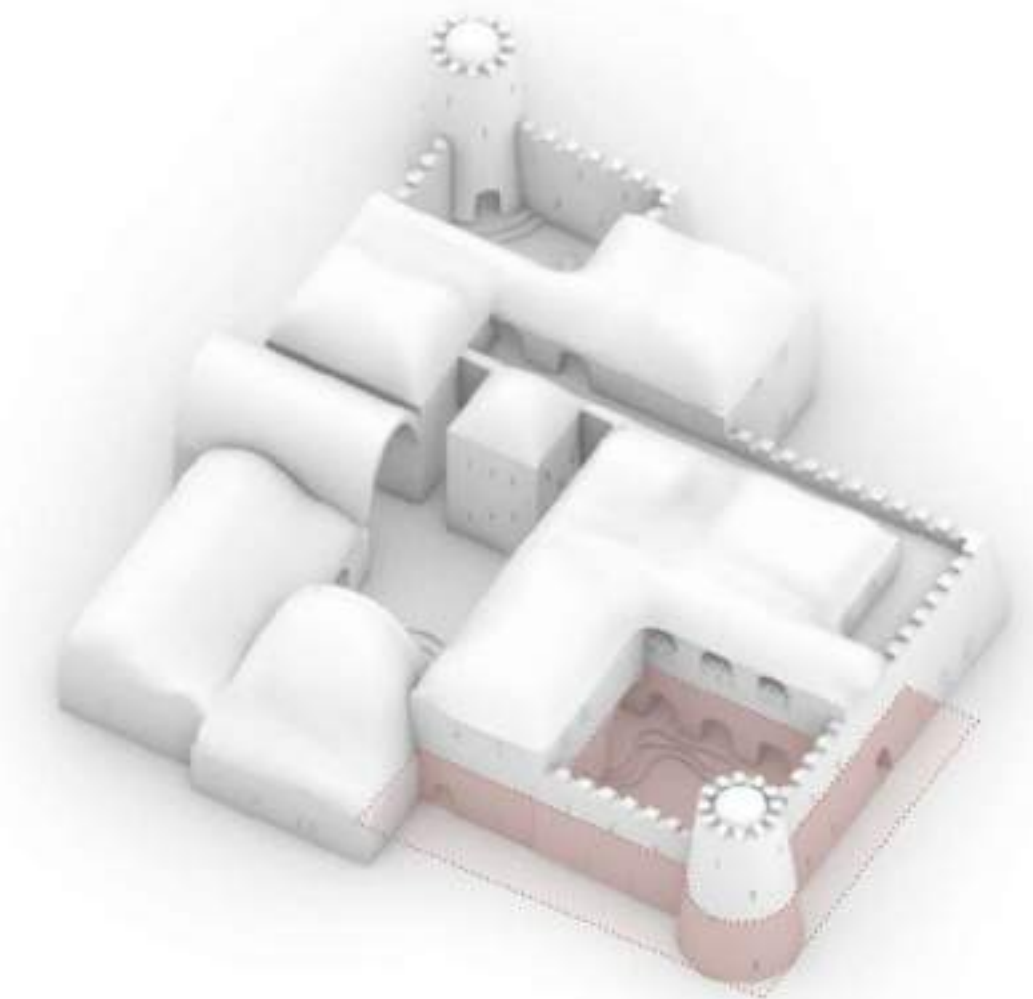


Figure 93 | Ground floor

Figure 94 | Brick stacking problem

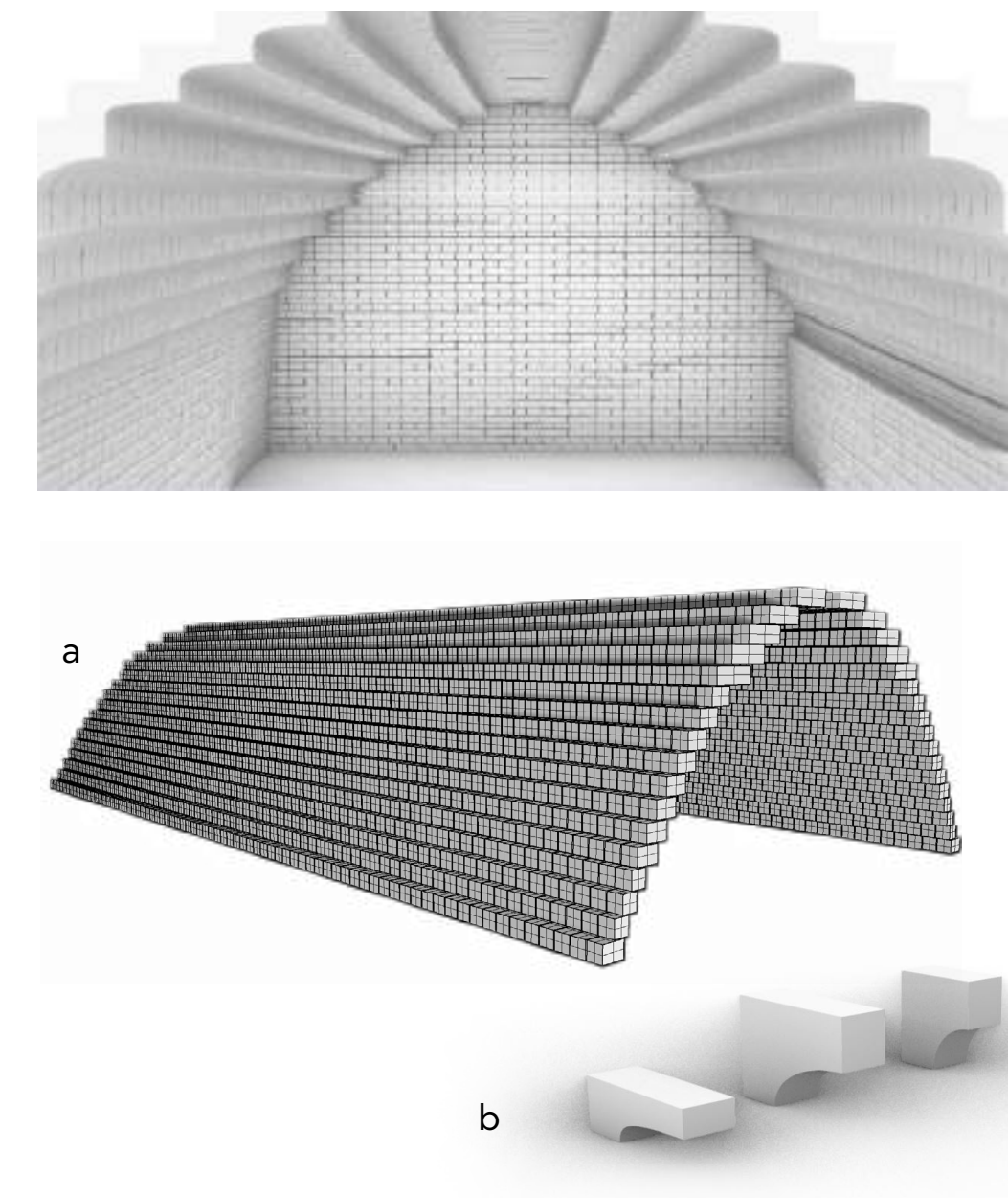


Muqarnas “half domes” and vaults were also considered, but eventually were ruled out. Muqarnas could have provided an easier manual for construction builders. As long as the right type of brick per layer was specified, the rest was simple bricklaying. The positioning of the bricks would be relatively easy as well, as muqarnas bricklaying do not require any scaffolding or temporary structures. Also the architectural expression in the classroom, would be very unique (figure 95).

To better understand if this solution could fit the design, a bricklaying script in Python was made and a C# code of Pr. Nourian was examined and further developed. (see Appendix K). In the first case, half of the ceiling surface (the other half would be mirrored after) and the four different types of muqarnas were imported (Figure 96b). The different bricks, accommodated for the changing curvature of the ceiling. The imported surface, was divided every 30cm in the z direction. Then, depending on the curvature of the slope angle of the surface, the appropriate brick was placed (figure 96a). With the inverted approach, the C# code, first voxelated the surface, to find which voxels were intersected by it, so eventually, the design of the bricks could be defined. Although the scripts were not perfected, the disadvantages of this construction method for the design were already clear.

Figure 95 | Muqarnas classroom impression

Figure 96 | Python muqarnas script
a. Vault
b. Brick types



The most concerning challenge was the insufficient overlapping surface. Large cantilevers were necessary, which a material such as adobe couldn't withstand. In addition, bricks would be then placed on this cantilever, significantly compromising the stability of the entire structure. Only muqarnas with a steep slope could be used efficiently, however this would lead to a very high ceiling, which was not practical for the ground floor spaces.

Figure 97 | C# muqarnas script

- a. shallow vault
- b. steep vault
- c. overlapping problem

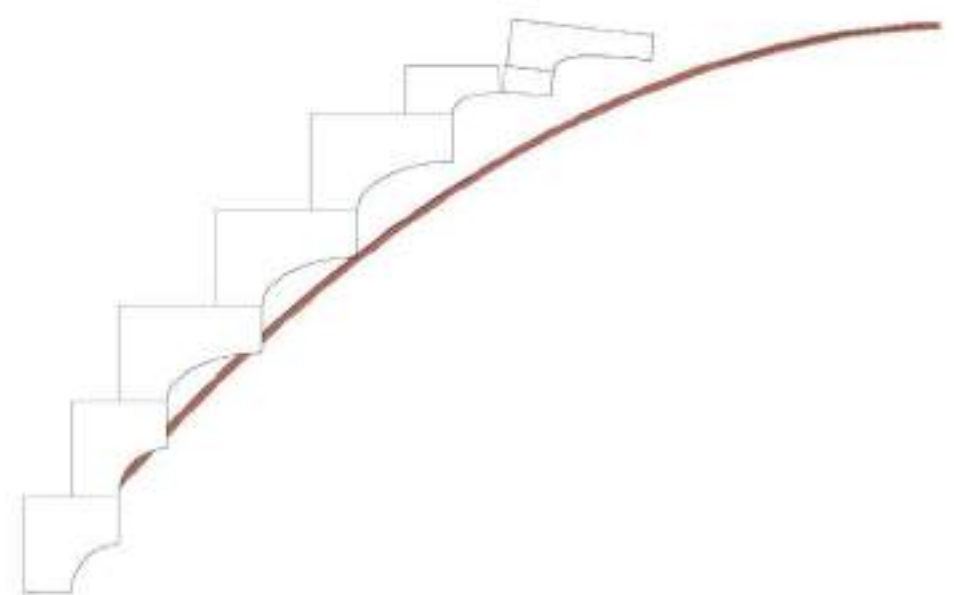


Figure 98 | Muqarna stacking problem

Figure 98

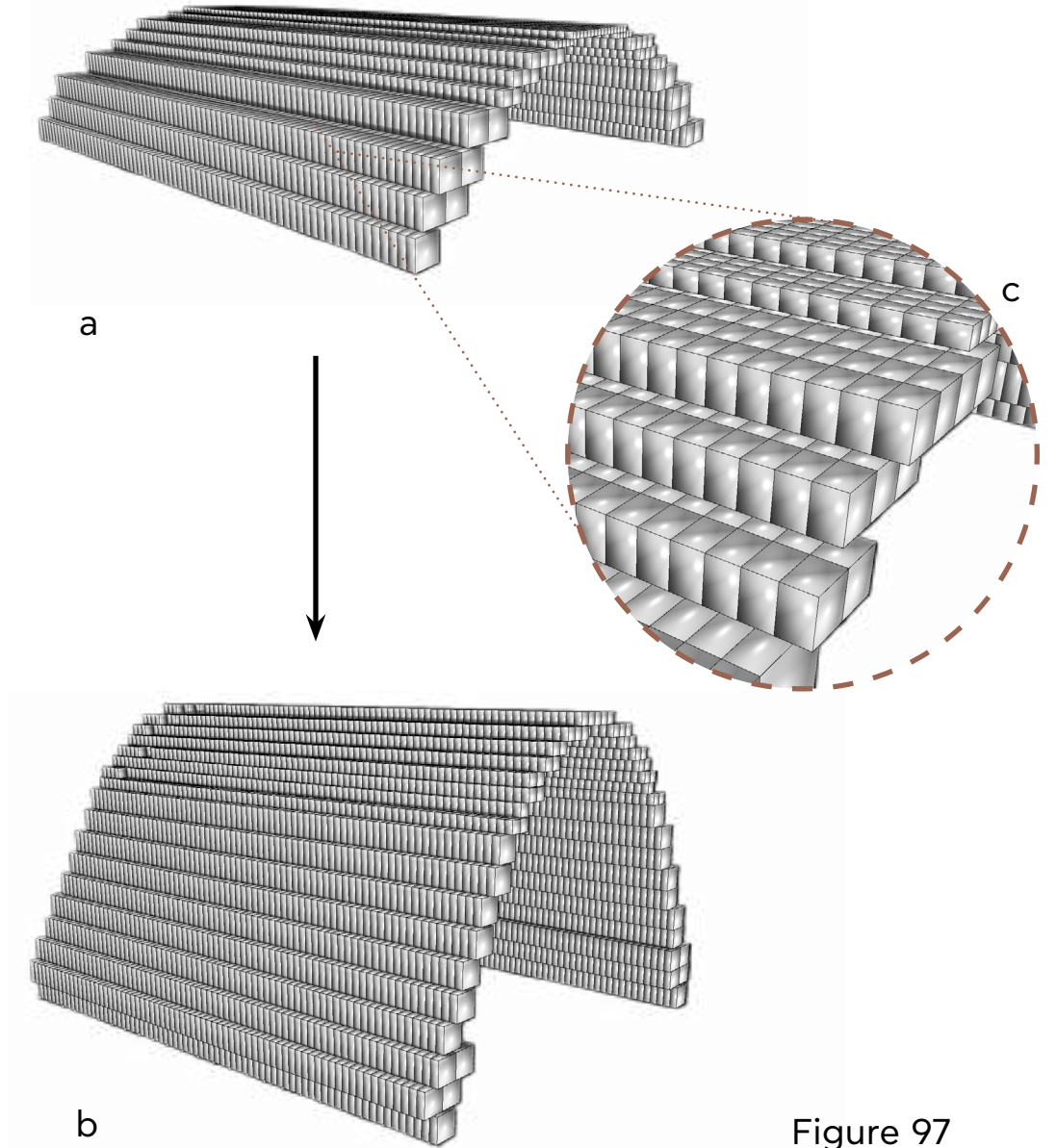


Figure 97

The greatest challenge of making the vault, was that the curve was a catenary curve, a geometry difficult to explain. However, making use of the catenary principle, the hanging of a chain to achieve the geometry, would be quite easy to do, as the spans are not too big. If one knows the spans and the maximum height of the two vaults (figure 99), the curve can be obtained. One has to find a wall, tape cardboard on it, and hang the chain to the desired dimensions. This method has been used on a one-to-one scale successfully by inexperienced builders before (reference the video). Then the cardboard can be cut on the curve and the cardboard can be placed on the wall, on the height of the vault (2.4m) to trace the curve with a knife on the wall (figure 100). The wall on which the vault will be built already exists, because it will be taller to reach the first floor.

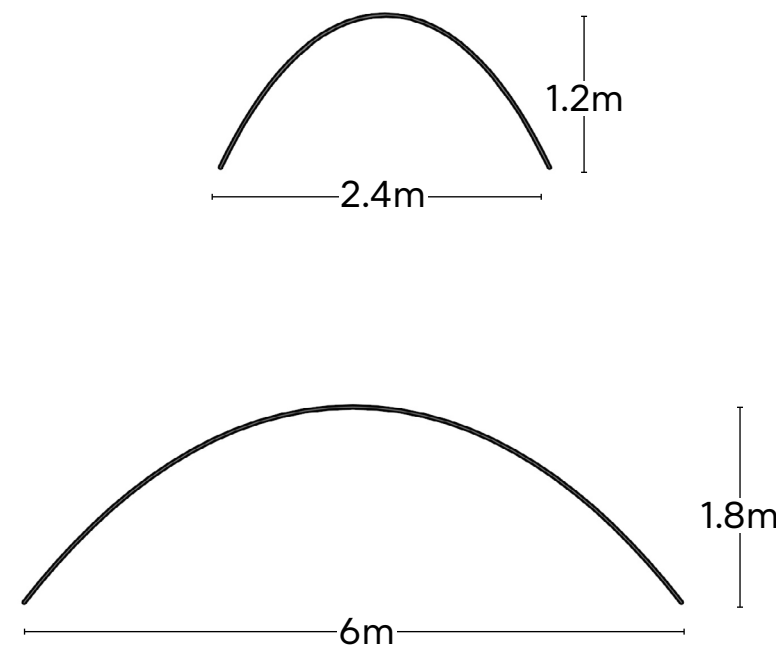
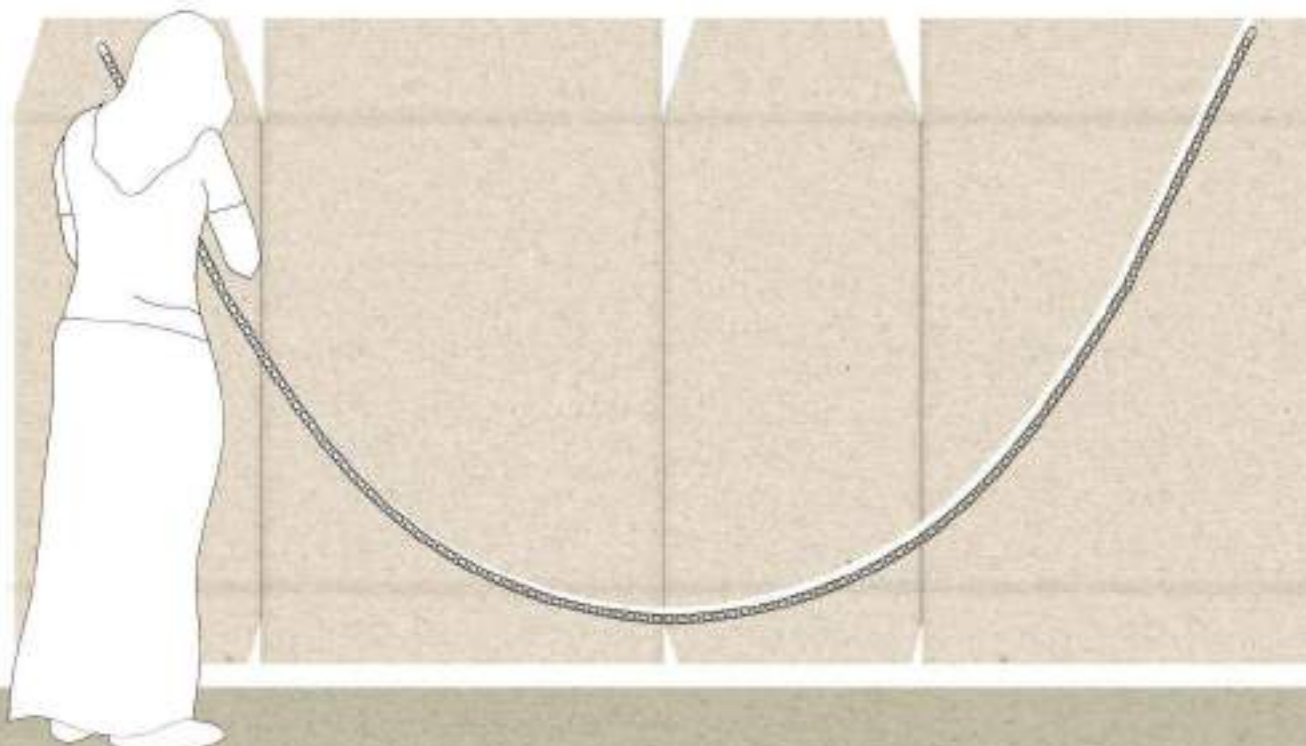
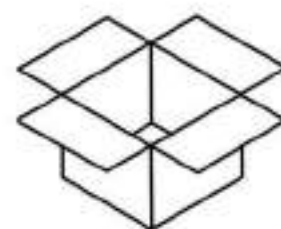


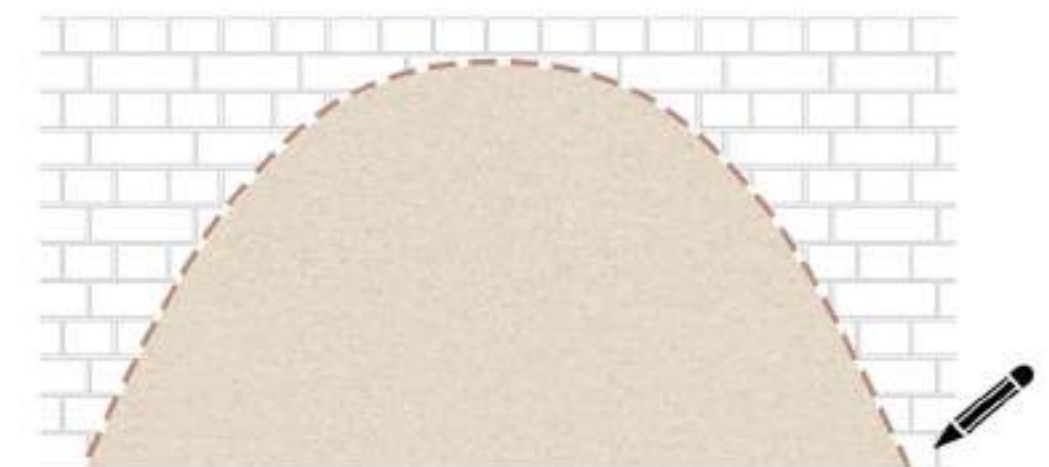
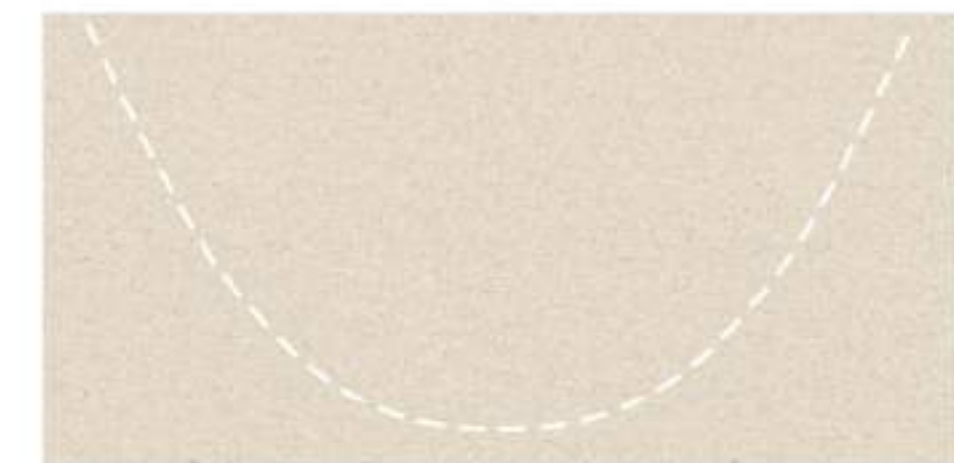
Figure 99 | Catenary curve dimensions

E Q U I P M E N T



T R A C I N G O F C U R V E

C U T C A R D B O A R D

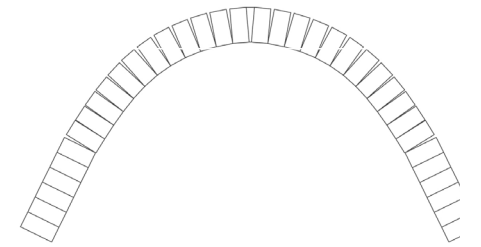


T R A C E C A R D B O A R D O N W A L L

Figure 100 | Catenary curve tracing process

After obtaining the trace of the catenary curve on the existing wall, the builder only needs the bricks (type c) and the mortar. The mortar used is adobe mortar and is meant to be sticky, which means it should have less water and more clay than the brick mixture. Having a sticky mortar allows for the bricks to be simply stuck onto the wall, without needing additional support or scaffolding (figure 102). The bricklaying in the vaults has two alternating patterns, for the grout lines to not align (figure 101).

PATTERN 1



PATTERN 2

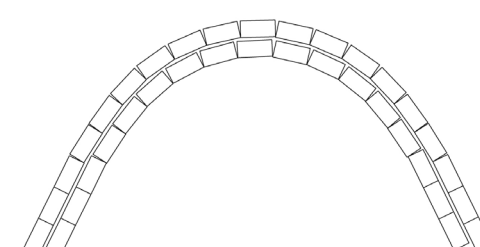


Figure 101 | Alternating brick patterns

Figure 101

Figure 102 | Bricklaying of vaults

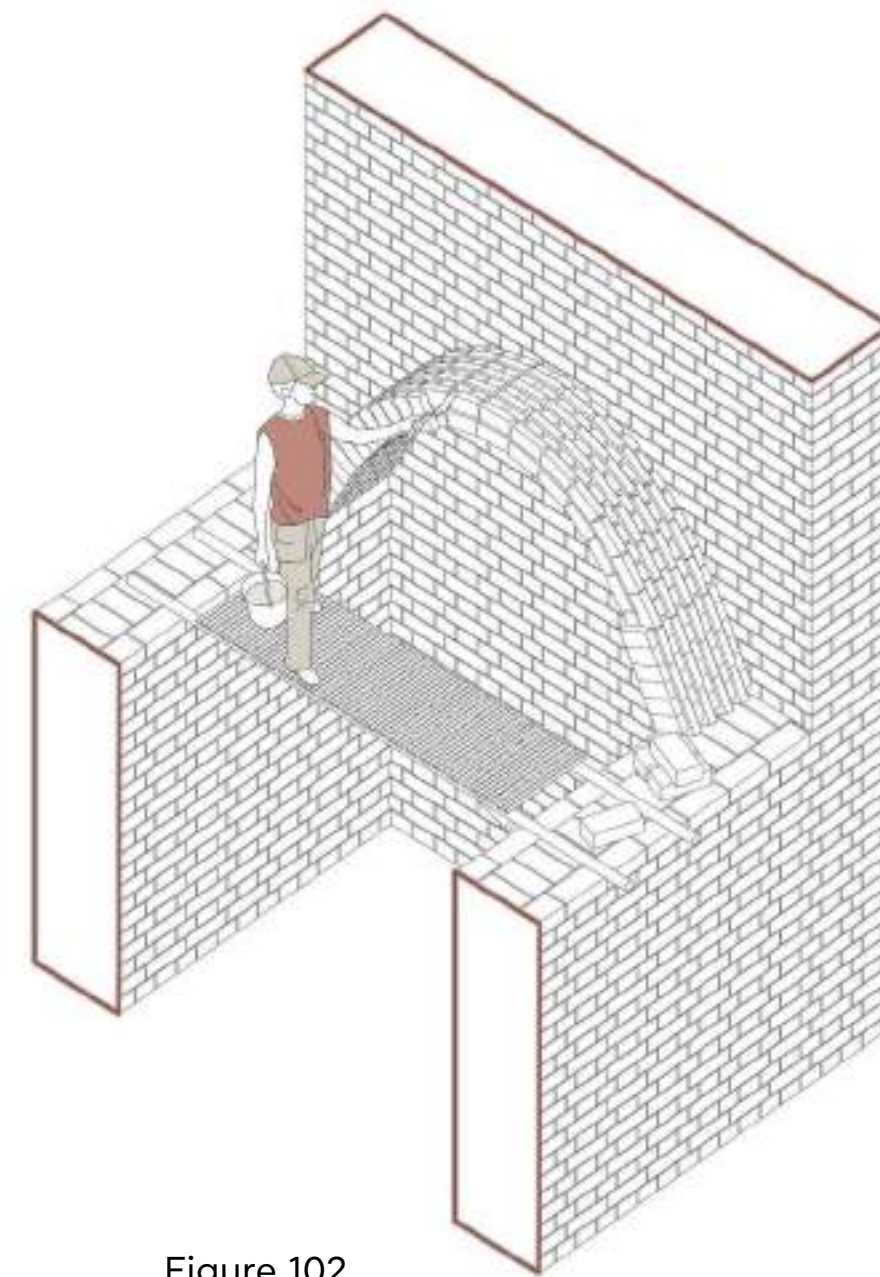
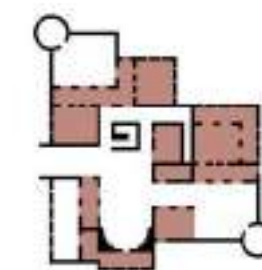


Figure 102

CEILING
STRUCTURES

TYPE
BARREL VAULT

BRICK
TYPE C



The bricklaying of these vaults was done with a Python script, which explained below (figure 103).

The script starts with importing the relaxed mesh from Rhino. Using the Bounding Box tool, the span direction of this mesh will be determined. This will be done by evaluating the X and Y domain of the shape. The shortest one will become the span direction of the bricks.

Once the coordinate system of the mesh is set, the dimensions of the brick will be imported in the script. These dimensions can be updated any time in Grasshopper, thereby changing the brick pattern of the vault.

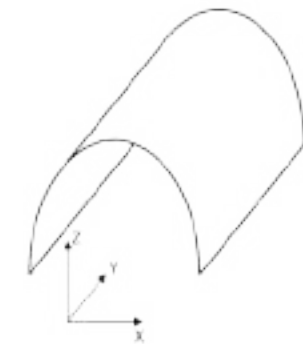
Thereafter the imported mesh will be contoured into the long direction. The distance between the contour curves depends on the dimensions of the bricks and how they are placed. In this case the bricks will be placed with the largest surface to the front. The distance between the curves will thereby be equal to the height of the brick + the thickness of the grout layer.

Once the contour curves are made, the list is split into two equal parts. One part only contains the curves with an odd index number the other one only contains the ones with even index numbers. By doing this, it is possible to make a shifted pattern in the bricklaying, which shifted pattern increases the strength of the structure.

The curves will thereafter be divided into segments. The size of these segments is, again, dependent on the dimensions of the bricks. In this case, the segment size equals half the length of the brick. Since that is the direction in which they are laid. On each segment a point is added. The next step is to divide the point lists again in even and odd items, to create the shifted pattern in the vault.

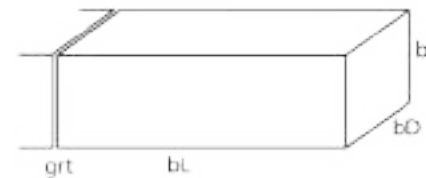
The final step is to place the bricks at the correct points. On the even curves, a brick will be placed at only the even points, on the odd curves, only at the odd points. This will eventually create the half-brick bond mentioned before. To make sure that the bricks are placed in the right direction, a new local coordinate system is made at each point. The normal of this plane is always perpendicular to the curve at that specific point, while the X-axis is equal to the tangent of the curve at that location.

If wanted, a second layer of bricks can be added on top of the first one. The only thing that should be altered are a second set of brick domains, this time with an offset distance to the curve. Also the even and odd points should be switched to keep the shifting pattern in the bricklaying.

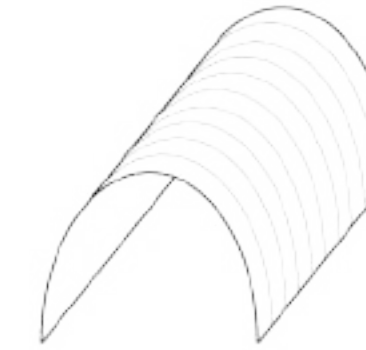


Step 1: Set up a new local coordinate system, based on span direction

bL = Brick Length
bD = Brick Depth
bH = Brick Height
grt = Grout Thickness



Step 2: Create the brick module, based on the input dimensions



Step 3: Create contour curves at a distance ($bH + grt$)

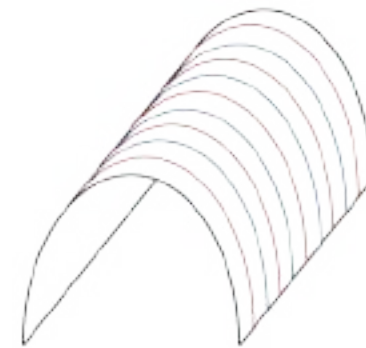
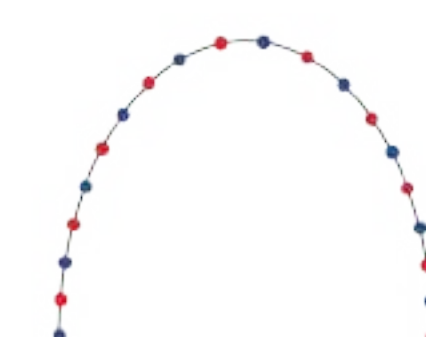
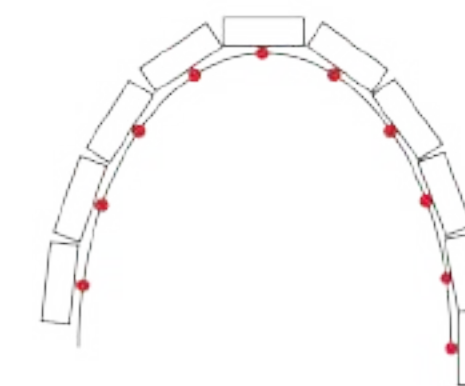


Figure 103 | Bricklaying python script

Step 4: Split the curves in even and odd lists. The base for the shifted brick pattern



Step 5: Create points on each curve, blue for even curve list, red for odd ones



Step 6: Assign the brick to the points to create the vault

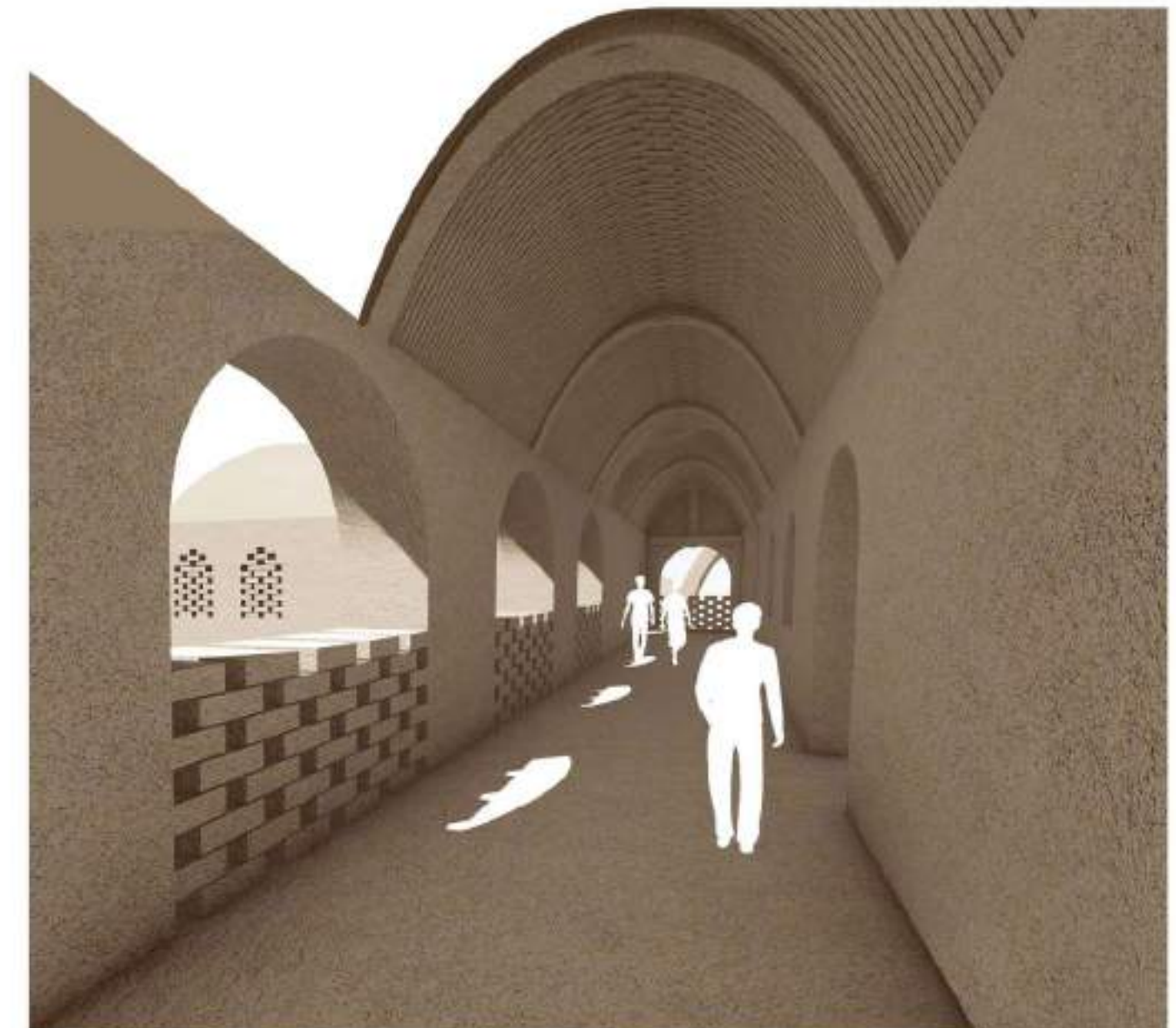
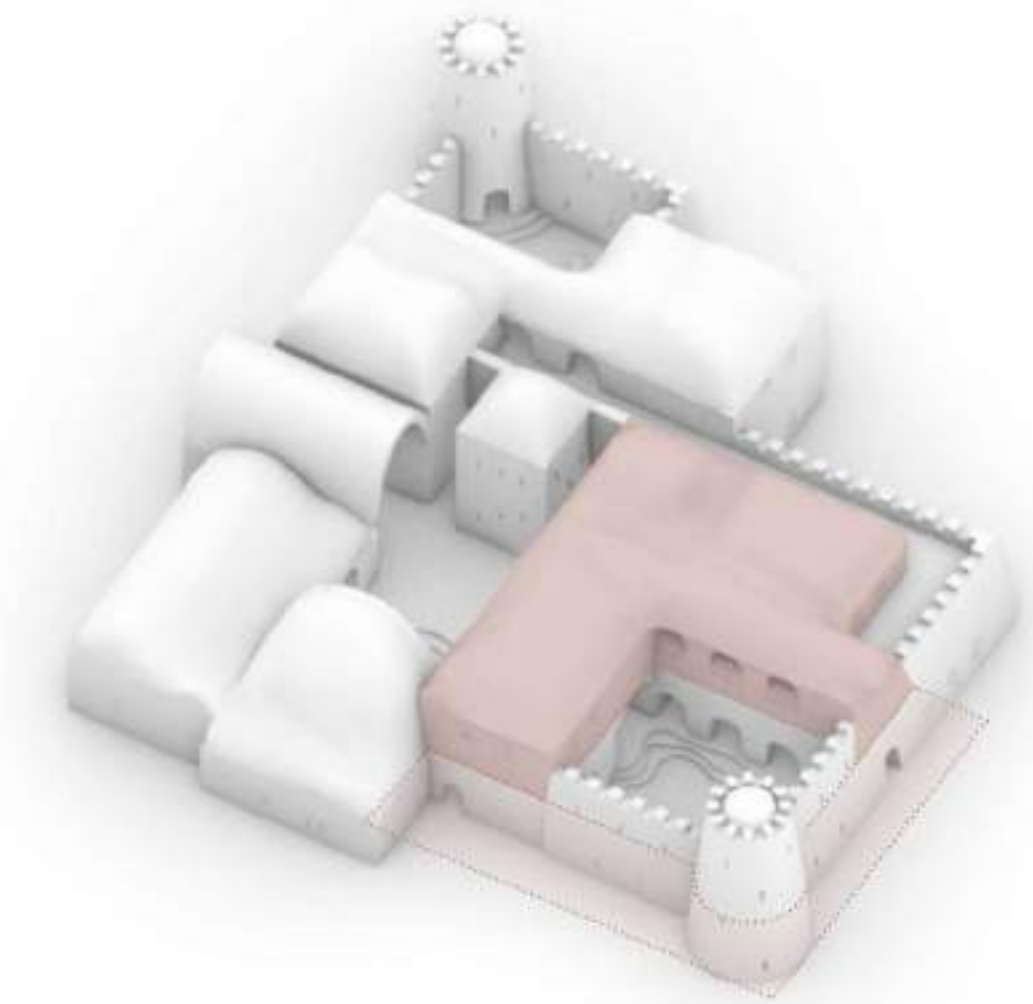


Figure 104 | Gallery vault

The top floor of the school no longer had the height limitation. For the galleries, the height remained unchanged, as it was adequately high for the according span, but for the galleries, the desired result was steeper than on the ground floor. The height was not the only difference from the ground floor though; it was decided that all the edges all would be anchored to the walls, otherwise the sharp edge of a vault would be exposed to water and weather corrosion. This meant that the construction method of the ground floor could not be repeated, as there would be no standing wall to lay the bricks on. However it would be a waste to not make any use of the acquired vault-making knowledge. That is how the solution of a ribbed vault was suggested. The ribs would define the corners of the spaces, while in between vaults could be made (with the same technique as the ground floor), that would be supported on the ribs.

After the amount of ribs was decided, the forces were evenly distributed to each rib, in order to calculate the required cross section area (see chapter 5.5). Eventually, that area was increased, to match the size of the bricks. Three different patterns for each layer of the rib were defined, to ensure the grout lines would overlap (figure 106).

Figure 105 | First floor



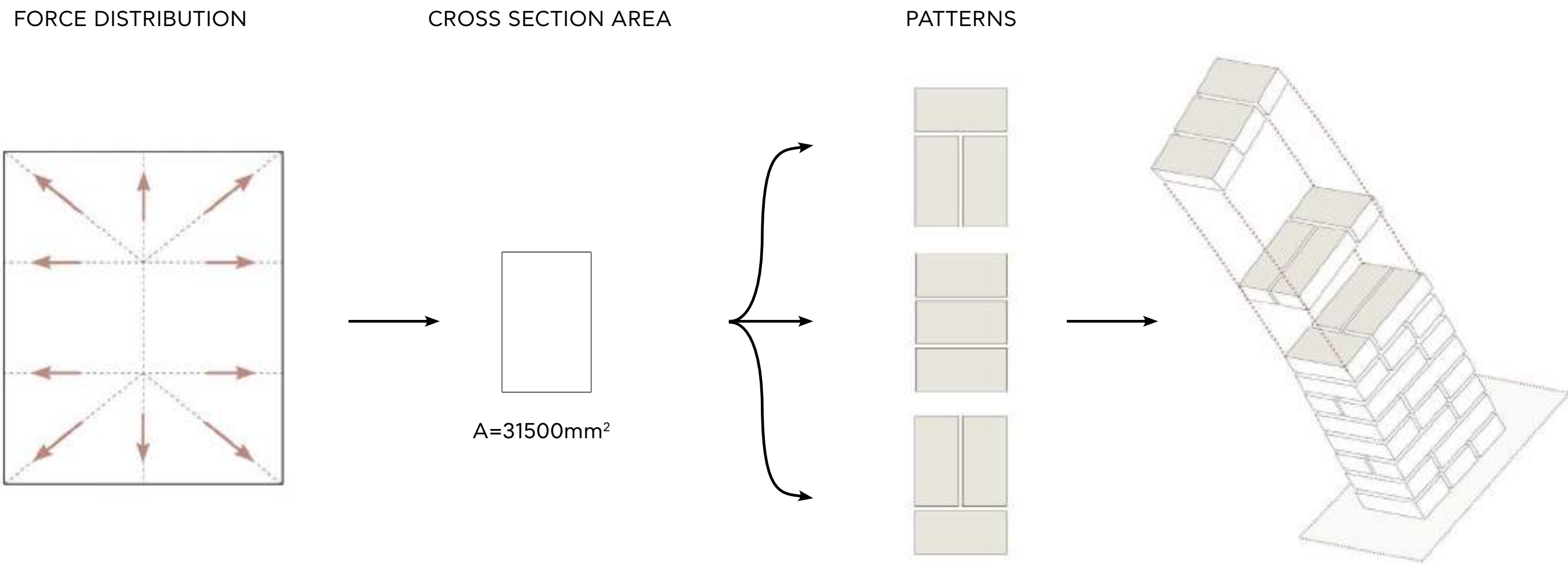


Figure 106 | Rib bricklaying



The construction of ribs, required formwork of some sort. To minimize the effect, all rooms had the same span. This way a lightweight formwork only had to be made once, and then could be moved around the complex 10 times to create the exact same structure. If the rooms making use of this structure were less, a temporary adobe wall might have been more sensible. Considering the repetitiveness though, building up and tearing down adobe structures so many times in the construction site, would only result in damaging the actual structure.

To support the formwork on the sides, the top floor walls should include protrusions, on which it will lay (figure 109a). In the center of the room, the formwork is supported by a pole. For the success of the construction another pole should be placed beneath the top one, otherwise the floor and ground floor ceiling will be damaged (figure 109b). After making the ribs, with an overlapping pattern at the point they meet, the vault in the middle section of the classroom is made, just as it was in the ground floor. Then, the rib over the vault is added, to receive the pressure from the ribs on both sides. Finally, the remaining spaces are small enough to be filled up with diagonally placed bricks and sticky mortar, without the need of any more guidance or supporting structure.

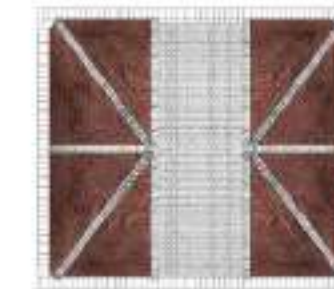
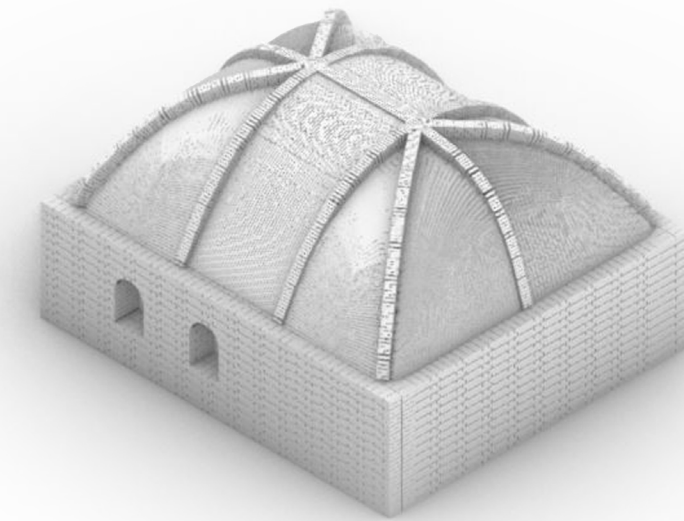
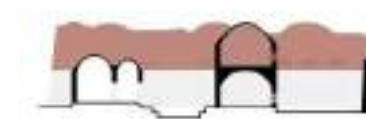
Figure 107 | Ribbed vault

Figure 108 | Classroom interior of ribbed vault

CEILING
STRUCTURES

TYPE
RIBBED VAULT

BRICK
TYPE C





FORMWORK BASE

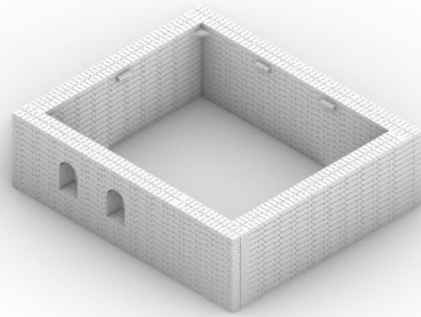
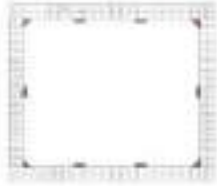


Figure 109a



PLACE FORMWORK

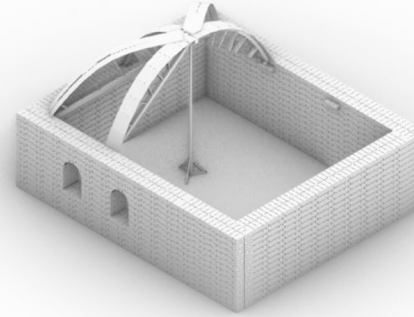
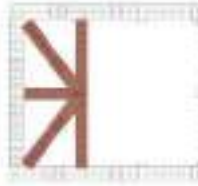


Figure 109b



BUILD RIBS

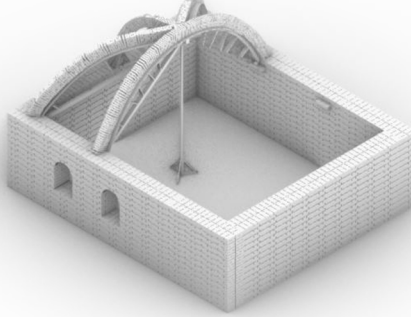
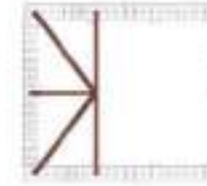


Figure 109c



BUILD VAULT

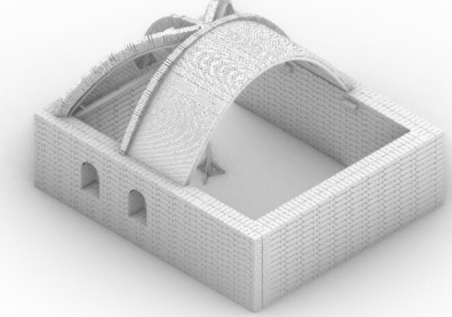
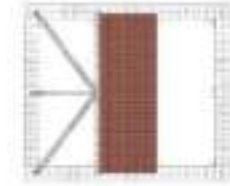


Figure 109d



BEWARE!

place a second pole on
the ground floor, beneath
the top floor one!

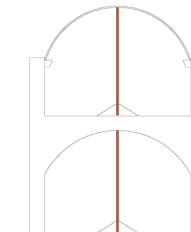
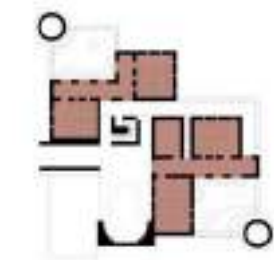
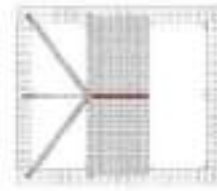
CEILING
STRUCTURESTYPE
RIBBED VAULTBRICK
TYPE C



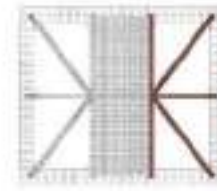
Figure 109e



BUILD RIBS



Figure 109f



FILL IN THE REST

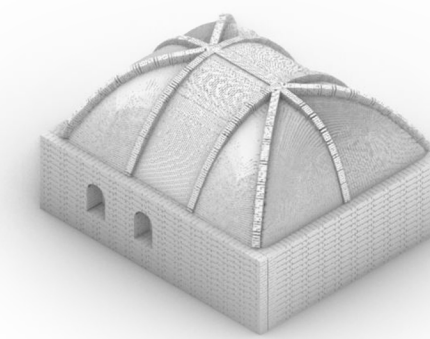
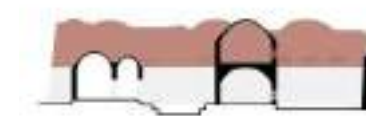
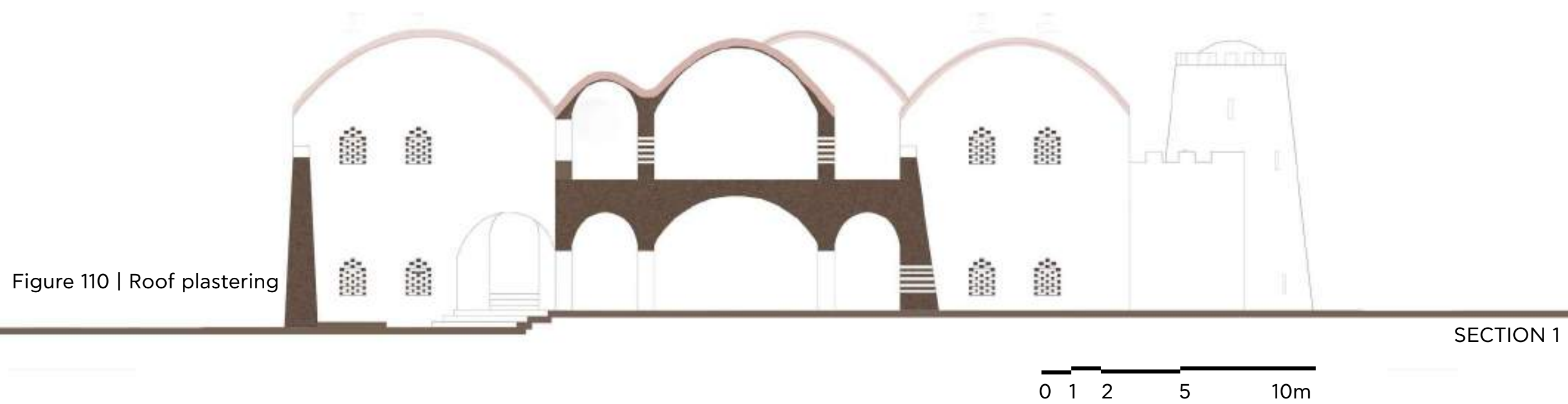


Figure 109g

CEILING
STRUCTURESTYPE
RIBBED VAULTBRICK
TYPE C

The roof should follow the ceiling, but also have smoother curves, so that water does not gather on it, but is led toward the edges of the building (figure 110). To achieve that, plaster should be used, simultaneously protecting the bricks of the structure from the weather. Usually a lime plaster is preferred, as it is harder than mud and needs less maintenance. However the soil composition of the area showed that there is no lime available in the area. As a result a mud plaster is used, that has the same materials as the adobe bricks mixture, only the sand should not be as coarse. To fill up the curves, spare bricks are used. The same plaster should be applied on all exterior walls and reapplied when the structure is revealed.



There were few exceptions to the ceilings of the complex. For the two towers, the library and the winter living room, domes were preferred to roof their circular floorplans. Although the dome bricklaying is quite simple (figure 112), the horizontal forces of the dome, posed an architectural challenge (figure 111). Three alternatives were suggested: to add mass on the base of the dome, to add buttresses or to make the domes much steeper. Of the three alternatives, the first one was preferred, as it could be incorporated in the castle complex. The mass added to the dome base was to be laid as a battlement wall (figure 113).

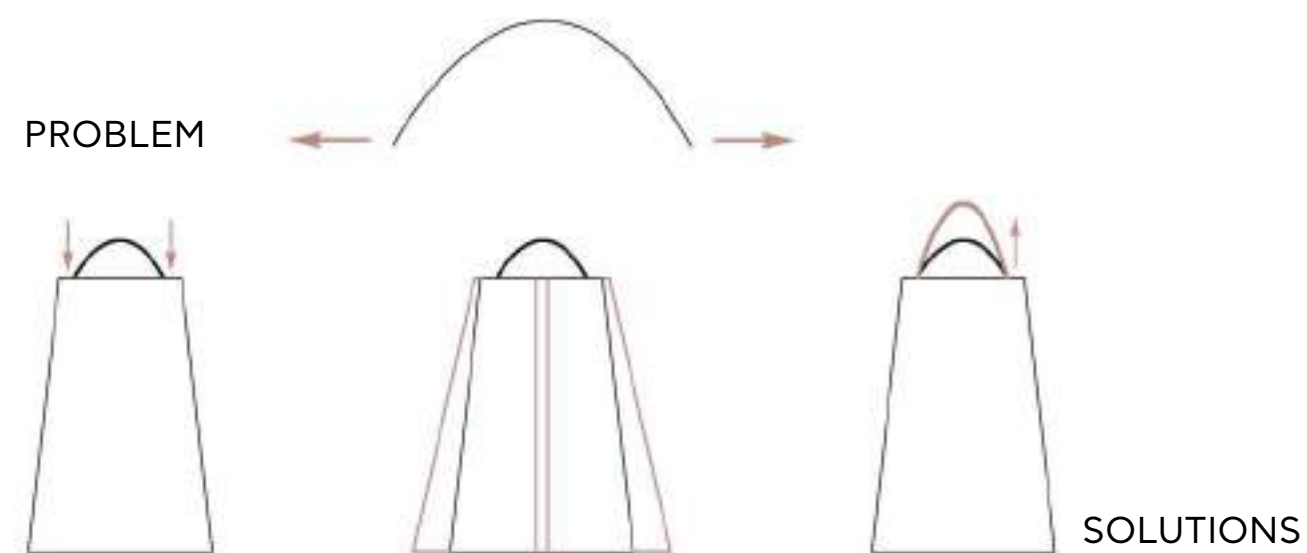
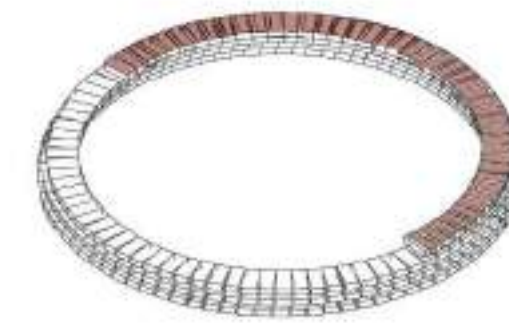
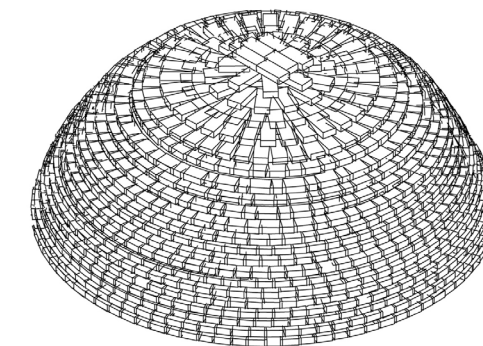


Figure 111 | Domes structural challenge

Figure 112 | Dome bricklaying



BRICK LAYING



FULL DOME

CEILING STRUCTURES	TYPE DOME	BRICK TYPE C		

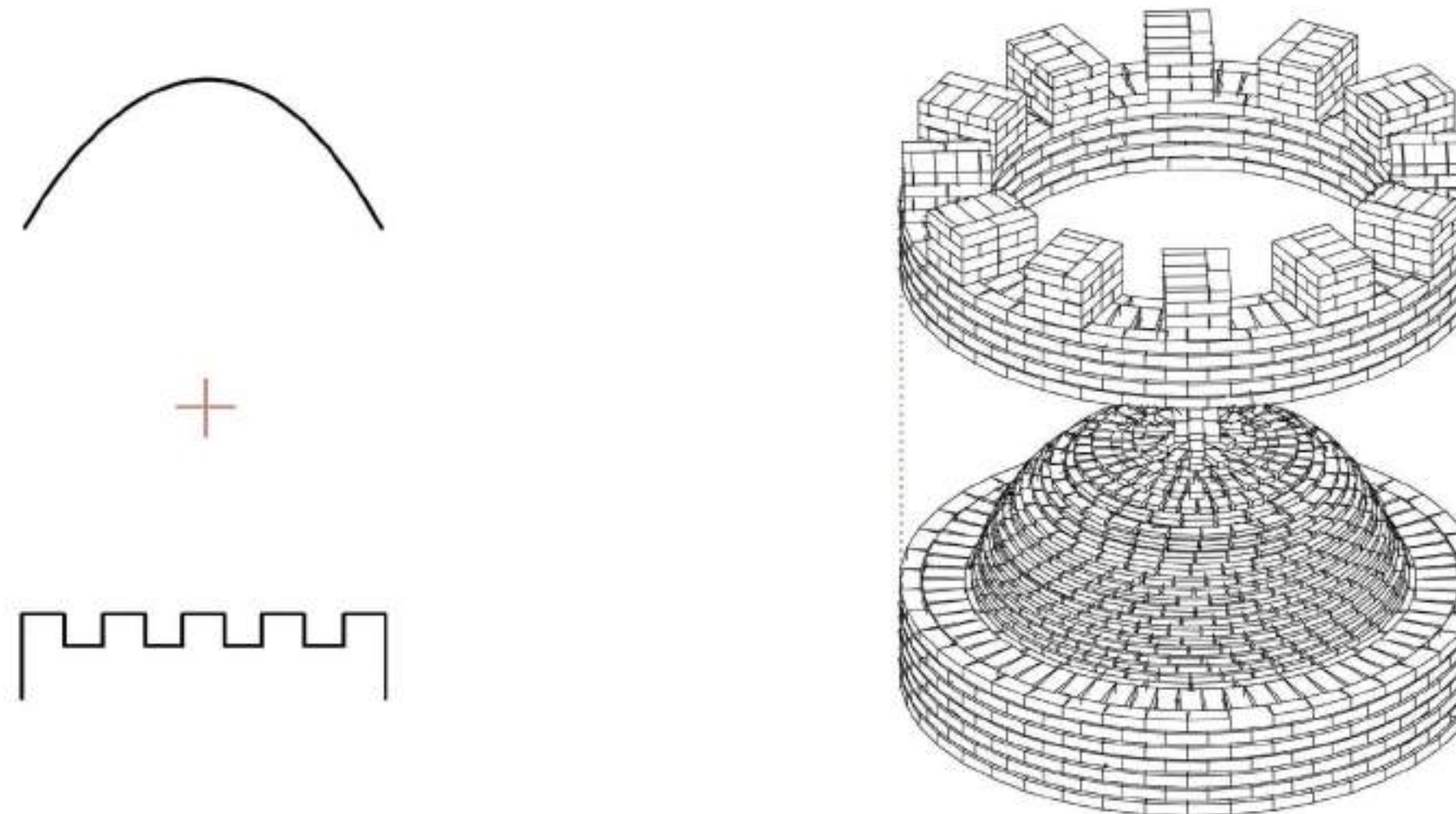
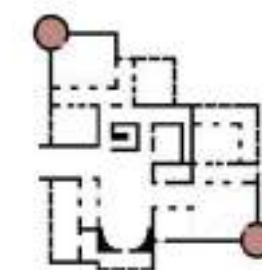
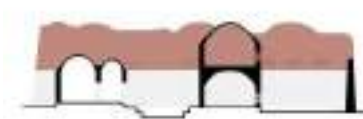


Figure 113 | Domes structural solution

CEILING
STRUCTURES

TYPE
DOME

BRICK
TYPE C



The second exception in ceiling was the case of the liwan. Liwan typically have a flat roof, but in the case of adobe that could not be possible. Instead the idea of replacing it with a half dome was conceived. Structurally, this would be quite a challenge, as the geometry is very difficult to achieve. Initially making consecutive arches instead of a half dome was proposed, but the lack of connections between the arches would result in a splitting of the arches from each other. Additionally the size of the liwan made it difficult to realize without any formwork. Eventually the most sensible method, was to create the back wall of the liwan with the semi-circular base and then place the bricks on it with a shifting to gradually build the truncated cone shape (figures 115, 116). The shifting should be limited to one third of the brick length, otherwise the risk of toppling over occurs (figure 114).

Figure 114 | Brick shifting

Figure 115 | Construction phases of liwan roof

Figure 116 | Resulting geometry of liwan ceiling

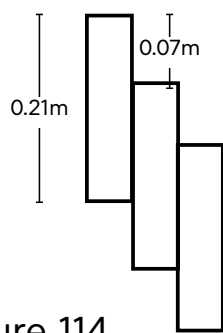


Figure 114

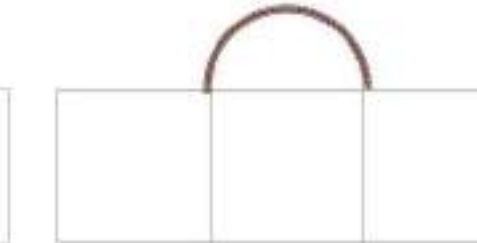
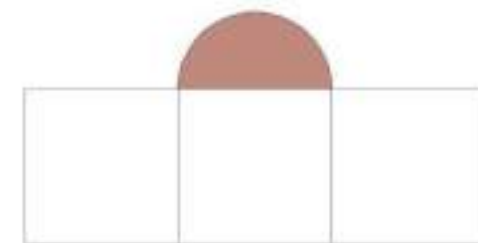
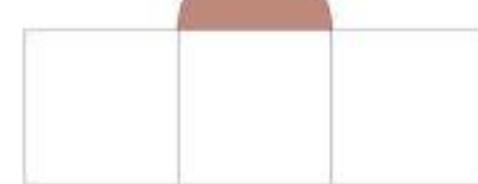


Figure 115

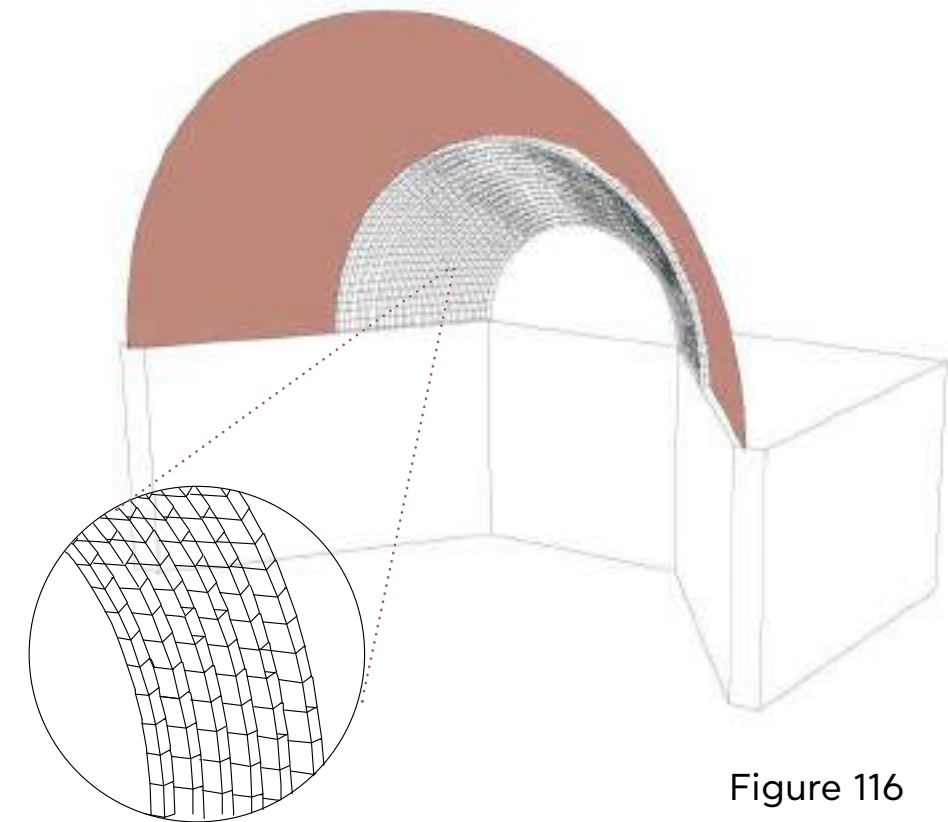
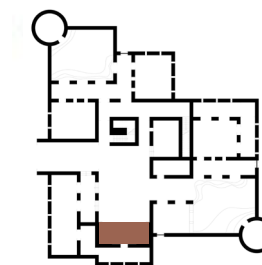
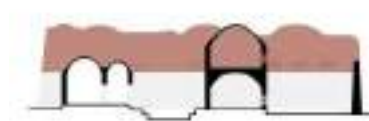


Figure 116

CEILING
STRUCTURES

TYPE
LIWAN

BRICK
TYPE C



To make the stairs, the same brick as the one in the walls was used, so the alignment with the rooms would be easier, and the steps would be on the architectural grid in the z direction. Every six steps, created a cluster that reached 1.2 height (figure 117). Four clusters are needed to reach the first floor, which is 4 architectural modules in height (4.8m). In length, these four clusters take up 5 architectural modules (6m). Because the staircase is linear and quite long, a landing step in the middle is required, increasing the total length of the stairs to 6 architectural modules (7.2m) (figures 118)

To ensure the stability of the staircase, the steps are filled with bricks beneath the entire length of the steps. The bricklaying of the steps is like the bricklaying of the walls. The top layer should always have the stretchers along the tread, to ensure an overlapping of the bricks and increase stability of the step.

Figure 117 | Stair module

Figure 118 | Stair module placement to reach top floor

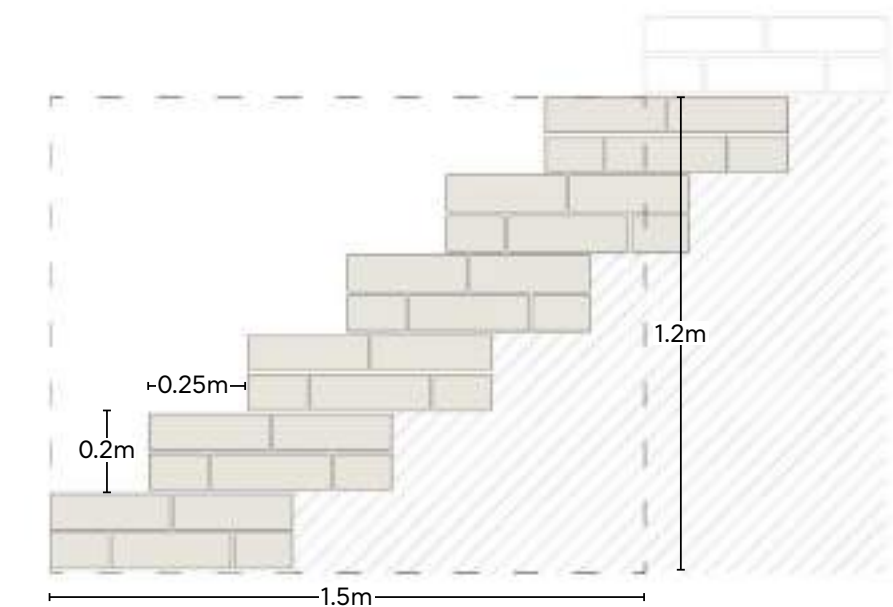


Figure 117

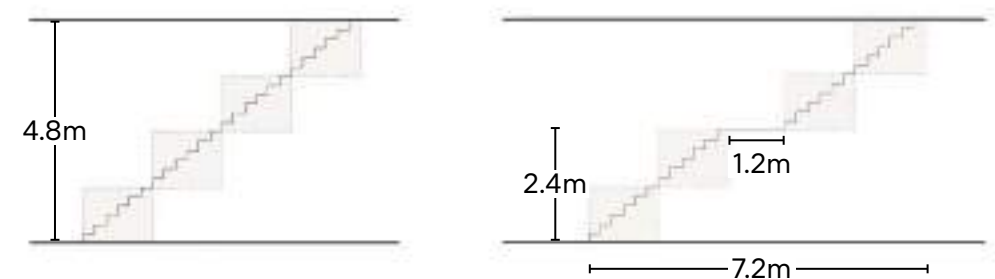


Figure 118

DETAILS	TYPE STAIRS	BRICK TYPE A		
---------	----------------	-----------------	--	--

The openings of the complex can be divided in doors, windows and gallery openings. For the doors and the gallery opening, which are both arched opening and only differ in width (doors are 1.20m and gallery openings are 1.80m) a compass is used to guide the bricklaying. As the structure is an arch, again brick type C is used.

To simplify the construction, the windows were limited to three different types, depending on the occasion; the arch window, the mashrabiya window and the arrow loop (figure 120). The arch window has the largest opening, brings in the most light, but also, if misplaced, the most dust. The mashrabiya window, imitates the wooden latticework patterns with bricks. It offers constant ventilation and lighting, while not disrupting the privacy of the room it is placed in. The arrow loop is the smallest opening, which is mostly used to disrupt large monotonous surfaces and help with the ventilation of the complex.

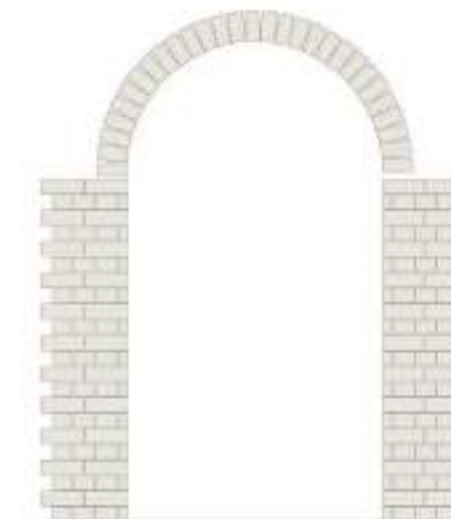
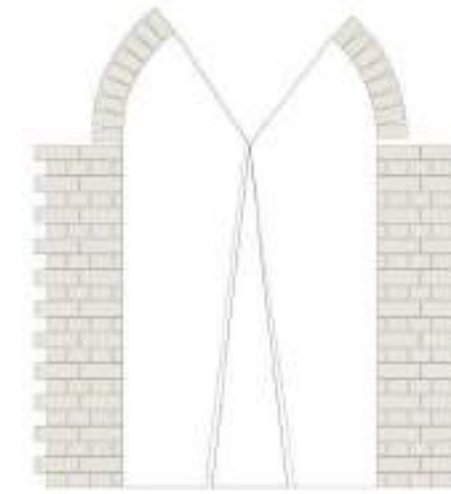
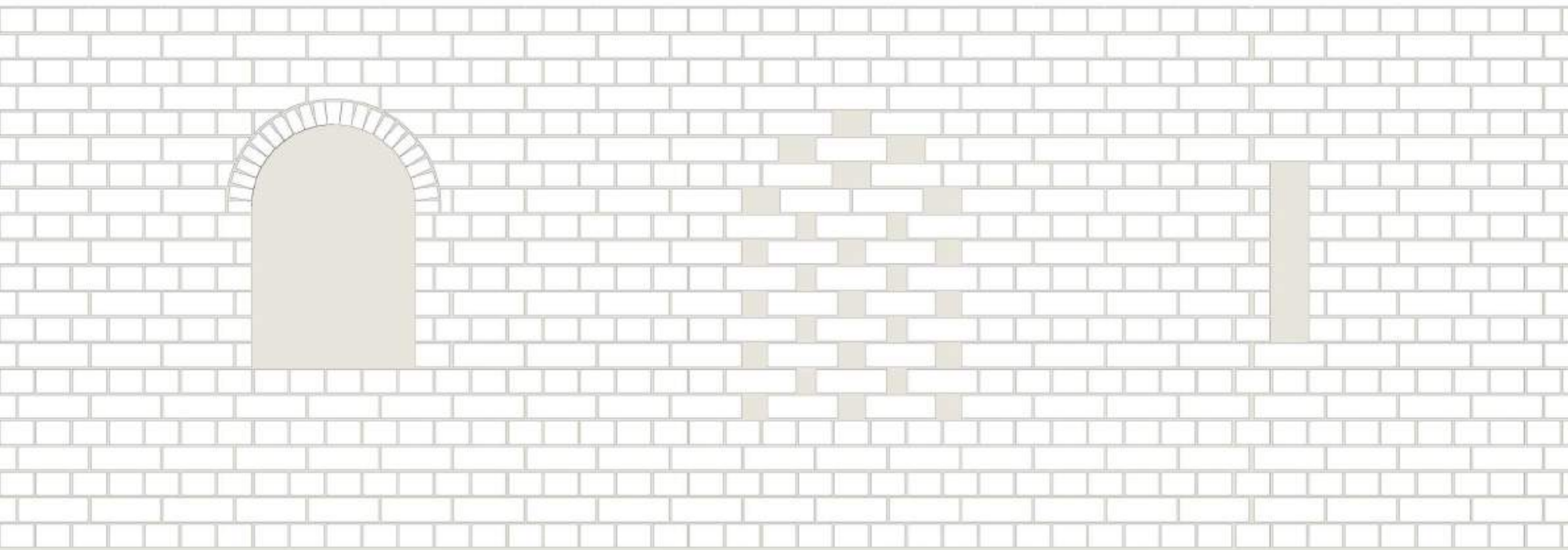


Figure 119 | Arch opening construction

Figure 120 | Window types in complex



ARCHED WINDOW

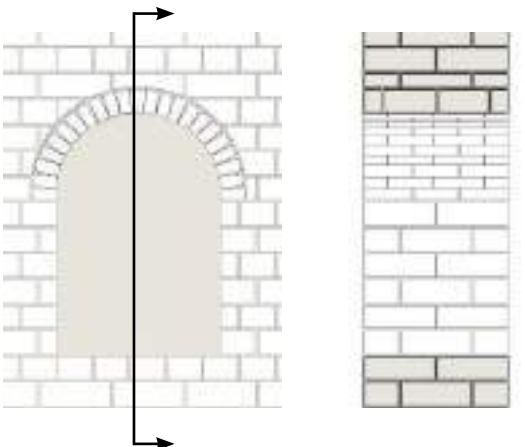
MASHRABIYA WINDOW

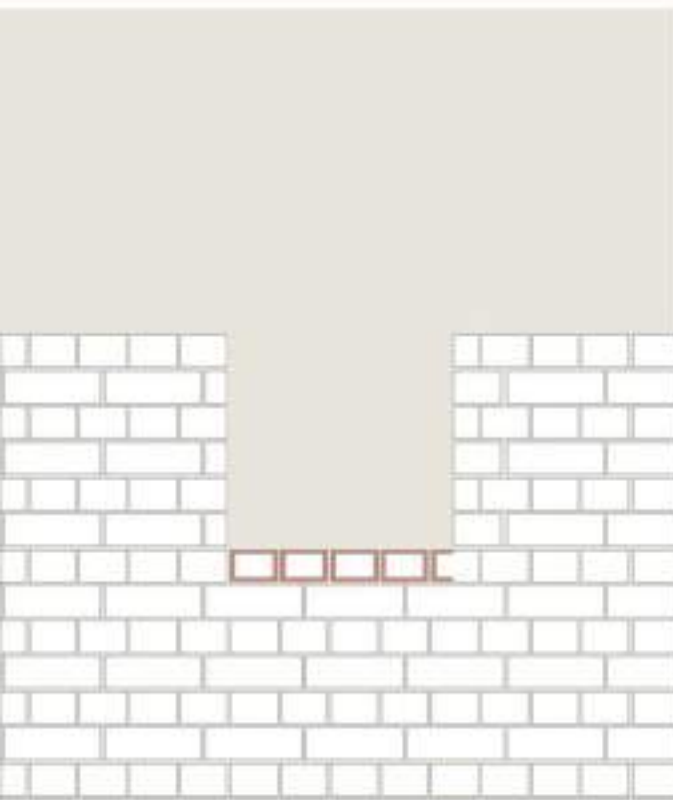
ARROW LOOP

As mentioned above the arch window provides the most light and ventilation, but also a clear viewing towards the interior. That is why it is not placed on any exterior walls. Instead, it is only placed on sheltered walls, to eliminate the amount of dust brought inside too. The arch window would be the most difficult to construct, as formwork is usually needed to construct an arch. However, items found within the camp could easily be used instead, such as a truck tire or a barrel. The most common truck tire size has a diameter of 70cm. To make the window four steps must be followed: first the gap has to be defined. That is 4 1/2 headers wide and 6 layers tall. Then, the tire is placed on top of some bricks. Truck tires are quite wide, so balancing it, shouldn't be a problem. Brick C is used to lay the arch on top of the tire. The use of the smaller, lighter brick, helps create a smoother arch and also reduces the tire deformation from the weight. Finally the wall bricklaying continues as usual, adding broken bricks around the arch border (figure 122).

Figure 121 | Arched window elevation and section

Figure 122 | Arched window construction phases



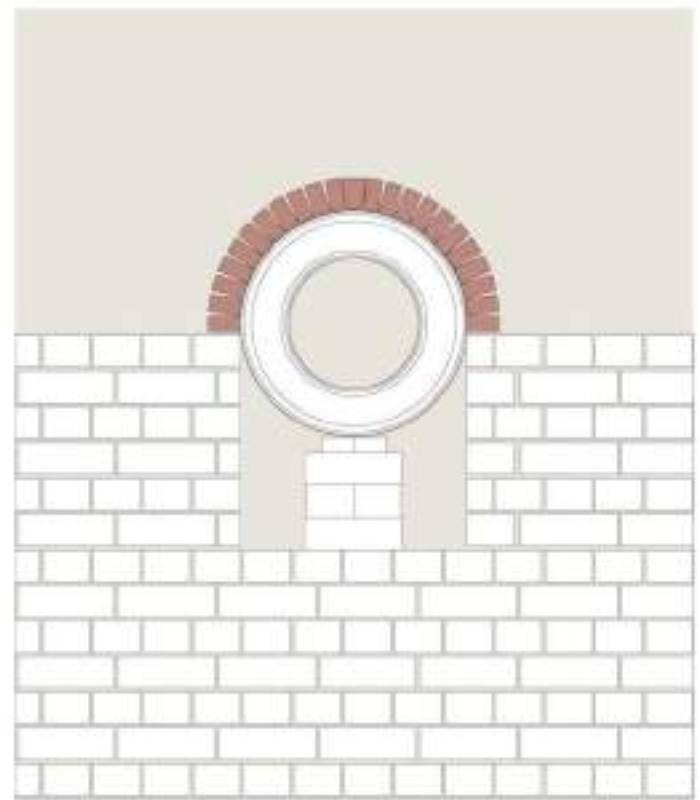


DEFINE THE GAP

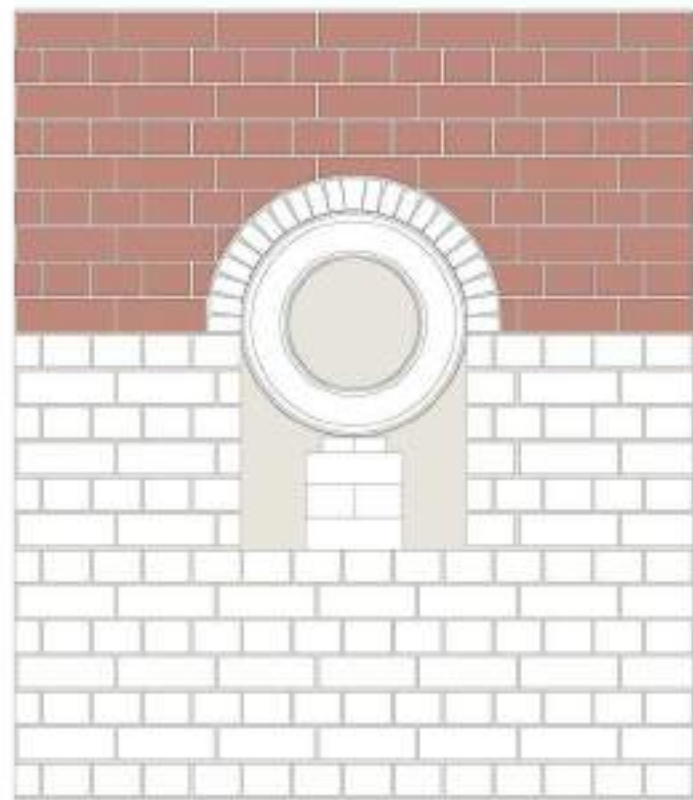
window width

=

4 1/2 headers brick A



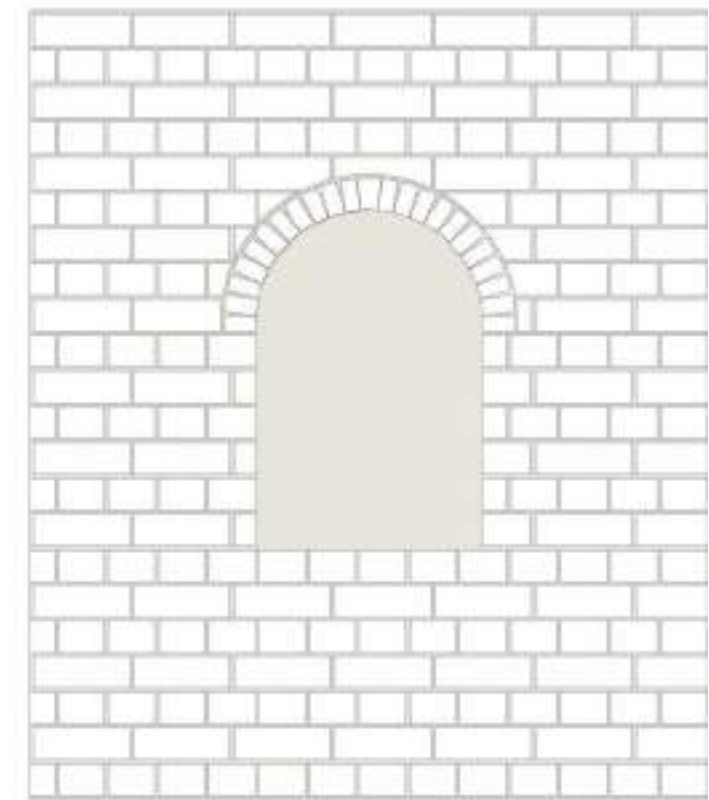
CREATE ARCH

temporarily place a truck tire on
bricksuse brick B to create the arch over
the tire

FILL UP WALL

continue bricklaying as usual

use broken bricks around the arch



REMOVE TIRE

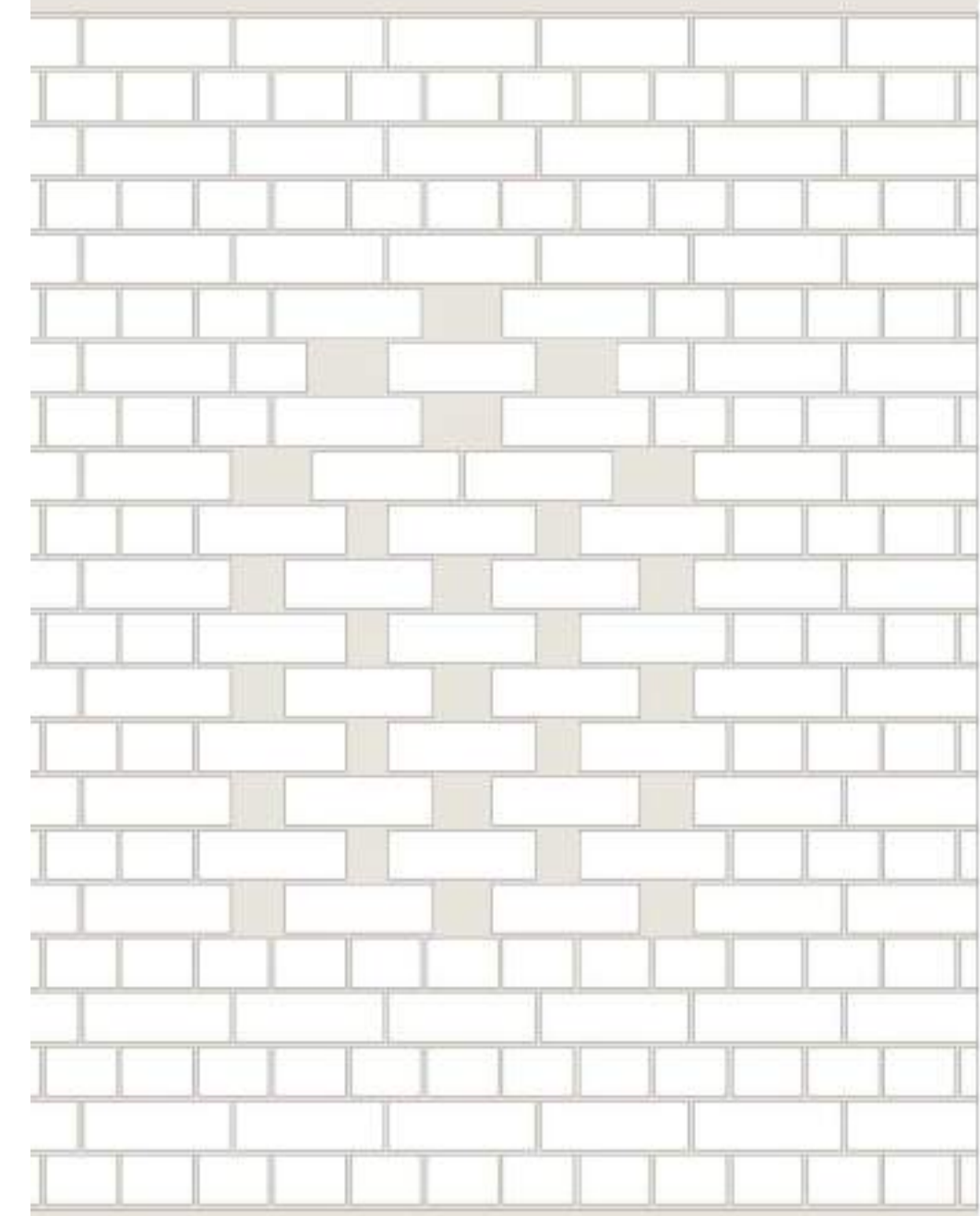
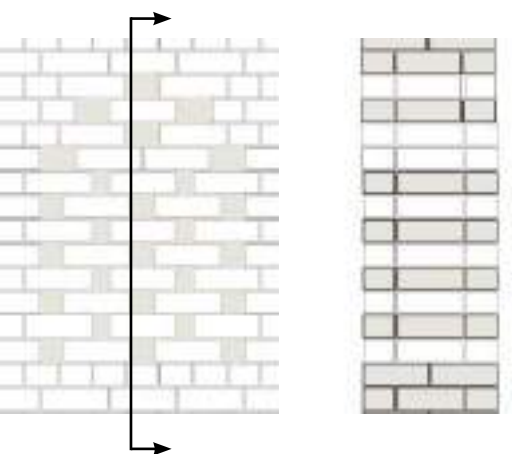
remove the tire

the window is ready!

The mashrabiya-like window, is inspired by vernacular architecture. Its discrete lighting and ventilation makes it the optimum choice for exterior walls as mentioned above. This particular window type could be made in any pattern preferred by the locals, but to avoid confusion two alternatives are described below. In the first one simple perforations are made, while in the second one creates an arch-like outline is created. Figure 124 shows the two alternating patterns and how the arch can be created. It is worth mentioning that for this type of window, only the stretcher of the brick is used. The same pattern is repeated throughout the thickness of the wall, to eliminate the effect of the perforations.

Figure 123 | Mashrabiya window elevation and section

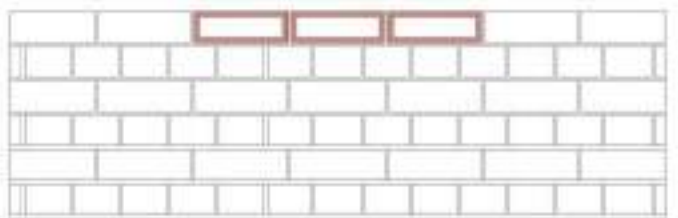
Figure 124 | Mashrabiya window construction phases



PATTERN 1 - STRETCHER ROW



PATTERN 2- HEADER ROW



DEFINE THE GAP

window width

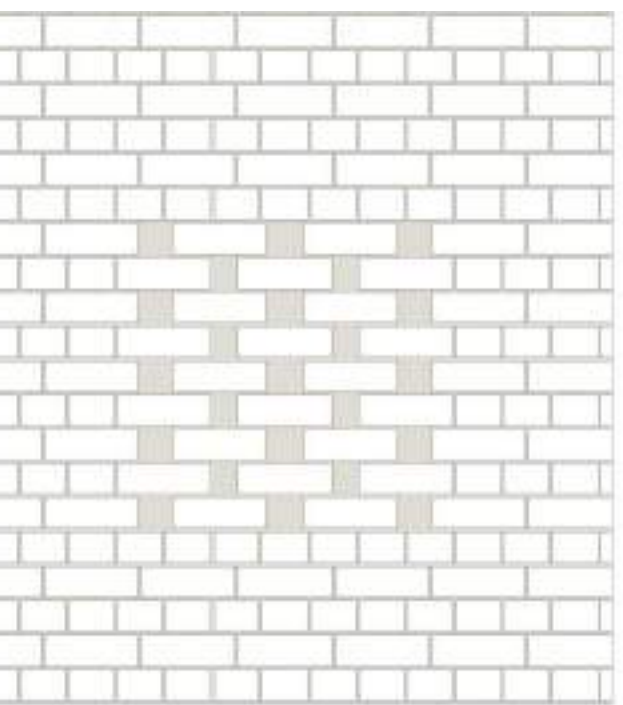
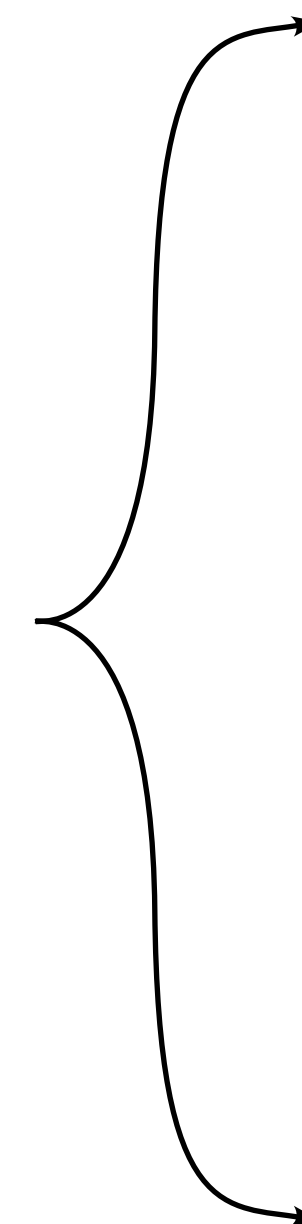
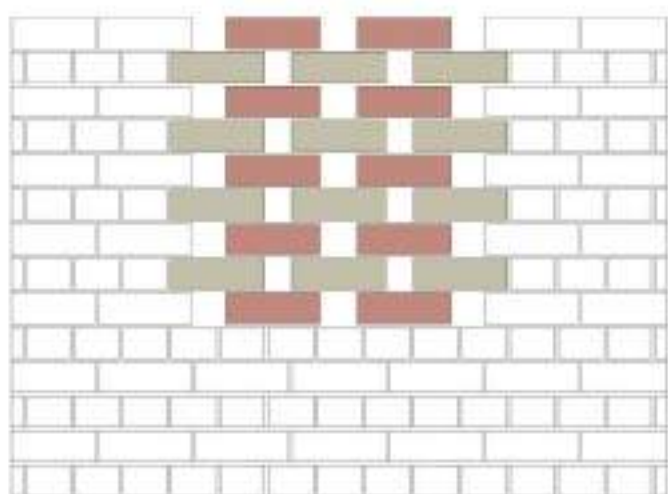
=

3 stretchers brick A

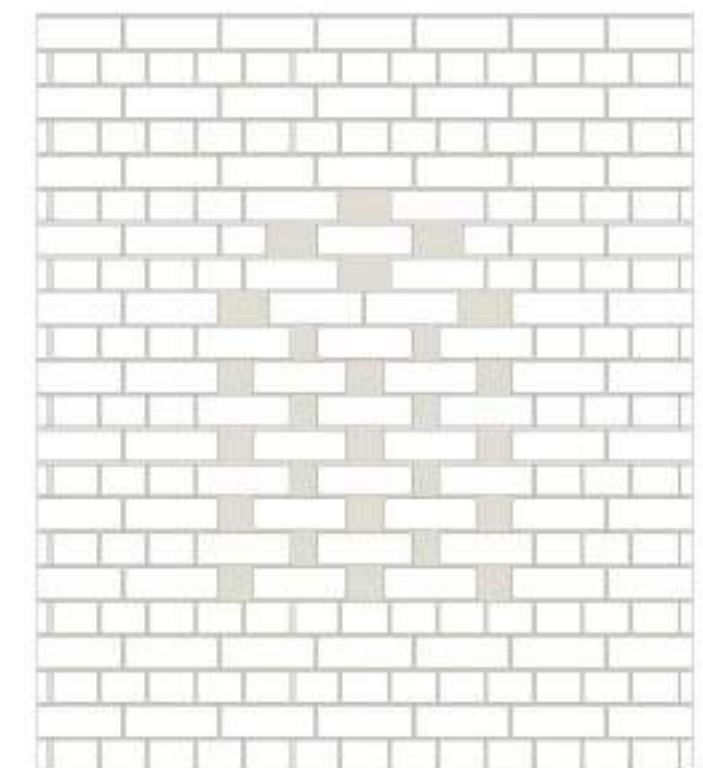
*remove the 3 bricks from bricklaying
and replace with pattern 1 instead*



ALTERNATE PATTERNS



STRAIGHT MASHRABIYA
end patter on stretcher row

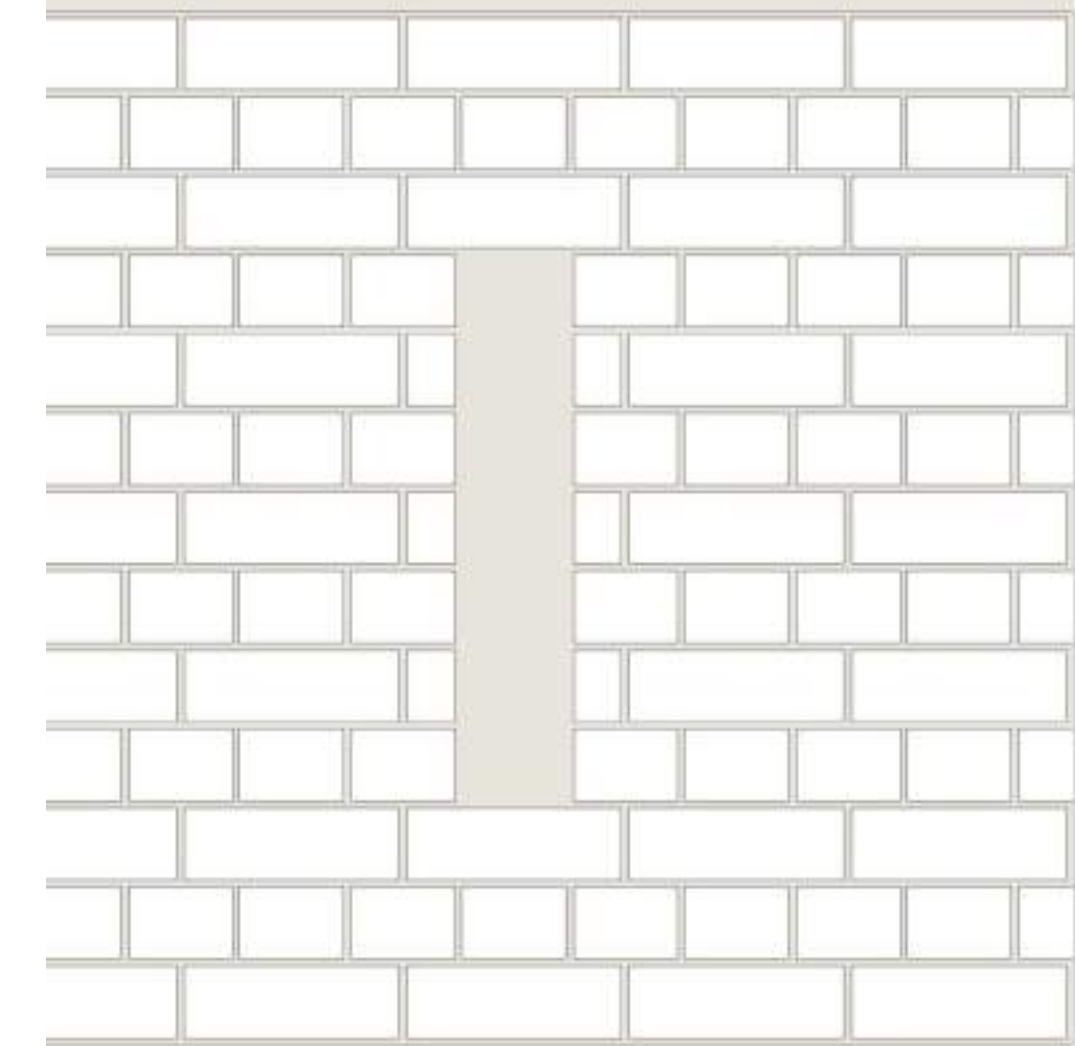
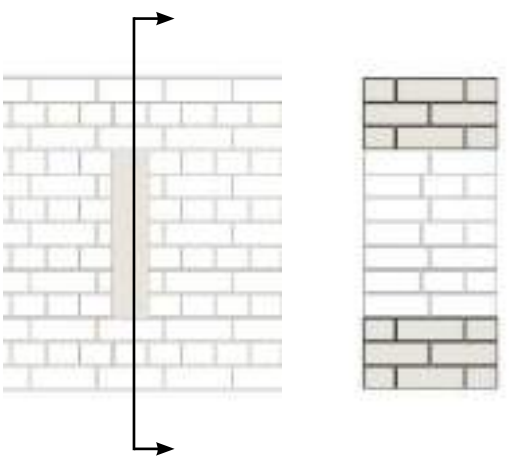


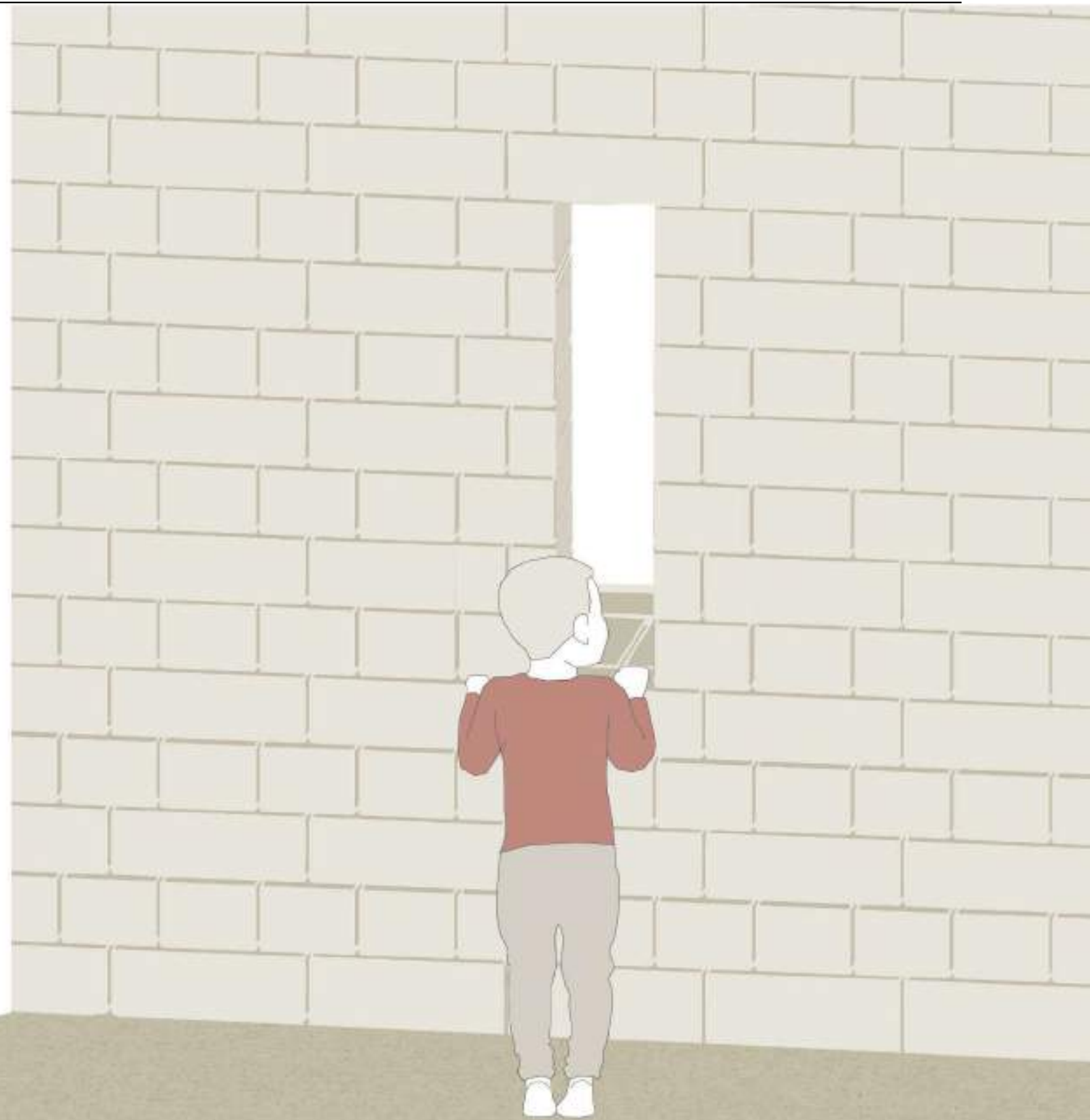
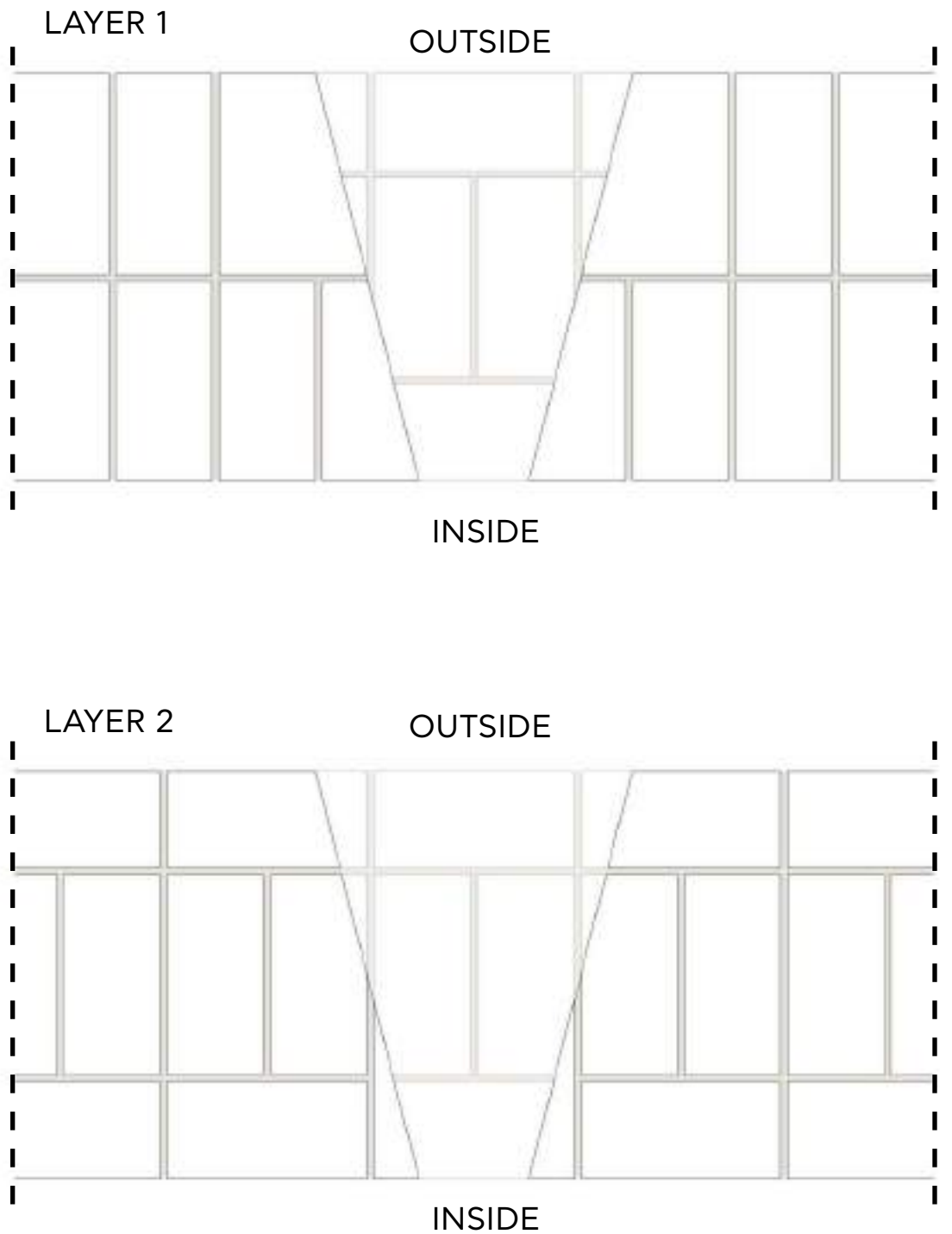
ARCH MASHRABIYA
end patter on header row

The arrow loop as mentioned in chapter 3.3, is an element of castle architecture. It is a slit in the wall, which opens towards the interior, from where soldiers shot their arrows, without being exposed. However, in the case of the project, the opening is inverted and placed outwards. This way, the venturi effect, accelerates the air entering from the openings, thus enhancing the air flow within the complex. The bricklaying is also quite simple, as the opening has the width of a header. The two bricklaying patterns in figure 126 alternate, and bricks broken diagonally create the opening towards the exterior.

Figure 125 | Arrow loop window elevation and section

Figure 126 | Arrow loop window construction phases





The placement of the windows is not random, but follows a very specific algorithm. Each space within the complex can be characterized as open (0), semi-open(1) or closed(2). Spaces out of the complex are null (N). If each of these numbers were placed within each architectural module (1.20x1.20cm), the layout of the complex would begin to reveal itself (figure 128). By defining which edges of the modules are walls, the layout would be clear. Depending on the numbers the wall edges border, the appropriate window could be known;

If an edge is bordering closed spaces (2-2), it means it is an interior wall, so no windows are assigned.

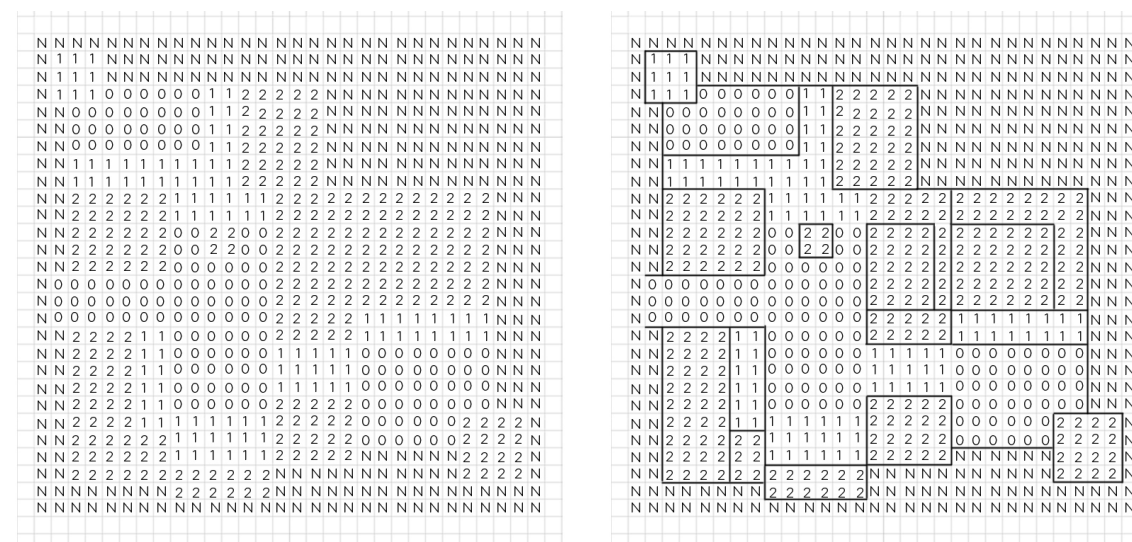
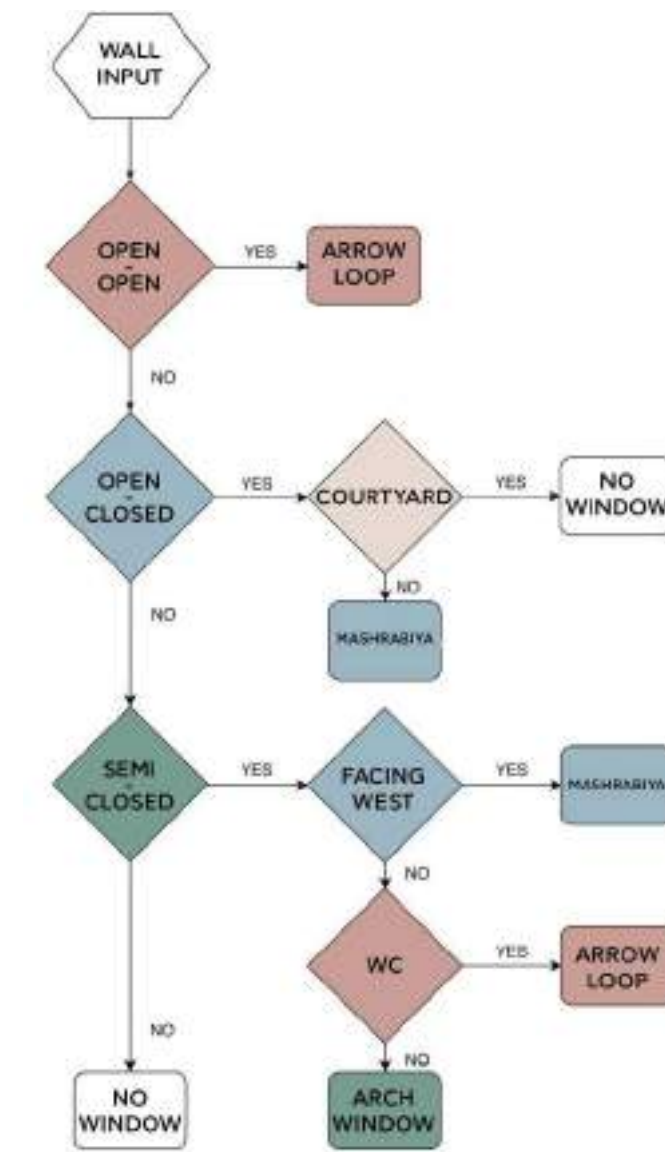
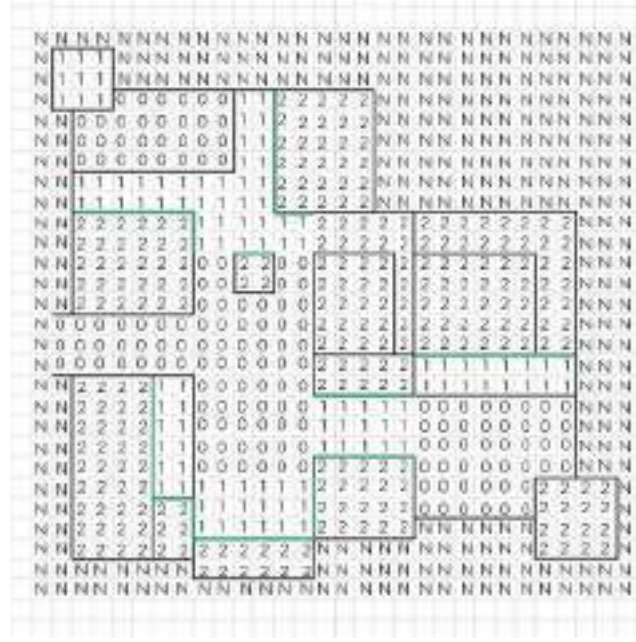


Figure 127 | Window placement flowchart

Figure 128 | Evolution of window placement algorithm

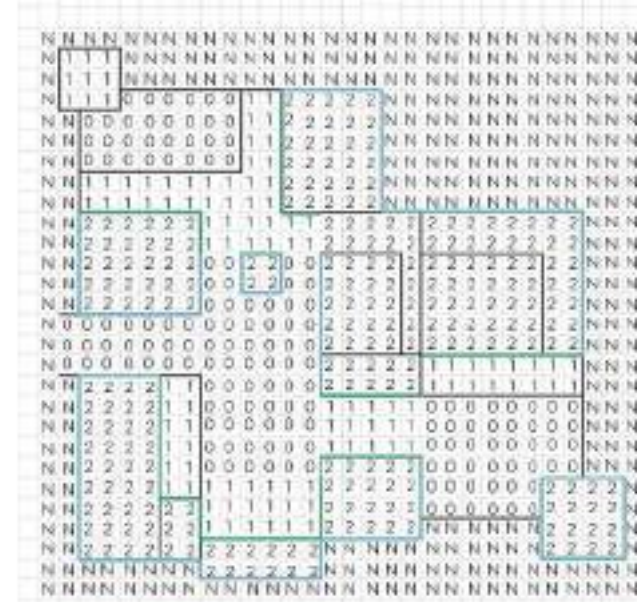


1-2



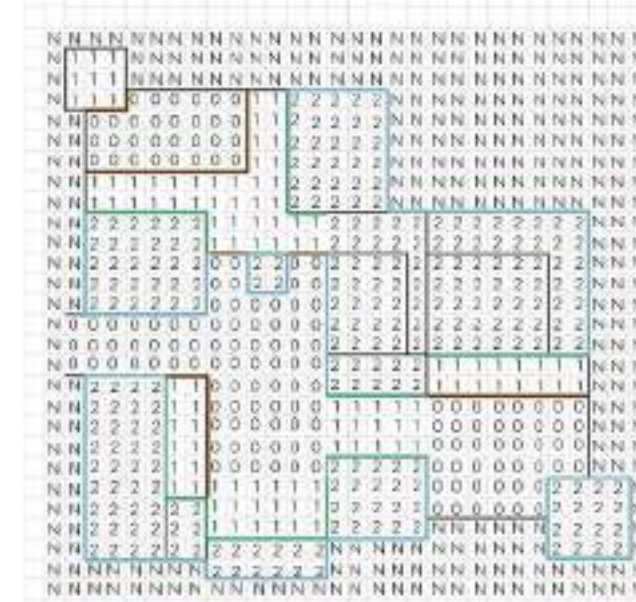
If an edge is bordering closed and semi-open spaces (1-2), it means it is a wall between a gallery and a room. The wall is well sheltered so it can receive arched windows. The arched windows have a width of 70cm, so they should be placed every 1.20m.

0-2



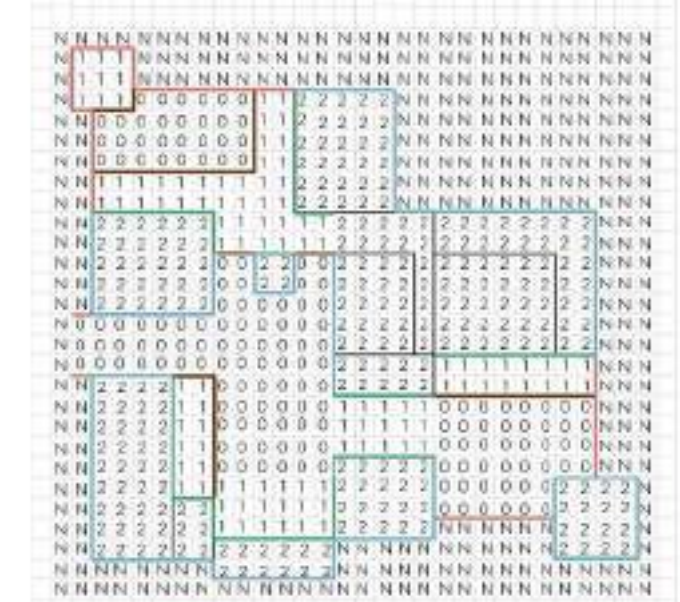
If it is bordering a closed and a null space (N-2), it means it is an exterior wall of a room, so mashrabiya windows are placed, to offer ventilation and lighting without invading the privacy of the castle. The mashrabiya windows have a width of 90cm, so they should be placed every 1.80m. The same happens if a closed and an open space (0-2) are bordering.

0-1



If an edge is bordering an open and a semi-open space (0-1), it means it is between a gallery and an open space. Then the opening placed is no longer a window, but an arched opening with a width of 1.80m, place every 3m.

N-1 & N-0

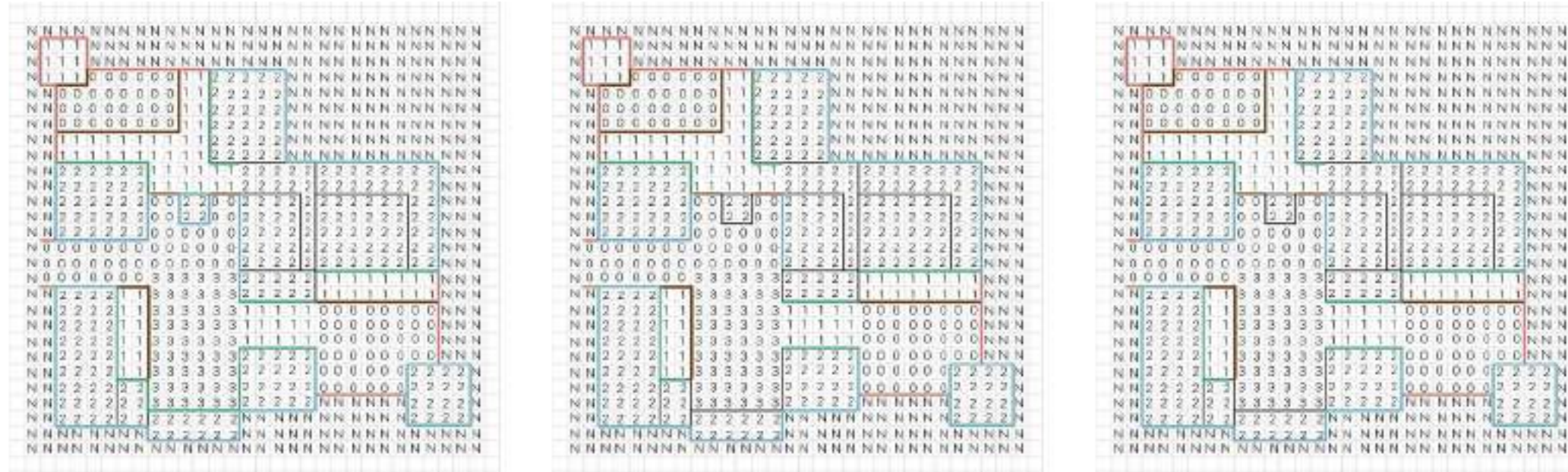


If an edge is bordering an open and null space (0-N), then is part of the defensive wall and arrow loops are placed. Arrow loops are very narrow (15cm) and can be place very often from a structural perspective, but are proposed to be placed every 1.50m. The same occurs if an edge is bordering a semi-open and null space (1-N), as it is part of the gallery end or winter living room, which do not require large openings.

3

3

W



As every rule has an exception, two are found in this algorithm as well. For architectural reasons, the public courtyard and the liwan should not have any windows overseeing it. Gallery openings are acceptable, as they are additional gathering spaces, but windows allow for unwanted contact with neighboring functions. As a result the courtyard and liwan area, are no longer characterized as 0s and 1s, but instead turn into a new category of 3's.

This adds a new if factor to the algorithm. If a wall was to obtain gallery openings and is bordering a 3, proceed as planned, but if a wall was to receive windows of any sort and is bordering a 3 add nothing.

The second exception concerns the orientation of the walls appropriate for arched windows. Even though the walls where such windows are placed are sheltered, it is not considered wise to place such large openings if the wall is facing the west. This is the main wind direction in this region and with a large window facing west, a lot of sand and dust will be blown into the building. This means that if a wall is between a 1-2 and 1 is on the left, mashrabiya openings are placed instead.

The final result is in line with the architectural vision of the project and complies with climate and privacy goals. The validation of the algorithm could be furthermore tested, if it was applied to different configurations and still had the desired results. The algorithm could be furthermore evolved, by including door placement, which would need to be limited to one per room.

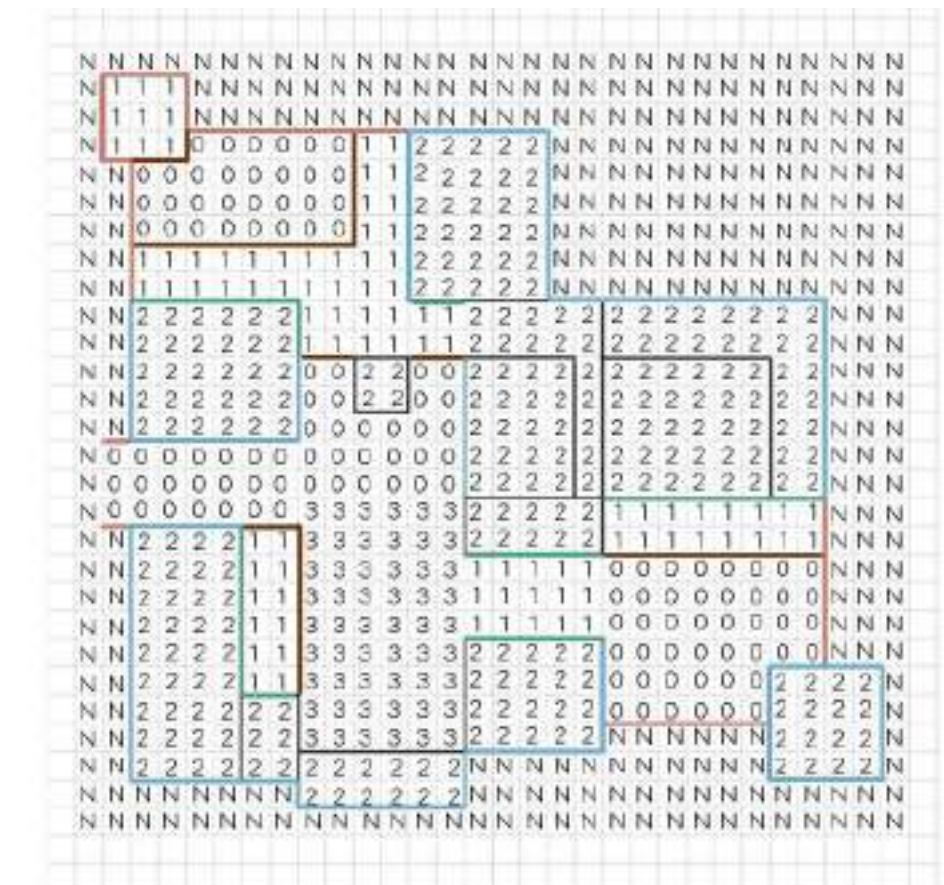
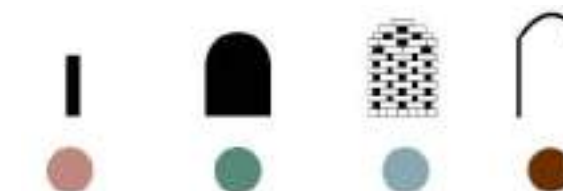


Figure 129 | Window placement final result

Figure 130 | Impression of
courtyard 1 and library

			SEMI-	
OUTSIDE	OPEN	OPEN	CLOSED	COURTYARD
N	0	1	2	3





REFLECTION & CONCLUSION

"Reflection is a vital part of creating design expertise."(Lawson & Dorst, 2009, P.64) Cross (2006,P.4-P.5) says that education cannot be referred to as such if the student is not 'self-aware' of what he/she learned by working on an assignment. Earthy studio was a very enjoyable, and educational course to follow and an enrollment we never regretted. As building technology students, the link between architecture and parametric computational design was appreciated. During AR3B011 EARTHY we learned new skills and sharpened our knowledge in a variety of scopes including spatial planning, earthy material, earthy construction design, designing via algorithms (Python programming), linear algebra, understanding of geometric topology, structural design, FEM, and low-tech masonry construction methods.

First, we have often heard from architecture teachers that floor plan design cannot be taught but rather one learned by practice. Van Dooren et al. (2013) wrote about generic elements that would help make design education explicit. Nevertheless, the methods still focus on the solution based approach rather than the problem based approach scientists use in comparison to designers. (Cross, 2006,P.6) By learning about the configurative approach to layout planning, through the graph theoretical methods for design and analysis of spatial configurations Nourian (2016) has developed, we came to rationalize floor plan planning in ways we have never thought of before. Now, even without

using the computational algorithm for spatial configuration, we can use the same logical approach manually. It's a thinking pattern that can be taught to others with using clear principles. This algorithm eloquently explicits that ambiguity of spatial planning.

Second, meshing, tessellation, dynamic relaxation, and FEM analysis during the form finding a structural verification phase were interchangeable and codependent steps in the design process. We learned that by controlling the lines of tessellation we could predetermine the form received by the relaxation. Meshing refinement level had an influence on the accuracy of the finite element analysis. An extremely fine mesh (high subdivision) takes an unnecessary long computational time. A rough or coarse mesh might mislead the interpretation of the FE analysis results. Some stresses in the corners or around an opening for example would only show if the mesh is finely subdivided. Meshing level has an effect of dynamic relation and form finding as well, but that is not the most important role of its accuracy level.

Third, working with a structurally brittle and climate sensitive material taught us a lot in the field of material processing, material science, and structural design. Adobe bricks are very appealing to work with due to their abundance and 100% environmental circularbility. The making-of and properties of these bricks solely depend on the composition of the soil

REFLECTION & CONCLUSION

in the location of the construction site. This taught us low-tech quality control methods. The material taught us how by means of designing from a structural starting point, material can be used sparingly. Usually people designing a structure and later on discovered that it can never stand unless reinforced concrete or a steel structure is used. Instead in this project, we chose the material of construction first and later we thought of how can we utilize its structural strengths. For earthy bricks this meant avoiding any tension forces in the structure, and designing a compression only structure. The same skill set and methodology can be used with any other material of choice like glass or inversely fabric.

Fourth, bricklaying bonds, python patterns and construction methods. The concept of an integrated design comes back in this phase. We learned how the ratio of our brick size is greatly linked to the module used in dimensioning the entire building, the human body size and mason's body strength. Even though this could be integrated manually, the use of computational scripting proved very useful. Bricklaying is a repetitive pattern. when it is applied on double curved surfaces, having a python script ensured a fast and accurate generation of various alternatives. The construction method had to be so easy that it would ensure achieving the accurate complex form we had designed even if laymen refugees were to build it.

As much as we have learned and achieved, we realize there is much more to learn and things to improve in our design. Given the time restriction we had, we are satisfied with our results. We would recommend however improving every single aspect of the project.

The subjects that the project could be improved upon, given that there would be more time to do so, are the following: Scripting the floorplan rules to see other resulting layouts. Eliminate the formwork from the construction methods. The removal of the formwork was something we tried during the entire project. But at the location where ribs were constructed no formwork-less method could be developed that supported the required shape. The computational part could be improved If more consultation on computational structural would have been given. A suggestion for next year would be to add Shibo Ren to the mentoring group. With the help of this the results could become more precise. For the scripting part, bricklaying of the ribs could have been done computationally. Finally construction methods for approximating the dynamically relaxed shape could be further researched and developed.

REFERENCES

- Cross, N. (2006). Designerly ways of knowing. London: Springer. Retrieved October 10, 2019, from <http://link.springer.com/book/10.1007/1-84628-301-9>
- Glamox. (2017). Classrooms. Retrieved October 23, 2019, from <https://glamox.com/uk/solutions/test-small-class-room>.
- Gubasheva, S. (2017). Adobe bricks as a building material. Czech Technical University, Faculty of Civil Engineering, Prague.
- Lawson, B., & Dorst, K. (2009). Design expertise. Oxford, UK: Architectural Press.
- Ligget, R., Milne, M., & UCLA. (2018). Retrieved from <http://www.energy-design-tools.aud.ucla.edu/climate-consultant/request-climate-consultant.php>
- Wikipedia. (2019, September 19). Zaatri refugee camp. Retrieved October 28, 2019, from https://en.wikipedia.org/wiki/Zaatari_refugee_camp#cite_note-12.
- Ledwith, A. (2014). Zaatri: The Instant City Retrieved from <http://sigus.scripts.mit.edu/x/files/Zaatari/AHIPublication.pdf>
- Nourian, P. (2016). Configraphics: Graph Theoretical Methods for Design and Analysis of Spatial Configurations (dissertation). Retrieved from <https://books.bk.tudelft.nl/index.php/press/catalog/book/isbn.9789461867209>
- Omondi, I., Hashem, M., & UNHCR, undefined. (2019, February). Jordan – Zaatri Refugee Camp Fact Sheet. Retrieved from <https://reliefweb.int/sites/reliefweb.int/files/resources/68566.pdf>.
- SamSamWater Foundation. (2018). SamSamWater Climate Tool- Location: Zaatri Refugee Camp, Mafraq, Jordan. Retrieved October 28, 2019, from <https://www.samsamwater.com/climate/climatedata.php?lat=32.2937&lng=36.3276&alt=0&loc=Zaatari+Refugee+Camp,+Mafraq,+Jordan,+Jordan>.
- Soulié, F., & Ababsa, M. (2018, May 9). An Urbanizing Camp? Zaatri Syrian Refugee Camp in Jordan. Retrieved October 28, 2019, from <https://lajeh.hypotheses.org/1076>.
- Steadman, J. (2018, May 9). The Global Refugee Crisis. Retrieved October 28, 2019, from https://helprefugees.org/news/the-refugee-crisis/?gclid=CjwKCAjwo9rtBRAAdEiwA_2N2toOaBRumAJIFYgk4QY7m1iOAoaqEiEx75I93WkyaCm7tUe55RoC13cQAvD_BwE.
- Strimel, G. (2014). Engineering Design: A Cognitive Process Approach. Old Dominion University. Retrieved from https://www.researchgate.net/profile/Greg_Strimel/publication/317054643_ENGINEERING_DESIGN_A_COGNITIVE_PROCESS_APPROACH/links/592335f2a6fdcc4443f7ef00/ENGINEERING-DESIGN-A-COGNITIVE-PROCESSAPPROACH.pdf

REFERENCES

- UNHCR. (2018, April). Zaatari Refugee Camp - Infrastructure and Facilities. Zaatari Refugee Camp - Infrastructure and Facilities. Retrieved from <https://reliefweb.int/map/jordan/zaatari-refugee-camp-infrastructure-and-facilities-april-2018>
- UNHCR. (2019). Operational Portal Refugee Situation. Retrieved from <https://data2.unhcr.org/en/situations/syria>.
- UNICEF-REACH. (2016a, January 13). JORDAN - Al Za'atari Refugee Camp - Population Density - December 2015. JORDAN - Al Za'atari Refugee Camp - Population Density - December 2015. Retrieved from https://www.impactrepository.org/document/reach/55176922/reach_jor_map_zaatari_mov_popdensity_dec2015_a1.pdf
- UNICEF-REACH. (2016b, January 13). JORDAN - Al Za'atari Refugee Camp - Number of People per Household (Block Level) - December 2015. JORDAN - Al Za'atari Refugee Camp - Number of People per Household (Block Level) - December 2015. Retrieved from https://www.impact-repository.org/document/reach/813fba0a/reach_jor_map_zaatari_mov_household_size_dec2015_a1.pdf
- UNICEF-REACH. (2016c, January 20). JORDAN - Al Za'atari Refugee Camp - School Enrolment by Block - December 2015. JORDAN - Al Za'atari Refugee Camp - School Enrolment by Block - December 2015. Retrieved from https://www.impactrepository.org/document/reach/dd254383/reach_jor_map_zaatari_mov_school_attendance_dec2015_a1.pdf
- Van Dooren, E., Boshuizen, E., Van Merriënboer, J., Asselbergs, T., & Van Dorst, M. (2013). Making explicit in design education: Generic elements in the design process. *International Journal of Technology and Design Education.*, 24 (1), 53-71. Retrieved October 10, 2019, from <http://link.springer.com/article/10.1007/s10798-013-9246-8>
- Windfinder. (2019). Windfinder - wind, wave & weather reports, forecasts & statistics worldwide. Retrieved from <https://nl.windfinder.com/#10/32.2090/35.8517>.

FIGURES

Figure 1, 2

UNHCR. (2019). FACT SHEET Jordan –Zaatari Refugee Camp Retrieved from <https://reliefweb.int/sites/reliefweb.int/files/resources/68566.pdf>

Figure 3

Omondi, I., Hashem, M., & UNHCR, undefined. (2019, February). Jordan – Zaatri Refugee Camp Fact Sheet. Retrieved from <https://reliefweb.int/sites/reliefweb.int/files/resources/68566.pdf>.

Figure 5

UNICEF-REACH. (2016c, January 20). JORDAN - Al Za'atari Refugee Camp - School Enrolment by Block - December 2015. JORDAN - Al Za'atari Refugee Camp - School Enrolment by Block - December 2015. Retrieved from https://www.impactrepository.org/document/reach/dd254383/reach_jor_map_zaatari_mov_school_attendance_dec2015_a1.pdf

Figure 7

b| Graham Brown, G. (2013, September 15). Zaatri Refugee Camp – Jordan. Retrieved November 4, 2019, from <http://learning-reimagined.com/zaatari-refugee-camp-jordan/>

c| Future Learning Space. (2015, October 11). Retrieved November 4, 2019, from <https://learningspacealive2015.wordpress.com/future-learning-space-3/>

d| Field Ready | Post. (2017, November 17). Retrieved November 4, 2019, from <https://www.fieldready.org/post/2017/11/17/zaatari-village-site-visit>

Figure 10

Ligget, R., Milne, M., & UCLA. (2018). Retrieved from <http://www.energy-design-tools.aud.ucla.edu/climate-consultant/request-climate-consultant.php>

Figure 11

Windfinder. (2019). Windfinder - wind, wave & weather reports, forecasts & statistics worldwide. Retrieved from <https://nl.windfinder.com/#10/32.2090/35.8517>.

Figure 12-15

Tomislav Hengl, Jorge Samuel Mendes de Jesus, T. (2019, November 4). SoilGrids. Retrieved November 4, 2019, from https://soilgrids.org/#!/?layer=ORCDRC_M_sl2_250m&vector=1

Figure 30

Retlaw Snellac Photography, R. (n.d.). Liwan at an old Damascene house. Afnan Hotel at present day. Damascus | Syria | Syria in 2019 | Islamic architecture, Damascus, Ancient architecture. Retrieved November 4, 2019, from <https://>

REFERENCES

gr.pinterest.com/pin/335799715945739340/?lp=true

Figure 31

Sabat. (n.d.). Retrieved November 4, 2019, from <https://yazd.today/sabat/>

Figure 34

Nourian, P. (n.d.). pirouznourian - SYNTACTIC. Retrieved November 4, 2019, from <https://sites.google.com/site/pirouznourian/syntactic-design>

Figure 38

Jebulon, . (2018, June 01). Arrow Loop. Ancient History Encyclopedia. Retrieved from <https://www.ancient.eu/image/8859/>

Figure 39

Mball93, . (2018, June 08). Arcade, Rochester Castle Keep. Ancient History Encyclopedia. Retrieved from <https://www.ancient.eu/image/8893/>

All other figures are made by the design team themselves and, as a result, do not have a reference.

APPENDIX A

Weather Chart

Climate Consultant 6.0 (Build 13, Jul 5, 2018)

File Criteria Charts Help

WEATHER DATA SUMMARY

LOCATION: DAMASCUS, -, SYR
 Latitude/Longitude: 33.42° North, 36.52° East; Time Zone from Greenwich 2
 Data Source: IWECC Data - 400800 WMO Station Number; Elevation 600 m

MONTHLY MEANS	JAN	FEB	MAR	APR	MAY	JUN	JUL	AUG	SEP	OCT	NOV	DEC	
Global Horiz Radiation (Avg Hourly)	226	238	436	476	532	576	579	560	514	434	330	271	Wh/sq.m
Direct Normal Radiation (Avg Hourly)	312	344	422	420	474	577	597	500	571	524	403	344	Wh/sq.m
Diffuse Radiation (Avg Hourly)	129	154	162	181	389	132	121	119	121	121	312	120	Wh/sq.m
Global Horiz Radiation (Max Hourly)	642	751	920	3009	1043	1047	1036	1009	943	835	683	582	Wh/sq.m
Direct Normal Radiation (Max Hourly)	884	942	927	959	947	947	947	936	895	835	935	885	Wh/sq.m
Diffuse Radiation (Max Hourly)	319	402	498	473	521	474	288	172	251	253	364	322	Wh/sq.m
Global Horiz Radiation (Avg Daily Total)	2783	3635	5366	6121	7339	8176	8086	7339	6385	4738	3199	2663	Wh/sq.m
Direct Normal Radiation (Avg Daily Total)	3149	3696	4994	5388	6528	8185	8331	7788	6972	5864	4156	3087	Wh/sq.m
Diffuse Radiation (Avg Daily Total)	1297	1657	1923	1941	2330	1877	1697	1380	1480	1247	1149	1185	Wh/sq.m
Global Horiz Illumination (Avg Hourly)	29887	36535	46912	51568	57430	61896	62590	60590	55535	49924	33509	29203	lux
Direct Normal Illumination (Avg Hourly)	29361	32067	41408	41436	47083	57286	59285	58722	56338	50211	38144	31072	lux
Dry Bulb Temperature (Avg Monthly)	6	7	10	14	21	24	26	26	23	17	12	7	degrees C
Dew Point Temperature (Avg Monthly)	2	0	2	3	5	7	11	11	9	9	4	1	degrees C
Relative Humidity (Avg Monthly)	80	65	63	52	41	40	48	48	46	60	66	67	percent
Wind Direction (Monthly Mode)	210	30	200	240	200	200	210	210	210	200	30	30	degrees
Wind Speed (Avg Monthly)	2	2	3	3	2	4	4	3	2	2	2	2	m/s
Ground Temperature (Avg Monthly of 3 Depths)	13	30	9	9	12	15	18	21	22	22	20	16	degrees C

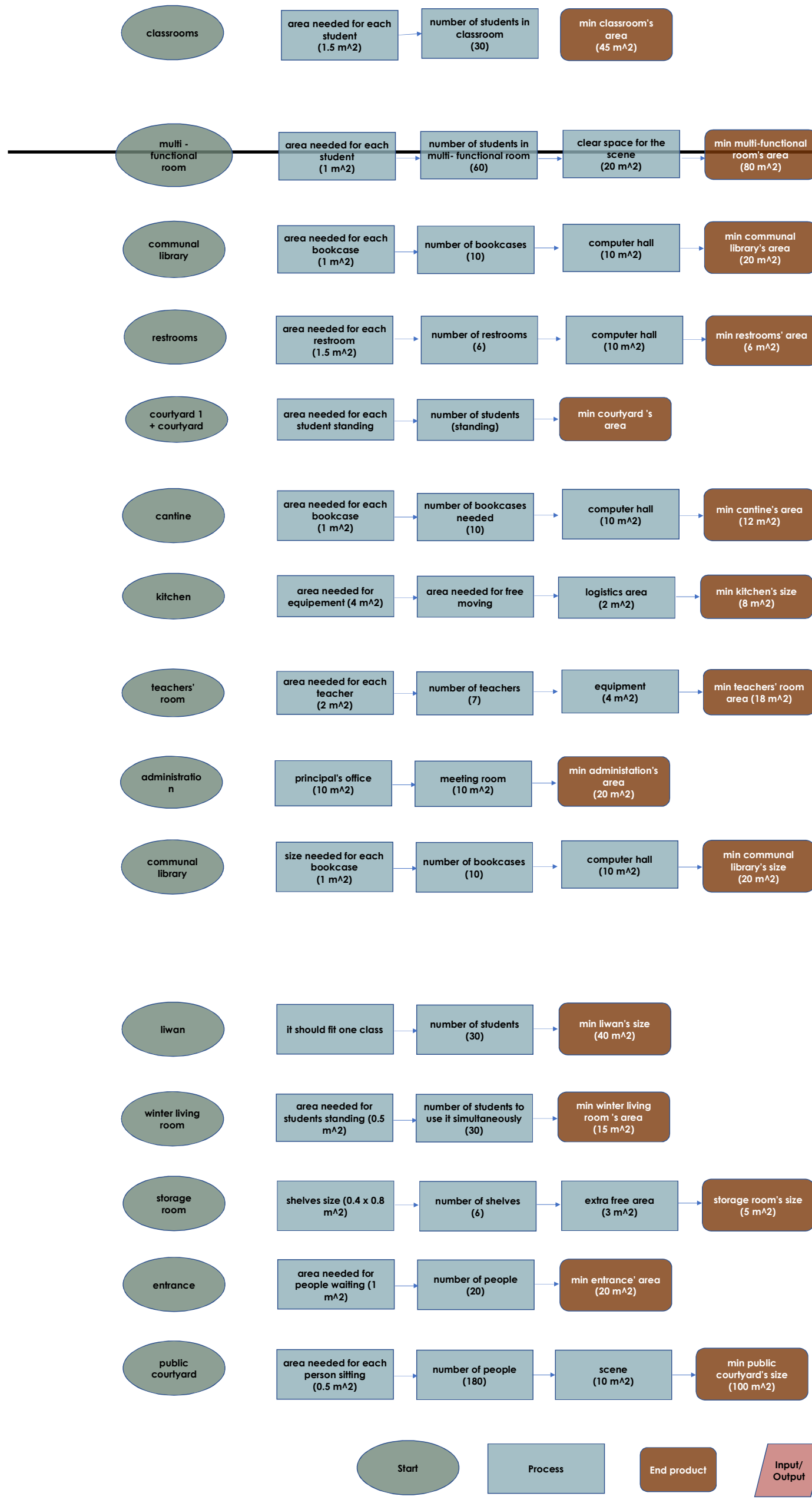
Back Next

APPENDIX B

Programme of requirements

Functional Areas (Bubble diagram)	Description	Connected to (REL Chart)	open / semi-open / closed space	min Free height requirements	Quantity	Size per room in functional cluster [m ²]	Accomodating (per room)	min Area for Cluster [m ²]	m ² per person	Orientation (N,E,S,W)	Day light requirement [LUX]
Class rooms 1	class room for younger children		closed	2700	4 class rooms	45	30 Pupils	172.8	1.5	-	300- 500
Class rooms 2	class room for elder children		closed	2700	3 class rooms	45	30 Pupils	129.6	1.5	-	300- 500
Multi Functional room	Music Art Gym Community ...etc	adjacent to courtyard, easy access from public and kids	Semi Open	4000	0	420	150 people / basket ball court	86.4		-	300
Communal Library	Might include a computer hall and is open to public out of school hours	Outside access as well as inside	Closed	2700	0	40	Book shelves only	23		-	200 (Shelves area) - 500 reading area
Restrooms 1			Closed	-	1	7.6	(3 * 0.9 * 1.7) + 3 m ²	5.76		-	150
Restrooms 2			Closed	-	1	7.6	(3 * 0.9 * 1.7) + 3 m ²	14.4		-	150
Court Yard 1	In the Center		Open	-	1	Proportional	-	54.7		-	-
Court Yard 2	In the Center		Open	-	1	Proportional	-	34.56		-	-
Cantine	kiosk for events and teachers while the multi functional room can host eating tables if needed	connected to kitchen	Semi Open	2700	1	6		12.96		South	200
Kitchen	needs a logistics point to get things in and out		Closed	2700	1	4		8.64		South	500
Teachers room		adjacent to administration	Semi Open	2700	1	50	20	28.8		-	500
Administration				2700	1	20	3	28.8		-	500
Liwan		open to courtyard	semi	5400	1	30	-	40.32		South	200
Winter living room		open to courtyard	semi	5400	1	30	-	17.28		North	200
storage room entrance		-	closed	-	1	20	-			-	-
public courtyard								23.04			
								110.88			

Program of Requirements Flochart

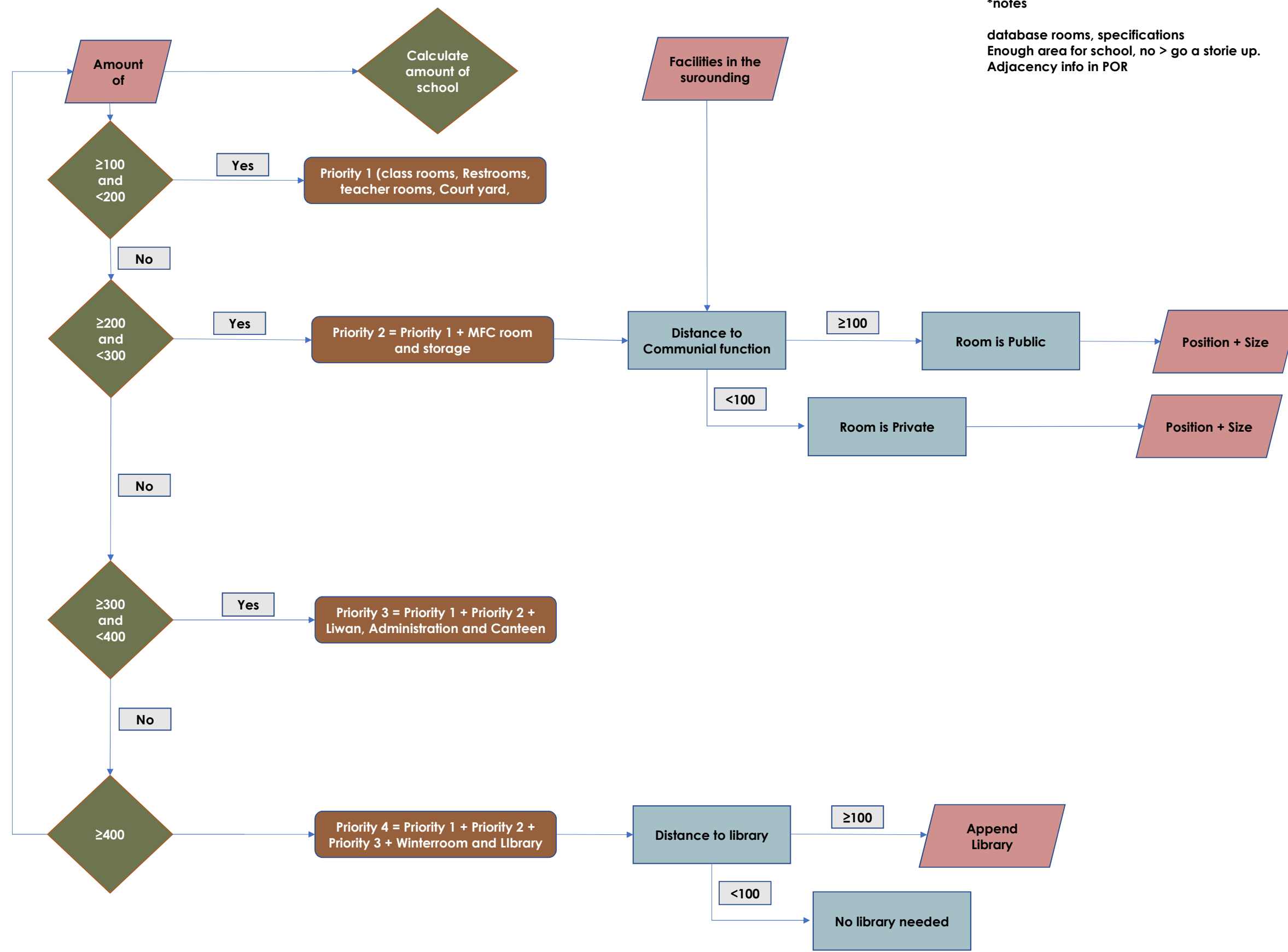


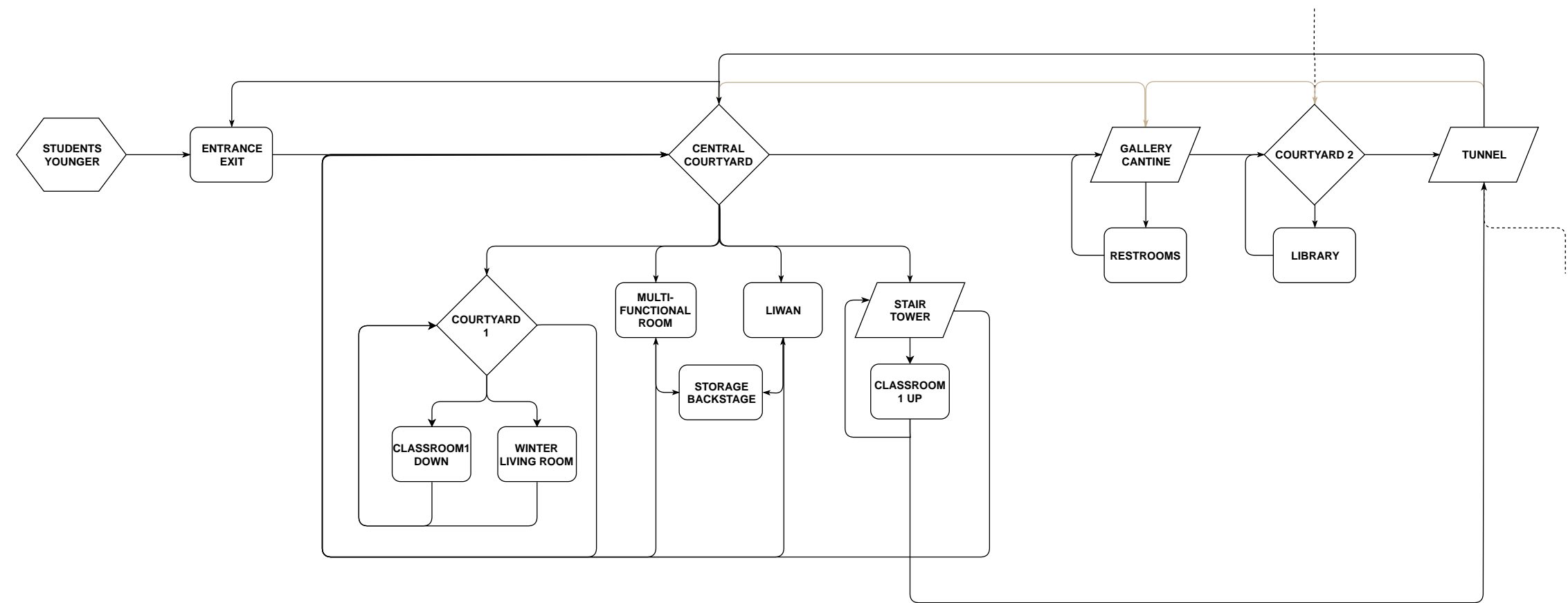
APPENDIX D

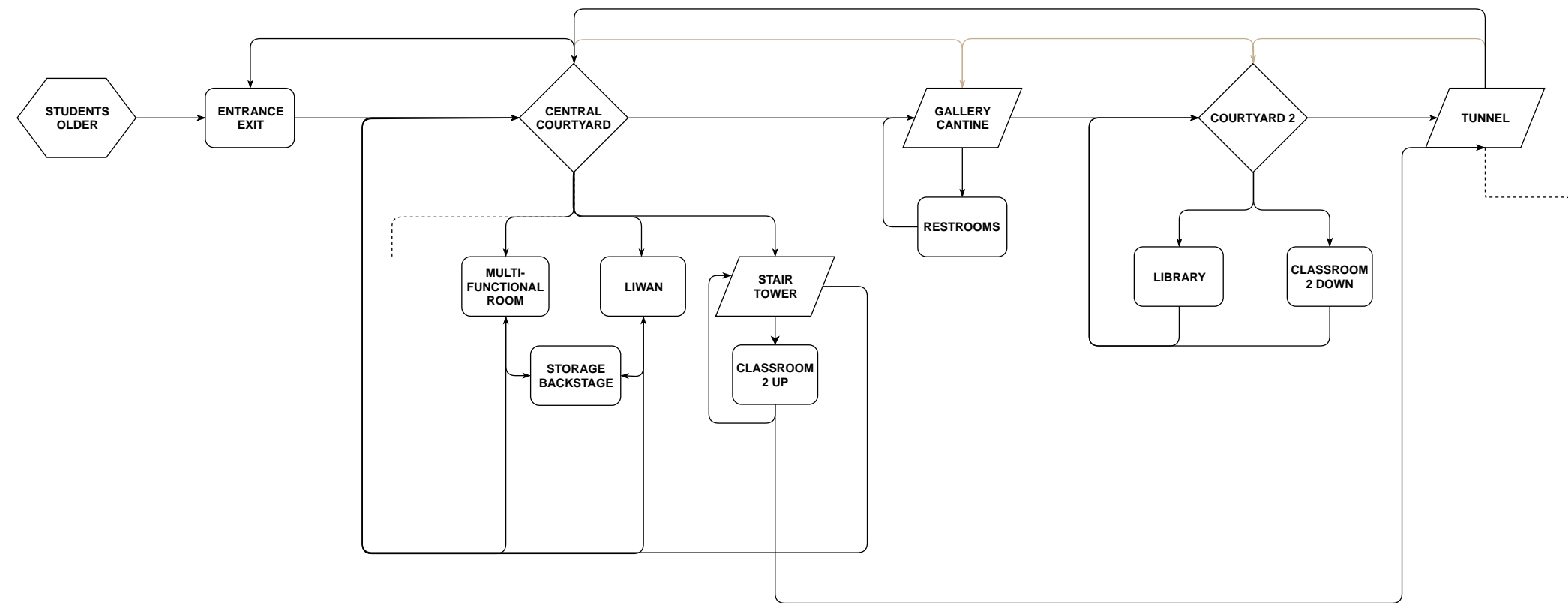
Priority 4 Floorplan Flowchart based on Psuedocode

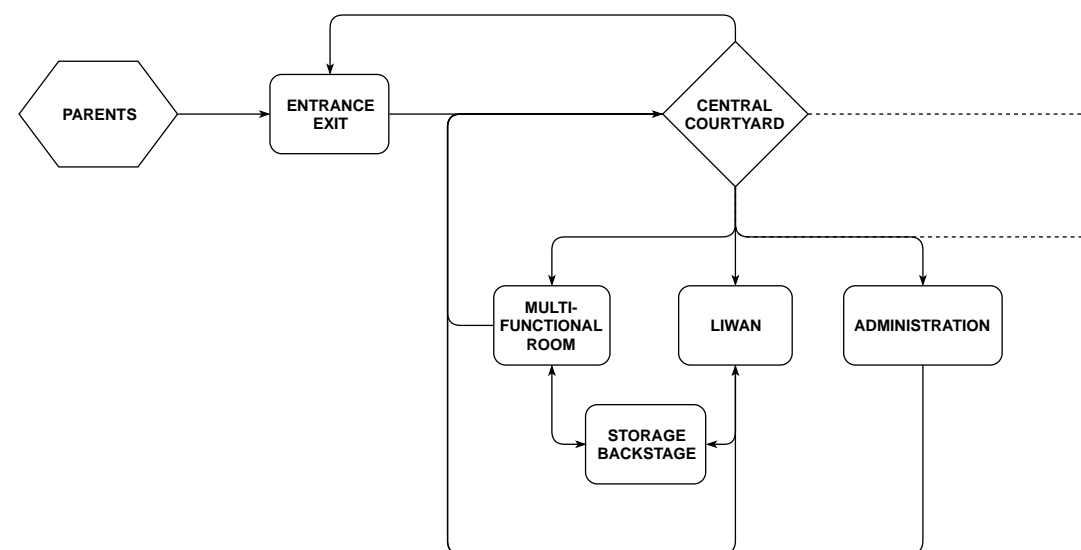
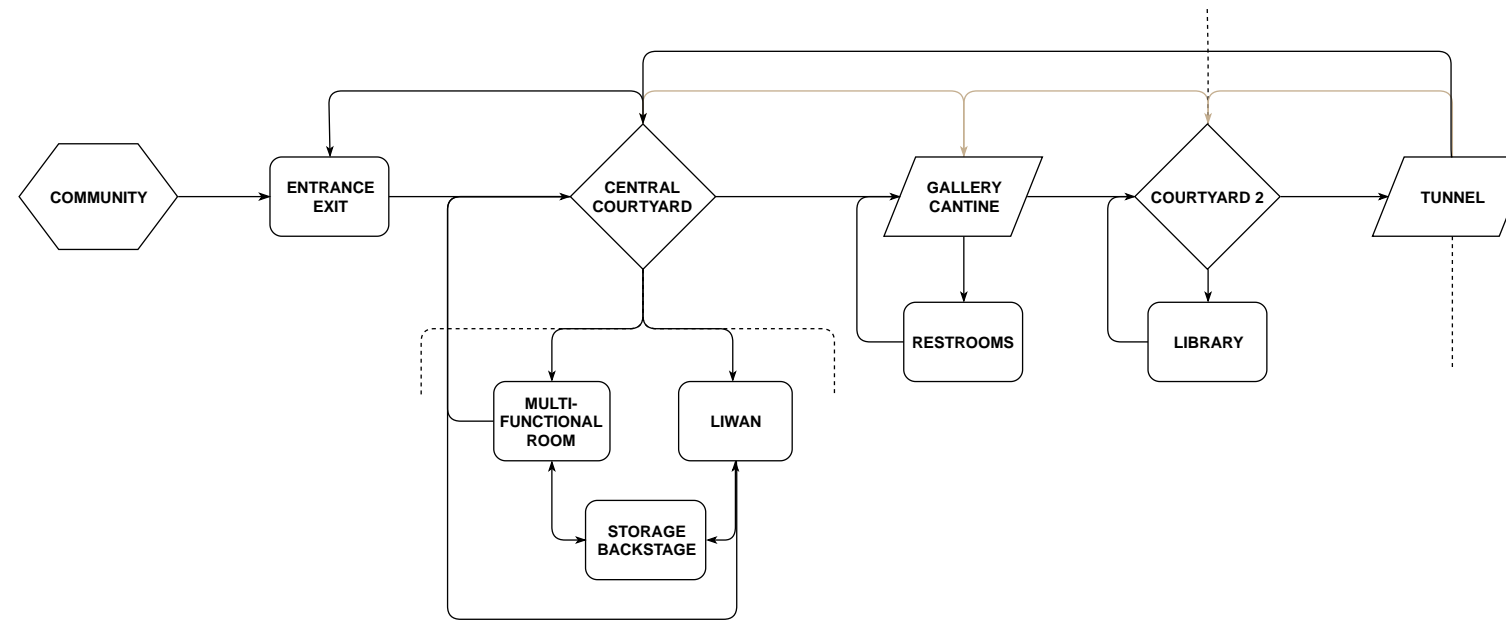


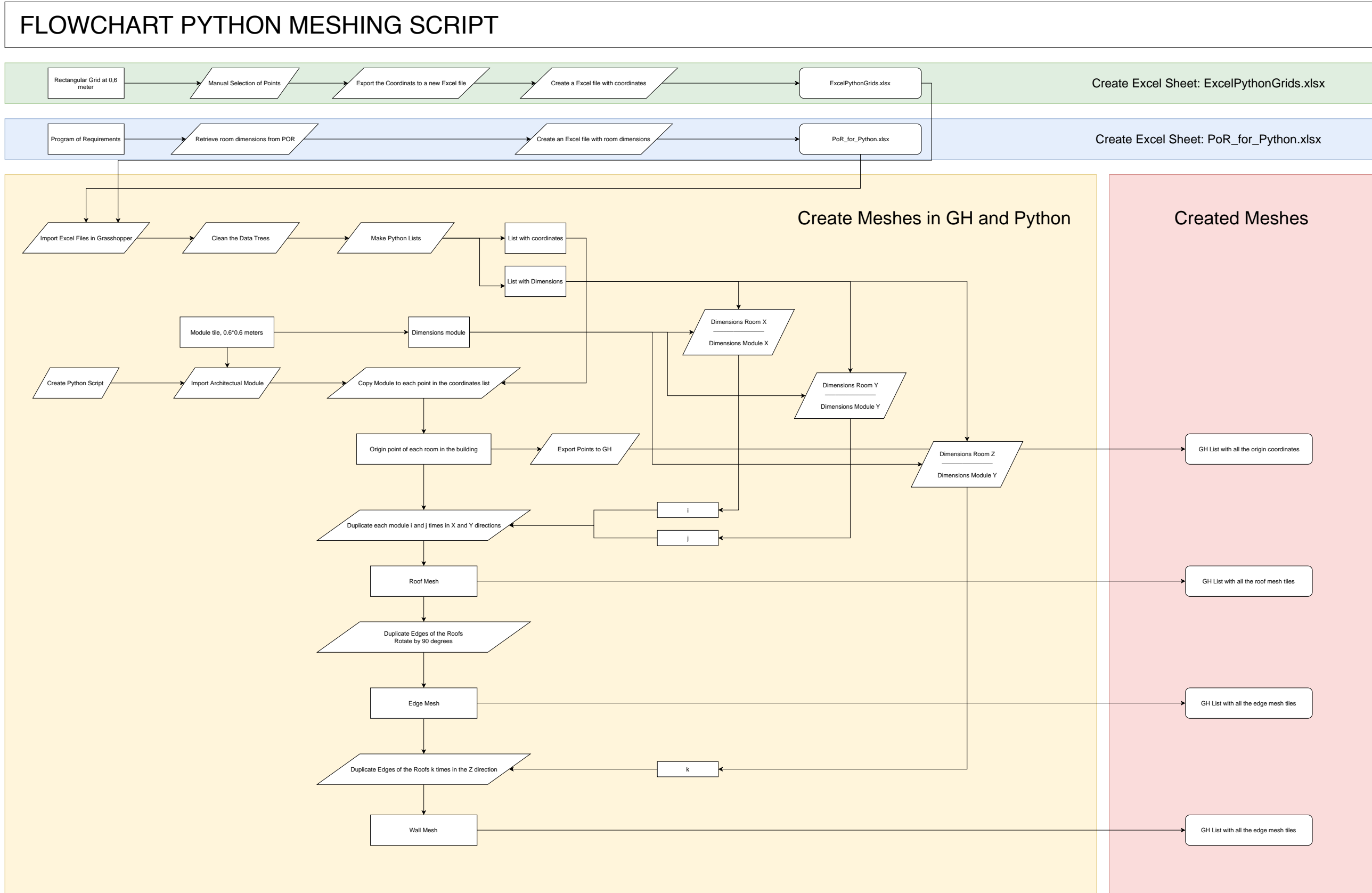
Flowchart School floorplan selection

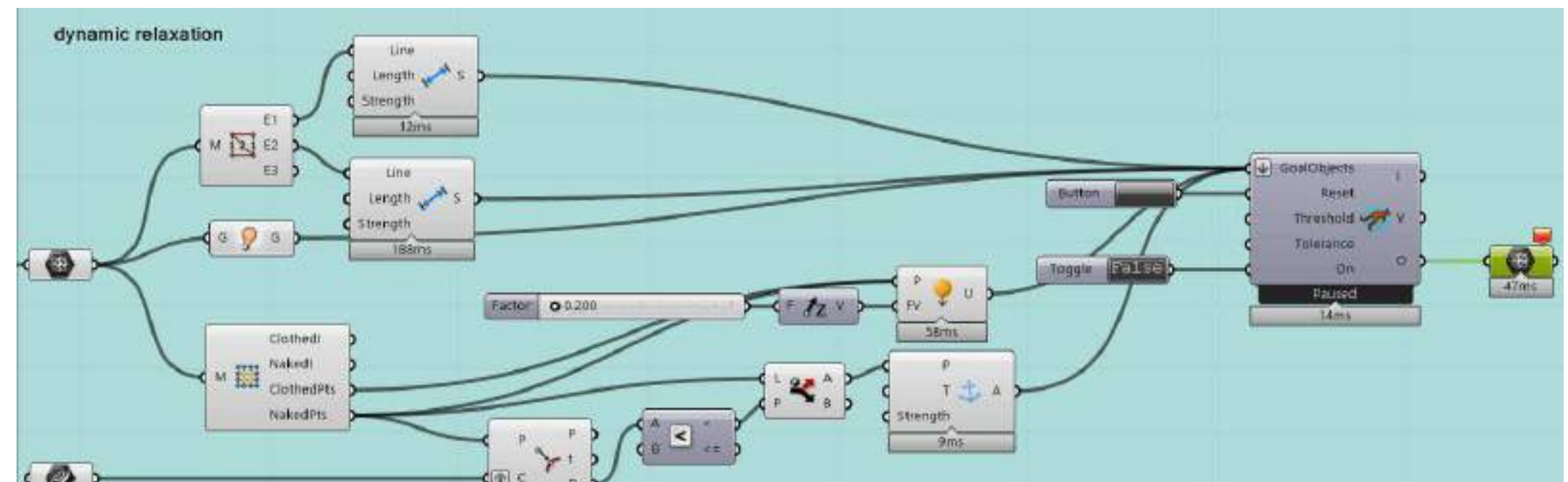












See following pages for the Brick Breaking Report

Laboratory experiments with adobe bricks
Strength of handmade adobe bricks

Earthy (AR3B011)
Delft, 4th November 2019
Mentors:
Prof.dr.ir.arch. Sariyildiz, I.S.
Dr.ir. Veer, F.A.
Dr.ir. Nourian, P.
Ir. Hoogenboom, J.J.J.G.
Ir. Rinze Visser, D.R.
Ir. Azadi, S.
Ir. Schnater, F.R.

Team:
Chouliara, K. - 4744292
Dimas, M. - 4893344
Engels, S.L. - 4813022
Naous, D. - 4290038
van Nimwegen, B. - 4484770
Rijsterborgh, R. - 4483014

Summary

This research is part of the EARTHY course, the subject of which is to design a structure that consists of only earthy materials in order to improve the quality of life in a district of Al Zaatri Refugee Camp in Jordan. The following main research question will be investigated in this study: *What are the structural properties of handmade adobe bricks and what is the impact of different additives in these bricks?* This research was done to determine the structural specifications for self handmade adobe bricks. Pure adobe specimens were chosen to determine the base strength of the adobe material and to make the additives comparable to this baseline.

To fabricate the adobe specimens the following steps were taken: mixing the materials, making the specimens and measuring and rotating. Then a specimen was taken and put under the machine and pressed down onto the brick until the maximum strength was reached.

Table of content

Summary

Notation

1. Introduction

2. Methodology

 2.1. Problem statement

 2.2. Research objective

 2.3. General research design

 2.4. How the specimens were made

 2.5. Method of testing

3. Results of the measurements

 3.1. Properties of the tested specimens

 3.2. Results

 3.2.1. Moisture content

 3.2.2. Stress

 3.2.3. Young's modulus

 3.2.4. Graphical analysis

 3.3.5. Accuracy

 3.3.6. Behavior during breaking

4. Discussion, limitation and conclusion of the research

 4.1. Discussion and limitations

 4.2. Conclusion

References

Appendix list

Notation

Table 1:
Symbols and unit of measure research (own table)

Description symbol	Symbol	Unit of measure
Force when breaking	F_{break}	N
Deflection breaking	dL at break	mm
Length	L	mm
Height	d	mm
Width	b	mm
Section area	a	mm ²
Stress	σ	N/mm ² (MPa)
Young's modulus	E	N/mm ² (MPa)
Deflection ratio	ϵ	N.A.
Mean value of the sample	\bar{x}	N.A.
Population standard deviation	σ	N.A.
Confidence factor	t	N.A.
Standard deviation of the measurements	S	N.A.
Confidence included a confidence factor	$\delta\bar{x}$	N.A.
Amount of test specimen	n	N.A.

1. Introduction

This research is part of the EARTHY course, the subject of which is to design a structure that consists of only earthy materials in order to improve the quality of life in a district of Al Zaatri Refugee Camp in Jordan. The goal is to design buildings that can ideally be constructed by their prospect inhabitants. Adobe was selected for these structures because it is locally available, it has relatively good structural capabilities and it has low fabrication and labor costs. The following main research question will be investigated in this study: *What are the structural properties of handmade adobe bricks and what is the impact of the different additives in these bricks?*

This research was done to determine the structural specifications of self handmade adobe bricks. To acquire these specifications specimens were made and tested by the students of this course. The results from these tests (including the making of the specimens) are discussed in this research.

In this report in chapter 2, methodology, the problem statement, research objective, general research design, are discussed. In chapter 3, the results of the measurements, the properties of the tested specimens and the results of the calculations are presented. Finally, in chapter 4, the discussion, the limitations and the final conclusion of the research will be analysed.

2. Methodology

2.1. Problem statement

The objective of the course EARTHY was the implementation of design strategies in a district of Al Zaatri Refugee Camp in Jordan in order to improve the life quality of the inhabitants. The approach of the course was to design and engineer earthy buildings, in particular from adobe materials. Earthy buildings are virtually 100% recyclable and they offer more comfort in comparison to tents. One of the focus points of the course is the relationship of the availability of the local materials with their structural properties. To use these local materials without definitive additions to build buildings that are 100% recyclable, research and experiments are required to understand the structural properties of the bricks made of these locally available materials.

2.2. Research objective

In this research, the structural properties and the influence of the different additives of adobe bricks will be discussed. The thirty different specimens which will be tested are self handmade with the same given basic recipe and with any selected additives. The shape of all the specimens are trapezoid prism in two different sizes, which are made in supplied molds. To test the structural properties, all the specimen types are tested by performing a true-experiment with a compression test. The property of the of the bricks will be defined by calculating the stress.

The following research question is defined: *What are the structural properties of self handmade adobe bricks and what is the influence of the different additives in these bricks?*

2.3. General research design

Table 2 shows the materials and mixtures that were used to make the adobe bricks. Pure adobe specimens were chosen to determine the base strength of the adobe material and to make the additives comparable to this baseline. With this baseline adobe mixture the following materials were mixed: clay, coarse sand, fine sand and water. The mixtures varied only in respect to the additive. The proportions of the different mixes can be found in table x.

For two of the five mixtures we used the hay and wood chips that were supplied by the university. These additives are a cheap and readily available material. Textile was chosen by the group, because this also represents a material that is easy to acquire. Rubber bands were selected to see what a stretchable material would do to the strength of the specimens. Other materials were also considered and rejected, due to lack of availability. For example, lime could have been a good alternative, but after studying the soil of the area, it was discovered that the percentage of available lime was actually very low, so it was rejected.

Table 2:
Materials and mixtures (own table)

	Clay %	% Coars Sand	% Fine Sand	% Water	% Hay	% Woodchips	% Rubberbands	% Textile
Pure Adobe	27	36	27	9	0	0	0	0
Adobe + Hay	27	36	27	9	0,65	0	0	0

Adobe + Woodchip	27	36	27	9	0	1	0	0
Adobe + Rubberbands	27	36	27	9	0	0	2,2	0
Adobe + Textile	27	36	27	9	0	0	0	1,3

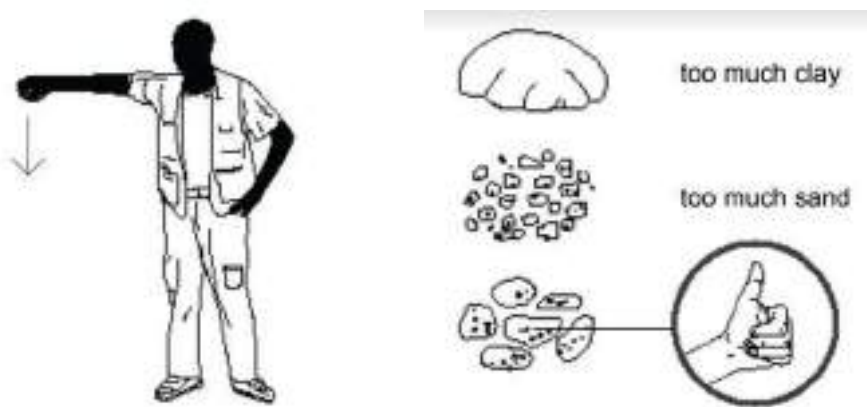
2.4. How the bricks were made

To fabricate the adobe bricks the following steps were taken:

1. Mixing the materials; the materials were taken from the bag that contained them and were put into buckets. The buckets were weighed on a person scale to determine the correct mixing ratios as seen in table 2. After this, the materials were put together in one bigger bucket and stirred with the help of a mixing machine. The materials were mixed until the consistency would not change anymore, which generally happened after ~5 minutes of mixing. The mixture was considered ready after it was tested with the ball rule, see figures 1 and 2.

2. Making the specimens; the molds that were used for making the specimens were the typical Tupperware trays. For the experiment two sizes of molds were used. The first mold had a dimension of 100x100x60 millimeter (LxWxH) and the second mold 60x60x50 mm. The mixture was put into the molds and hand-pressed to make the mixture compact in the mold. After this, the bricks were directly released from the mold and put onto a pallet.

3. Measuring and rotating; after the specimens were made they were directly weighed. Every day, excluding weekends, the specimens were rotated to ensure that they would dry equally. The specimens were also placed away from direct sunlight. On the last two days of drying the specimens were removed from the pallet and placed directly on to the heated floor. Right before the destructive testing the specimens were weighed again to determine the final weight and moisture content.



Figures 1 and 2: Mixture ball test, (Granier, 2014, p. 9)

2.5. Method of testing

The destructive testing was done in the following manner. All the specimens in the test had an age of 7 days. First the specimens were grouped depending on the additive. Then a specimen was taken and put under the machine on a piece of plywood and pictures were taken. The machine was put into action and pressed down onto the brick until the maximum strength was reached. The maximum strength was then documented in an excel file. After this the sample was removed, pictures were taken and the sample was discarded into a bucket. Figures 3 and 4 showing a brick before and after the compression test.



Figures 3 and 4: A brick before and after the compression test (own figures)

The pure adobe mixtures were separated from the ones with additives, as pure adobe could be reused (figures 5 and 6). After the tests the final results were emailed to use for further analysis. Afterwards, the data from all the groups were exchanged to get a larger test group for the only adobe specimens, straw and wood chip mixtures.



Figures 5 and 6: Division of mixtures (own figures)

3. Results of the measurements

In this chapter, the properties of the tested specimens and the results will be discussed. For this research five different brick mixtures were tested, molded in two different brick sizes; pure adobe, adobe with rubber, adobe with textile, adobe with wood chips and adobe with hay. Additional information and calculations in this chapter are added in appendix I.1 till I.4. If there will be looked in the literature for earlier tests, it can be made clear in what order of magnitude the values of the properties should be. If the 2007 Gubasheva tests were seen as reliable and as comparison material, the values of the maximum stress would be approximately between 2.14 and 2.88 MPa. The values of the Young's modulus between 98 and 211 MPa.

3.1. Properties of the tested specimens

The conditions and the way in which the specimens were made were different for each group. The reason for this is because all the groups made and mixed their own mixtures. In this research the results of all the groups for pure adobe specimens will be examined. Every group made its own adobe mixtures. Even though, all adobe mixture were based on the same given recipe, the procedure was not entirely precise, so all mixtures should be considered slightly different.

Two batches of pure adobe were made in this group to make all of our specimens. The same molds were used for all - bricks, so as the dimensions are not to differ considerably. However since they were hand-made, no - specimens can be considered identical. Two sizes of molds were used to make the pure adobe specimens. The molds used per group were different, so the dimensions will differ considerably. This must be corrected in the calculations. The measured dimensions and the failure stress of the tested specimens are shown in tables in appendix I.1.

3.2. Results

For the results the different series of specimens are used. In this paragraph the graphical analysis, accuracy and stress will be discussed.

3.2.1. Moisture content

The day that the bricks were made the initial moisture content was also measured. On the day of the destructive testing the moisture content of the bricks was measured again. These measurements were done to determine the remaining moisture content. This in terms would determine if the bricks are fully dried and therefore have reached their maximum strength.

Observations after breaking the specimens showed that the core of the specimens was still moist. The expectation is that if the specimens were completely dried out, the stress values would be higher than the results of the experiments.

Table 3 shows the results of the moisture measurements. The table shows that many samples have lost more moisture than that originally was put in them in the form of water. This is of course not possible. The reason for this faulty results is probably because there was moisture in one of the materials prior to mixing. When the mixture was measured on the day of making it was noted that the coarse sand was very moist. This is possibly the source of the extra moisture.

Table 3:

Moisture content (own table)

Specimen type:	Mass specimen before drying (average) [kg]:	Mass specimen after drying (average) [kg]:	Δ Mass [kg]:	Moisture content before drying (average) [%]:	Moisture content after drying (average) [%]:
Only adobe (big)	1,61	1,42	0,19	9,1%	-3,3%
Only adobe (small)	0,53	0,47	0,06	9,1%	-1,6%
Rubber additive	0,45	0,42	0,03	8,9%	5,4%
Textile additive	0,46	0,39	0,07	9,0%	-6,3%
Wood chips additive	0,48	0,40	0,08	9,0%	-8,6%
Hay additive	0,46	0,40	0,06	9,0%	-4,2%

3.2.2. Stress

The stress is calculated with the maximum force that the machine has exerted on the specimens (F_{max} [N]) and the smallest horizontal section area [mm^2]. With these two values, the failure stress [Mpa] can be calculated using formula 1. The measured dimensions and the failure stress of the tested specimens are shown in tables in appendix I.1.

$$\text{Failure stress} = \frac{\text{Maximum force}}{\text{Horizontal section area}} \quad \sigma [\text{Mpa}] = \frac{F_{max} [\text{N}]}{a [\text{mm}^2]} \quad (1)$$

3.2.3. Young's modulus

The Young's modulus is calculated with the failure stress [MPa] and the deflection ratio [-]. The deflection ratio can be determined by dividing the determined deflection [mm] by the starting level [mm]. With these two values, the E-modulus can be calculated using formula 2.

$$E = \frac{\sigma}{\epsilon} \quad E = \frac{\sigma}{\frac{\Delta l}{l_0}} \quad (2)$$

If this calculation is applied with the measured values, an average E-modulus of 9.52 MPa is obtained. This value seems unreliable, since the values from the literature are 10-15 times higher, without applying any statistics, so that this value will end even lower. That is why this report is not discussed further in the E-modulus. The E-modulus that is ultimately chosen will therefore come from the literature and not from this research.

3.2.4. Graphical analysis

After comparing all the results in a scatter plot, a pattern emerge can be seen. This pattern shows exactly the samples of each group (separated by redlines). Some groups show a consistency in there testing results whilst other groups are much more divided over the spectrum. This division and grouping is seen throughout the different additives. Figure 7 shows the scatter plots with separating of each group of the only adobe specimens. The other scatterplots can be found in appendix I.2. In these scatter plots, the values are not ranked by size but per group that has tested them specimens.

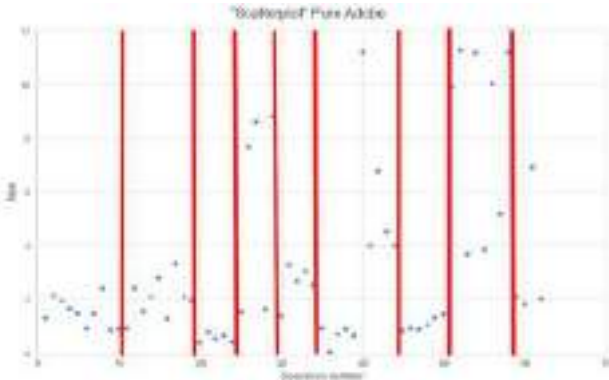


Figure 7: Scatterplot pure adobe (own figure)

By using a box plot, the extremely high and low values can be filtered. A box plot is a much simplified, but useful, representation of the distribution of the data. The spacings between the different parts of the box indicate the degree of dispersion (spread) and skewness in the data, and show outliers. In the box plots it can be seen that the values between 0 and the median are closer to each other than the values from the median to the maximum value. As a result, the average is always higher than the median, due to the peaks upwards. In figure 8 the box plot only of the adobe specimens is shown. All the boxplots of all the different additives can be found in appendix I.2.

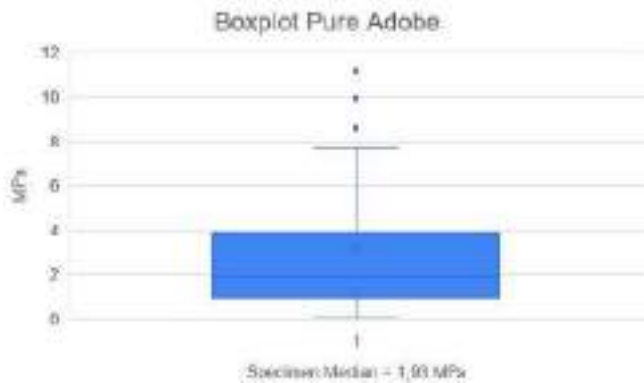


Figure 8: Boxplot pure adobe (own figure)

After starting to look at the differences in testing between all the additives, the following can be concluded. When looking at the pure adobe this is to be the weakest material. But comparing the scatterplots it also seems that the results are the most inconsistent, showing large divisions between groups. Straw seems to be the most consistent of all the additives. The strength of the bricks differ greatly between additives, the strongest additive seems to be straw.

3.2.5. Accuracy

With the different types of specimens, it is possible to make a histogram of the mean values of all the repeated measurements to show a normal distribution. Since there are only 5 specimens per series for three of the six additives, it is better to just look at the values in table xx. For the groups with a relatively large n it can be useful to look at the histograms to determine a value. Table 4 shows the frequency table of the failure stress for the only adobe specimens and the corresponding histogram/normal distribution (figure 9). For the other frequency tables and histograms see appendix I.2.

Table 4:
Frequency table pure adobe (own table)

Lower limit	Upper limit	Range	\bar{x}_i	n _i	f _i	c _{ni}	c _{fi}
0,001	0,250	[0;0,25]	0,126	1	2%	1	2%
0,251	0,500	[0,25;0,5]	0,376	2	3%	3	5%
0,501	0,750	[0,50;0,75]	0,626	4	6%	7	11%
0,751	1,000	[0,75;1]	0,876	10	16%	17	27%
1,001	1,250	[1;1,25]	1,126	1	2%	18	29%
1,251	1,500	[1,25;1,5]	1,376	7	11%	25	40%
1,501	1,750	[1,5;1,75]	1,626	4	6%	29	47%
1,751	2,000	[1,75;2]	1,876	4	6%	33	53%
2,001	2,250	[2;2,25]	2,126	4	6%	37	60%
2,251	2,500	[2,25;2,5]	2,376	2	3%	39	63%
2,501	2,750	[2,5;2,75]	2,626	2	3%	41	66%
2,751	3,000	[2,75;3]	2,876	1	2%	42	68%
3,001	3,250	[3;3,25]	3,126	1	2%	43	69%
3,251	3,500	[3,25;3,5]	3,376	2	3%	45	73%
3,501	3,750	[3,5;3,75]	3,626	1	2%	46	74%
3,751	4,000	[3,75;4]	3,876	3	5%	49	79%
4,001	4,250	[4;4,25]	4,126	0	0%	49	79%
4,251	4,500	[4,25;4,5]	4,376	0	0%	49	79%
4,501	4,750	[4,5;4,75]	4,626	1	2%	50	81%
4,751	5,000	[4,75;5]	4,876	0	0%	50	81%
5,001	More	More	5,001	12	19%	62	100%
SOM:		82	100%				

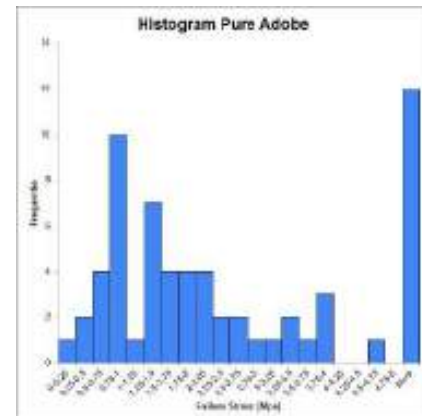


Figure 9: Histogram pure adobe (own figure)

As discussed earlier at the box plots, some values are considerably higher than others. These values influence the average and therefore these values will not be considered. These values fall outside the first and last quartiles. In the histograms, these bars can also be ignored in the search for the bell shape. A bell shape can be discovered in the different histograms. The top of this bell shape should roughly indicate the value to be chosen. For the groups with a small n this form is more difficult to discover and the value will therefore deviate from reality. The range between which the values must be chosen is shown per material and addition in table 5, derived from the histograms.

Table 5:
The range between which the values must be chosen (own table)

Specimen type:	Range chosen values Failure Stress [Mpa]
Only adobe	0,75 - 1,5
Rubber additive	0,75 - 1,25
Textile additive	1,0 - 1,2
Wood chips additive	1,0 - 3,1
Hay additive	1,4 - 1,8
Straw additive	3,0 - 4,0

For each group of measurements, the statistical estimation of the imprecision is calculated, see appendix I.3. For each group of measurements (n) the imprecisions are given in table 6. To have a confidence statement, including statistical estimations of

measurements, of 95% confidence the factor that expresses the confidence which states the imprecision is correct (t) is depending on the number of measurements (n), (Tenpierik, 2018)

Table 6:
Statistical estimation of the imprecision: 95% confidence (own table)

Specimen type:	Statistical estimation of imprecision:
Only adobe	$\pm 7,9E-01$
Rubber additive	$\pm 3,1E-01$
Textile additive	$\pm 1,5E-01$
Wood chips additive	$\pm 7,7E-01$
Hay additive	$\pm 2,9E-01$
Straw additive	$\pm 8,9E-01$

Each building material has a safety factor to make the material weaker in the calculation, so that the construction is ultimately extra strong, over dimensioned. Since adobe is a still unknown material, it will have a relatively higher safety factor than other building materials. Other materials are used to determine this safety factor. In the Netherlands and Belgium, this safety factor for reinforced concrete is 1.5, for solid wood 1.3 and for structural steel 1.15. These factors show that the quality of steel can be better controlled than the quality of concrete. For masonry, the values are between 1.5 and 3. (Van Normen & Reglementen, 2003) For this project, Adobe will also fall under masonry. Therefore, a safety factor for adobe will be chosen between 2 and 3.

3.2.6. Behavior during breaking

For the behavior during breaking analysis only the stress diagrams of the specimens, which were made and tested by this group, are examined. This because, the different additives of the samples, could not be determined from the excel sheet. These diagrams are provided in appendix I.4.

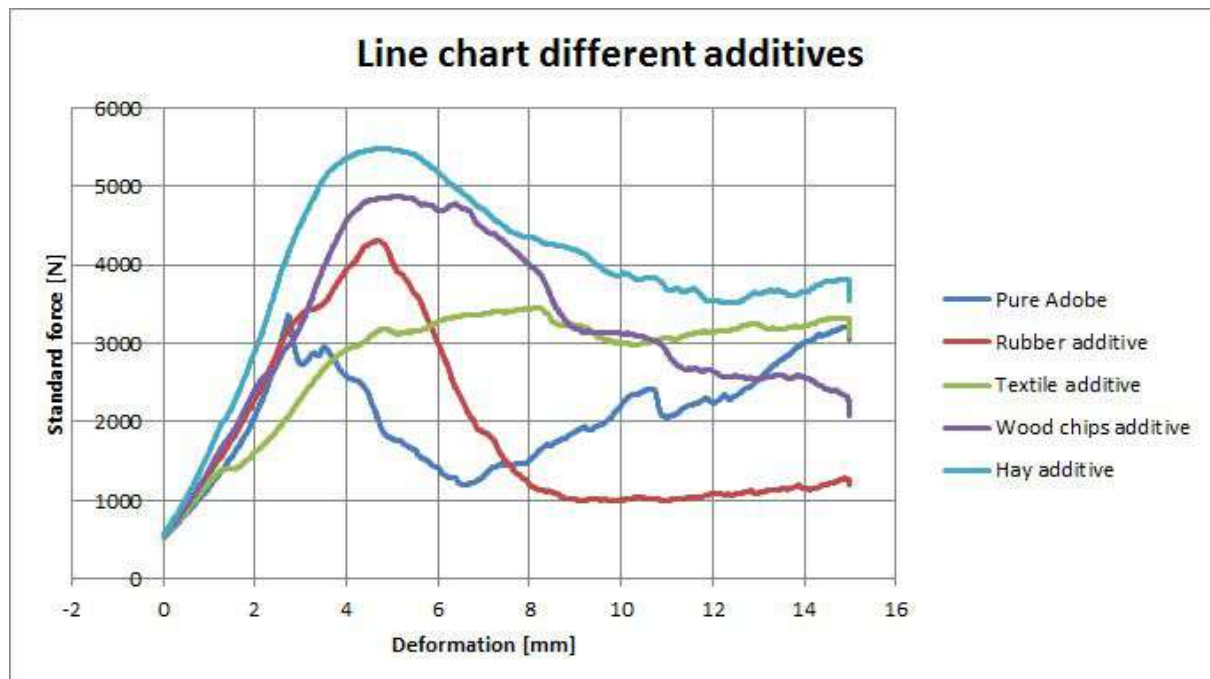


Figure 10: Line chart behavior during breaking (own figure)

The graph in figure 10, shows the deformation for all the small bricks with and without different additives. The machine sinks at a constant speed and the force that is exerted thereby always increases to guarantee this speed. For this graph, the average lines have been selected for all additions that are (approximately) characteristic of these additions. These lines show the behavior of the different specimens. The graph for the rubber additive gives a different pattern in comparing the other specimens, the strength builds up to a certain point at which it in turn fails instantly. The same is true for wood chips, but the failure is less critical. Hay and textile both show a different pattern. These materials build up until a relatively high stress and then withstand this stress for a longer period without it breaking. The reason for this is probably the fibrous nature of both materials.

4. Discussion, limitations and conclusion of the research

In this chapter the discussion, limitations and conclusion of the research regarding the main research question.

4.1. Discussion and limitations

During the making of the specimens, a number of things came to light that could influence the results of the research:

- Inconsistencies in the measurements because a person scale was used to measure out the materials for the mixtures. These scales are not accurate enough to weigh such small quantities of material. The ratios may therefore differ in each different mixture of each group.
- Inconsistencies because of mixing the materials. This was done by machine and with the pure adobe mixtures this was relatively consistent. With the different mixtures it proved hard to make consistent mixtures due to the additives sticking to the mixing machine.
- Inconsistencies because of the way the specimens were molded. There was no way of guaranteeing the same pressure was used for pressing each stone. Another factor that could have influenced the results is that the bricks were made by different members of the team. The same applies of course that each group made its own specimens in different ways.

During the testing of the specimens, a number of things were noticed that could possibly influence this research:

- Because the specimens did not dry through and through, the measured value could deviate from the actual situation where the bricks were completely dried.
- Inconsistencies in the measured deformations, it is very probable that the piece of plywood that was used to put the specimens on when testing the strength also took some of the deflection. This causes the specimens to “appear” more deformed than they in reality could deform.

The limitations of this study are the five specimens for some groups of specimens are used. The accuracy is limited as this small test group.

When analysing the results it was found that there was a large deviation in the results, especially for the pure adobe bricks. According to research (Sasui, 2017) where they looked at the variations in the strength of adobe bricks, the biggest factor that caused this deviation was the variances of pressure when making the bricks with molds. This caused a difference in compaction of the soil in the molds and thus they become less strong.

4.2. Conclusion

The main question that was central to this research was as follows: *What are the structural properties of handmade adobe bricks and what is the impact of the different additives in these bricks?* Before answering this question based on the interpretation of the results, something general can be said about the results.

The results showed outliers that were high or low compared to the other values. It can be said that the lowest measured value must be used for building with the material. If this value is chosen, the design is certainly safe. The design is then probably overdimensioned since most bricks of this material will be a lot stronger than the lowest measured value. It will always be that there will be bad bricks among the large amount of bricks. This does not mean that the building will collapse if these bad stones are in the construction. The forces in the building will look for the foundation via the strongest route in the construction. To solve this problem it is also possible to add a safety margin to the forces and material values that will be exerted on the building, so that the structure will never reach the maximum value that it can handle.

From the results, a range is given for each type of specimen, each with a different addition,(sth unclear with the syntax) Table 7 shows the estimated safe design strength per specimen type with the 95% confidence statistical estimation of the imprecision. It should be noted that the test group of the specimens with rubber, textile and hay as additive had only a n of 5 per group and is therefore not reliable.

Table 7:
Chosen estimated safe design strength (own table)

Specimen type:	Chosen estimated safe design strength [Mpa]:	Statistical estimation of imprecision:
Only adobe	1,1	$\pm 7,9\text{E-}01$
Rubber additive	1,0	$\pm 3,1\text{E-}01$
Textile additive	1,1	$\pm 1,5\text{E-}01$
Wood chips additive	2,1	$\pm 7,7\text{E-}01$
Hay additive	1,6	$\pm 2,9 \text{ E-}01$
Straw additive	3,5	$\pm 8,9 \text{ E-}01$

It can be deduced from this table that fibrous materials as additive influence the strength of the material. The additives also influence the behavior during breaking. The specimens with straw as an addition come the strongest from this research with a strength of 3.5 Mpa. If the statistical estimation of imprecision or 95% confidence is removed to be safe, a calculation value of 2.6 Mpa remains. A safety factor for adobe will be 2.5 to weaken the material in the calculation to make the final structure strong enough, a safe over-dimensioned structure.

A more structured research should be done to improve reliability and repeatability to determine the adobe characteristics, because the results from this research have too many uncontrolled variables that make the results very undependable. This is also seen when comparing results between groups. Because of these undependable results there can be only given an estimated safe design strength.

References

- Granier, T. (Ed.). (2014). *The Nubian Vault Mason's Manual* (4th ed., Vol. 1). la vout e nubienne.
- Gubasheva, S. (2017). *Adobe bricks as a building material*. Czech Technical University, Faculty of Civil Engineering, Prague.
- Huwaja, S., Jinwuth, W., & Hengrasmee, S. (2017). Variation in Compressive Strength of Handmade Adobe Brick, 1–43.
- Tenpierik, M.J. (2018). AR1B025-D3_Lecture 3a_Measurements and data analysis_MJTENPIERIK. TU Delft Brightspace, AR1B025-D3, p.30.
- Van Normen & Reglementen, (2003). "Ontwerpen en dimensionering van constructies volgens Eurocode 0 (EN 1990)." WTCB tijdschrift.

Appendix list

- Appendix I.1: The measured dimensions and the failure stress
- Appendix I.2: Graphical analysis
- Appendix I.3: Statistical estimation of imprecision
- Appendix I.4: Behavior during breaking

Appendix I.1: The measured dimensions and the failure stress

Table 1:
The measured dimensions and the failure stress adobe only (own table)

Code	Dimensional Properties [mm]			Fmax (N)	dL at Fmax	Section Area [mm ²]	Failure Stress [Mpa]
	L	W	H				
ADDOE ONLY							
A1	160,00	100,00	60,00	14908,00	-	16000,00	0,931
A2	95,00	70,00	30,00	15037,38	5,81	6650,00	2,419
A3	95,00	70,00	30,00	10380,37	4,91	6650,00	1,561
A4	95,00	70,00	30,00	14003,23	3,90	6650,00	2,196
A5	95,00	70,00	30,00	18570,73	7,75	6650,00	2,793
A6	95,00	70,00	30,00	6604,43	5,11	6650,00	1,294
A7	170,00	90,00	40,00	51253,27	19,53	15300,00	3,352
A8	170,00	80,00	40,00	31973,98	7,55	15300,00	2,098
A9	170,00	90,00	40,00	29826,87	9,68	15300,00	1,952
1A	164,00	121,00	71,00	8319,96	11,76	19644,00	0,419
1B	159,00	124,00	63,00	15680,92	11,81	19716,00	0,795
1C	155,00	124,00	67,00	10478,11	11,19	19220,00	0,545
1D	159,00	114,00	64,00	12005,94	13,08	18126,00	0,662
1E	159,00	128,00	68,00	8844,50	12,41	20352,00	0,435
2A	113,00	113,00	43,00	19500,00	-	12768,00	1,527
2B	109,00	111,00	40,00	93036,24	24,98	12095,00	7,690
2C	109,00	108,00	36,00	101160,80	24,30	11772,00	8,893
2D	116,00	109,00	42,00	20709,00	-	12644,00	1,637
2E	111,00	102,00	40,00	91968,26	24,05	11322,00	8,830
S1a	95,00	70,00	30,00	9216,00	7,91	6650,00	1,386
S2a	95,00	70,00	30,00	21900,00	-	6650,00	3,293
S3a	95,00	70,00	30,00	17900,00	-	6650,00	2,692
S4a	95,00	70,00	30,00	20200,00	-	6650,00	3,038
S5a	95,00	70,00	30,00	16900,00	-	6650,00	2,641
1	100	100	60	13310,3	9,126376	10000,00	1,331
2	100	100	60	21595,4	9,896349	10000,00	2,169
3	100	100	60	19246,79	12,69633	10000,00	1,925
4	100	100	60	16456,54	14,32644	10000,00	1,646
5	100	100	60	14791,9	8,94633	10000,00	1,479
6	60	60	50	3360,184	2,725414	3600,00	0,933
7	60	60	50	5351,55	12,53665	3600,00	1,487
8	60	60	50	8721,683	3,744479	3600,00	2,423
9	60	60	50	3059,625	3,816359	3600,00	0,850
10	60	60	50	3241,821	6,386316	3600,00	0,901
1	105,00	105,00	65,00	16122,84	8,98	17325,00	0,931
2	105,00	105,00	65,00	1104,09	0,09	17325,00	0,064
3	105,00	105,00	65,00	12435,69	9,90	17325,00	0,718
4	105,00	105,00	65,00	15507,39	8,49	17325,00	0,800
5	105,00	105,00	65,00	11456,90	9,87	17325,00	0,681
6	110,00	80,00	30,00	98453,83	14,98	8800,00	11,188
7	110,00	80,00	30,00	35100,00	9,97	8800,00	3,889
8	110,00	80,00	30,00	59763,43	14,99	8800,00	6,791
9	110,00	80,00	30,00	39892,43	9,97	8800,00	4,633
10	110,00	80,00	30,00	35138,97	9,98	8800,00	3,893
A1	175,00	85,00	40,00	12457,81	11,32	14875,00	0,837
A2	175,00	85,00	40,00	13624,26	9,28	14875,00	0,916
A3	175,00	85,00	40,00	13027,70	11,29	14875,00	0,876
A4	175,00	85,00	40,00	15851,05	14,85	14875,00	1,072
A5	175,00	85,00	40,00	19770,12	8,58	14875,00	1,329
A6	175,00	85,00	40,00	21831,98	10,02	14875,00	1,468
A7	105,00	75,00	30,00	78228,37	14,87	7875,00	9,934
A8	105,00	75,00	30,00	88700,0	-----	7875,00	11,263
A9	105,00	75,00	30,00	29158,42	15,00	7875,00	3,703
A10	105,00	75,00	30,00	87904,19	14,89	7875,00	11,162
A11	105,00	75,00	30,00	30334,83	15,00	7875,00	3,882
A12	105,00	75,00	30,00	79126,34	14,98	7875,00	10,848
A1	100,00	75,00	30,00	38708,00	-	7500,00	5,160
A2	100,00	75,00	30,00	63980,44	11,87	7500,00	11,290
A3	100,00	75,00	30,00	15700,00	-	7500,00	2,093
A4	100,00	75,00	30,00	13872,56	9,43	7500,00	1,823
A5	100,00	75,00	30,00	52000,00	-	7500,00	6,833
A6	100,00	75,00	30,00	14998,25	11,98	7500,00	2,000

Table 2:

The measured dimensions and the failure stress rubber additive (own table)

Code	Dimensional Properties [mm]			Fmax (N)	dL at Fmax	Section Area [mm ²]	Failure Stress [Mpa]
	L	W	H				
Rubber additive							
11	60	60	50	3874,103	4,300693	3600,00	1,076
12	60	60	50	3798,812	5,726472	3600,00	1,055
13	60	60	50	2433,258	14,34663	3600,00	0,676
14	60	60	50	4825,335	4,856345	3600,00	1,340
15	60	60	50	4309,289	4,8967	3600,00	1,197

Table 3:

The measured dimensions and the failure stress textile additive (own table)

Code	Dimensional Properties [mm]			Fmax (N)	dL at Fmax	Section Area [mm ²]	Failure Stress [Mpa]
	L	W	H				
Textile additive							
16	60	60	50	4018,924	14,91635	3600,00	1,116
17	60	60	50	3698,73	6,386354	3600,00	1,027
18	60	60	60	3454,65	8,226385	3600,00	0,960
19	60	60	50	2954,478	14,80639	3600,00	0,832
20	60	60	50	4007,874	6,076674	3600,00	1,113

Table 4:

The measured dimensions and the failure stress wood chips additive (own table)

Code	Dimensional Properties [mm]			Fmax (N)	dL at Fmax	Section Area [mm ²]	Failure Stress [Mpa]
	L	W	H				
Wood chips additive							
WD1	170	90	40	24253,13	6,72	15300	1,585
WD2	170	90	40	43393	16,73	15300	2,836
WD3	90	90	40	9842,557	7,28	8100	1,215
4A	125	118	50	38373,860	19,958	14750	2,602
4B	122	115	52	65834,380	24,965	14030	4,700
SW1s	95	70	30	15800		6650	2,391
Sw2s	95	70	30	22700		6650	3,414
Sw3s	95	70	30	16700		6650	2,511
21	60	60	50	5277,722	4,866442	3600	1,466
22	60	60	50	4846,897	6,488415	3600	1,291
23	60	60	50	5063,669	4,01638	3600	1,407
24	60	60	50	4873,333	5,03645	3600	1,354
25	60	60	50	4665,315	4,4643	3600	1,296
17	135	90	40	32480,30	9,24	12150	2,673
18	135	90	40	35830,86	9,97	12150	2,949
19	135	90	40	27850,94	14,94	12150	2,292
20	135	90	40	26406,52	9,44	12150	2,174
21	135	90	40	35840,77	14,69	12150	2,950
W1	105	75	30	43293,21	11,96	7875	5,498
WD1	100	75	30	56650,17	11,98532	7500	7,553
WD2	100	75	30	38300	-	7500	5,107
WD3	100	75	30	52495,67	11,98119	7500	6,999

Table 5:
The measured dimensions and the failure stress hay additive (own table)

Code	Dimensional Properties [mm]			Fmax (N)	dL at Fmax	Section Area [mm ²]	Failure Stress [Mpa]
	L	W	H				
Hay additive							
26	60	60	50	5483,833	4,788423	3800,00	1,523
27	60	60	50	6759,478	11,73845	3800,00	1,878
28	60	60	60	6607,645	5,546422	3800,00	1,835
29	60	60	50	6904,746	11,15651	3800,00	1,918
30	60	60	50	5017,568	6,716428	3800,00	1,394

Table 6:
The measured dimensions and the failure stress straw additive (own table)

Code	Dimensional Properties [mm]			Fmax (N)	dL at Fmax	Section Area [mm ²]	Failure Stress [Mpa]
	L	W	H				
Straw additive							
S1	170	90	40	53932,71	24,86	15300	3,525
S2	170	90	40	60108,58	18,18	15300	4,517
S3	170	90	40	100489,4	16,27	15300	5,569
S4	170	90	40	72196,41	23,67	15300	4,719
3A	115	111	40	100549,50	14,95	12765	7,877
3B	116	114	41	100384,60	19,83	13224	7,591
3C	111	110	41	100284,40	20,94	12210	8,214
SS1b	175	85	40	35400	9,94	14875	2,380
SS2b	175	85	40	28000	-	14875	1,882
SS3b	175	85	40	29300	-	14875	1,970
SS4b	175	85	40	31600	9,92	14875	2,124
SS5b	175	85	40	44800	9,94	14875	3,018
11	135	90	40	46286,38	14,94	12150	3,810
12	135	90	40	29810,99	8,86	12150	2,454
13	135	90	40	63061,82	14,95	12150	5,190
14	135	90	40	46270,21	14,94	12150	3,808
15	135	90	40	43370,08	13,16	12150	3,570
16	135	90	40	36758,87	14,94	12150	3,190
S1	175	85	40	36582,63	14,94	14875	2,460
S2	175	85	40	33957,98	14,79	14875	2,283
S3	175	85	40	56105,79	14,94	14875	3,772
S4	175	85	40	51784,55	14,93	14875	3,481
S5	175	85	40	56502,25	14,94	14875	3,798
S6	105	75	30	27459,32	9,97	7875	3,487
S1	100	75	30	78581,88	11,98106	7500	10,478
S2	100	75	30	47607,38	11,965	7500	6,348
S3	100	75	30	66655,61	11,96496	7500	8,887

Appendix I.2: Graphical analysis

Graphical analysis only adobe

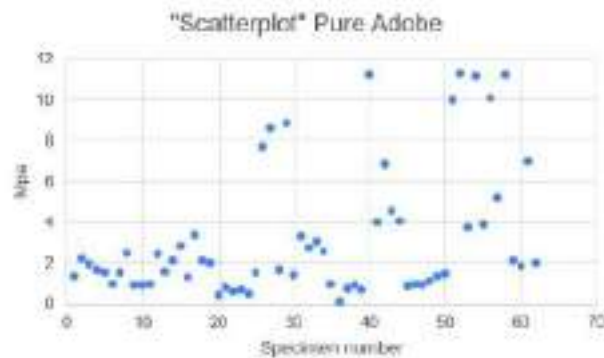


Figure 1: Scatterplot pure adobe (own figure)

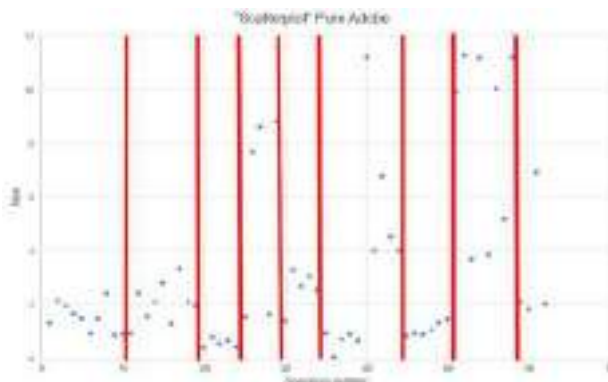


Figure 2: Scatterplot divided in groups pure adobe (own figure)

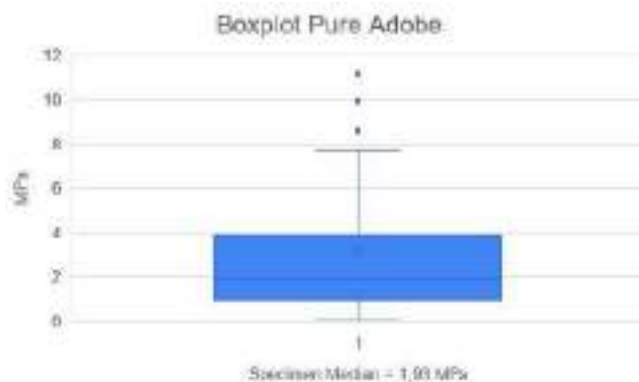


Figure 3: Boxplot pure adobe (own figure)

Table 1:
The measured dimensions and the failure stress pure adobe (own table)

Lower limit	Upper limit	Frequency table Pure Adobe				
		Range	x_i	n_i	f_i	c_{ni}
0,001	0,250	[0;0,25]	0,126	1	2%	1
0,251	0,500	[0,25;0,5]	0,376	2	3%	3
0,501	0,750	[0,5;0,75]	0,626	4	6%	7
0,751	1,000	[0,75;1]	0,876	10	18%	17
1,001	1,250	[1;1,25]	1,126	1	2%	18
1,251	1,500	[1,25;1,5]	1,376	7	11%	25
1,501	1,750	[1,5;1,75]	1,626	4	6%	29
1,751	2,000	[1,75;2]	1,876	4	6%	33
2,001	2,250	[2;2,25]	2,126	4	6%	37
2,251	2,500	[2,25;2,5]	2,376	2	3%	39
2,501	2,750	[2,5;2,75]	2,626	2	3%	41
2,751	3,000	[2,75;3]	2,876	1	2%	42
3,001	3,250	[3;3,25]	3,126	1	2%	43
3,251	3,500	[3,25;3,5]	3,376	2	3%	45
3,501	3,750	[3,5;3,75]	3,626	1	2%	46
3,751	4,000	[3,75;4]	3,876	3	5%	49
4,001	4,250	[4;4,25]	4,126	0	0%	49
4,251	4,500	[4,25;4,5]	4,376	0	0%	49
4,501	4,750	[4,5;4,75]	4,626	1	2%	50
4,751	5,000	[4,75;5]	4,876	0	0%	50
5,001	More	More	5,001	12	19%	62
		SOM:		62	100%	

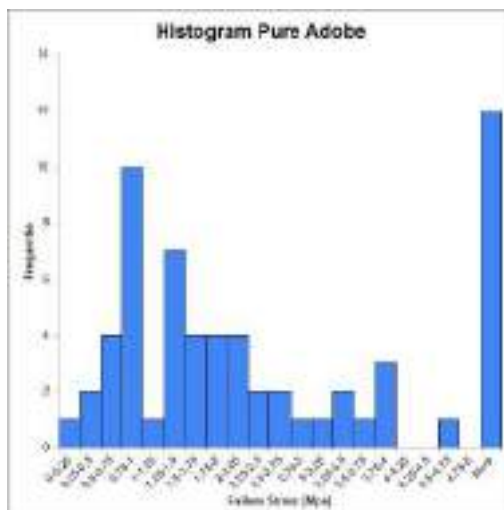


Figure 4: Histogram pure adobe (own figure)

Graphical analysis rubber additive

Table 2:
The measured dimensions and the failure stress rubber additive (own table)

Lower limit	Upper limit	Frequency table Rubber additive					
		Range	x_i	n_i	f_i	$c_n i$	$c_f i$
0,501	0,750	[0,5;0,75]	0,626	1	20%	1	20%
0,751	1,000	[0,75;1]	0,876	0	0%	1	20%
1,001	1,250	[1;1,25]	1,126	3	60%	4	80%
1,251	1,500	[1,25;1,5]	1,376	1	20%	5	100%
		SOM:		5	100%		

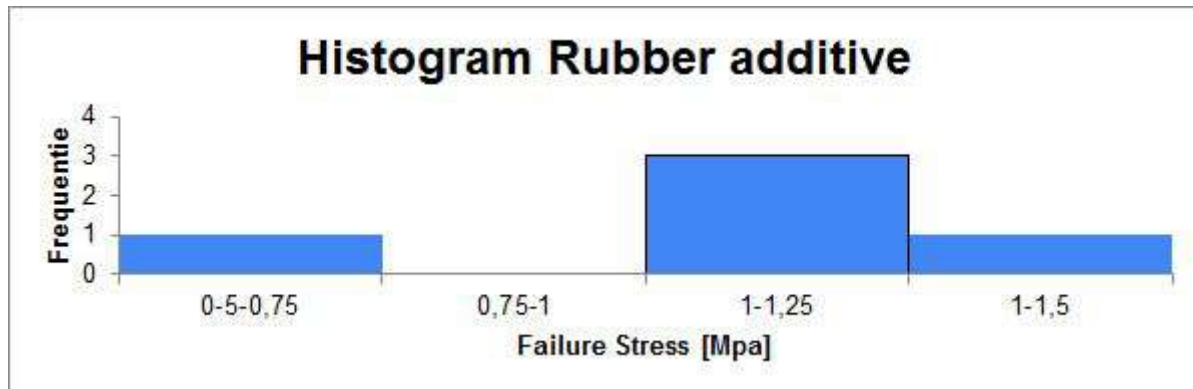


Figure 5: Histogram rubber additive (own figure)

Graphical analysis textile additive

Table 3:
The measured dimensions and the failure stress textile additive (own table)

Lower limit	Upper limit	Frequency table Textile additive					
		Range	x_i	n_i	f_i	c_{ni}	c_{fi}
0,601	0,800	[0,5;0,75]	0,701	1	20%	1	20%
0,801	1,000	[0,75;1]	0,901	2	40%	3	60%
1,001	1,200	[1;1,25]	1,101	2	40%	5	100%
		SOM:		5	100%		

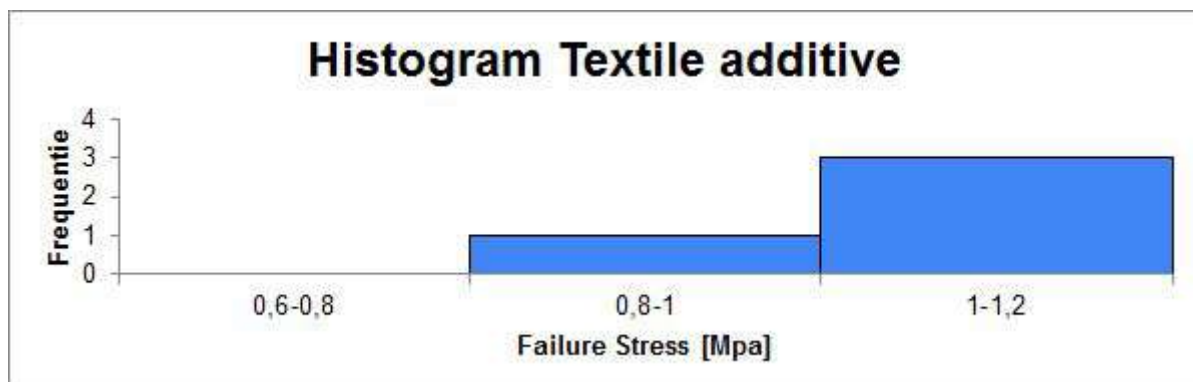


Figure 6: Histogram textile additive (own figure)

Graphical analysis wood chips additive

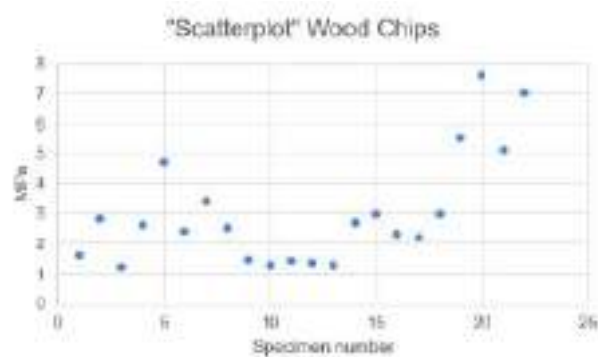


Figure 7: Scatterplot wood chips additive (own figure)

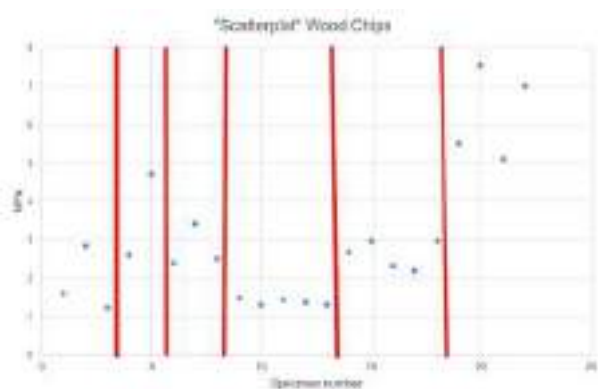


Figure 8: Scatterplot divided in groups wood chips additive (own figure)



Figure 9: Boxplot wood chips additive (own figure)

Table 4:
The measured dimensions and the failure stress wood chips additive (own table)

Lower limit	Upper limit	Frequency Wood chips additive					
		Range	x_i	n_i	f_i	c_{ni}	c_{fi}
1,01	2,00	[1;2]	1,505	2	8%	2	8%
2,01	3,00	[2;3]	2,505	5	21%	7	29%
3,01	4,00	[3;4]	3,505	10	42%	17	71%
4,01	5,00	[4;5]	4,505	2	8%	19	79%
5,01	6,00	[5;6]	5,505	1	4%	20	83%
6,01	7,00	[6;7]	6,505	2	8%	22	92%
7,01	8,00	[7;8]	7,505	2	8%	24	100%
		SOM:	24	100%			

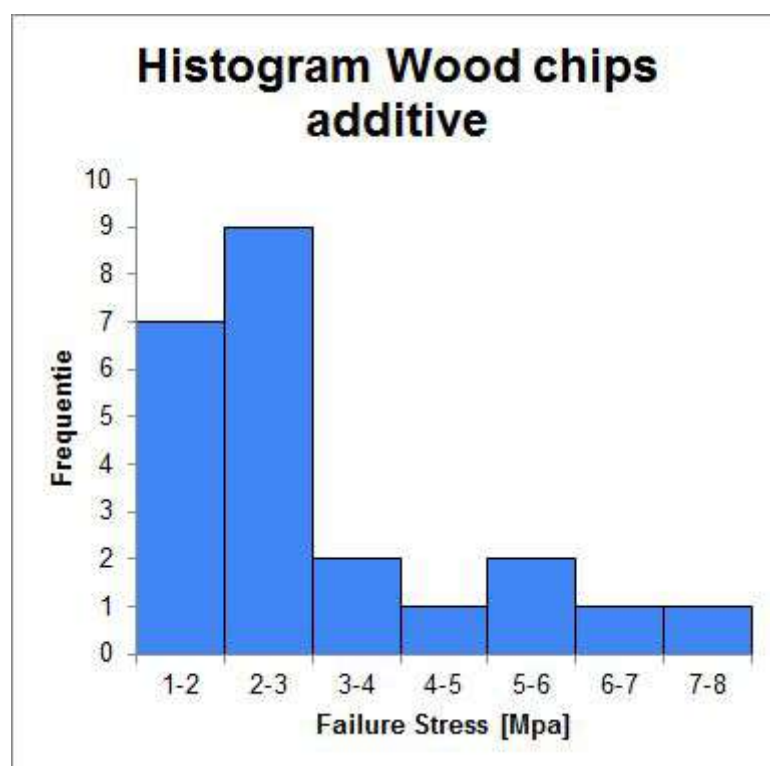


Figure 10: Histogram wood chips additive (own figure)

Graphical analysis hay additive

Table 5:
The measured dimensions and the failure stress hay additive (own table)

Lower limit	Upper limit	Range	x_i	n_i	f_i	c_{ni}	c_{fi}
0,601	0,800	[0,5;0,75]	0,701	1	20%	1	20%
0,801	1,000	[0,75;1]	0,901	2	40%	3	60%
1,001	1,200	[1;1,25]	1,101	2	40%	5	100%
SOM:				5	100%		

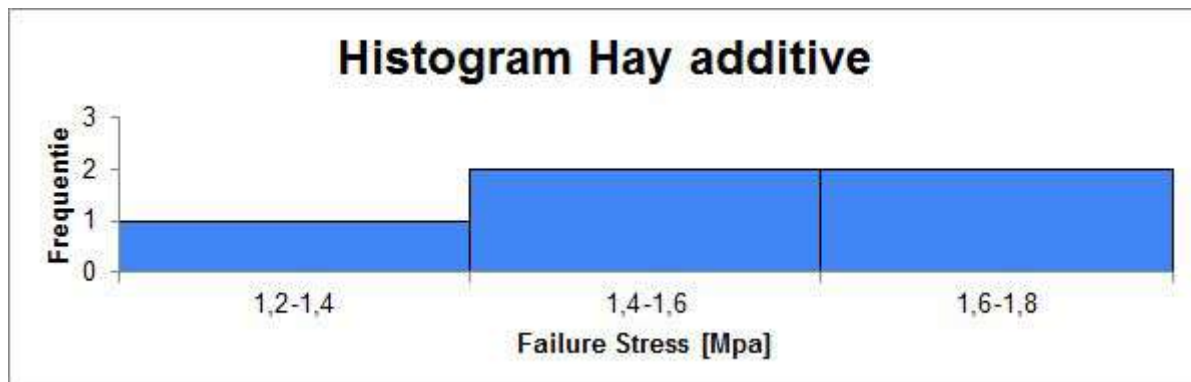


Figure 11: Histogram hay additive (own figure)

Graphical analysis straw additive

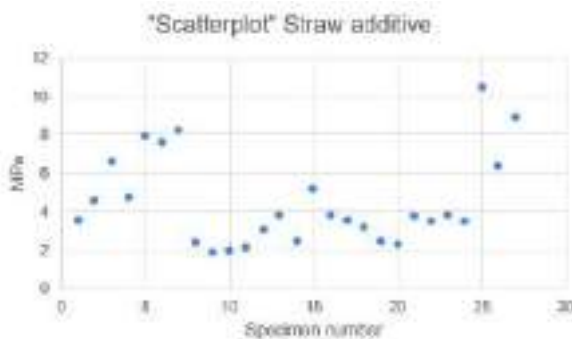


Figure 12: Scatterplot straw additive (own figure)

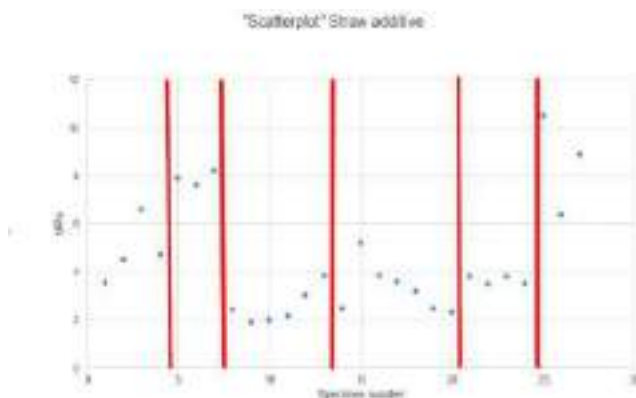


Figure 13: Scatterplot divided in groups straw additive (own figure)

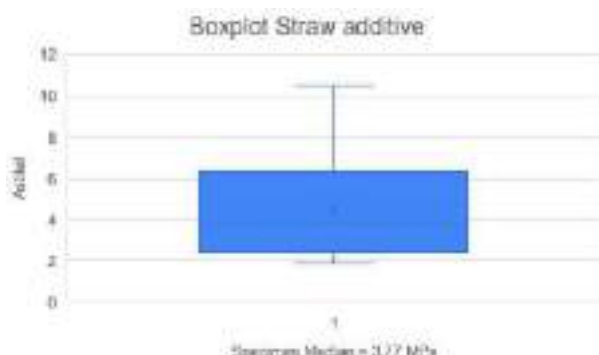


Figure 14: Boxplot straw additive (own figure)

Table 6:
The measured dimensions and the failure stress straw additive (own table)

Lower limit	Upper limit	Frequency table Straw additive					
		Range	xi	ni	fi	cni	cfi
1,01	2,00	[1;2]	1,505	2	7%	2	7%
2,01	3,00	[2;3]	2,505	5	19%	7	26%
3,01	4,00	[3;4]	3,505	10	37%	17	63%
4,01	5,00	[4;5]	4,505	2	7%	19	70%
5,01	6,00	[5;6]	5,505	1	4%	20	74%
6,01	7,00	[6;7]	6,505	2	7%	22	81%
7,01	8,00	[7;8]	7,505	2	7%	24	89%
8,01	9,00	[8;9]	8,505	2	7%	26	96%
9,01	10,00	[9;10]	9,505	0	0%	26	96%
10,01	11,00	[10;11]	10,505	1	4%	27	100%
		SOM:	27	100%			

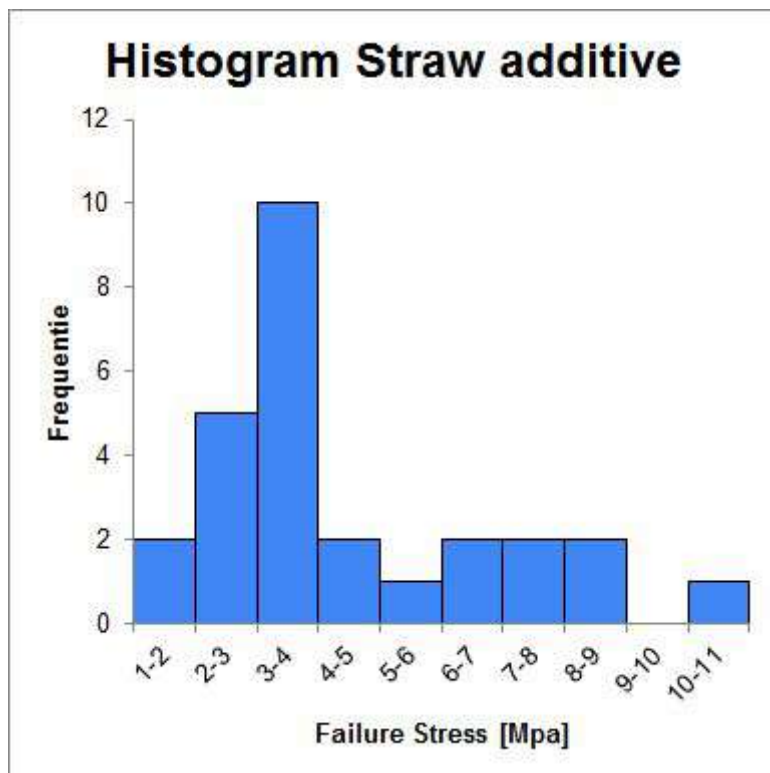


Figure 15: Histogram straw additive (own figure)

Appendix I.3: Statistical estimation of imprecision

Statistical estimation of the imprecision: 95% confidence, only adobe

$$n = 62$$

$$\bar{x} = \frac{1}{n} \sum_{i=1}^n x_i$$

$$\bar{x} = 3,179852$$

$$s = \sqrt{\frac{1}{n-1} \sum_{i=1}^n (x_i - \bar{x})^2}$$

$$s = 3,187213$$

$$\sigma = \frac{s}{\sqrt{n}}$$

$$\sigma = 0,404776$$

$$t = 1,96$$

$$\delta x = t \cdot \sigma$$

$$\delta x = 0,793362$$

Statistical estimation of the imprecision: 95% confidence, rubber additive

$$n = 5$$

$$\bar{x} = \frac{1}{n} \sum_{i=1}^n x_i$$

$$\bar{x} = 1,068811$$

$$s = \sqrt{\frac{1}{n-1} \sum_{i=1}^n (x_i - \bar{x})^2}$$

$$s = 0,247393$$

$$\sigma = \frac{s}{\sqrt{n}}$$

$$\sigma = 0,110638$$

$$t = 2,78$$

$$\delta x = t \cdot \sigma$$

$$\delta x = 0,307573$$

Statistical estimation of the imprecision: 95% confidence, textile additive

$$n = 5$$

$$\bar{x} = \frac{1}{n} \sum_{i=1}^n x_i$$

$$\bar{x} = 1,009704$$

$$s = \sqrt{\frac{1}{n-1} \sum_{i=1}^n (x_i - \bar{x})^2}$$

$$s = 0,118933$$

$$\sigma = \frac{s}{\sqrt{n}}$$

$$\sigma = 0,053189$$

$$t = 2,78$$

$$\delta x = t \cdot \sigma$$

$$\delta x = 0,147864$$

Statistical estimation of the imprecision: 95% confidence, wood chips additive

$$n = 22$$

$$\bar{x} = \frac{1}{n} \sum_{i=1}^n x_i$$

$$\bar{x} = 3,011879$$

$$s = \sqrt{\frac{1}{n-1} \sum_{i=1}^n (x_i - \bar{x})^2}$$

$$s = 1,840897$$

$$\sigma = \frac{s}{\sqrt{n}}$$

$$\sigma = 0,39248$$

$$t = 1,96$$

$$\delta x = t \cdot \sigma$$

$$\delta x = 0,769262$$

Statistical estimation of the imprecision: 95% confidence, hay additive

$$n = 5$$

$$\bar{x} = \frac{1}{n} \sum_{i=1}^n x_i$$

$$\bar{x} = 1,709626$$

$$s = \sqrt{\frac{1}{n-1} \sum_{i=1}^n (x_i - \bar{x})^2}$$

$$s = 0,235564$$

$$\sigma = \frac{s}{\sqrt{n}}$$

$$\sigma = 0,105347$$

$$t = 2,78$$

$$\delta x = t \cdot \sigma$$

$$\delta x = 0,292866$$

Statistical estimation of the imprecision: 95% confidence, straw additive

$$n = 27$$

$$\bar{x} = \frac{1}{n} \sum_{i=1}^n x_i$$

$$\bar{x} = 4,496346$$

$$s = \sqrt{\frac{1}{n-1} \sum_{i=1}^n (x_i - \bar{x})^2}$$

$$s = 2,356487$$

$$\sigma = \frac{s}{\sqrt{n}}$$

$$\sigma = 0,453506$$

$$t = 1,96$$

$$\delta x = t \cdot \sigma$$

$$\delta x = 0,888872$$

Appendix I.4: Behavior during breaking

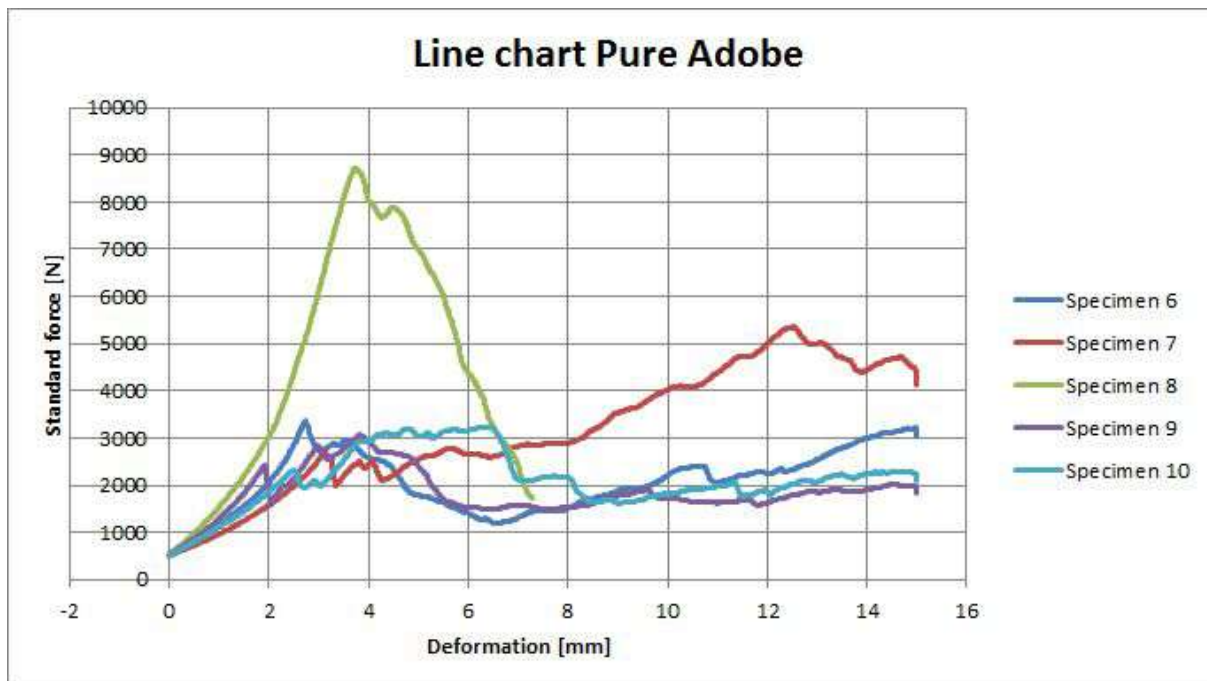


Figure 1: Line chart behavior during breaking pure adobe (own figure)

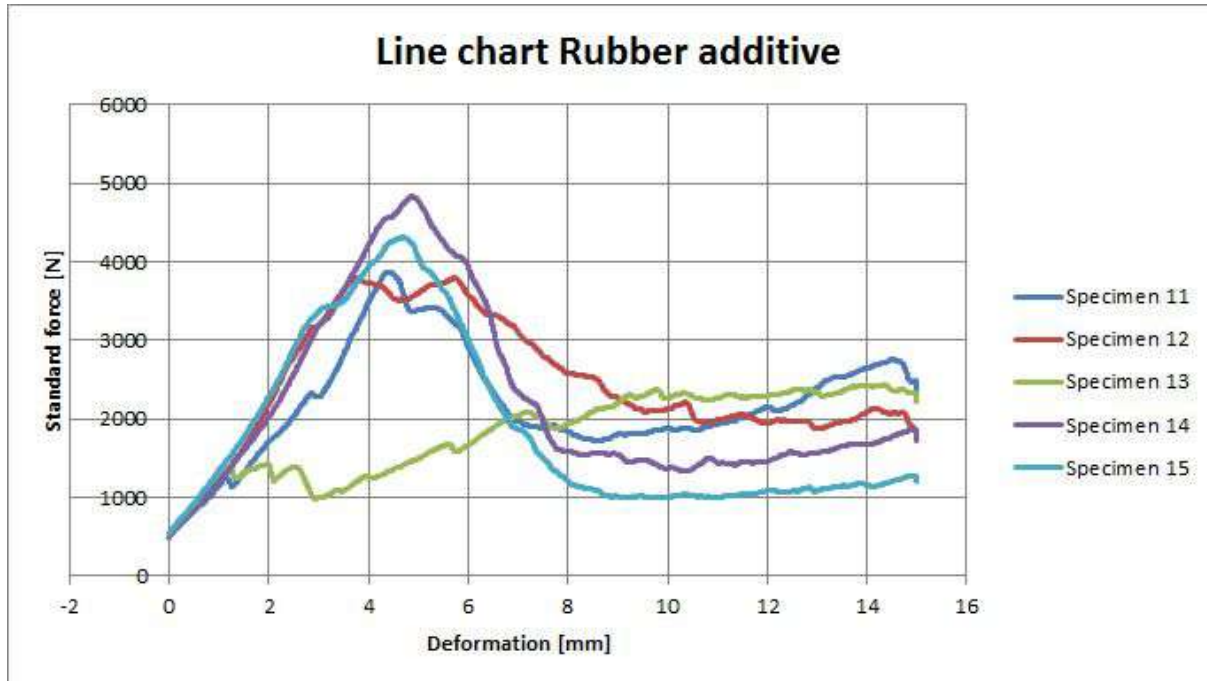


Figure 2: Line chart behavior during breaking rubber additive (own figure)

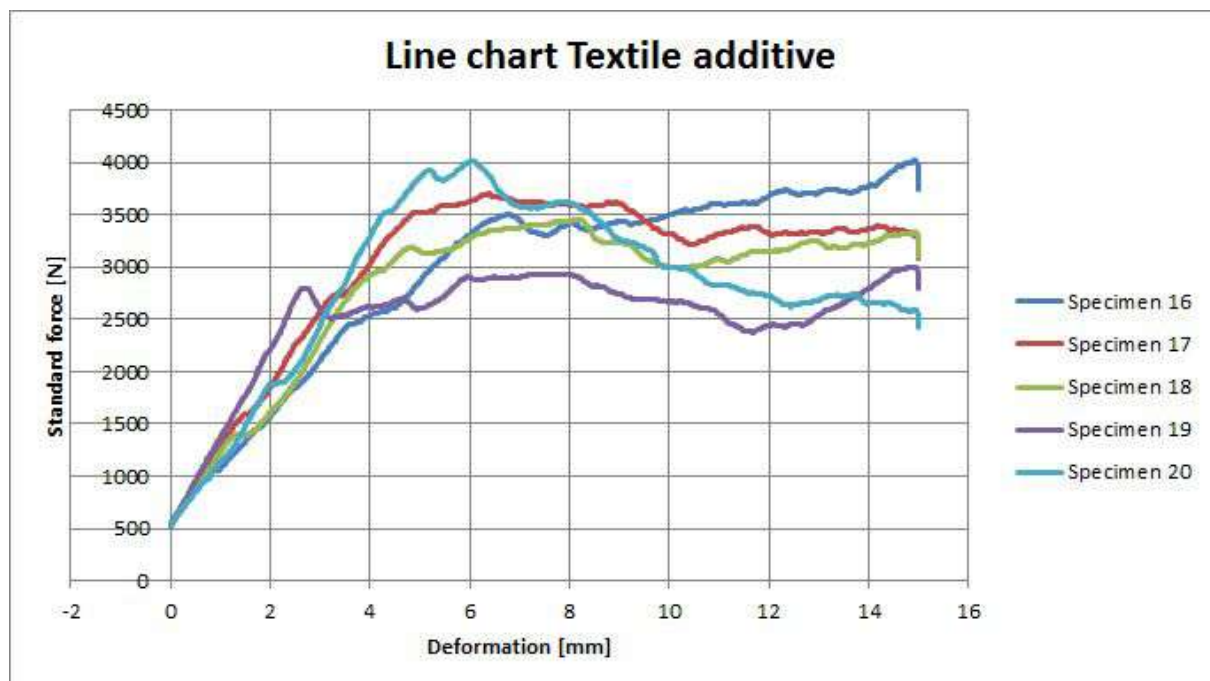


Figure 3: Line chart behavior during breaking textile additive (own figure)

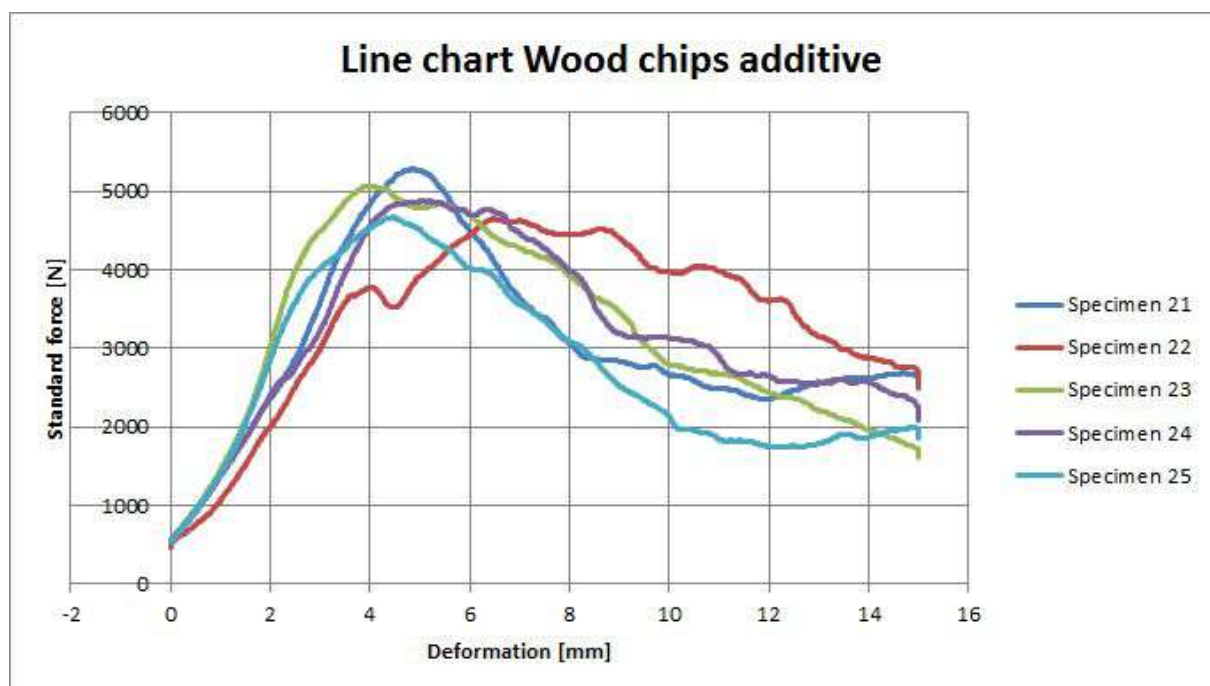


Figure 4: Line chart behavior during breaking wood chips additive (own figure)

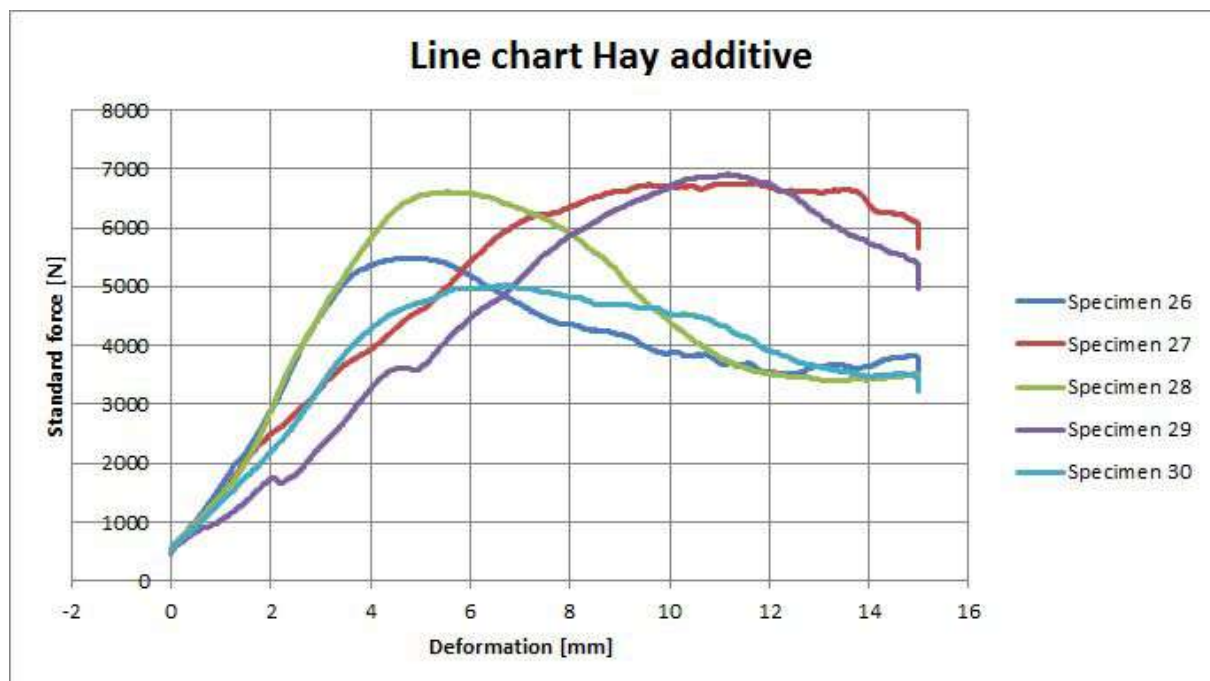


Figure 5: Line chart behavior during breaking hay additive (own figure)

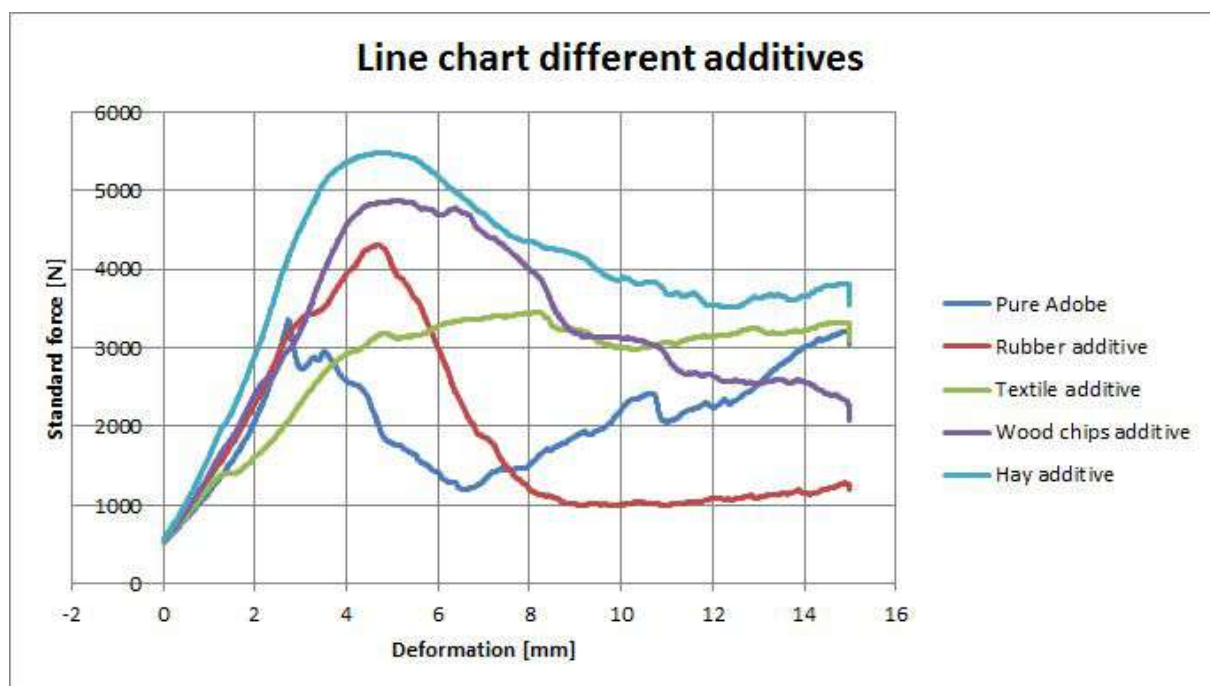
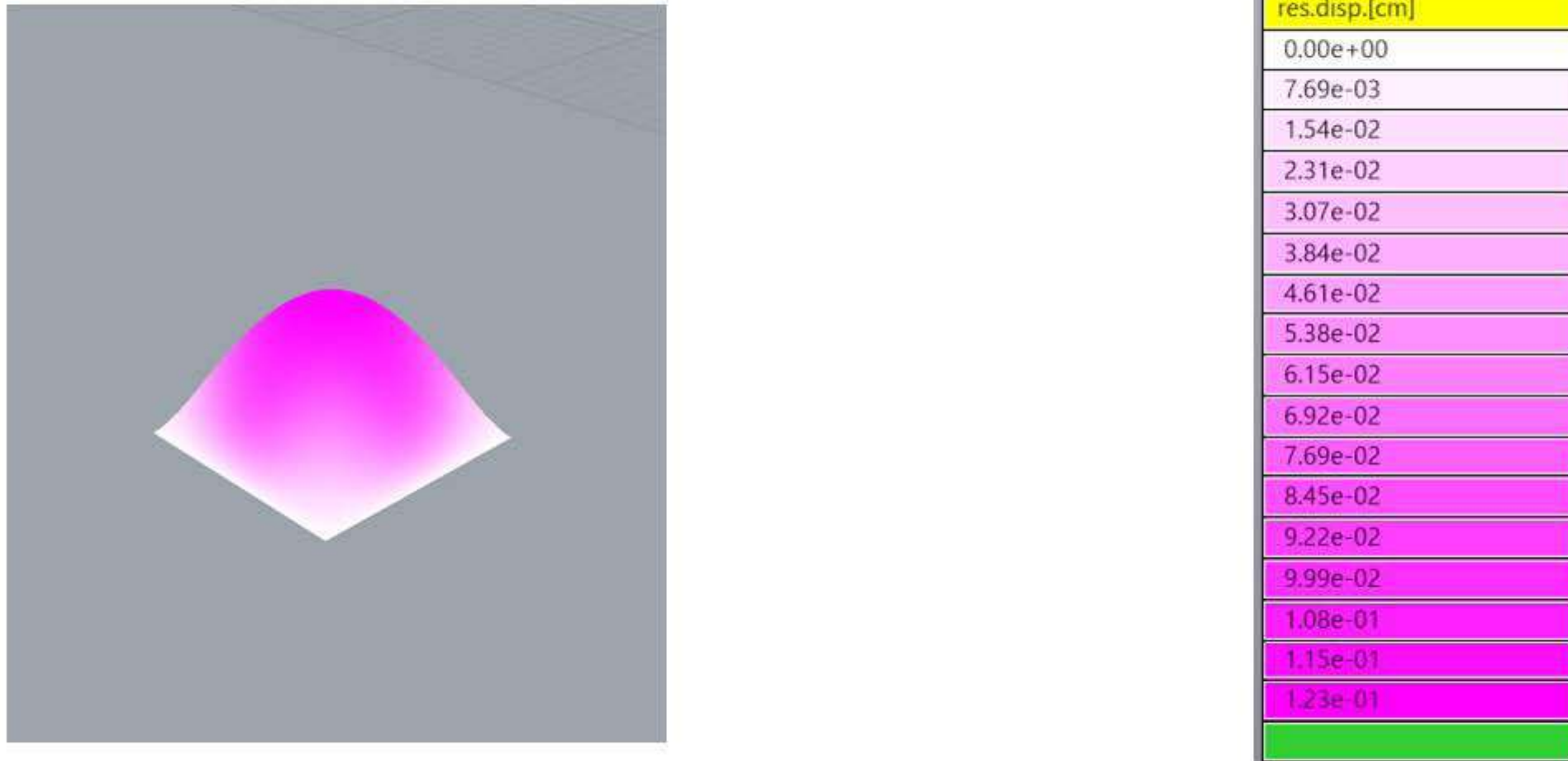
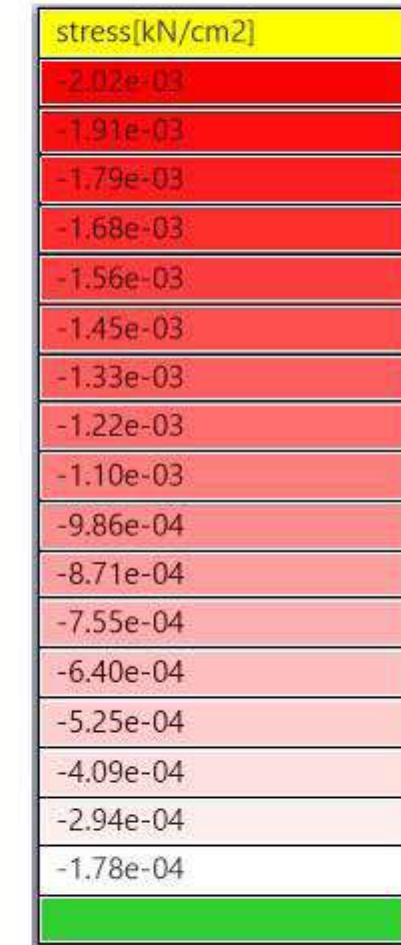
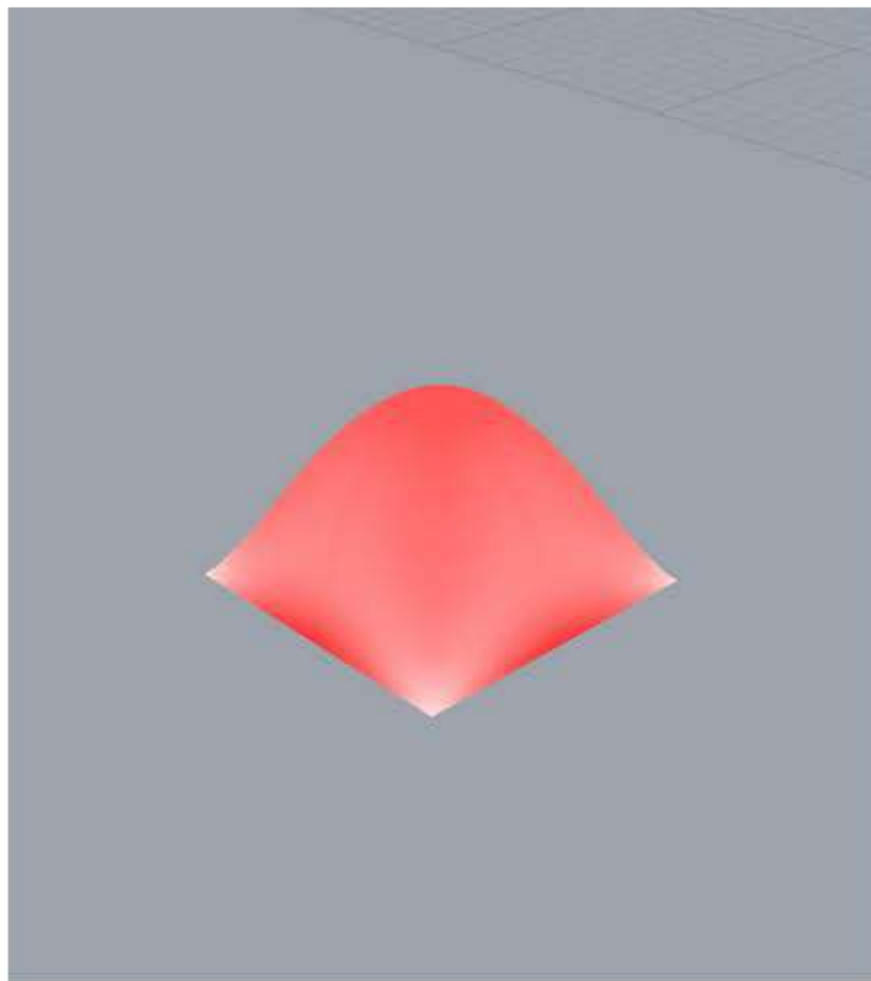


Figure 1: Line chart behavior during breaking different additives (own figure)

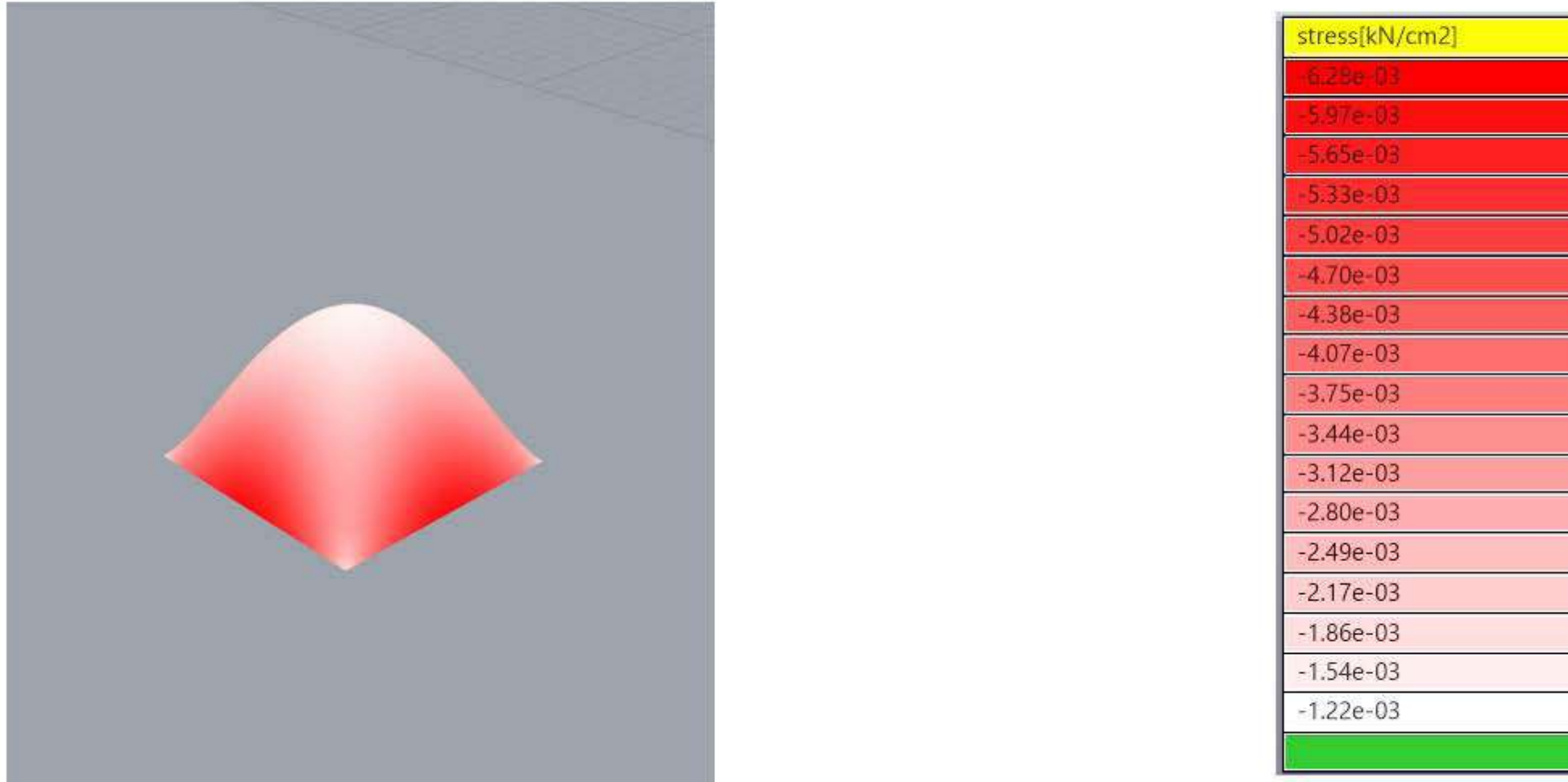
Dome Library Displ.



Dome Library princ 1



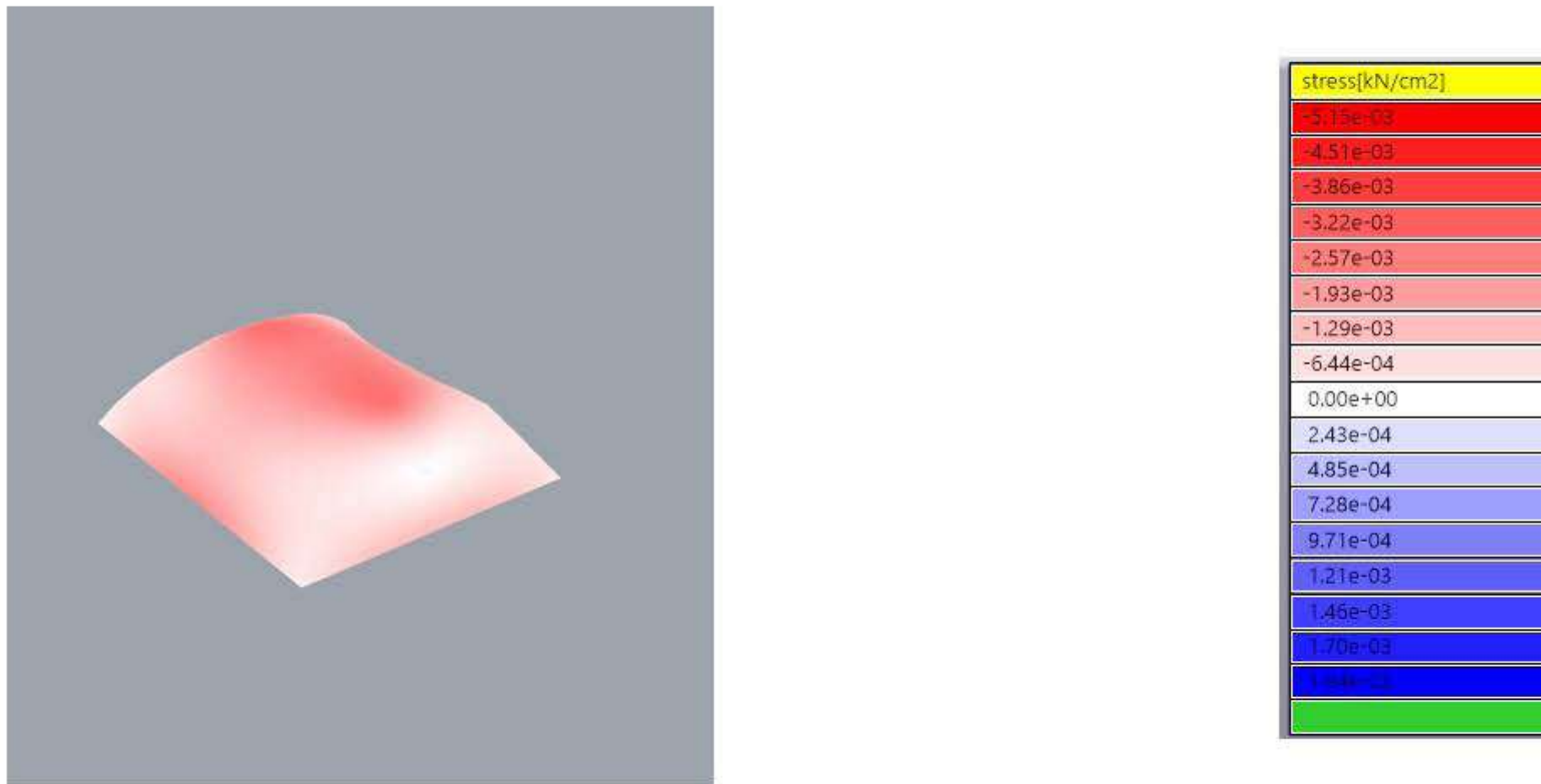
Dome Library princ 2



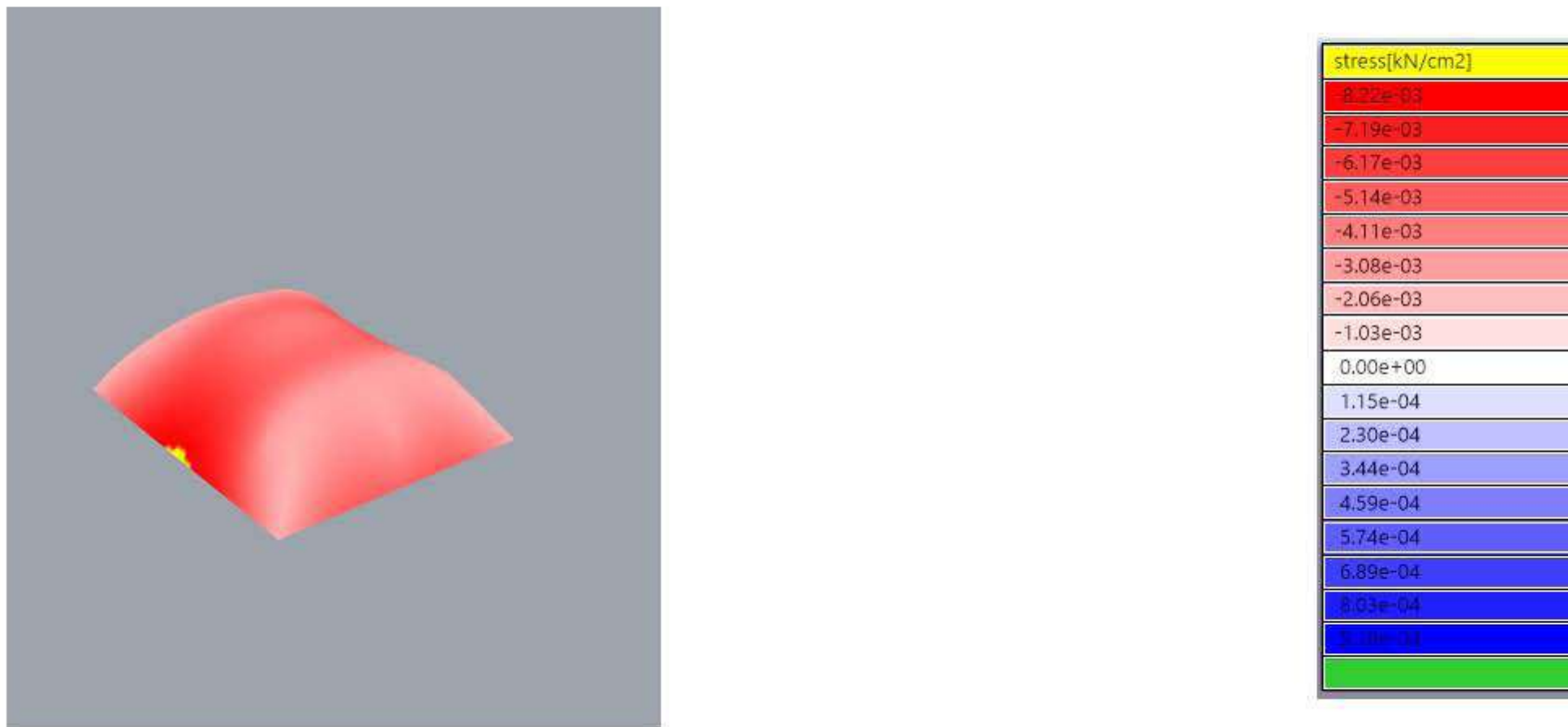
Vault classroom floor 1 Disp.



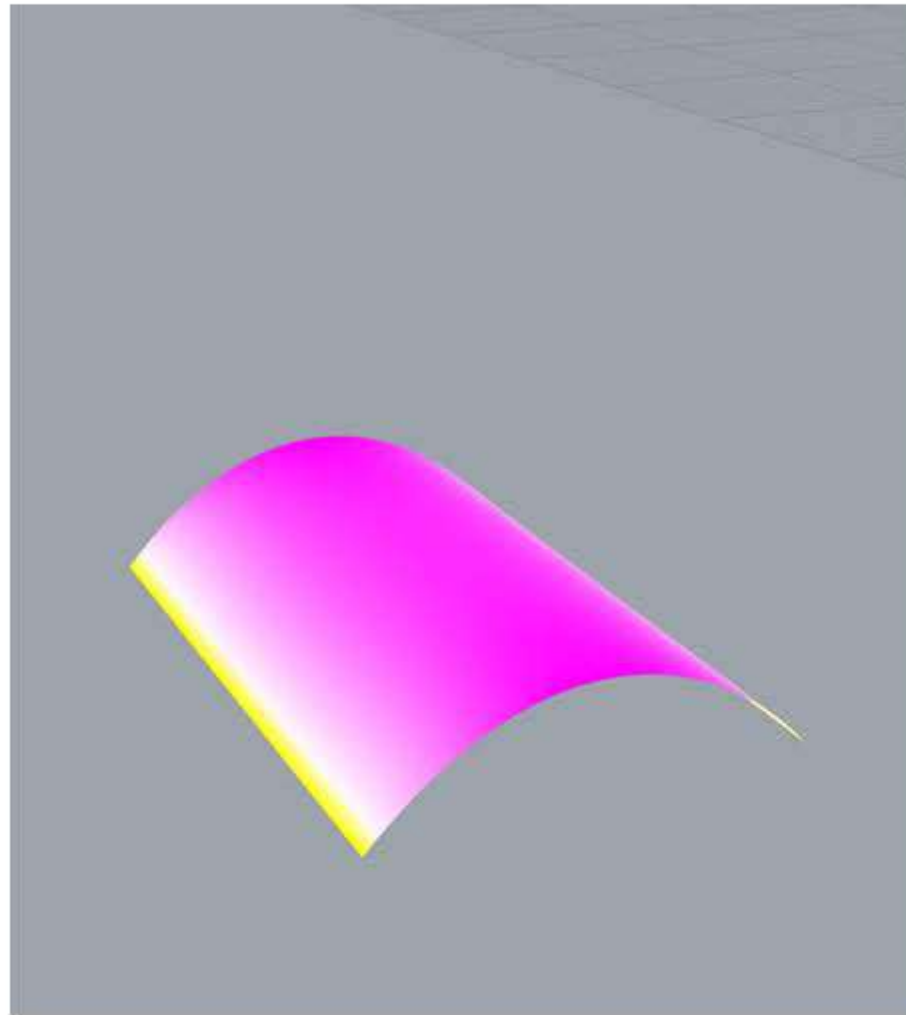
Vault classroom floor 1 princ 1



Vault classroom floor 1 princ 2

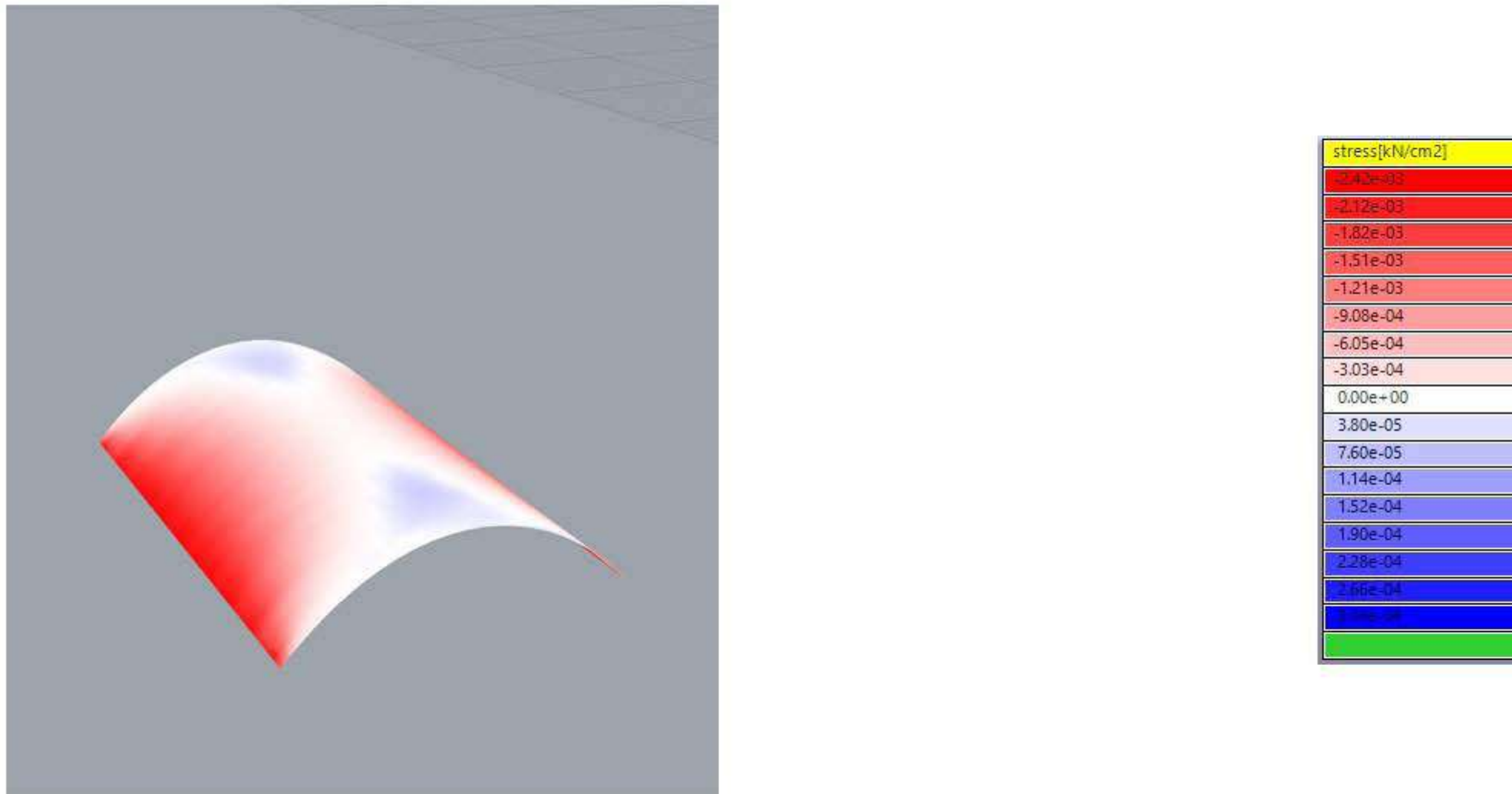


Vault classroom floor 0 displ. 2



res.disp.[cm]
3.77e-02
6.06e-02
8.36e-02
1.07e-01
1.29e-01
1.52e-01
1.75e-01
1.98e-01
2.21e-01
2.44e-01
2.67e-01
2.90e-01
3.13e-01
3.36e-01
3.59e-01
3.82e-01
4.05e-01

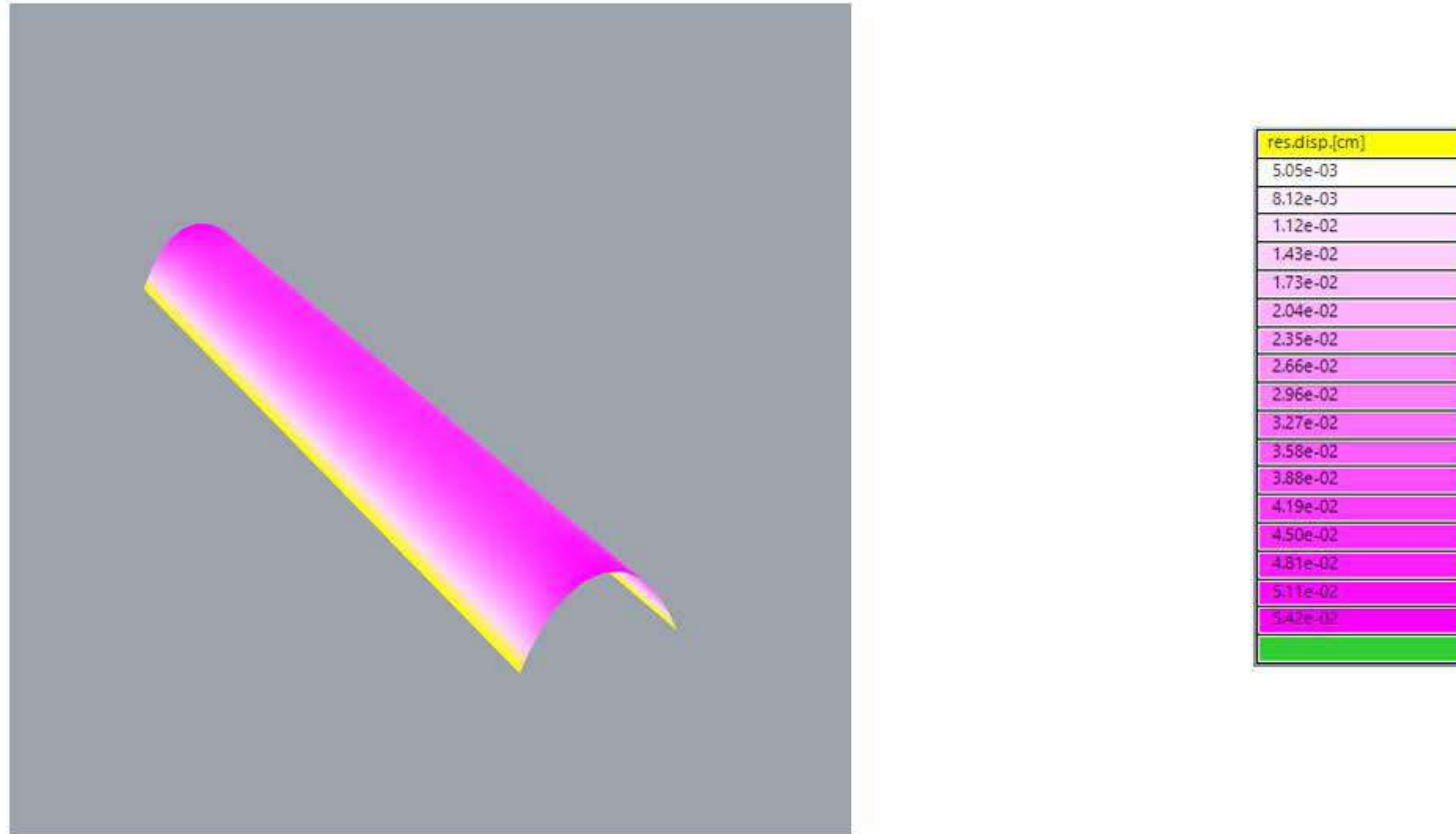
Vault classroom floor 0 princ 1



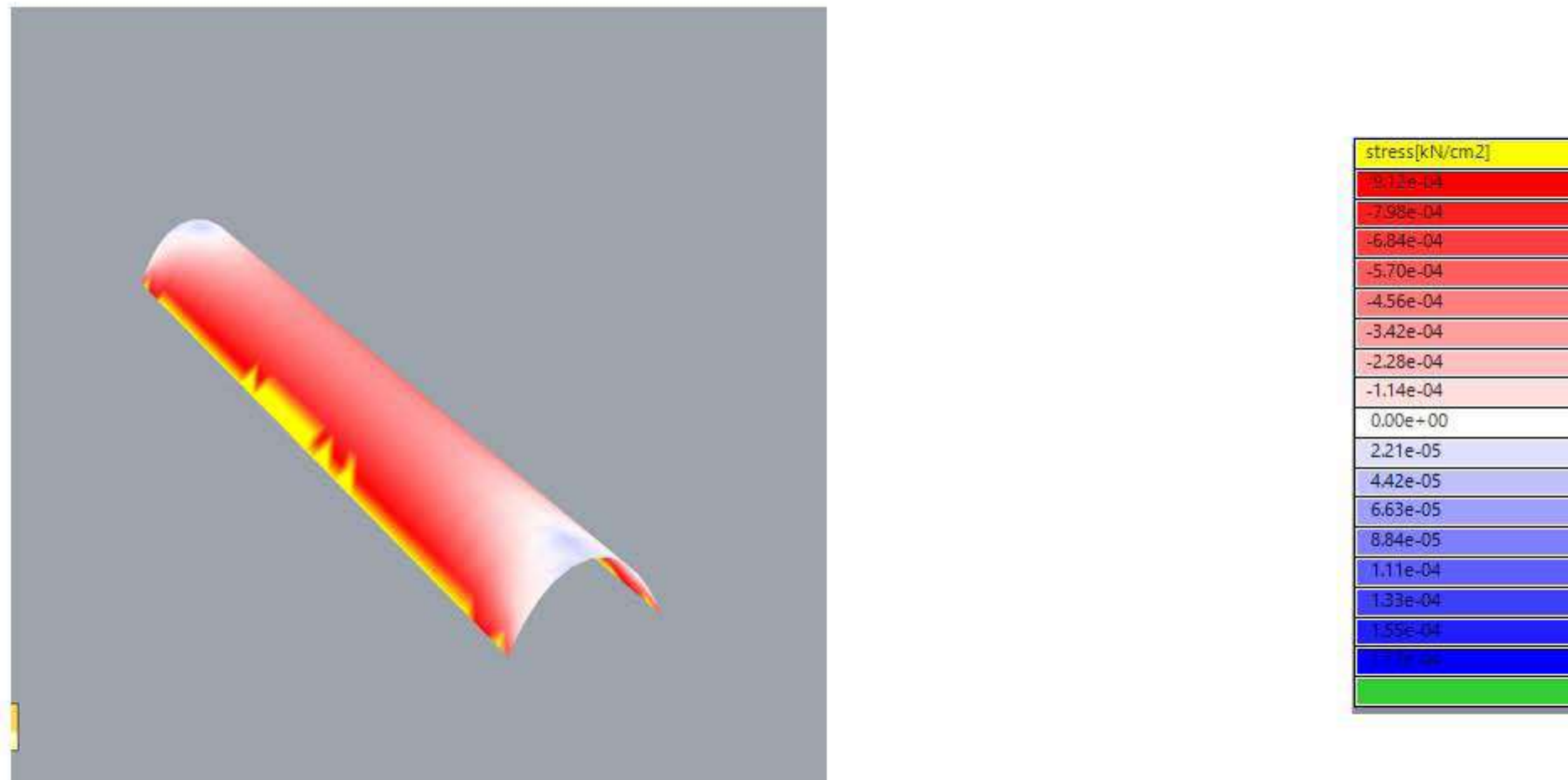
Vault classroom floor 0 princ 2



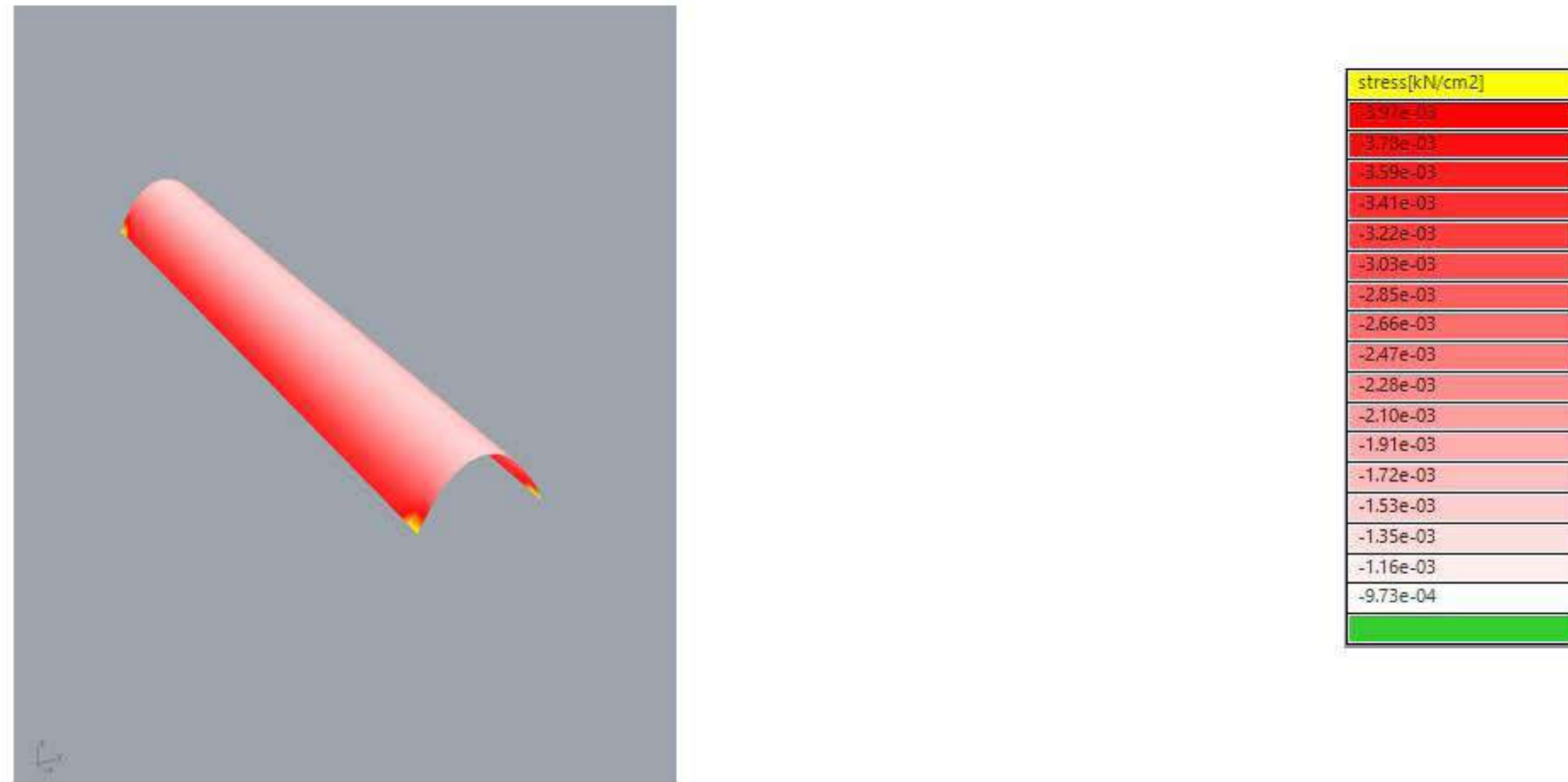
Vault gallery floor 0 displ.



Vault gallery floor 0 princ 1



Vault gallery floor 0 princ 2



This is how the trials were done:

Python Trial Description:

Inputs:

srf: Surface of vault: The surface imported is cut in the middle since it is symmetrical. Later it will be mirrored.

 typeA45:geometry of type A muqarnas brick with 45 cm depth (with diagonal force transfer slope ~ 30/45)

 typeB30:geometry of type B muqarnas brick with 30 cm depth (with diagonal force transfer slope ~ 30/30)

 typeC15:geometry of type C muqarnas brick with 15 cm depth (with diagonal force transfer slope ~ 30/15)

 typeD_45_15:geometry of type D muqarnas brick with 45 cm depth and 15 height (with diagonal force transfer slope ~ 15/45)

These are the imported muqarnas bricks

Step1:

 Import the relaxed vault surface shape from rhino (baked kangaroo geometry)

Step2:

 Import the four types of mukarnas bricks as Breps (internalize them)

Step3:

 create a contour / curve lines every 30cm in z direction

Step4:

 Measure the curvature angle of the vault surface where the next brick at every brick row.

Step5:

 #If curvature slope angle (inverseTan) is between the range of 90 - 54 degrees, then use brick typeC15

 #If curvature slope angle (inverse tan) is between the range of 54 - 39 degrees, then use brick typeB30

```
#If curvature slope angle (inverse tan) is between the range of 39-26 degrees, then use brick typeA45)
#If curvature slope angle (inverse tan) is between the range of 39-26 degrees, then use brick typeA45)
#If curvature slope angle (inverse tan) is between the range of 18 - 0 degrees, then use brick typeD_45_15)
#The range of angles have been adjusted to accommodate more variations of bricks. Initially the range
was calculated with a +/- range around the slope of the diagonal of the brick. Force transfer vector
```

Some improvements could have been made like overlapping half brick over gap. But the challenges and disadvantages outweigh potential solutions in this scenario.

This was the result:

The second method was used the C# code of Pirouz Nourian and further developed.

The second method was used the C# code of Pirouz Nourian and further developed.

Step1:

In this method three cubic bricks are imported. The dimensions are 30x30x10cm, 15x15x10cm, and 7.5x7.5x10cm.

Step 2:

The code creates a 3D grid of modules based on these bricks sizes.

Step 3:

The curvature/ vault surface is placed inside this grid.

Step 4:

Wherever the surface intersects a module, the module is kept and a brick type, corresponding to the size of the module, is placed in this location.

This is the result of this algorithm:

In this script the alternating gap overlap is solved in the y direction but the x directional overlap is a greater issue.

When the vault height is increased (see image below), the cantilevering problem is less of an issue, but the result is not optimal yet. Nevertheless, a height ceiling is not desired.